ASYMMETRIC INDUCTION AND PHOTOCHEMISTRY OF 7-BENZOYLBICYCLO[2.2.1]HEPTANE DERIVATIVES

by

CHARLES JAMES SCOTT

B.Sc. (Hons.), The University of Western Ontario, 1997

A THESIS SUBMITTED IN PARTIAL FULFILMENT OF

THE REQUIREMENTS FOR THE DEGREE OF

DOCTOR OF PHILOSOPHY

in

THE FACULTY OF GRADUATE STUDIES

(Department of Chemistry)

We accept this thesis as conforming

to the required standard

THE UNIVERSITY OF BRITISH COLUMBIA

JULY 2003

Department of Chemistry

The University of British Columbia
Vancouver, Canada

September 17, 2003

Abstract

The Norrish/Yang photochemistry of two series of norbornane derivatives, 7-methyl-7-benzoylnorbornanes and 7-benzoylbenzonorbornenes, has been studied in both the solid state and solution. In the 7-benzoylbenzonorbornene system, photolysis in the solid state leads to a significant alteration in the ratio of photoproducts, from a complex mixture of two Yang cyclobutanols and a Norrish type II cleavage product in solution, to a single product, an *endo*-aryl cyclobutanol, in the solid state due to the confining effects of the crystal lattice. Photolysis of the 7-methyl-7-benzoylnorbornanes in the solid state or solution led to formation of an *endo*-aryl cyclobutanol as the sole photoproduct.

By utilizing ionic chiral auxiliaries it was possible to form chiral ammonium carboxylate salts between optically pure amines and the achiral norbornane derivatives containing a carboxylic acid functional group. Photolysis of the chiral salts in the solid state gave variable results, but through the use of a number of auxiliaries it was possible to achieve a high degree of enantioselectivity in the photoproducts (up to 98% ee at 100% conversion of the starting ketone). Photolysis of the same salts in solution gave only a racemic mixture of photoproducts, highlighting the critical role that the chiral crystal lattice plays in the asymmetric induction.

Through the use of X-ray crystallography, solid state reactivity-crystal structure relationships were developed to explain the observed reactivity in 11 of the ketone substrates. Fortuitously, two of the molecules studied underwent single crystal-to-single crystal reactions, allowing for a detailed study of the reaction through a series of X-ray crystal structures. In this case, because the molecules studied were chiral ammonium carboxylate salts used in the asymmetric induction studies, it was possible to predict and confirm the absolute configuration of the photoproduct, as well as validate the crystal structure-reactivity relationships. Comparison of the results obtained in the studies presented have also been compared to previous work in order to develop a greater understanding of how conformational changes in the geometry of a ketone can affect the outcome of Norrish/Yang reactions.

Table of Contents

v

List of Figures

List of Schemes

LIST OF TABLES

List of Symbols and Abbreviations

v_{max}	absorption maxima (IR spectroscopy)
λ_{max}	absorption maxima (UV spectroscopy)
Å	angstrom
δ	chemical shift (ppm)
°C	degrees Celsius
Δ	heat to reflux
ε	molar extinction coefficient
λ	wavelength
anal.	analysis
APT	attached proton test
Ar	aryl
bp	boiling point
br	broad
Bu	butyl
calcd	calculated
cat.	catalytic
CDI	carbonyldiimidazole
conc.	concentrated
COSY	^{1}H-^{1}H correlation spectroscopy
d	doublet
DCI	desorption chemical ionization
DMF	dimethylformamide
DMPU	*N,N'*-dimethylpropyleneurea
DMSO	dimethylsulfoxide
ee	enantiomeric excess
EI	electron impact
EtOAc	ethyl acetate
EtOH	ethanol
eV	electron volts
g	grams

GC	gas chromatography
h	hour(s)
hν	light
HMBC	heteronuclear multiple bond connectivity
HMQC	heteronuclear multiple quantum coherence
HPLC	high performance liquid chromatography
HRMS	high resolution mass spectrometry
Hz	hertz
ID	inner diameter
IPA	isopropanol
^{i}Pr	isopropyl
IR	infrared
J	coupling constant (Hz)
LDA	lithium diisopropylamide
lit.	literature
LRMS	low resolution mass spectrometry
LSIMS	liquid secondary ionization mass spectrometry
m	multiplet
M	molarity
Me	methyl
MeCN	acetonitrile
MeOH	methanol
mg	milligram
MHz	megahertz
min	minutes
mmol	millimole
mol	mole
MOM	methoxymethyl
mp	melting point
MS	mass spectrometry
NMR	nuclear magnetic resonance
NOE	nuclear Overhauser effect
NOESY	two-dimensional nuclear overhauser spectroscopy

ORTEP	Oak Ridge Thermal Ellipsoid Program
pet.	petroleum
Ph	phenyl
ppm	parts per million
psi	pounds per square inch
py	pyridine
q	quartet
quint	quintet
s	singlet
SEM	2-(trimethylsilyl)ethoxymethyl
sept	septet
t	triplet
THF	tetrahydrofuran
TLC	thin layer chromatography
UV/VIS	ultraviolet / visible
W	watt

Acknowledgements

First and foremost I would like to thank my supervisor, Professor John Scheffer, for his guidance and support during my time at UBC. I am also indebted to Drs. Eugene Cheung and Brian Patrick for determining the X-ray crystal structures presented in this thesis. Thanks are also given to the staff of the Electrical and Mechanical Engineering shops, who were always able to fix the equipment that broke at the least opportune times, and the NMR and Mass Spectrometry labs for their assistance and advice. Finally, I would like to thank the members of the Scheffer research group, past and present, who have had to put up with me over the years.

INTRODUCTION

Chapter 1 Introduction

1.1 Preamble

Although often overlooked, it is interesting to note that both the first organic chemical reaction, Wöhler's synthesis of urea in 1828,[1] and the first organic photochemical reaction, Trommsdorff's 1834 discovery that sunlight caused santonin crystals to become yellow and shatter,[2] were conducted in the solid state. Since then, however, the vast majority of both organic and organic photochemical reactions have been conducted in solution. In recent years there has been a growing interest in the solid state reactivity of molecules, particularly in terms of crystal engineering and materials science.[3] In addition, polymorphic crystal forms of the same molecule have been found to have different chemical and physical properties, a factor that has had a significant impact on the design and manufacture of pharmaceuticals as well as reactivity studies.[4]

That the two enantiomeric forms of a molecule can exhibit different biological activity is a pharmacological effect that has been known for nearly eighty years.[5] However, it was not until the disastrous effects of thalidomide (1) were discovered in the early 1960s that the full implications of racemic pharmaceuticals were recognized. In this extreme case of differing biological activity it was eventually found that the (+)-enantiomer of thalidomide (1, Figure 1.1) gave the desired sedative/antinausea effects while the (-)-enantiomer was a severe teratogen.[6] Among many other known examples in which enantiomeric forms of a molecule have drastically different biological effects are propoxyphene (2), where the (+)-enantiomer (2, Figure 1.1) is an analgesic, while the (-)-enantiomer is an antitussive, and α-(2-bromophenoxy)propionic acid (3), where the (+)-enantiomer (3, Figure 1.1) is a plant growth stimulant while the (-)-enantiomer acts as a growth retardant.[7] Owing to the potential differences in biological activity based on the stereochemical configuration of a molecule, extensive information about the reactivity of chiral substances is now required before a pharmaceutical may be approved for use. These requirements and the inherent challenge involved in selectively constructing each chirality centre in a molecule to match the desired product have made asymmetric synthesis a major focus of organic chemistry.

1   **2**   **3**

Figure 1.1 Molecules whose enantiomers exhibit different types of biological activity.

Photochemical processes are among the most important chemical reactions in nature; photosynthesis in plants harnesses the sun's energy, converting water and carbon dioxide into oxygen and glucose,[8] and the earth's protective ozone layer is generated through photolysis of oxygen.[9] In addition to the role of light in reactions essential for maintaining life, photochemical reactions have also been shown to be a valuable synthetic tool in organic synthesis, with the ability to facilitate molecular transformations not possible thermally.[10]

These three areas: solid state chemistry, asymmetric chemistry, and photochemistry, are brought together in the present work, where it has been found that by conducting photochemical reactions in the solid state it is possible to achieve high chemical and optical selectivity in the formation of complex organic molecules.

1.2 Solid State Organic Chemistry

With the increasing interest in solid state chemistry on a number of different fronts, a clarification of some commonly used terms and concepts will first be presented. First are the four general classifications of solid state reactions: solid-phase, solvent-free, solid-state or solid-solid, and single crystal (see Figure 1.2).[11] Solid-phase reactions are concerned with the use of insoluble polymer supports as a platform for conducting chemical reactions in solution. Solvent-free reactions occur when two solid reagents are mixed together without a solvent to produce either a solid, through a liquid/melt intermediate, or a liquid/melt. Solvent-free reactions are not necessarily solid state reactions and may also include solid-liquid, liquid-liquid, gas-solid, gas-liquid, and gas-gas reactions that do not require the use of a solvent. Solid-state or solid-solid reactions are those in which two solids react to form a third without forming an intermediate liquid or vapour phase. The final class, single-crystal reactions, are

those in which a chemical reaction occurs within a crystal without the involvement of other chemical reagents, but instead uses heat or light to induce reactivity in uni- or bimolecular reactions. Reactivity of all four classes of solid-state reactions can take place by three general means: thermal, mechanochemical (phase transitions, detonations, solid-solid reactions, catalyst activation), and photochemical.[12] The work presented within this thesis is concerned only with photochemical, single-crystal reactions even though the term solid-state or crystalline state is often used.
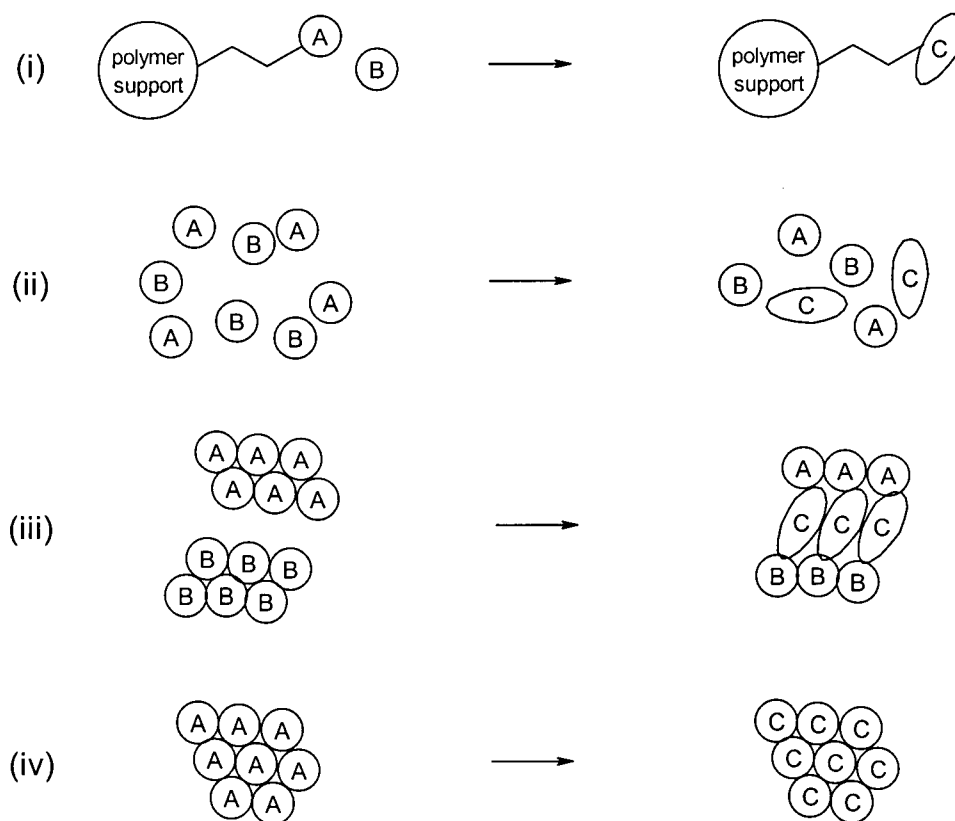
Figure 1.2 Solid-state reaction classes: (i) solid-phase, (ii) solvent-free, (iii) solid-state or solid-solid, and (iv) single crystal.

Although the solid state is not commonly thought of as practical for conducting reactions, it can, in many cases, have significant advantages over the same reaction conducted in solution. While this is particularly true for unimolecular rearrangements, the pioneering work of Schmidt and co-workers in the 1960s was conducted on bimolecular reactions.[13] In all cases,

(a)

(b)
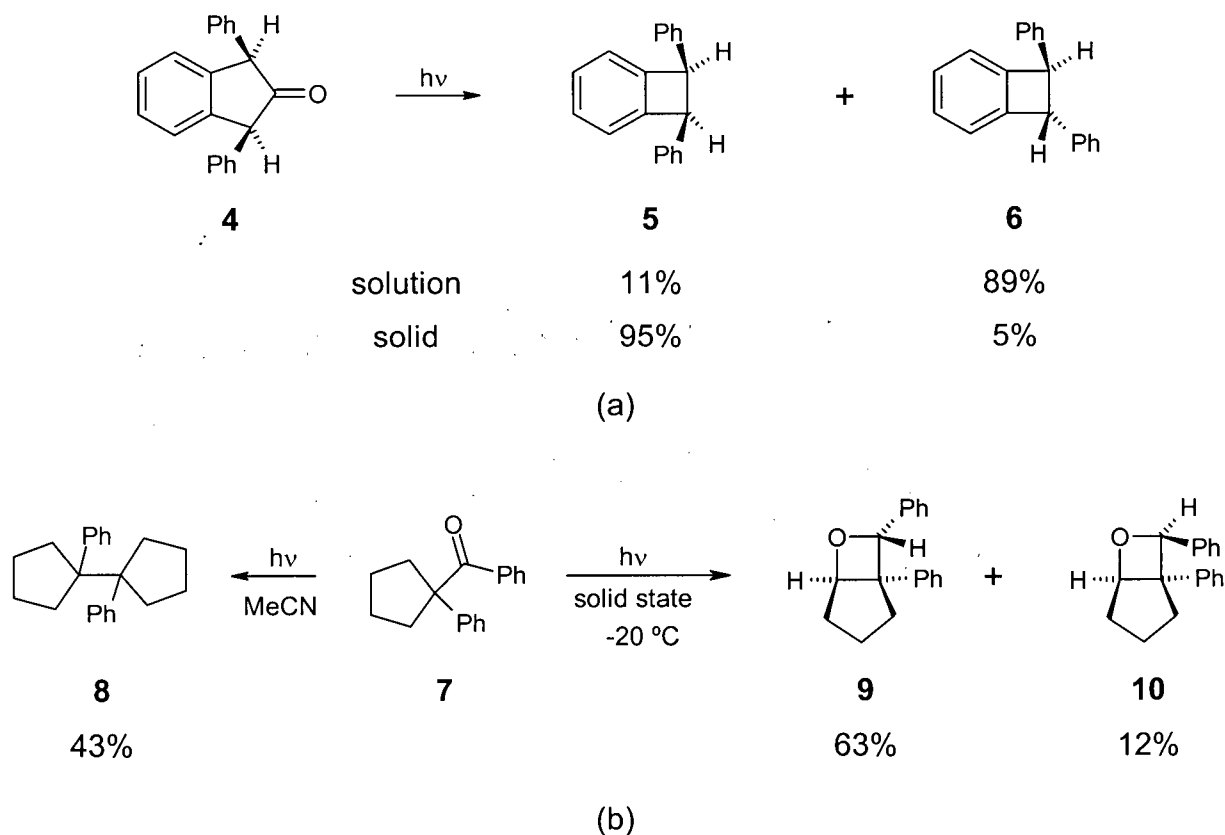
Figure 1.3 Examples of solid state reactions showing: (a) differences in selectivity between the solution and solid state, (b) latent reactivity.

the effect of the crystal lattice upon the reacting molecule can be truly remarkable in terms of altering product ratios, acting as a chiral source for enantioselectivity,[14] and, in some cases, even providing a pathway to the latent reactivity of a molecule where new products are observed.[15] Examples of reactions showing these benefits are shown in Figure 1.3 for reaction selectivity and latent reactivity; asymmetric induction in the solid state will be discussed in a following section. Figure 1.3a shows the Norrish type I cleavage reaction of diphenylindanone **4**, which forms primarily *cis*-diphenylcyclobutane **5** in the solid state but forms the more stable *trans*-isomer **6** in solution.[16] An example of latent reactivity is shown in Figure 1.3b, where ketone **7** undergoes a Norrish type I cleavage reaction in solution to give primarily dimer **8**.[15e] Ketone **7** also undergoes Norrish type I cleavage in the solid state, however, oxetanes **9** and **10** are formed as the major products because dissociation of the cleavage intermediates through the crystal

lattice is not possible. There are also potential benefits to be observed in areas of green, or environmentally friendly, chemistry by eliminating the use of solvents.[17]

As mentioned previously, both the first organic,[1] and organic photochemical,[2] reactions were conducted in the solid state in the early nineteenth century. While conducting reactions in solution soon became the norm, research still took place in the solid state, a notable example being the 1895 synthesis of indigo by Engler and Dorant (Figure 1.4).[18] This particular example is illustrative of a number of shortcomings of solid state chemistry at the time because there was no general understanding of how the transformation of 2'-nitrochalcone (11) to indigo (12) occurred, although it is now obvious that molecular conformation must play a large role in the success of the reaction. A proposed mechanism offered by Luwisch involves addition of two molecules of water, which would co-crystallize in the crystal lattice, and formation of benzoic acid as a byproduct.[14] Even with the limited understanding of how reactions occurred in the solid state several of these types of reactions were used commercially, such as the Kolbe-Schmitt synthesis of phenolic acids (gas-solid reaction),[19] used in the synthesis of salicylic acid.
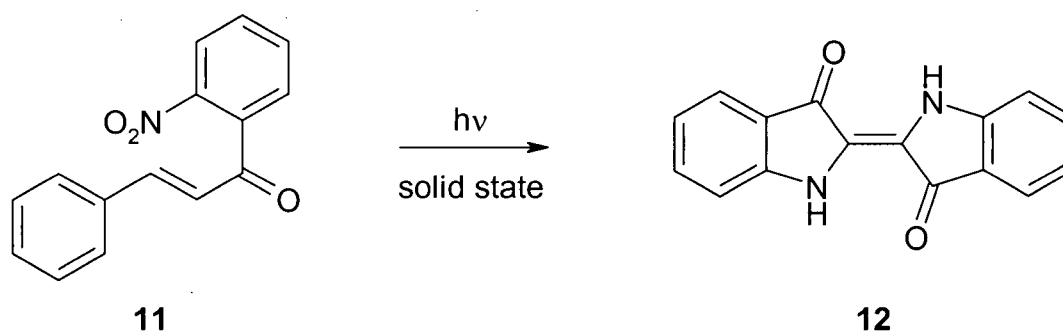
Figure 1.4 Solid-state synthesis of indigo (12) from 2'-nitrochalcone (11).

Kohlshutter, who proposed the topochemical postulate in 1918, brought forward the first insights into how reactions occur in the crystalline state.[20] In this postulate, the idea was advanced that the reaction of molecules in the crystalline state occurs with a minimum of atomic and molecular movements. As X-ray crystallographic techniques advanced, further research by Schmidt and co-workers in the 1960s on the intermolecular [2π + 2π] dimerization of *trans*-cinnamic acid derivatives **13** led to a much greater understanding of solid state reactivity.[13,21]
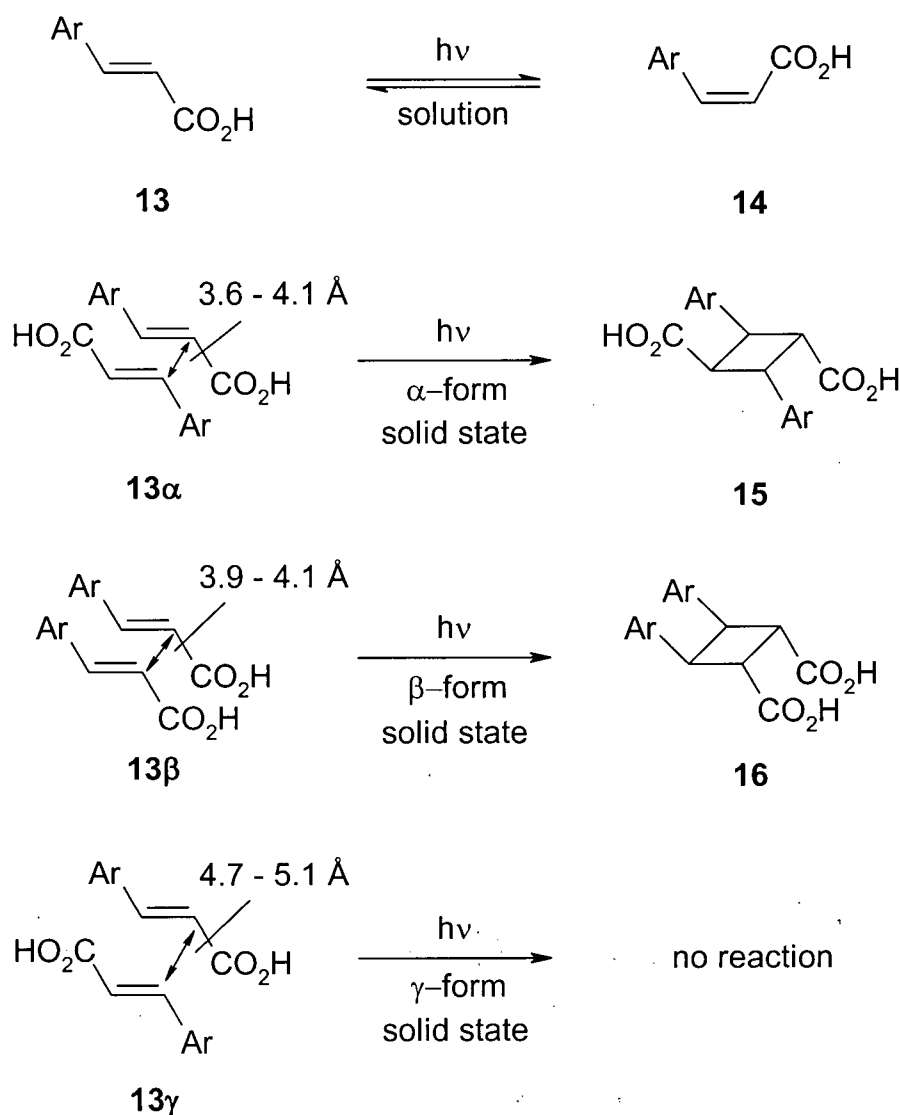
Figure 1.5 *trans*-Cinnamic acid photochemistry in solution and three crystal forms.

While this photochemistry had been studied previously by Libermann (1889),[22] de Jong (1922),[23] Stobbe (1922),[24] and also by Bernstein and Quimby (1943),[25] a consensus could not be reached on the details of the reaction. Investigation by the Schmidt group, shown in Figure 1.5, was finally able to explain the reactivity and, in the process, laid the groundwork for all future crystalline state studies. Although all *trans*-cinnamic acids **13** were found to undergo *trans-cis* isomerization to *cis*-cinnamic acids **14** in solution, photolysis in the solid state of different crystal forms gave rise to three different modes of reactivity. When crystals of the α-form cinnamic acids **13α** were irradiated, head-to-tail dimers, α-truxillic acids **15**, were obtained as

the sole product in a $[2\pi + 2\pi]$ cycloaddition. Crystals of the β-form cinnamic acids **13β** underwent a similar $[2\pi + 2\pi]$ cycloaddition but gave head-to-head dimers, β-truxillic acids **16**, while irradiation of the γ-form cinnamic acids **13γ** gave no observable photoproduct. Examination of the crystal structures of the three crystal forms of acid **13** revealed that it was the crystal packing of the molecules that gave rise to the differing reactivity. For the α-form cinnamic acids **13α**, the acid molecules were found to lie in a head-to-tail orientation with double bond-to-double bond distances of 3.6 - 4.1 Å. Similarly, the β-form cinnamic acids **13β** were aligned in a head-to-head orientation, with adjacent double bond distances of 3.9 - 4.1 Å. The unreactive γ-form cinnamic acids **13γ**, while orientated head-to-tail, had much longer adjacent double bond distances of 4.7 - 5.1 Å, a distance that was evidently enough to hinder cycloaddition. From the results obtained in this study, Schimdt was able to construct the following topochemical rules: 1) compounds sharing similar chemical structures may show significantly different behaviour in the solid state, 2) reaction in the solid state may differ from reaction of the same compound in solution; and 3) different crystal forms of a molecule may show different reactivity in the solid state.[13]

The understanding of reactivity in solids was further elaborated by Cohen, who introduced the concept of the *reaction cavity*.[26] This theory proposed that each individual molecule within a crystal is isolated within a cavity composed of the neighbouring molecules, and that the success of any reaction is subject to how well the product fits within the cavity. Figure 1.6 shows a molecule(s) (dashed line) lying within its reaction cavity (solid line) that can react in one of two ways, either through the allowed pathway, where the product fits within the original cavity, or the forbidden pathway, where the product is not able to fit within the cavity. One of the main consequences of the reaction cavity is that if a reaction can produce two or more possible products, the one(s) that are able to best fit within the cavity should be preferred upon reaction in the solid state. As well, the concept can be applied to other organized or confined media, such as zeolites and host-guest complexes, where a reacting molecule is isolated within a confined space.[27]
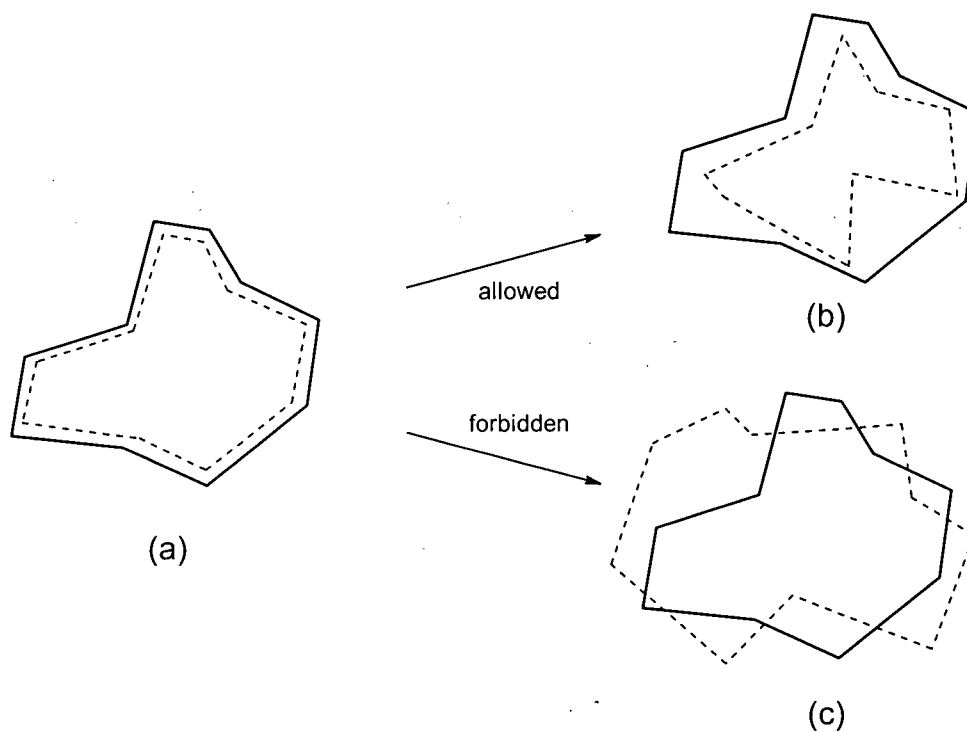
Figure 1.6 Graphical representation of the reaction cavity. (a) starting material (dashed line) fits within the surrounding reaction cavity (solid line); (b) allowed solid state reaction - product (dashed line) fits within the cavity; (c) forbidden reaction - product (dashed line) does not fit within the cavity.

The use of X-ray crystallography as a tool for gaining a deeper understanding of crystalline state chemistry by Schmidt was later expanded through the work of Thomas, who not only used the initial crystal structure of a molecule to explain its reactivity, but also followed this reactivity through a series of X-ray crystal structures, mapping the transition from starting material to product.[28] This relatively rare form of solid state reactivity has been termed *single crystal-to-single crystal reactivity* because the initial crystal lattice remains intact throughout the entire reaction.[29] The dimerization of 2-benzyl-5-benzylidenecyclopentanone (**17**, see Figure 1.7) and its derivatives are without doubt the most widely studied single crystal-to-single crystal reactions.[30] When following the reaction of cyclopentanone **17** by X-ray crystallography, through 11 crystal structures, a seamless transition to [$2\pi + 2\pi$] dimer **18** could be observed. A surprising finding in this study was that although topochemical lattice control is maintained throughout the reaction, changes in the unit cell parameters were observed; all of the unit cell

axes were altered during the course of the reaction (a, 0.06%; b, 0.28%; c, -0.69%). Even larger changes were observed for irradiation of a *para*-bromo derivative, where the axis changes were -3.77% for a, -5.61% for b, and 6.52% for c. Since both molecules crystallized in the orthorhombic space group Pbca, changes in the angles α, β, and γ could not be studied.

17   **18**
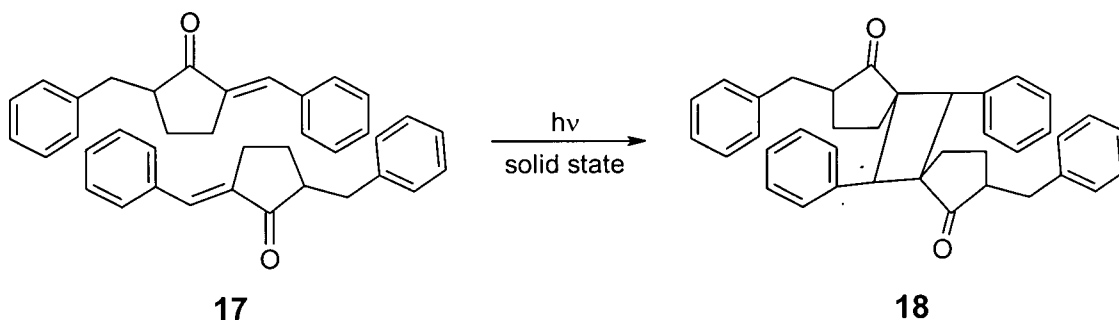
Figure 1.7 Single crystal-to-single crystal dimerization of cyclopentanone **17**.

1.3 Ketone Photochemistry

1.3.1 General Aspects of Photochemistry

A photochemical reaction occurs when a photon is absorbed by the chromophore of a molecule, producing an electronically excited state, which then undergoes a chemical transformation (or other competing decay process). Populating the excited states of a molecule has been found to allow transformations, both intra- and intermolecular, that would be impossible to achieve thermally. For example, consider a molecule, containing a suitable chromophore, in which irradiation with 320 nm light readily populates an excited state; thermally, a 1% population of the same excited state would require temperatures approaching 10,000 °C.[31] This would invariably lead to destruction of the molecule rather than the desired reaction. Figure 1.8 shows the energy level diagram for reactions involving reactant R^o. Paths (a) and (b) show thermal reactions into products **P1** and **P2** respectively, where it is seen that reaction to **P1** is exothermic but reaction to **P2** is highly endothermic. When the thermodynamics of pathway (b) are considered, it is not a realistic route to product **P2** since it would be thermally unstable due to the differences in activation energies required for the forward ($R^o \rightarrow$ **P2**) and reverse (**P2** $\rightarrow R^o$) reactions. An alternative pathway to product **P2** is

through (c) where the reactant, **R°**, is irradiated with light (hv), forming the excited state intermediate **R***, which then undergoes a thermodynamically favourable, exothermic reaction to **P2**.
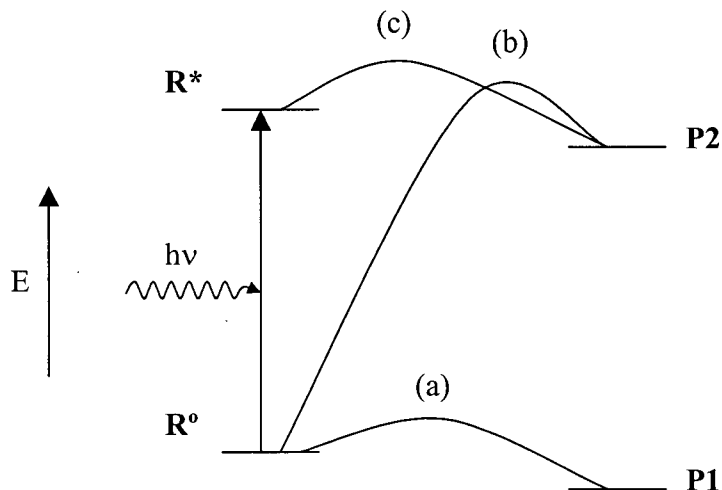
Figure 1.8 Energy level diagram for transformation of reactant **R°**: (a) thermal reaction into product **P1**; (b) thermal reaction into product **P2**; (c) photochemical reaction into product **P2** via photoexcited species **R***.

Upon excitation there are a number of radiative and non-radiative decay processes available as shown in Figure 1.9.[32] Absorbance of light energy by a molecule in its ground state (S_0) leads to electronic population of a singlet excited state (S_2 in Figure 1.9), which then undergoes rapid internal conversion (ic), a vibrational, non-radiative decay process, to the lowest energy excited state S_1. From S_1 there are four possible decay processes: (i) internal conversion back to the ground state S_0; (ii) fluorescence, a radiative decay process that will emit a photon of light and return the molecule back to ground state S_0; (iii) chemical reaction, producing a photoproduct; or (iv) intersystem crossing (isc), a non-radiative process in which the electron residing in excited state S_1 undergoes spin inversion through spin-orbit coupling (soc), placing the molecule in a triplet excited state (T_1). From the triplet excited state (T_1) there are three possible decay processes: (i) intersystem crossing to ground state S_0; (ii) phosphorescence, a radiative decay process that produces a photon and returns the molecule to S_0; and (iii) chemical reaction to produce a photoproduct.
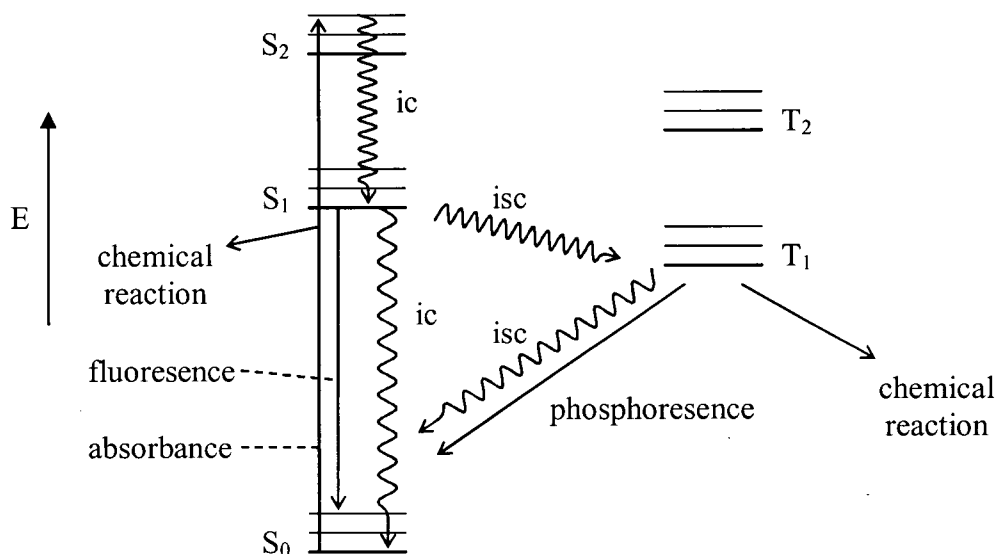
Figure 1.9 Jablonski diagram illustrating radiative and nonradiative processes.

Illustrated in Figure 1.10a are spin diagrams and orbitals for excitation of a ketone, the chromophore present in the molecules that were investigated for the present work. In the ground state configuration of a ketone (Figure 1.10i and iv), 2 electrons are present in the C-O σ-bond, 2 in the C-O π-bond and 4 in the two non-bonding n-orbitals. Excitation by light will cause promotion of one electron in an n-orbital into the π* anti-bonding orbital (Figure 1.10ii and v) with retention of spin. This type of excitation, producing a singlet excited state, is denoted $^1(n,\pi^*)$ and is symmetry allowed but spatially forbidden since the n and π* orbitals are orthogonal. From the singlet excited state, spin inversion or intersystem crossing (isc) may occur through spin-orbit coupling, producing a triplet excited state, denoted $^3(n,\pi^*)$, where the electrons in the singly occupied n-orbital and π* orbital have the same spin (Figure 1.10iii and vi). Chemical reactions may take place from either the singlet or triplet excited state.

(a)

(b)
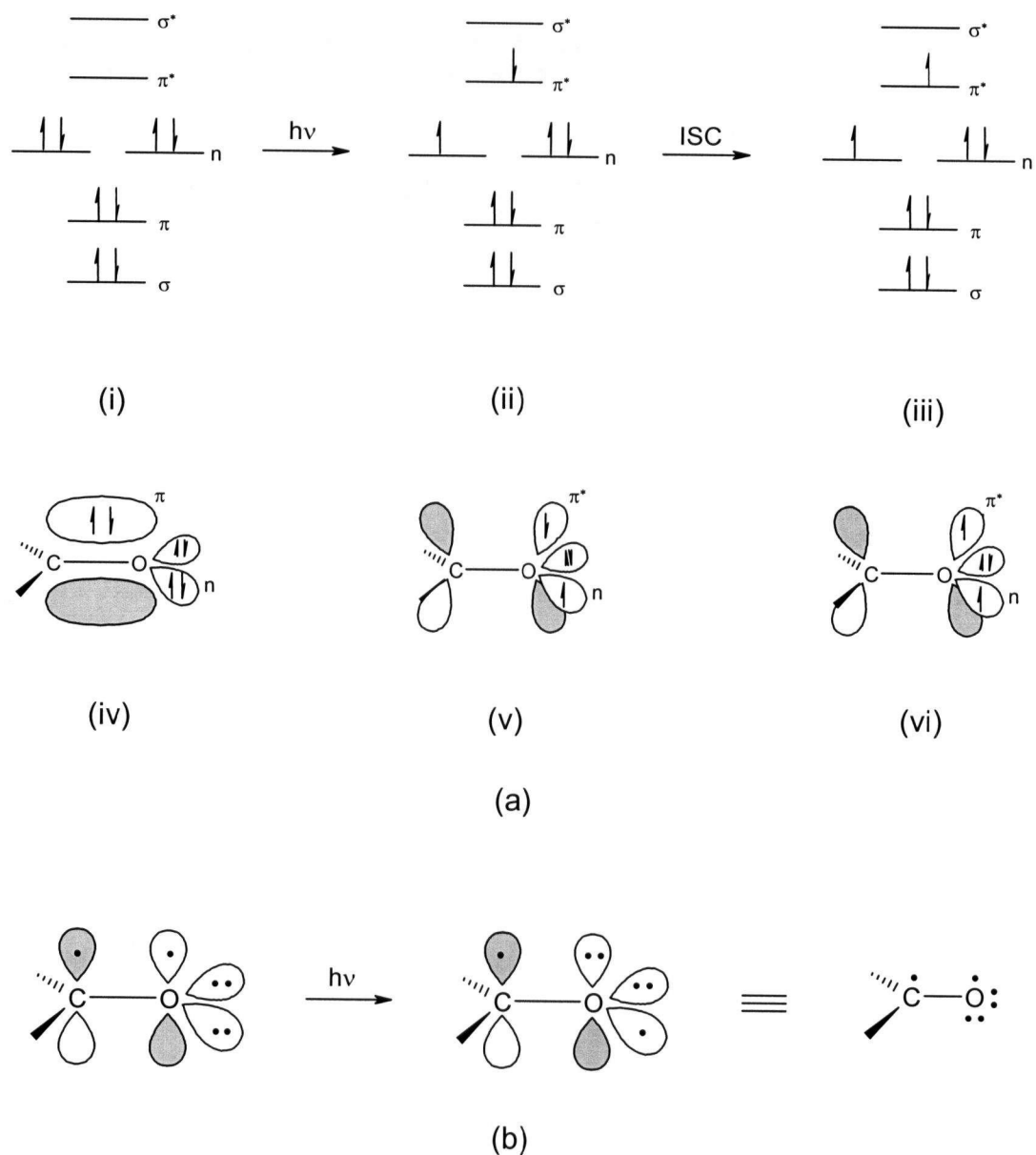
Figure 1.10 (a) The spin diagrams and orbital depictions of a ketone (lone pair orbitals on oxygen are shown as being sp^2 hybridized). (i), (iv) ground state; (ii), (v) singlet excited state; (iii), (vi) triplet excited state. (b) Depiction of the electron distribution in excited state ketones giving rise to alkoxy radical-like behaviour.

1.3.2 The Norrish/Yang Photochemistry of Ketones

Perhaps the most widely studied of the photochemical reactions is the Norrish/Yang transformation of ketones,[33] involving abstraction of a γ-hydrogen atom by the (n,π*) excited state ketone to give either a Norrish type II cleavage product,[34] or a Yang cyclization product,[35] as illustrated in Figure 1.11 for ketone **19**. Upon absorption of a photon of light by the chromophore of ketone **19**, the molecule enters an (n,π*) excited state (singlet or triplet) and may then undergo a reversible γ-hydrogen (1,5 hydrogen) abstraction to produce 1,4-hydroxybiradical **20**. Biradical **20** may then undergo one of three processes: (1) reverse hydrogen abstraction to reform ketone **19**, (2) Norrish type II cleavage, or (3) Yang cyclization.
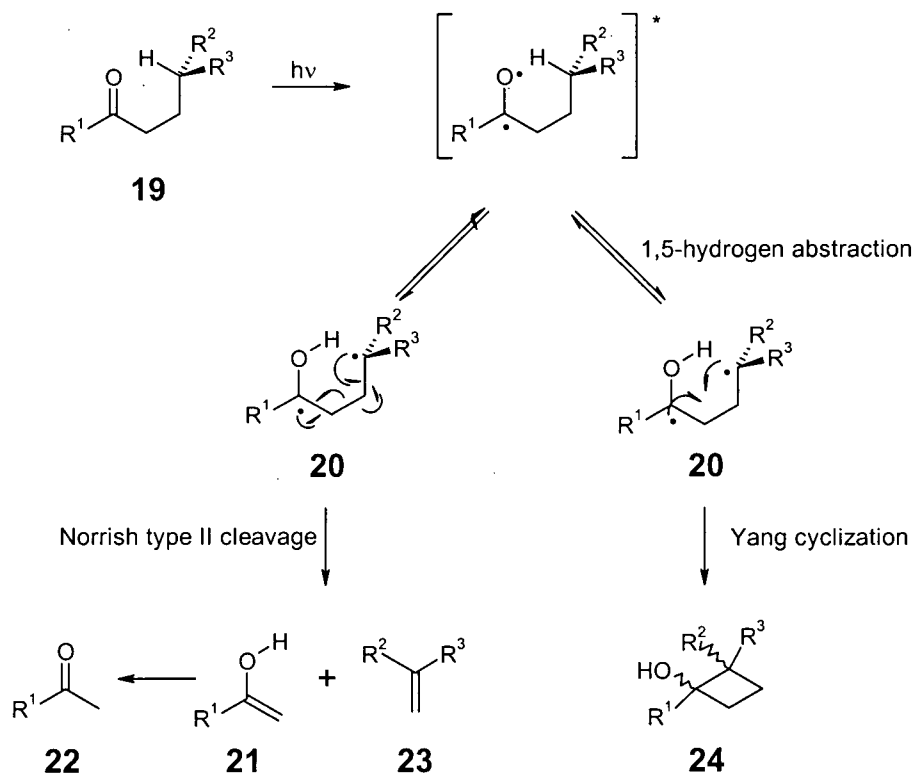
Figure 1.11 Norrish/Yang photochemistry of ketones.

In the Norrish type II cleavage reaction biradical **20** undergoes a fragmentation, giving enol **21**, which tautomerizes to ketone **22**, and alkene **23**. For the Yang cyclization reaction, biradical **20**

undergoes ring closure to form cyclobutanol **24**. Since biradical **20** is an intermediate with a lifetime greater than that required for bond rotation, there are stereochemical consequences for the products. Cyclobutanol **24** may be formed as one of two different stereoisomers. However, if there is further substitution on the α or β carbons then there would be 4 isomers possible through bond rotation in the biradical. Similarly, β substitution would lead to an alkene that could be formed as either *cis* or *trans*. For these reasons it is desirable to be able to control Norrish/Yang photochemistry in terms of both reactivity (cyclization vs. cleavage) and stereochemistry.

For the hydrogen abstraction process, the excited state carbonyl group may be thought of as being similar to an alkoxy radical, with one electron of the double bond centred on the carbon atom and the second on the oxygen (see Figure 1.10b).[36] Reactivity may occur from either the singlet or triplet excited state of the molecule, however, phenyl ketones have been found to react exclusively from the triplet excited state.[37] Generally, reaction from the triplet state has been found to be more efficient than from the singlet,[33b] but is much less stereospecific.[38] Following excitation, the γ-hydrogen is preferentially abstracted through a six-membered transition state although in the absence of an abstractable γ-hydrogen, δ-hydrogen abstraction (1,6-hydrogen abstraction) may occur through a seven-membered transition state,[39] and in some cases where a γ-hydrogen is present, may be a competitive process.[40] Less common, though still possible, are β-hydrogen abstraction (1,4-hydrogen abstraction) through a five-membered transition state,[41] and ε-hydrogen abstraction (1,7-hydrogen abstraction) through an eight-membered transition state.[42]

Unlike other photochemical reactions,[43] there are few reported uses of Norrish/Yang photochemistry in natural product syntheses. One example, however, is Paquette's synthesis of Punctatin A (**25**), where the Yang cyclization of ketone **26** into cyclobutanol **27** is a key step in the synthetic pathway as shown in Figure 1.12.[44] While there are no problems associated with isomerization through bond rotation for this example, there is a lower than desired chemical selectivity between the cyclization (cyclobutanol **27**) and cleavage (ketone **28**) reactions (~2:1 favouring cyclization) and a low chemical yield. When considering that this photochemical step occurs near the end of a 16-step synthesis, ways in which the selectivity of the reaction can be enhanced become crucial before wider use of photochemical reactions in synthesis can be realized.
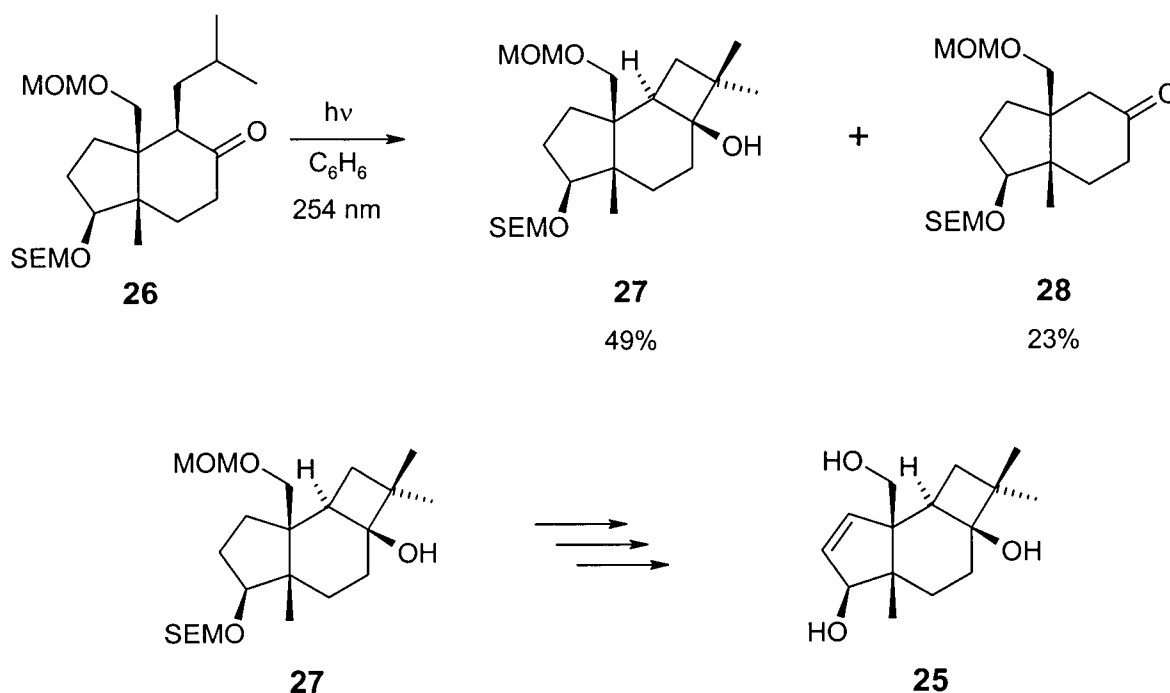
Figure 1.12 Yang cyclization as the photochemical key step in the synthesis of Punctatin A (**25**).

1.3.3 Geometric Requirements for Norrish/Yang Photochemistry

The use of X-ray crystallography is an invaluable tool in the study of solid state reactions as it makes possible the development of crystal structure-solid state reactivity relationships. These relationships provide a correlation between the crystallographically determined structure of a molecule and its observed reactivity in the solid state. From such relationships it is possible to gain a greater understanding of how the geometry of the molecule affects the partitioning between cyclization, cleavage and reverse hydrogen transfer reactions in Norrish/Yang chemistry. While this method has proven valid, there are some differences between the ground state structure obtained in a crystal structure and the excited state structure of the same molecule that must be considered. These changes mainly involve the differences in excited state geometries (the carbonyl carbon may pyramidalize slightly) and bond lengths (n,π* excitation lengthens the carbonyl bond by ~0.1 Å)[45] upon excitation. As well, the use of X-ray crystallography itself is known to have some inaccuracies associated with hydrogen atoms.[46]

The pyramidalization of the excited state carbonyl group is not a major concern for the present work as it deals with phenyl ketones, which are believed to maintain a planar geometry in the excited state.[47] For dialkyl ketones, however, a significant amount of pyramidalization (22-45°) may be expected based on theoretical calculations,[48] although the amount of reorientation possible in the solid state should be less than in solution based on least-motion principles. This is in agreement with the excited state structure of formaldehyde, which is known to be significantly pyramidalized upon excitation.[49] Despite the minor differences in ground and excited state geometries, crystal structure-reactivity correlations have been shown to provide information in full agreement with the observed chemical reactivity, legitimizing their use as a predictive tool in solid state chemistry.

1.3.3.1 Hydrogen Abstraction Parameters

Norrish type II hydrogen abstraction reactions have been widely studied in the solid state for numerous systems by Scheffer and co-workers. By comparing the observed results to data extracted from the crystal structures of the starting materials, it has been possible to postulate an idealized system of parameters necessary for the abstraction process to occur.[50] As shown in Figure 1.13 there are 4 main parameters, one distance and three angles, associated with the γ-hydrogen abstraction reaction: d, θ, Δ, and ω. The symbol d, represents the distance between the carbonyl oxygen and the γ-hydrogen to be abstracted. Ideally these atoms should lie within 2.72 Å of each other, the sum of their van der Waals radii.[51] The first angle of interest, θ, represents the O$\cdots$H$_\gamma$-C$_\gamma$ angle and should be 180°, allowing for maximum overlap between the oxygen atom and the C-H σ-bond.[52] Complementing θ is Δ, denoting the C=O$\cdots$H$_\gamma$ angle, with an optimal value in the 90° to 120° range depending on the model of hybridization used for the n-orbital on oxygen. If the Kasha model for the carbonyl group is used then the ideal value of Δ will be 90°, corresponding to the angle between the unhybridized 2p orbital and the carbonyl oxygen,[53] but if the "rabbit ear" model is used the two hybridized sp^2 orbitals will have a 120° angle to the carbonyl group axis. The final angle of interest in describing the hydrogen abstraction process is given the symbol ω and represents the 'out-of-plane' angle between the γ-hydrogen and the carbonyl group, where orbital overlap will be maximized at 0°.

16
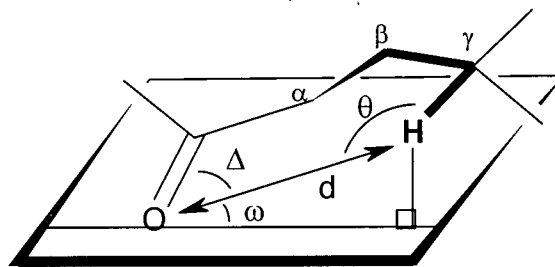
Figure 1.13 Parameters for γ-hydrogen abstraction.

While these values represent the ideal values for the parameters based on the structure and geometry of the interacting orbitals, in reality large variations are routinely observed. There are a number of reasons for this but the biggest factor involved is likely that the angles are chosen for maximum overlap, with a best-case scenario based on a line through the centre of the orbital, and does not take into consideration the actual shape of the orbital. Therefore, parameters may lie outside the ideal values but still lead to reaction as long as there is sufficient orbital overlap. Deviations are most commonly observed in the parameters θ and ω and are likely due to the fact that it is often not geometrically possible to have the orbitals aligned in the optimal position. Values for θ are rarely above 125° or lower than 100°, and values for ω are most often observed in the range of 17 to 63°, although higher values have been observed.

1.3.3.2 Cyclization versus Cleavage

Following the formation of the biradical intermediate in the hydrogen abstraction process there are three possible reactions that may occur: reverse abstraction, reforming the starting material; Norrish type II cleavage, forming an alkene and enol; or cyclization, forming a cyclobutanol. As in the case of abstraction, a set of parameters has been developed for rationalizing the occurrence of these reactions based on crystal structure-reactivity relationships. Once again, the possibility of the cleavage or cyclization process occurring relies on orbital overlap, with the quantum yield-lowering reverse abstraction taking place as the predominant reaction pathway when neither is favoured.
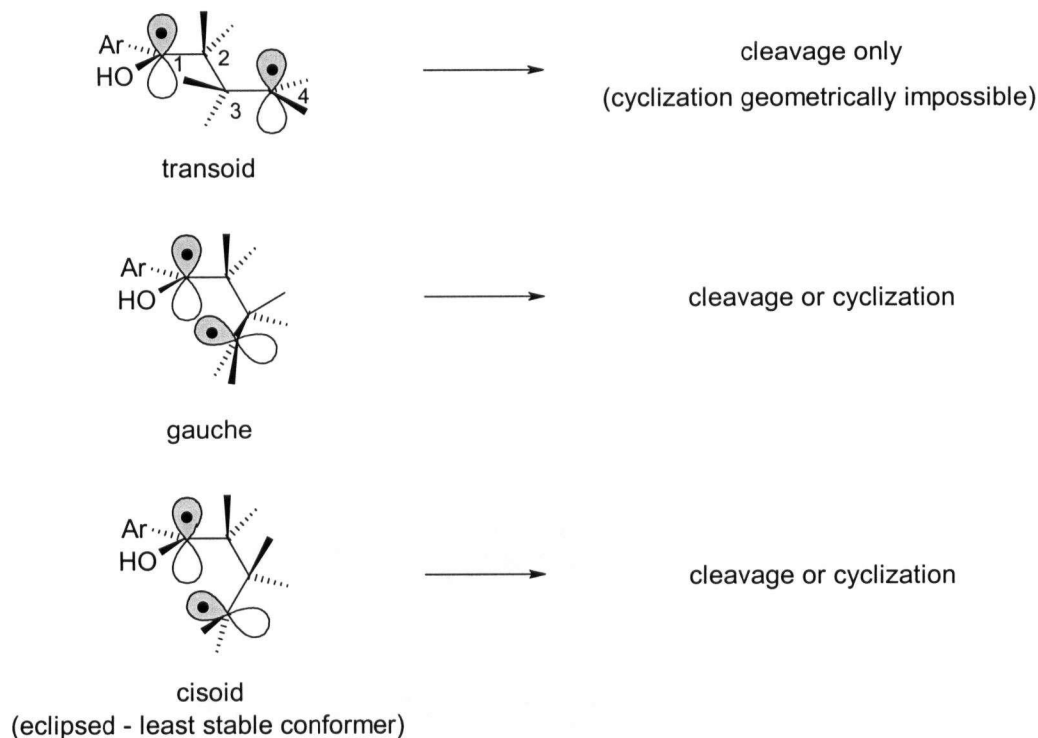
Figure 1.14 1,4-Biradical conformations and their reaction products.

Figure 1.14 shows how different conformations of the hydroxybiradical intermediate encountered in Norrish/Yang photochemistry can affect the product distribution.[54] For the transoid biradical, in which the C_1-C_2 and C_3-C_4 σ-bonds are anti-periplanar, only a cleavage product is possible since cyclization is geometrically impossible. In the transoid conformation, cleavage will occur when there is maximum overlap between the p-orbitals on C_1 and C_4, and the C_2-C_3 σ-bond (*i.e.* the p-orbitals are parallel to the σ-bond).[54,55] Rotation around the C_2-C_3 σ-bond produces a gauche conformation for the biradical in which C_4 lies above the plane of the other carbon atoms. This allows for the cyclization reaction to become a competitive reaction and either process may be observed. Further rotation around the C_2-C_3 σ-bond forms a cisoid biradical in which the C_1-C_2 and C_3-C_4 σ-bonds are eclipsed, making it the least stable conformer. For both the cisoid and gauche conformations cleavage would be the expected process when there is good overlap between the p-orbitals and the C_2-C_3 bond, while cyclization would be preferred when the p-orbitals on C_1 and C_4 are directed towards each other, allowing for ring closure to occur.

In terms of developing structure-reactivity relationships, the favourability of the cleavage reaction is gauged through the dihedral angles φ_1 and φ_4 (see Figure 1.15).[56] The dihedral angle φ_1 represents the overlap between the p-orbital on C_1, the carbonyl carbon, with the C_2-C_3 σ-bond that would be fragmented in a cleavage reaction. Dihedral angle φ_4 represents the overlap between the p-orbital on C_4 with the same C_2-C_3 bond. For both cases an optimum value of 0° indicates maximum overlap and the ideal geometry for cleavage. These angles may be obtained from the ketone crystal structure with the following assumptions: (1) that the C_4 carbon becomes sp^2 hybridized and that the C_1 carbon maintains planarity following hydrogen abstraction, and (2) that there are no conformational changes in the molecule immediately after hydrogen abstraction.
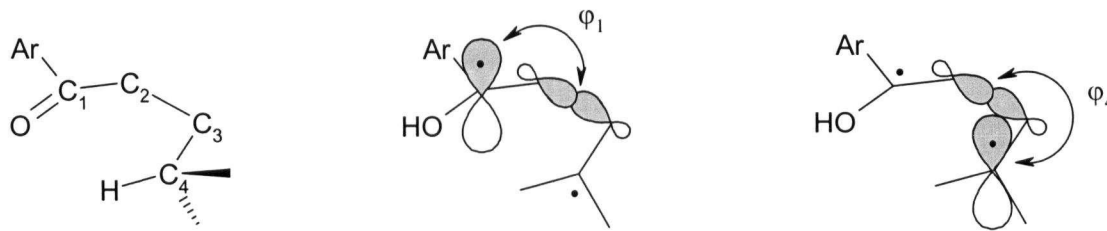
Figure 1.15 Illustration and numbering of the cleavage parameters φ_1 and φ_4.

Cyclization is dependent on two factors, the distance between the radical centres and the alignment of the p-orbitals. The symbol D (Figure 1.16a) is defined as the distance between the two reacting centres, C_1 and C_4, and should be less than 3.4 Å, the sum of the van der Waals radii for two carbon atoms.[51] The second parameter of interest is β (Figure 1.16b),[57] the dihedral angle formed between the p-orbital on C_1 and the C_2-C_4 vector. In the ideal situation this will be 0°, meaning that the p-orbital is pointed directly towards the p-orbital on the C_4 carbon, allowing for closure of the cyclobutane ring. At the further extreme, if β is equal to 90° then the p-orbital of the C_1 carbon will be orthogonal to the p-orbital on the C_4 carbon and ring closure will be disfavoured.

(a)   (b)
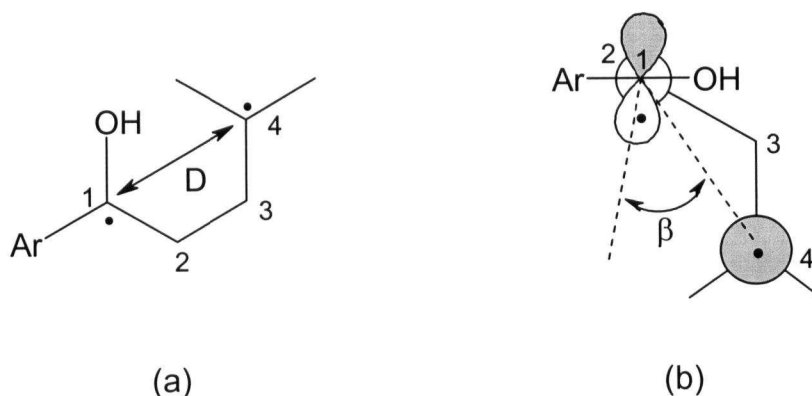
Figure 1.16 Illustration of (a) distance D and (b) cyclization angle β.

1.4 Asymmetric Photochemistry

Photochemical methods have been used in a variety of natural product syntheses so there has been a growing focus in developing methods for carrying out the corresponding reactions enantioselectively.[58] However, unlike the wealth of successes for asymmetric reactions in the ground state, general, reliable methods for carrying out photochemical reactions in an asymmetric manner have not been as forthcoming. The difficulties involved in the study of asymmetric photochemistry have made it a challenging area of research since the latter half of the nineteenth century, when Le Bel and van't Hoff first proposed using circularly polarized light to obtain an enantiomerically enriched solution though selective photodestruction of a racemate in solution using circularly polarized light.[59] These ideas were first realized in 1929 by Kuhn who performed the first asymmetric photoreaction.[60] Since that time there have been many advances in asymmetric photochemistry in solution using a variety of methods ranging from circularly polarized light to chiral solvents, optically active photosensitizers, and chiral auxiliaries.[58] Perhaps the most promising results have been seen in solid state photochemistry, where the crystal lattice is used to impart chiral information through crystal chirality, pre-association of host-guest complexes, and chiral auxiliaries.[61]

1.4.1 Solid-State Asymmetric Induction

When an achiral compound crystallizes, it may do so in any of the 230 crystallographic space groups, chiral or achiral. Optically pure, chiral molecules, on the other hand, must crystallize in one of the 65 chiral space groups, which do not possess a mirror plane or inversion centre. Therefore, for any enantioselectivity to be observed, the reaction of a prochiral molecule must occur within a crystal that occupies a chiral space group. The spontaneous crystallization of an achiral molecule in a chiral space group occurs when the molecule adopts a chiral packing arrangement. This is most easily visualized by considering the case of a brick (achiral), which can be used to construct either a right or left-handed spiral staircase (chiral) as shown in Figure 1.17.
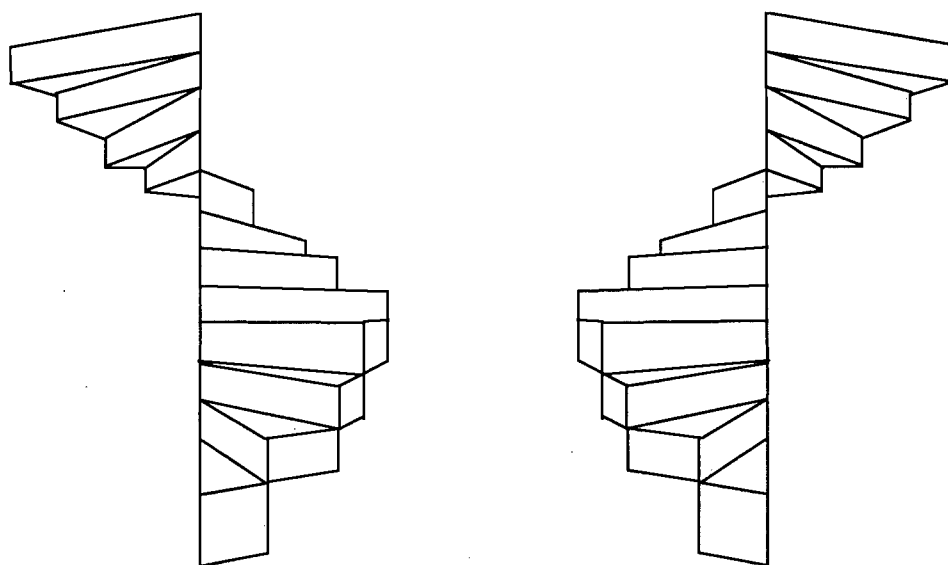
Figure 1.17 Chiral right and left-handed spiral staircases constructed from an achiral object (brick).

The first reaction of an achiral molecule in a chiral space group was conducted by Schmidt and co-workers, who demonstrated that enantiomorphously pure single crystals of achiral chalcone **29**, which spontaneously crystallizes in the chiral space group $P2_12_12_1$, could be converted into chiral dibromide **30** upon exposure to bromine vapour (see Figure 1.18).[62]

Although the enantiomeric excess (ee) obtained was low at 6%, this example showed that chirality could successfully be transferred from a chiral crystal lattice to an achiral molecule.

Space group: P2$_1$2$_1$2$_1$

29   **30**
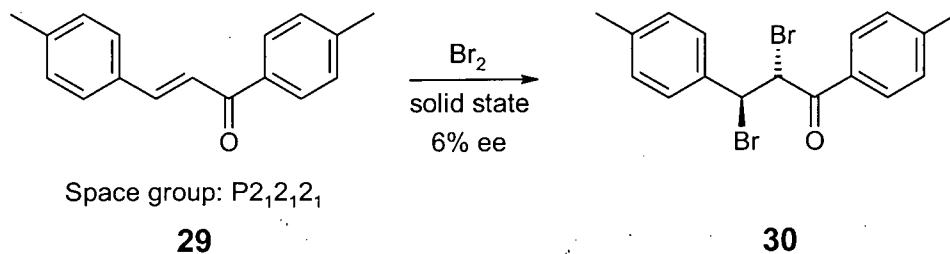
Figure 1.18 Absolute asymmetric synthesis of dibromide **30** from achiral chalcone **29**, which crystallizes in the chiral space group P2$_1$2$_1$2$_1$.

Absolute asymmetric synthesis (asymmetric reactions with no externally imposed source of chirality) was also found to be possible for photochemical reactions in cases where prochiral photoreactive molecules spontaneously crystallize in chiral space groups. This was first demonstrated by Schmidt for the [2π + 2π] cycloaddition of dilute solid solutions containing two similar aromatic dienes that co-crystallize in the chiral space group P2$_1$2$_1$2$_1$ and gave up to 70% ee.[63] Since the first photochemical asymmetric synthesis in the solid state there have been numerous other examples for a variety of different inter- and intramolecular reactions,[61] one example of which is shown in Figure 1.19. The conversion of achiral dibenzobarrelene **31** is chosen because its photochemistry was studied in both chiral and achiral crystals, and for its historical connection with the ionic chiral auxiliary concept presented in the next section. In a study by Scheffer and co-workers (Figure 1.19),[64] it was found that dibenzobarrelene **31** crystallized in two polymorphic forms, one chiral (P2$_1$2$_1$2$_1$) and one achiral (Pbca). Upon irradiation to 25% conversion of a single crystal of **31** having the chiral space group P2$_1$2$_1$2$_1$, a 95% enantiomeric excess of photoproduct **32** was achieved. When a crystal of dibenzobarrelene **31** with the achiral space group Pbca was irradiated, photoproduct **32** was obtained as a racemic mixture.

Based on the multitude of examples available, it is clear that irradiation of chiral crystals is one of the most reliable ways in which to routinely achieve a highly enantioselective
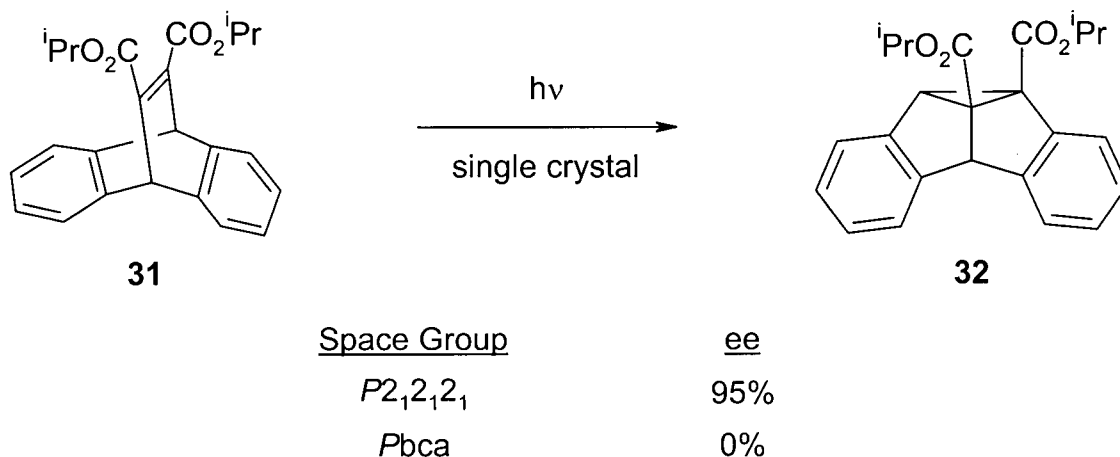
Figure 1.19 Absolute asymmetric synthesis for a photochemical reaction.

photoreaction. However, there are some major drawbacks to this method: 1) spontaneous crystallization in a chiral space group is a random and unpredictable process,[65] 2) irradiation of polycrystalline samples will lead to lowered ees unless the recrystallization solution is seeded with an enantiomorphously pure single crystal to ensure chiral homogeneity, and 3) only solid samples may be studied. The problems associated with the random crystallization of achiral molecules in chiral space groups are easily overcome by introducing an element of chirality into the molecule in the form of a chiral auxiliary. By attaching a chiral auxiliary to the achiral molecule, crystallization in a chiral space group is ensured, allowing for the possibility of enantioselectivity in the reaction, following which the auxiliary is removed.

1.4.2 The Ionic Chiral Auxiliary Concept

The ionic chiral auxiliary concept, developed by Scheffer and co-workers, has proven to be a reliable method of asymmetric photochemistry for a wide range of different reactions.[66] In this method an optically pure amine is ionically bonded to an achiral carboxylic acid (or an optically pure acid is bound to an achiral amine) as shown in Figure 1.20. Using optically pure amines to obtain enantioenriched materials is not new, being the basis of the racemate resolution procedure discovered by Pasteur in the nineteenth century.[67] However, Scheffer's method does overcome one major limitation of the Pasteur technique by maximizing the potential chemical yield of optically pure enantiomer. From a racemic mixture the maximum possible yield of an

optically pure enantiomer is 50%, whereas the *in situ* resolution procedure of Scheffer has a maximum possible yield of 100% optically pure enantiomer.

Ionic Chiral Auxiliary Concept

Pasteur Resolution Technique
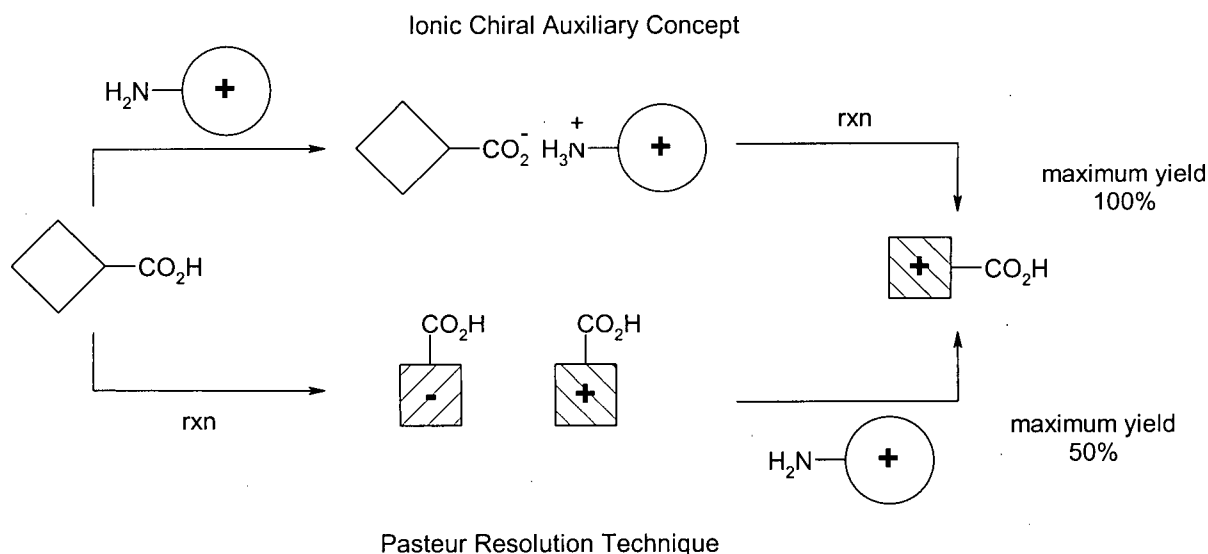
Figure 1.20 Comparison of the ionic chiral auxiliary approach to asymmetric induction and the Pasteur resolution method.

The ionic chiral auxiliary approach to asymmetric induction was first demonstrated by Gudmunsdottir and Scheffer during asymmetric induction studies on dibenzobarrelenes (see Figure 1.21),[68] previous research having shown that the diisopropyl ester derivative underwent absolute asymmetric induction.[64] Rather than having to rely on the unpredictable crystallization of an achiral molecule in a chiral space group, it was decided to make use of a chiral auxiliary that could be easily removed following the reaction. Salt **33**, formed between an achiral acid and optically pure amine, was photolysed in the solid state and found, following diazomethane workup, to give diester **34** with an enantiomeric excess of 80%. Formation of an ammonium carboxylate salt linkage rather than the more traditional application of covalently bound amines (amides) and alcohols (esters) was chosen in an attempt to give higher melting crystals, thus eliminating the problems associated with crystal melting in solid state reactions.
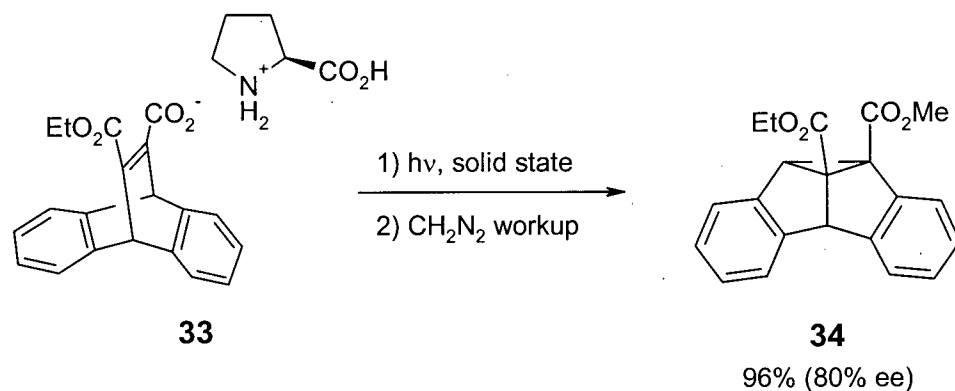
Figure 1.21 Application of the ionic chiral auxiliary concept in the photolysis of dibenzobarrelenes.

The energy level diagrams shown in Figure 1.22 illustrate the differences in conducting the photolyses in solution and the crystalline state. When a photolytic reaction is conducted in solution (Figure 1.22a), there is little energy difference between the two diastereomeric transition states leading to the (+) and (-) forms of the photoproduct due to the nature of the auxiliary used. When dissolved, the chiral auxiliary will be loosely bound to, and in most cases far removed from, the reacting site of the prochiral substrate, and therefore be unable to influence the rapid equilibrium between conformers leading to the diastereomeric transition states. However, when the same reaction is conducted in the solid state (Figure 1.22b), both the chiral auxiliary and prochiral substrate are confined within the crystal lattice and a substantial energy barrier may be present between the diastereomeric transition states, leading to an observed chiral discrimination. Depending on the nature of the photolabile molecule there are two possible reasons for the increased energy difference. If an achiral molecule preferentially crystallizes in a homochiral conformation then the resulting energy difference would be due to the increased rotational energy required to interchange between the two chiral conformations. Due to the confines imposed by neighbouring molecules in the crystal lattice this will be a "forbidden" or unfavoured process in the solid state based on the topochemical principles. In this case the diastereomeric discriminating step occurs during the crystallization process, before the photochemical reaction. If a molecule is unable to adopt an enantiomeric conformation then the resulting energy barrier would be due to the differences in energy between the two
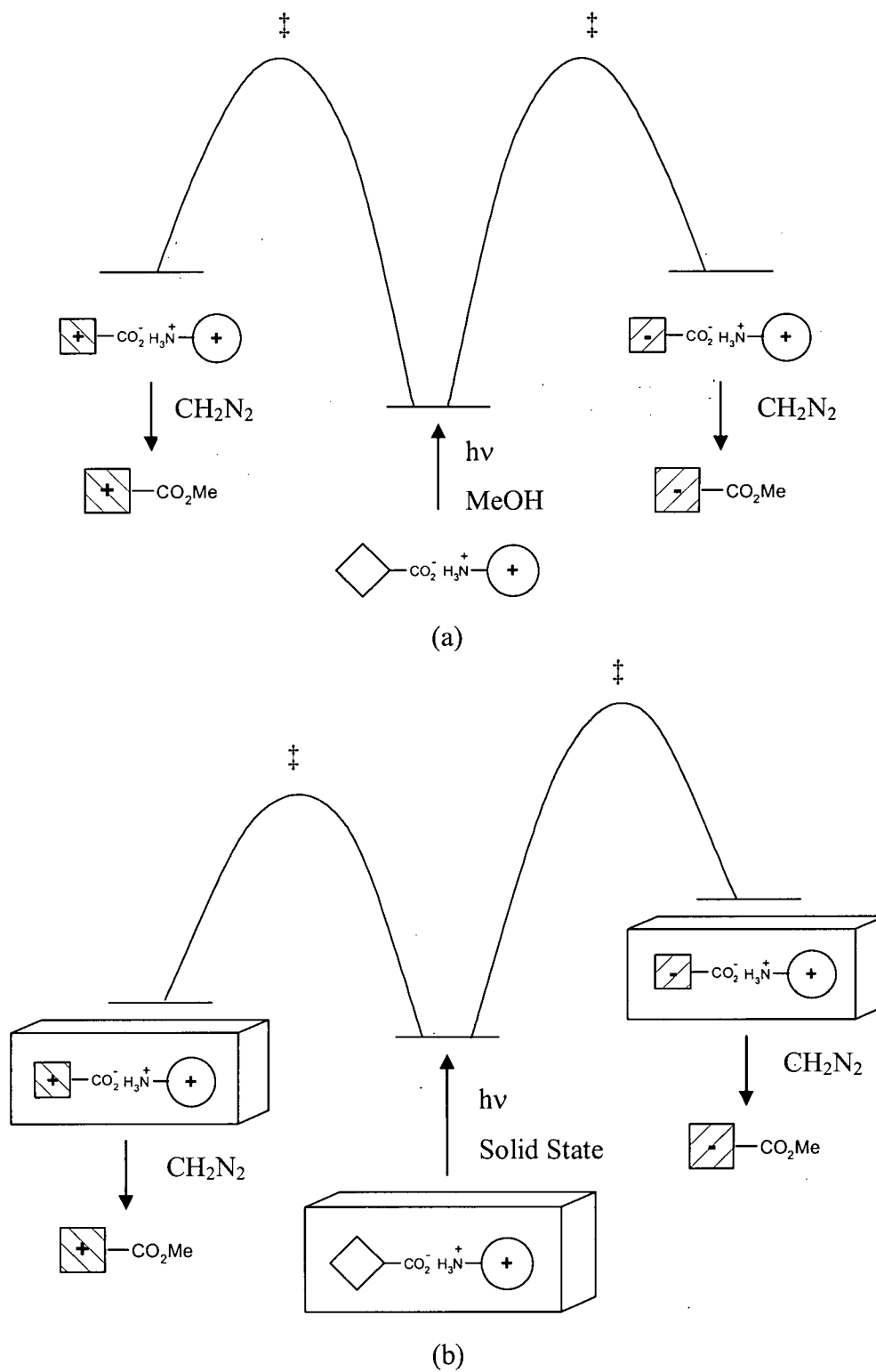
Figure 1.22 Energy level diagrams for photolysis of ammonium carboxylate salts in (a) solution, (b) solid state.

diastereomeric transition states formed upon photolysis in the crystal lattice. Once again, due to the topochemical considerations, if one diastereomeric transition state has a better fit within the confines of the chiral reaction cavity then it will have a lower energy relative to the unfavoured transition state. In this case the diastereomeric discriminating step occurs during the photochemical reaction.

There are a number of features that make this particular method attractive in terms of general applicability: 1) it makes use of a large pool of commercially available, inexpensive, optically pure amines and acids; 2) either optical isomer may be produced in a reaction by switching the chirality of the auxiliary; 3) the auxiliary is easily attached and removed through acid-base chemistry; 4) ionic solids are generally high melting, giving robust crystals (essential for studying reactions in the solid state); 5) the technique is easily scalable, without loss of enantioselectivity, by running the reaction as a suspension of the crystalline solid in hexanes,[69] making this approach synthetically practical.

1.5 Research Objectives

The work presented in this thesis was conducted with two goals in mind: to further study the ability of the ionic chiral auxiliary approach to induce enantioselectivity in solid state photochemical reactions, and to study the photochemistry in both solution and the solid state of 7-benzoylbicyclo[2.2.1]heptane derivatives. These objectives have been encompassed in two series of related systems involving Norrish/Yang photochemistry from within the symmetrical, conformationally locked, five-membered rings of norbornane in the 7-benzoylnorbornene derivatives **35** and 7-benzoyl-7-methylnorbornane derivatives **36** shown in Figure 1.23.

The benzoylnorbornane system was selected as a target for continued studies on the Yang cyclization reaction to complement previous work on phenyladamantanyl and phenyl(tert-butylcyclohexyl)ketones within our research group.[70] In both of these systems hydrogen abstraction occurred from a six-membered ring, while in the norbornyl system hydrogen abstraction occurs from a five-membered ring, allowing for the effects of ring geometry on the abstraction process and product distribution to be examined. Although photochemical studies have been undertaken for 2-benzoylnorbornanes,[71] there have not been any prior reports published on the photochemistry of 7-benzoylnorbornanes.
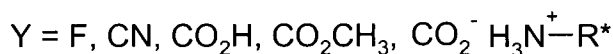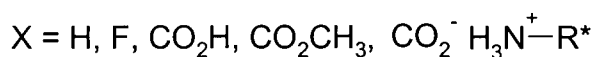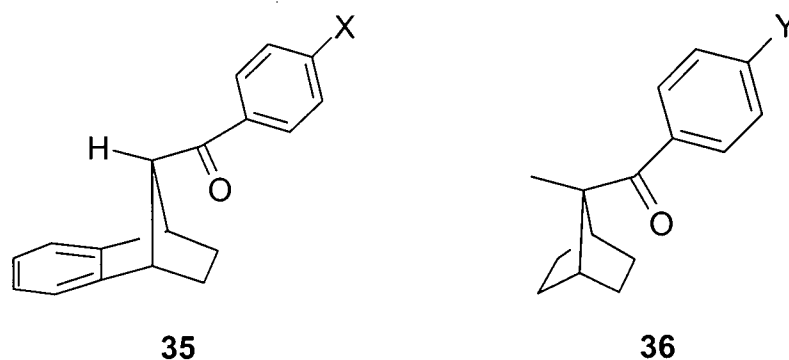
Figure 1.23 7-Benzoylnorbornane derivatives selected for photochemical study.

Initial work proceeded on a series of benzonorbornene derivatives (**35**), a system chosen in hopes that the presence of the benzo substituent would aid in enhancing the formation of robust, high-melting crystals that are essential for solid state studies. Due to solubility problems encountered with some benzonorbornene derivatives, and difficulties in attaching an α-methyl substituent on the bridge carbon with the desired stereochemistry, further studies were undertaken on 7-methyl-7-benzoylnorbornane derivatives (**36**). By studying both types of norbornane derivative (with or without an α-methyl substituent) it would be possible to gain a greater understanding of the effects that carbonyl group geometry plays in the partitioning of the cyclization, cleavage and reverse hydrogen abstraction reactions in Norrish/Yang photochemistry.

The norbornane skeleton, with a 7-benzoyl and/or 7-methyl substituent(s), was specifically chosen because it is an achiral molecule that forms a chiral molecule upon irradiation, through abstraction of one of the two enantiotopic γ-hydrogens, allowing for the enantioselectivity of the photochemical reaction to be studied. Based on previous successes it was decided to apply the ionic chiral auxiliary concept, in which optically pure amines can be used to form chiral ammonium carboxylate salts with achiral carboxylic acids. By conducting

the photolyses in the solid state it is known that crystal chirality can be transferred to the photoproducts through topochemically controlled reactions to give very high enantiomeric excesses. Further studies have revealed that in many cases crystallization of achiral substrates into chiral environments causes them to adopt chiral conformations that will favour selective formation of one enantiomer over another.

Through the use of X-ray crystallography, it is possible to develop crystal structure-reactivity relationships allowing the correlation of the molecular structure in a crystal lattice with its observed reactivity. X-ray crystallography may also be used directly in the study of solid state reactions in the rare event that a single crystal of the reactant may be seamlessly converted into a single crystal of the product, a single crystal-to-single crystal reaction. Such studies, where it is possible to obtain crystal structures at the beginning, middle and end of a chemical reaction, allow for a direct confirmation of structure-reactivity relationships, and in some cases prediction and confirmation of the absolute configuration of photoproducts. By forming these relationships a greater understanding of the factors affecting hydrogen abstraction and product formation can be reached. By forming structure-reactivity relationships with numerous substrates it should become possible to predict the outcome of future photochemical reactions through correlations between known reactions and the parameters of theoretical molecules obtained through molecular modeling.

RESULTS AND DISCUSSION

Chapter 2 Substrate Preparation

35   **36**
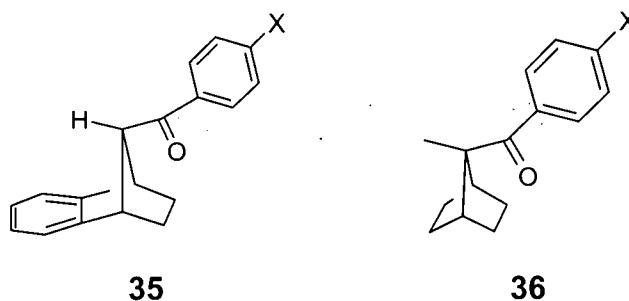
Figure 2.1 Bicyclo[2.2.1]heptane derivatives required for photochemical and asymmetric induction studies.

The molecules of interest for the present studies have the general structures of **35** and **36** (Figure 2.1), common to which is the bicyclo[2.2.1]heptane skeleton with a benzoyl substituent at the 7- position. While the molecules themselves were previously unknown, both were accessible through synthetic manipulation from previously prepared compounds and commercially available materials. The retrosyntheses of ketone derivatives **35** and **36** are shown in Scheme 2.1. The benzonorbornene derivatives (**35**) were synthesized from the known *anti*-9-carboxybenzonorbornadiene (**37**),[72] which could be prepared from commercially available cyclopentadiene (**38**) and *o*-bromofluorobenzene (**39**). The related norbornane derivatives (**36**) were synthesized from the known 7-carboxy-7-methylnorbornane (**40**),[73] following methylation of 7-carboxynorbornane (**41**),[74] prepared from commercially available norbornene (**42**). Both syntheses followed analogous pathways from the parent carboxylic acids (**37** and **40**) utilizing Grignard reactions to add the benzoyl functionality.
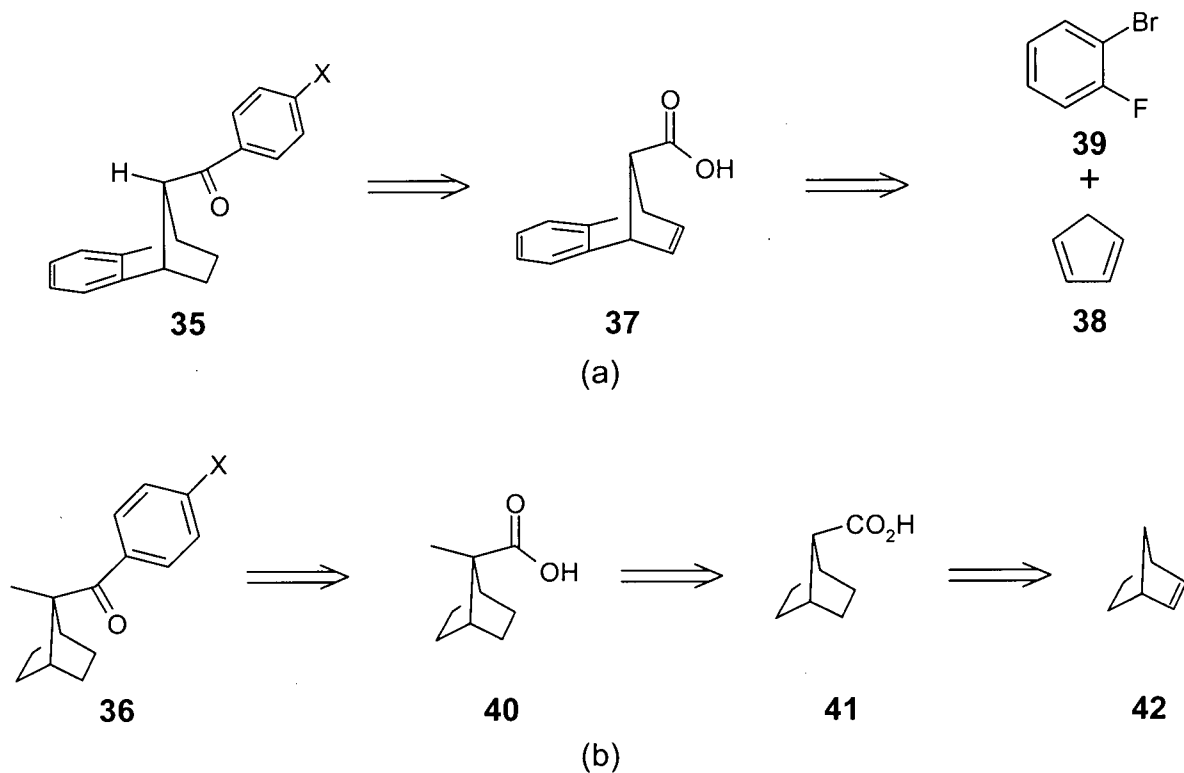
Scheme 2.1 Retrosynthetic analysis of ketones **35** (a) and **36** (b).

2.1 Synthesis of Benzonorbornene Derivatives
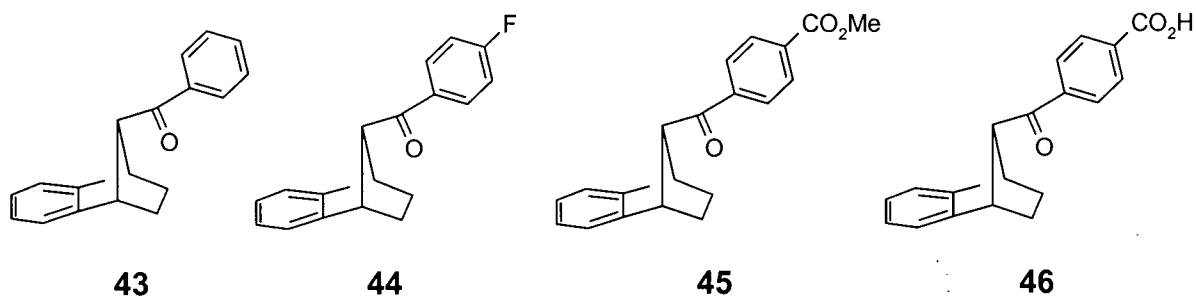
Figure 2.2 Benzonorbornene phenyl ketones **43**, **44**, **45**, and **46**.

The benzonorbornene phenyl ketones, **43**, **44**, **45**, and **46**, illustrated in Figure 2.2, were synthesized using common synthetic methodologies, with some modifications, starting from the known *anti*-9-carboxybenzonorbornadiene (**37**).[72]

2.1.1 Synthesis of the Benzonorbornene Skeleton

Anti-9-carboxybenzonorbornadiene (**37**) served as the source of the benzonorbornene skeleton found in the phenyl ketones studied and was prepared using a known procedure (Scheme 2.2) that was in turn based on modifications of literature preparations.[75] Starting from commercially available 1-bromo-2-fluorobenzene (**39**) and freshly cracked cyclopentadiene (**38**), benzonorbornadiene (**47**) was synthesized in 77% yield via a [$4\pi + 2\pi$] cycloaddition of benzyne with diene **38**. The required benzyne was generated *in situ* upon addition of *o*-bromofluorobenzene (**39**) to magnesium via α-elimination of the generated *o*-fluorophenylmagnesium bromide Grignard reagent. Wagner-Meerwein rearrangement of the bromonium ion formed on addition of bromine to the double bond of alkene **47** led to the selective formation of *exo*-2-*anti*-9-dibromide **48** in 57% yield. This was followed by dehydrobromination of dibromide **48** with a refluxing solution of KDA in THF to give monobromide **49** in 76% yield. Monobromide **49** was then converted into the desired carboxylic acid **37** in 87% yield by performing a lithium-halogen exchange at -78 °C between monobromide **49** and 'BuLi, followed by addition of gaseous carbon dioxide and acidification with concentrated hydrochloric acid.
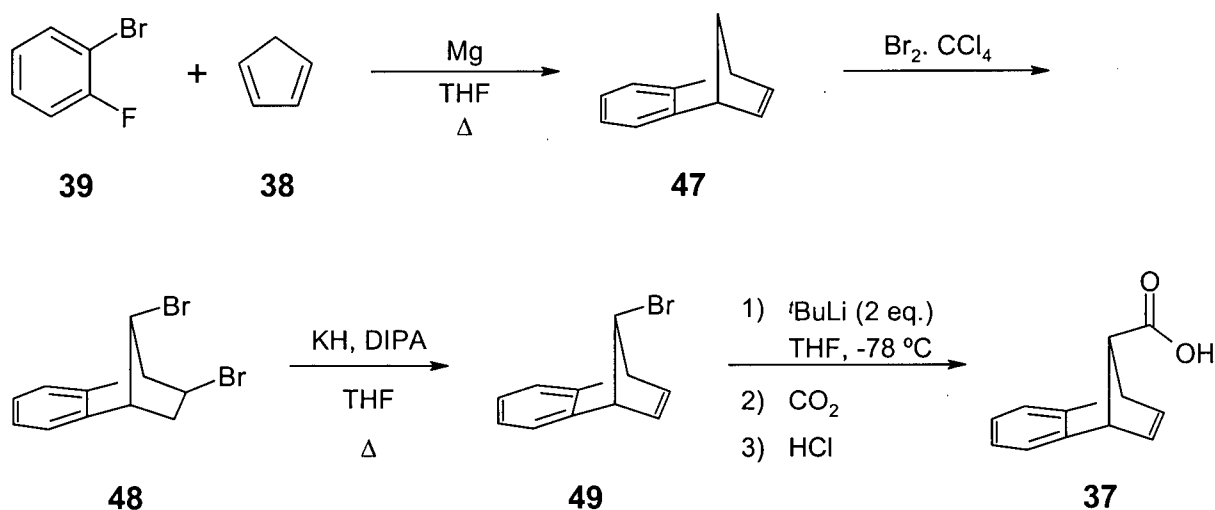
Scheme 2.2 Synthesis of the *anti*-9-benzonorbornene skeleton.

Reduction of the double bond in acid **37** was easily accomplished to form acid **50** (Scheme 2.3) in quantitative yield, using hydrogen gas at atmospheric pressure in the presence of palladium on a carbon support, completing the synthesis of the desired benzonorbornene substructure.
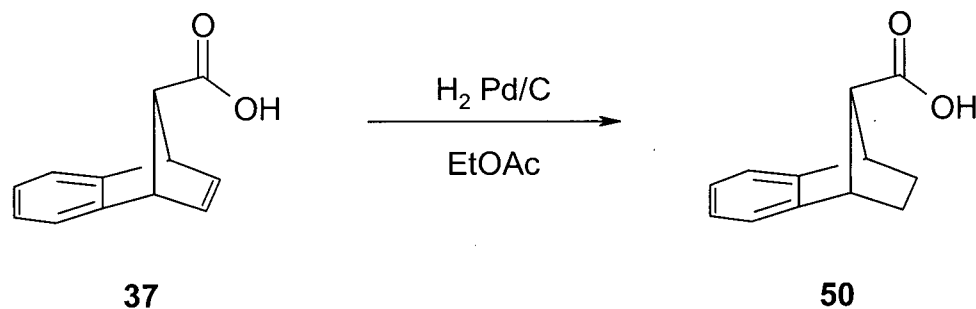
Scheme 2.3 Synthesis of acid **50**.

2.1.2 Synthesis of Phenyl Ketone 43
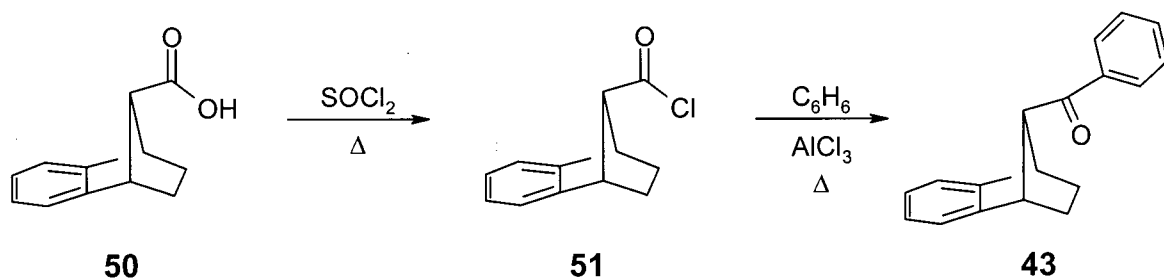
Scheme 2.4 Synthesis of ketone **43**.

As outlined in Scheme 2.4, the method chosen for the synthesis of ketone **43** involved the Friedel-Crafts arylation of acid chloride **51** in an approach which had been previously utilized within our research group for related studies.[70] Following the generation of acid chloride **51** by refluxing acid **50** in thionyl chloride, the Friedel-Crafts arylation was conducted by dissolving the acid chloride in benzene in the presence of aluminum trichloride. While the desired ketone **43** was obtained, there were a number of unisolated side products formed, resulting in a low overall yield of 27%. Hindsight allows that perhaps the low yield of product

would not be totally unexpected due to the presence of the aromatic ring in the starting material, which may have been activated by the presence of the bicylic [2.2.1] system, allowing for the formation of undesired products. As this compound was not going to be used as a precursor in the synthesis of the other ketones, no attempts were made to optimize the yield. Spectral data for this compound were in agreement with the assigned structure, which was confirmed by X-ray crystallography (Figure 2.3a).

(a)   (b)
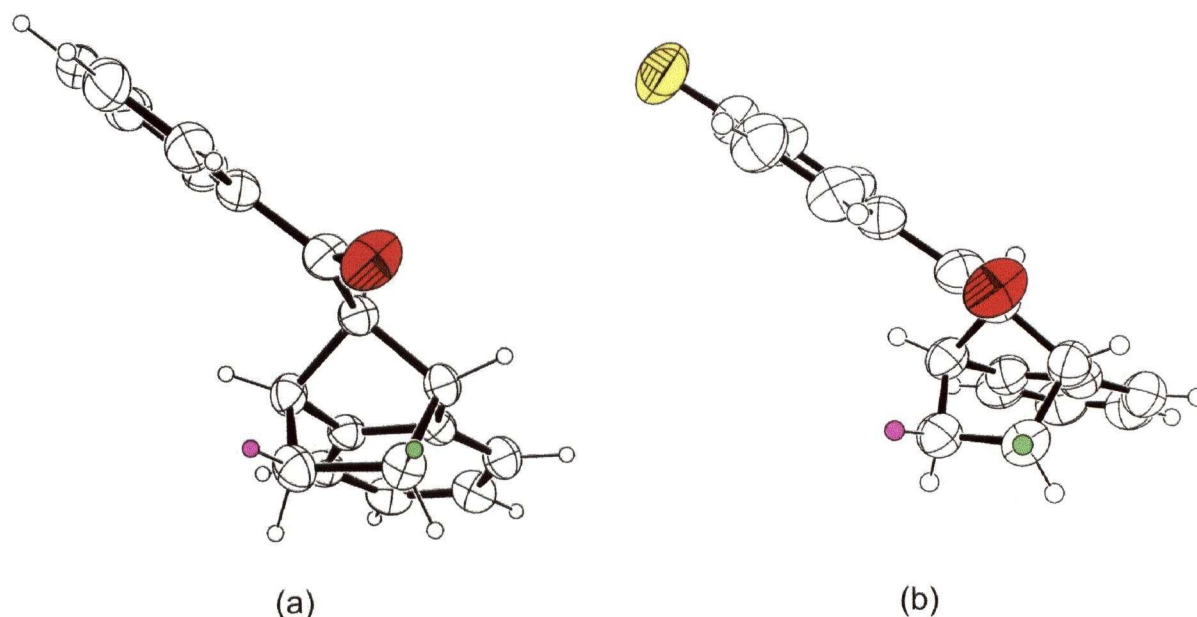
Figure 2.3 ORTEP representations of (a) **43**; (b) **44**. Oxygen atoms are shown in red with the abstractable γ-hydrogens shown in green (most favoured for abstraction) and purple. The fluorine atom in **44** has been coloured yellow.

2.1.3 Synthesis of Phenyl Ketone 44

Initially it had been planned to prepare ketone **44** using an analogous approach to that of ketone **43**, with benzene being replaced by fluorobenzene in the Friedel-Crafts reaction. Unlike ketone **43**, which was not to be used as a starting point in further syntheses, ketone **44** was a precursor and therefore a higher yielding procedure was desired. Following an obvious route, attempts at performing a Grignard addition to acid chloride **51** were conducted but proved unsatisfactory due to a substantial amount of product resulting from the addition of a second

34

equivalent of the Grignard reagent to **44**. This type of problem could be overcome by conducting the Grignard addition on the corresponding aldehyde, rather than the acid chloride, producing a secondary alcohol that would be unable to add a second equivalent of Grignard reagent. Oxidation of the alcohol would then give the desired product. A second approach would be to make use of a Weinreb amide (*N,N*-methoxymethylamide),[76] rather than an acid chloride. The presence of this functional group has been shown to result in the addition of only one equivalent of a Grignard reagent, even in the presence of large (75 eq.) excesses.[76] Since the required amide could be prepared in one step from acid **50**, and ketone **44** would be formed directly in the reaction, this route was chosen over the aldehyde method. Amide **52** was prepared from acid **50** in 76% yield following the procedure of Jones *et al.*[77] and addition of *p*-fluorophenylmagnesium bromide proceeded cleanly, giving ketone **44** in 90% yield (Scheme 2.5). The structural assignment of **44** is supported by spectral data and an X-ray crystal structure (Figure 2.3b).
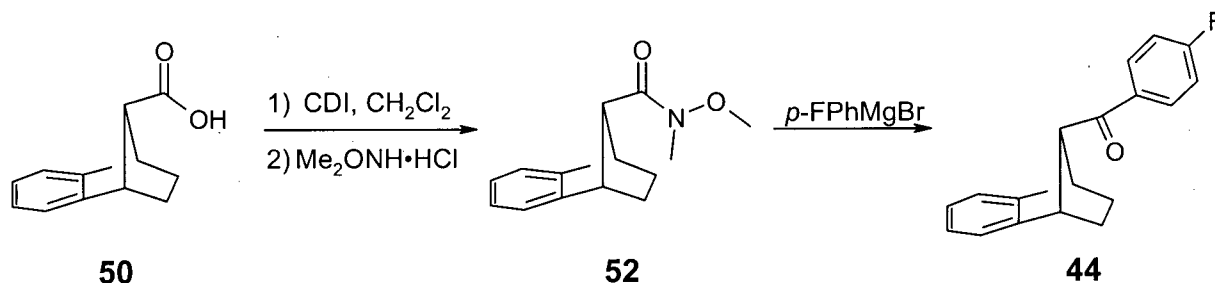
Scheme 2.5 Synthesis of ketone **44**.

2.1.4 Synthesis of Ketones 46 and 45

Following the procedure of Leibovitch for the synthesis of *para*-carboxylic acid substituted phenyl ketones,[70] ketone **44** would have been converted to ketone **46** as shown in Scheme 2.6. However, it was found that while treatment of ketone **44** with KCN did successfully cause substitution of the cyano group at the para position through a S$_N$Ar reaction, forming cyanoketone **53**, epimerization at the C-7 bridge carbon also occurred, resulting in a nearly equal mixture of the two epimers. Attempts to alter the equilibrium ratio by using KCN as the limiting reagent and reducing the reaction time were unsuccessful and also resulted in

epimerization, even when the reaction was not carried to completion. Attempts at conducting the reaction at lower temperatures were also unsuccessful with only starting material being recovered. While the two epimers could be separated by chromatography, hydrolysis of the
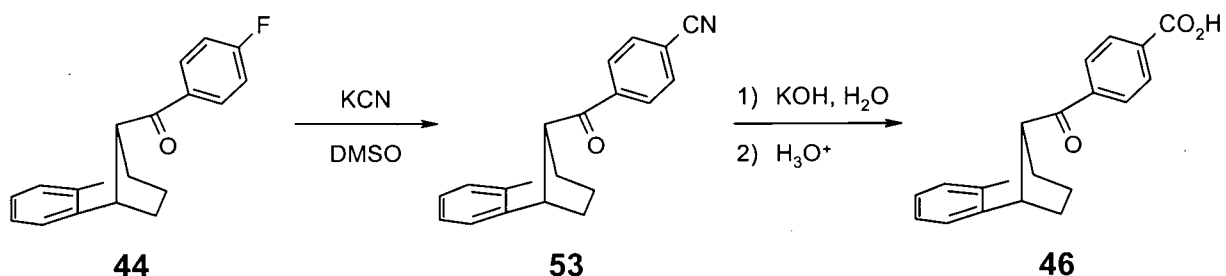
Scheme 2.6 Proposed synthesis of ketone **46**.

cyano group with potassium hydroxide also resulted in an equal mixture of the epimers. Since using this method for the synthesis would result in a 50% reduction in the possible yield, with further reductions owing to the difficulty in obtaining pure acid **46** through multiple recrystallizations, an alternative strategy for the synthesis was sought.
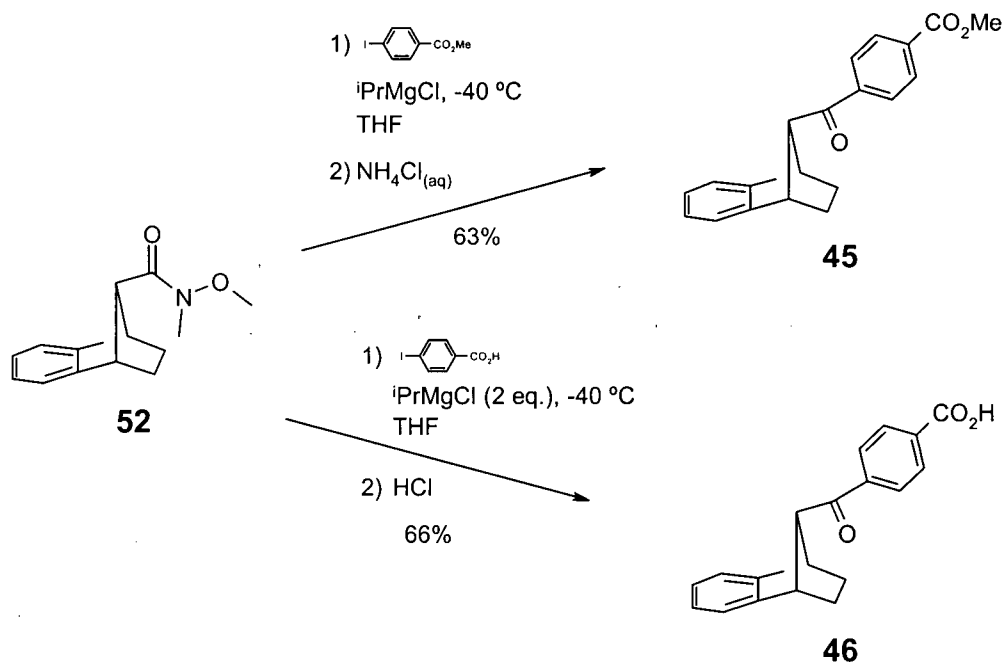
Scheme 2.7 Synthesis of ketones **45** and **46**.

At the time this difficulty in the synthesis arose a paper describing recent work by the groups of Cahiez and Knochel on functionalized Grignard reagents was reported.[78] Of greatest interest to the present work was the use of the ethyl and *tert*-butyl esters of *p*-iodobenzoic acid as Grignard reagents, generated *in situ* with diisopropylmagnesium chloride. This technique was successfully applied to the analogous methyl iodobenzoate forming ketone **45** in a one step reaction with a yield of 63% from amide **52** as shown in Scheme 2.7.

(a)   (b)
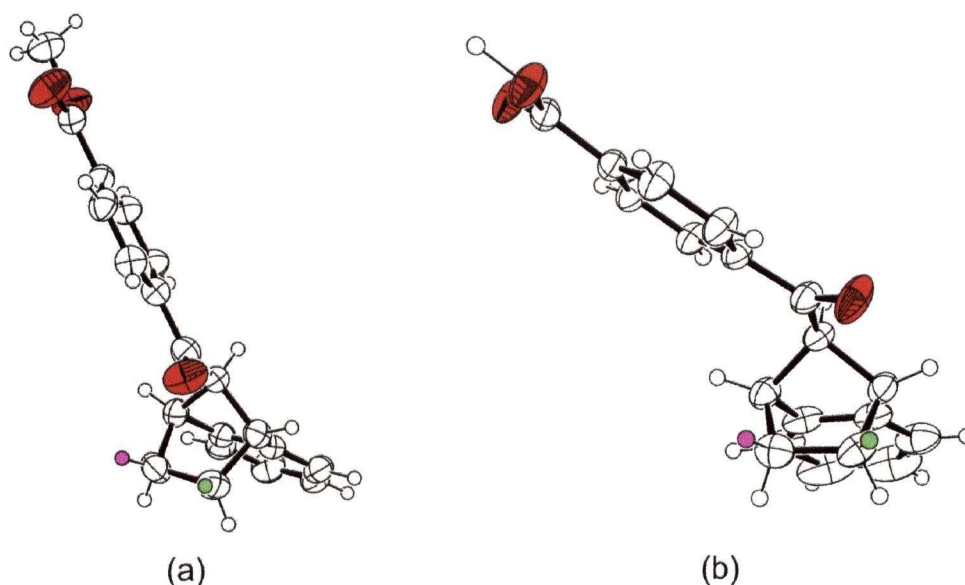
Figure 2.4 ORTEP representations of (a) **45**; (b) **46**. Oxygen atoms are shown in red with the abstractable γ-hydrogens shown in green (most favoured for abstraction) and purple.

As was observed for ketone **44**, the bridge position once again proved to be very susceptible to epimerization in acidic or basic media, thus hindering hydrolysis of the ester, even with "mild" techniques. Once again the methodology of Knochel and Cahiez was adapted. For the preparation of ketone **46** (see Scheme 2.7) a Grignard reagent was prepared using *p*-iodobenzoic acid (rather than one of its ester derivatives) and two equivalents of isopropylmagnesium chloride. With slow addition of ^{i}PrMgCl to a solution of the acid at -40 °C it was possible to selectively deprotonate the carboxylic acid before formation of the Grignard reagent through magnesium-iodide exchange. Following an acidic workup ketone **46** was obtained directly from amide **52** with a yield of 66% after recrystallization from ethanol, to

remove a small amount of the unwanted epimer, and from methanol, to remove the benzoic acid present as a byproduct from any unreacted Grignard reagent. The spectral data obtained were in full accordance with the assigned structures and were supported by X-ray crystallographic structures (Figure 2.4).

2.2 Synthesis of 7-Methylbicyclo[2.2.1]heptane Derivatives
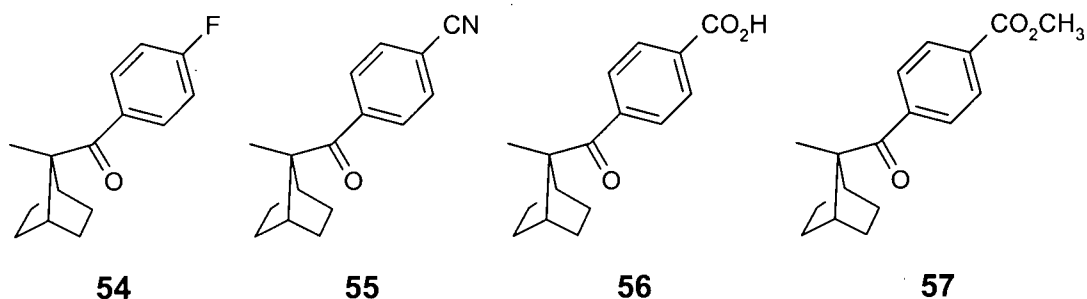
Figure 2.5 7-Methylnorbornane phenyl ketones **54, 55, 56** and **57**.

Owing to the problems encountered during attempts to place a 7-methyl substituent on any of the benzonorbornene substrates prepared in the previous section, it was decided to simplify the substrate and study the photochemistry of bicyclo[2.2.1]heptanes. While this system contains the same core skeleton, the absence of the benzo substituent negates the epimerization problems encountered during methylation. The 7-methylnorbornane derivatives **54, 55, 56** and **57** depicted in Figure 2.5 were prepared using 7-carboxynorbornane (**41**) as the source of the bicyclo[2.2.1]heptane skeleton.

2.2.1 Synthesis of the Bicyclic Skeleton

The bicyclo[2.2.1]heptane skeleton required for this study was found in the known acid **41**, which was synthesized following literature procedures as outlined in Scheme 2.8.[74,79] Starting with commercially available norbornene (**42**), addition of bromine in carbon tetrachloride with one equivalent of pyridine formed dibromide **58** in 32% yield following vacuum distillation. While this reaction is analogous to the one used in the preparation of

dibromide **48** in the previous section there has been a substantial decrease in the selectivity of the reaction. As noted by Kwart and Kaplan, conducting this reaction in the absence of pyridine decreases the yield of **58** even further through HBr assisted isomerization.[74] Following a procedure by Shultz et al.,[79] selective elimination of the 2-bromo substituent was possible using potassium *tert*-butoxide in refluxing dimethylsulfoxide to give monobromide **59** in 93% yield. From the monobromide the carboxylic acid was once again produced through a lithium-halogen exchange reaction followed by addition of gaseous carbon dioxide. This allowed for the formation of carboxylic acid **60** in 87% yield and was followed by reduction to acid **41** in 89% yield with hydrogen over palladium on a carbon support.
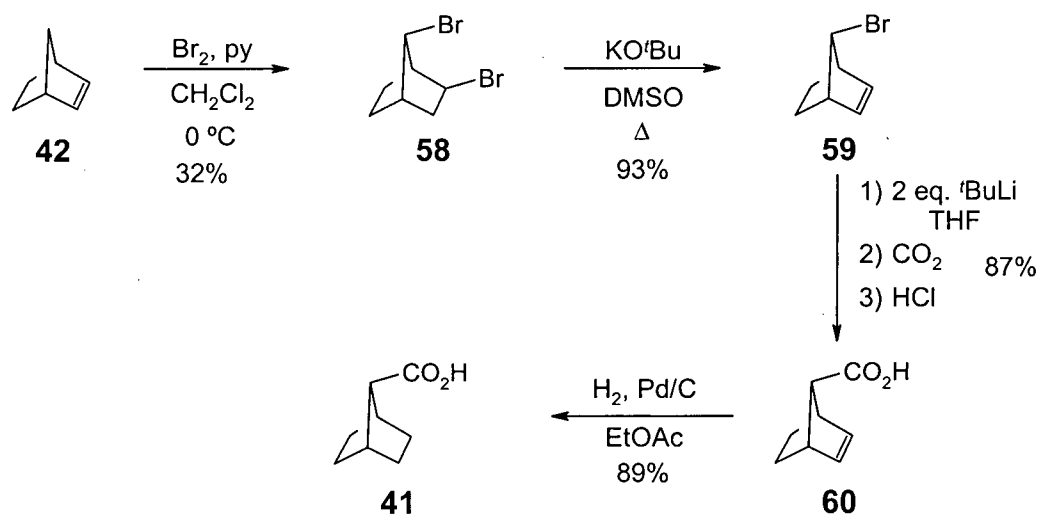
Scheme 2.8 Synthesis of the bicyclo[2.2.1]heptane skeleton.

2.2.2 Synthesis of *p*-Fluorophenyl Ketone 54

The synthesis of ketone **54** from carboxylic acid **41** is outlined in Scheme 2.9. Acid **41** was transformed into its methyl ester derivative by treatment with oxalyl chloride, followed by the addition of methanol. Although the yield of ester **61** was lower than expected at 81%, it was possible to recover the unreacted acid for use in subsequent reactions. A methyl substituent at the 7- position of ester **61** was introduced via formation of an enolate with LDA in the presence of DMPU followed by addition of methyl iodide to give ester **62** in 89% yield. Numerous methods were attempted for the hydrolysis of ester **62**, however these were largely unsuccessful

owing to the steric hindrance created by the α-methyl substitution in the previous step. Eventually the method of Olah *et al.*,[80] using trimethylsilylchloride and sodium iodide in refluxing acetonitrile was found to facilitate the hydrolysis of ester **62** to acid **40** although the yield was low (56%), even after four days of reflux. Once again, however, it was possible to recycle the unreacted material.

The initial approach desired for the preparation of ketones **56** and **57** was to follow the successful use of functionalized Grignard reagents used in the synthesis of benzonorbornene derivatives **45** and **46**. Unfortunately, it was found that the increased steric hindrance provided by the presence of the methyl substituent at the C-7 bridge carbon hindered addition of the Grignard reagent. The temperature sensitive nature of the Grignard reagents formed from methyl iodobenzoate and iodobenzoic acid made it impossible to increase the yield of the reaction to acceptable levels without resulting in their destruction. Based on this problem it was decided to revert to the traditional strategy used within our group.
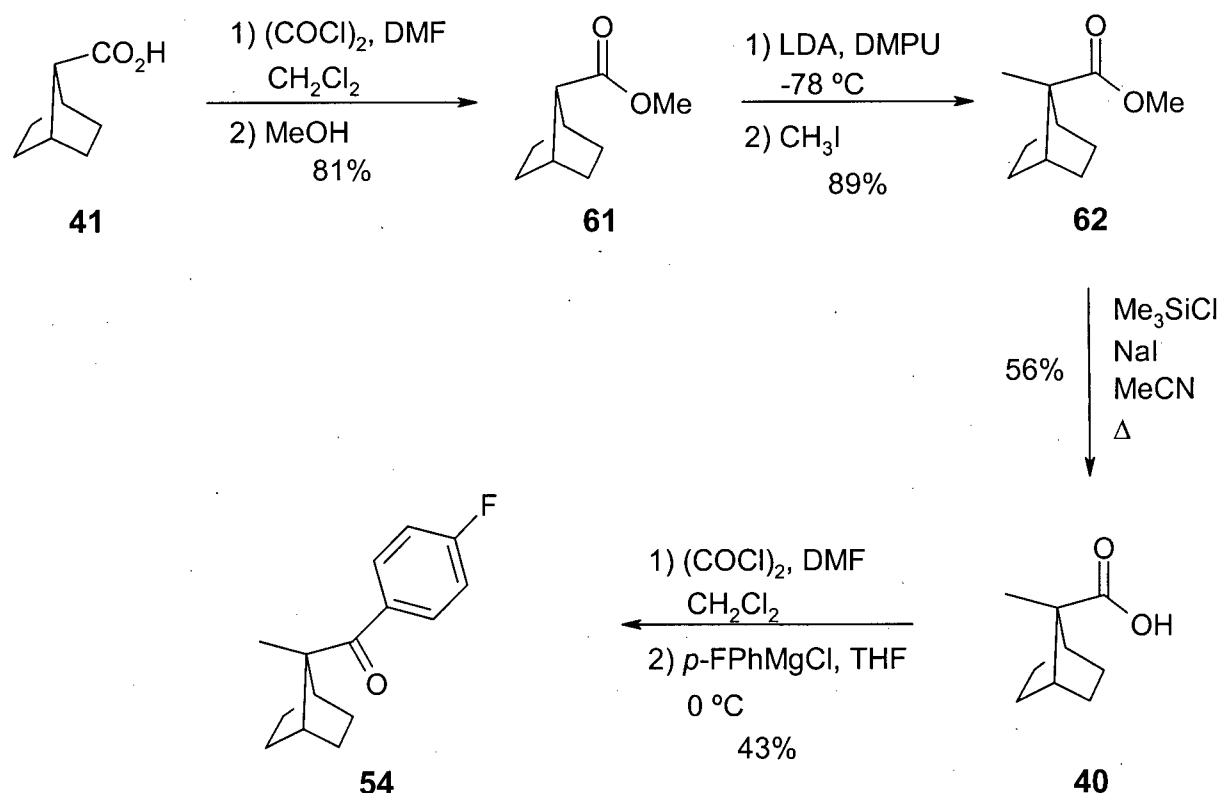
Scheme 2.9 Synthesis of ketone **54**.

Addition of the *p*-fluorophenyl ketone functionality was accomplished by adding the corresponding Grignard reagent (*p*-fluorophenylmagnesium bromide) to the acid chloride of acid **40**. The yield for this reaction, at 43% after purification, was disappointingly low and is likely due in part to the steric hindrance of the quaternary centre adjacent to the carbonyl group. Spectral data obtained for this compound were in agreement with the assigned structure, which was confirmed by X-ray crystallographic analysis (Figure 2.6a).

(a)   (b)
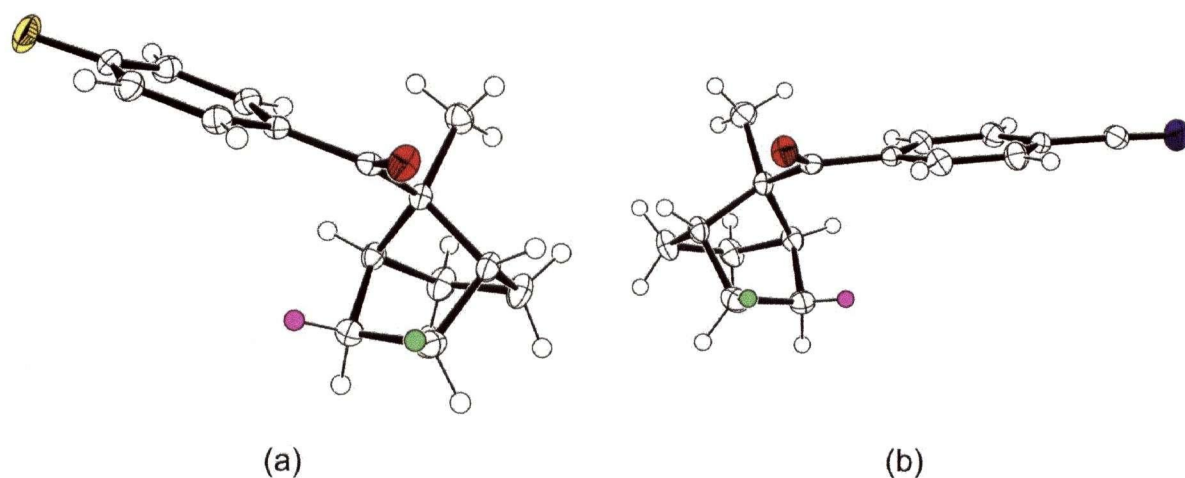
Figure 2.6 ORTEP representations of (a) ketone **54** and (b) ketone **55**. Oxygen atoms have been coloured red, nitrogen blue and fluorine yellow. The γ-hydrogen most favoured for abstraction is shown in green and the least favoured in purple.

2.2.3 Synthesis of Acid 56 and Ester 57

Following formation of *p*-fluorophenyl ketone **54**, completion of the synthesis proceeded as shown in Scheme 2.10. *p*-Fluorophenyl ketone **54** was readily converted to its *para*-cyano analogue **55** in 93% yield through treatment with potassium cyanide in refluxing DMSO. This was followed by hydrolysis of the nitrile with KOH in aqueous ethanol to afford acid **56** in 98% yield. The preparation of ester **57** was accomplished through esterification of acid **56** from its acid chloride following addition of methanol. All three ketones gave spectra in agreement with the assigned structures, which were confirmed by X-ray crystallography (**55**, Figure 2.6b; **56** and **57**, Figure 2.7).
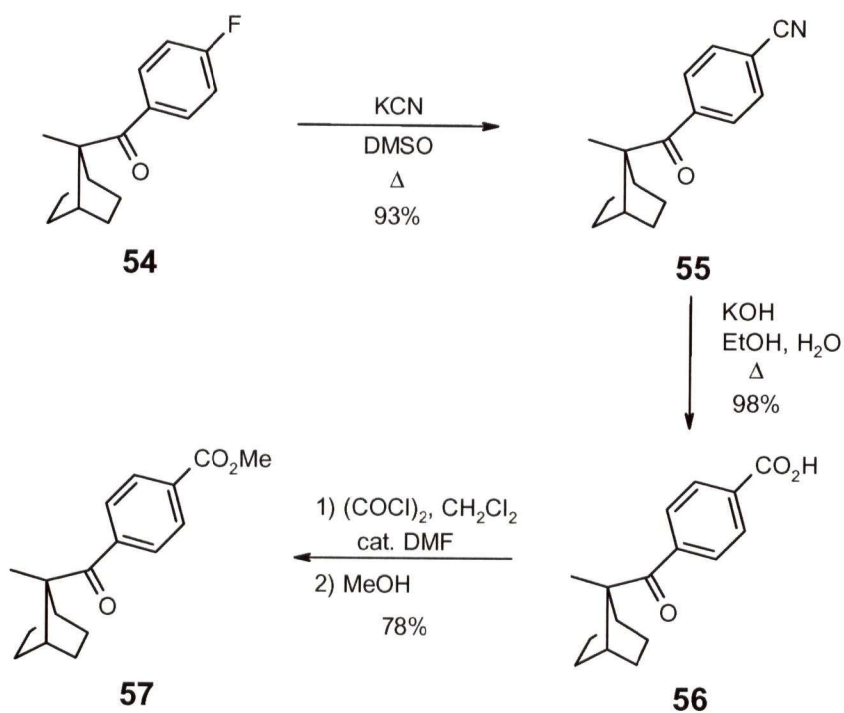
Scheme 2.10 Synthesis of ketones **55**, **56** and **57**.

(a)

(b)
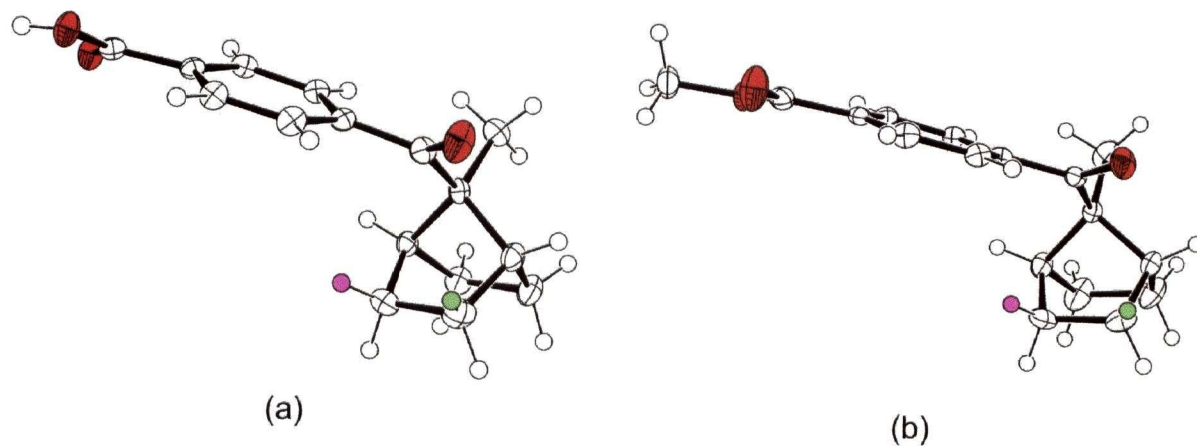
Figure 2.7 ORTEP representations of ketones **56** (a) and **57** (b). Oxygen atoms have been coloured red with the γ-hydrogen most favoured for abstraction green and the least favoured purple.

Chapter 3 Photochemical Studies and Identification of Photoproducts

3.1 Photochemical Studies of Ketones 43, 44, 45 and 46

The four phenyl ketones synthesized for this study were all previously unknown compounds and therefore their photochemistry had not been studied. A further search of the literature revealed that the photochemistry of the 7-benzoylbicyclo[2.2.1]heptane system in general had also not been studied, although the photoreactivity of the isomeric 2-benzoylnorbornane system had been investigated by Lewis and co-workers.[71] While the primary focus of the present work was to study the reactivity of the ketones, especially optically active salts of acid **46**, in the solid state, their photochemistry in solution was first explored. This served the dual purpose of allowing for the isolation and identification of the photoproducts, and to serve as a point of comparison in judging the selectivity of the photoreaction in different reaction media (crystalline state and solution).

3.1.1 Solution Photochemistry of Phenyl Ketones 43, 44 and 45

Preparative photolyses of ketones **43**, **44** and **45** were carried out in acetonitrile under an atmosphere of nitrogen at room temperature using Pyrex filtered light ($\lambda > 290$ nm). Absorption of light by the phenyl ketone preferentially forms a triplet excited state capable of abstracting one of the two accessible γ-hydrogens to give an intermediate 1,4-hydroxy biradical. The biradical intermediate is then able to undergo a number of different reactive processes: degenerate back abstraction to reform the starting ketone; formation of an *endo*-arylcyclobutanol (**63, 64, 65**) or *exo*-arylcyclobutanol (**66, 67, 68**) in a Yang cyclization reaction; or formation of a Norrish type II cleavage product (**69, 70, 71**). These processes are outlined in Scheme 3.1 along with the results of the solution photolyses in Table 3.1. From Table 3.1 it is seen that all three ketones behave photochemically in a similar manner with the major photoproduct being the *endo*-aryl cyclobutanol derived from Yang photocyclization of the biradical. Substantial amounts of the Norrish type II cleavage product were also found along with smaller amounts of a second Yang cyclization product, the *exo*-aryl cyclobutanol.

43   (X = H)
44   (X = F)
45   (X = CO$_2$Me)

X = H   63
X = F   64
X = CO$_2$Me 65

69
70
71

66
67
68
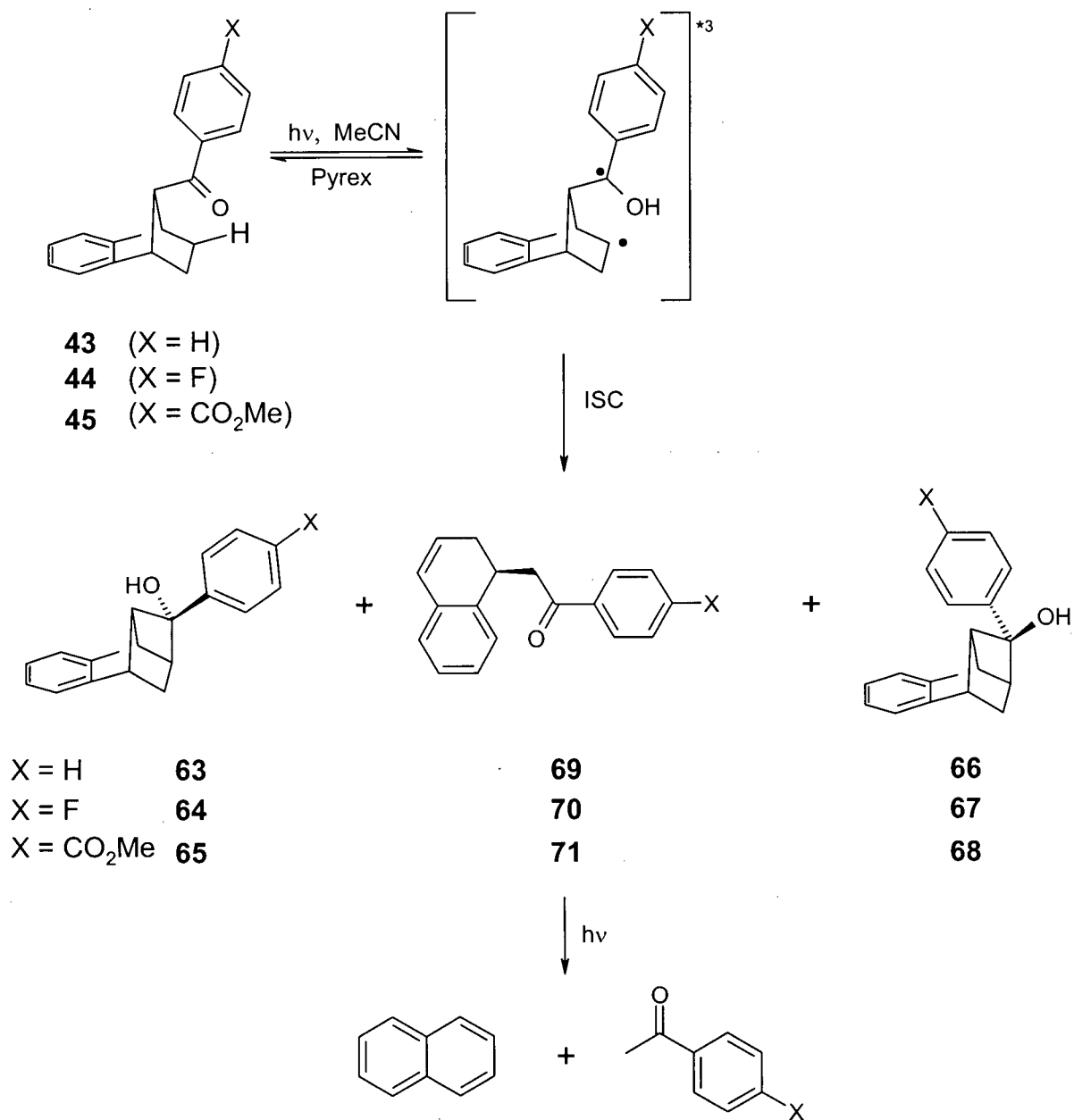
Scheme 3.1 Solution photolysis of ketones **43**, **44**, and **45**.

Table 3.1 Solution photolyses of phenyl ketones **43**, **44** and **45**.[a]

Ketone	X	time (h)	Conv. (%)[b]	Products (%)[c,d]		
43	H	6.75	91	**63**	**69**[e]	**66**
				60	19	8
44	F	4	93	**64**	**70**[e]	**67**
				57	31	5
45	CO_2Me	6	100	**65**	**71**[e]	**68**
				46	52	2

[a]All photolyses were conducted using Pyrex filtered light ($\lambda > 290$ nm) in acetontrile at room temperature under a nitrogen atmosphere. [b]Percentage of total GC integral due to the disappearance of the corresponding ketone. [c]Percentage of the total GC integral of photoproducts due to the corresponding compound. [d]Any remaining products were present in minor amounts and not isolated. [e]Products arising from secondary photolysis of this product, naphthalene and the corresponding acetophenone derivative, were observed but not isolated. Therefore, the reported percentage yield may not accurately reflect the true amount of this product actually formed.

3.1.2 Photoproduct Identification for Photolyses of Ketones 43, 44, and 45

Following isolation by chromatography the structures of the three primary photoproducts were elucidated using 1- and 2-D NMR spectroscopy, with corroborating information as to the presence of certain functional groups being obtained by IR spectroscopy. Additional molecular information was obtained by mass spectrometry and, where possible, by elemental analysis to confirm that the photoproducts were indeed structural isomers of the starting material. The secondary photoproducts, obtained from the irradiation of the cleavage products **69**, **70** and **71**, were identified by gas chromatography using a mass selective detector, followed by comparison of the mass spectra and GC retention times of authentic samples. Confirmation of the assigned structures for two of the photoproducts (*endo*-arylcyclobutanol **64** and cleavage product **71**) was obtained by X-ray crystallography. As the *exo*-arylcyclobutanol was only formed in small amounts and was difficult to obtain in pure form, its structure was not confirmed by X-ray crystallography.

Since phenyl ketones **43, 44,** and **45** have similar structures and spectra, only one example of each of the photoproducts resulting from the photolysis of each ketone in solution is described. For each type of photoproduct analogous spectra were obtained, with the exception of the carbon and proton signals owing to the differing phenyl substitutions. Since the methyl ester derivative photoproducts were used in the analyses of the optically active salts (following diazomethane workup) these photoproducts have been selected for presentation. Following the table containing the comprehensive NMR assignments for each photoproduct derived from ketoester **45,** a second table is included comparing the signals for the analogous molecules resulting from photolysis of ketones **43** and **44.**

3.1.2.1 Identification of *endo*-Aryl Cyclobutanols 63, 64 and 65

The three *endo*-aryl cyclobutanols, one of the two major products formed by photolysis of the corresponding ketones, were isolated by repetitive radial chromatography (for **65,** repetitive preparative HPLC was also necessary) and characterized by NMR spectroscopy, IR spectroscopy, and mass spectrometry. The structural connectivity was primarily determined through interpretation of the NMR spectroscopic data, while IR spectroscopy served mainly to confirm the presence of the alcohol functionality through the characteristic O-H stretching frequency observed as a broad signal in the 3300 - 3500 cm^{-1} range. Mass spectrometry served to confirm that each photoproduct was indeed a structural isomer of the starting ketone.

Listed in Table 3.2 are the signals from the ^{1}H and ^{13}C NMR spectra of *endo*-arylcyclobutanol **65,** along with the correlations determined from HMQC, HMBC and NOESY NMR experiments. These data were sufficient for the determination of the structure and its relative stereochemistry at C10. The assignment was further corroborated by an X-ray crystal structure obtained for *endo*-aryl cyclobutanol **64** (Figure 3.1), which is structurally analogous to **65,** differing only in the substitution of the phenyl ring. As shown in Table 3.3, the signals from the atoms relevant to the structural determination are similar for *endo*-aryl cyclobutanols **66** and **64,** deriving from photolysis of ketones **43** and **44** respectively, with the only major differences lying in the aromatic region due to the *para-* substituent.
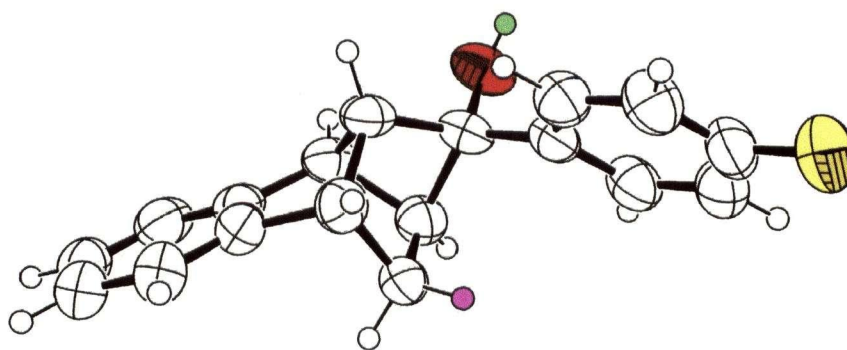
Figure 3.1 ORTEP representation of *endo*-arylcyclobutanol **64**, resulting from photolysis of phenyl ketone **44**. The oxygen atom is shown in red, fluorine in yellow, abstracted γ-hydrogen in green and the unabstracted γ-hydrogen in purple.

Table 3.2 Comprehensive NMR assignments for *endo*-arylcyclobutanol **65** in CD_2Cl_2.

Carbon #	^{13}C δ (ppm)	^1H δ (ppm) (correlations from HMQC)	^1H-^1H COSY correlations	HMBC (long-range) ^{13}C-^1H correlations	^1H-^1H NOESY correlations
1	48.97	4.26 m, 1H	H2, H4 (w), H9	H3$_b$, H4, OH	H2, H9, OH
2	46.51	2.95 m, 1H	H1, H3$_a$, H9	H3$_a$, H3$_b$, H4, H9, OH	H1, H3$_a$, H3$_b$, H12
3	32.18	H$_a$ 0.55 dd, J = 11.2, 2.4 Hz, 1H	H2, H3$_b$	H1 (w), H9	H2, H3$_b$, H4 (w)
		H$_b$ 1.60 dd, J = 11.2, 5.9 Hz, 1H	H3$_a$, H4		H2, H3$_a$, H4, H12

4	44.46	3.18 m, 1H	H1 (w), H3$_b$, H9 (w)	H1, H2, H3$_a$, H3$_b$	H3$_b$, H5, H12
5a	155.19	-	-	H1, H3$_a$, H3$_b$, H7, H8	-
5	119.65	7.17 m, 1H	H6	H4, H6/7	-
6	126.21	7.10 m, 1H (obscured)	H5, H7	H8	-
7	125.87	7.10 m, 1H (obscured)	H6, H8	H5	-
8	123.57	7.29 m, 1H	H7	H5 (w), H6/7	-
8a	142.12	-	-	H4, H5 H6/7	-
9	66.37	3.31 m, 1H	H1, H2, H4 (w)	H2, H3$_a$, H4 (w)	H1, H4, H12
10	83.62	-	-	H3$_a$, H3$_b$, H12, OH (w)	-
11	129.89	-	-	H12	-
12	126.52	7.37 m, 2H	H13	H13 (w)	H2, H4, H9, H13
13	130.27	8.05 m, 2H	H12	H12	H12
14	147.93	-	-	H12 (w), H13	-
15	167.02	-	-	H12 (w), H13, H16	-
16	52.37	3.90 s, 3H	-	-	-
-	-	OH 2.20 (s)	-	-	H1, H2 (w), H9 (w), H12 (w)

The signals of primary importance for the identification of the *endo*-arylcyclobutanol structure were those originating from the six carbons, with the associated proton signals, of the alkyl portion of the structure. APT and HMQC experiments revealed that there were 7 alkyl carbons: one methyl (belonging to the methyl ester), one methylene (C3), four methine (C1, C2, C4, C9) and one quaternary (C10), as would be expected for the formation of a cyclobutanol from the starting material (**45**). Also of importance was the absence of any peaks in the ^{13}C spectra that could be attributed to a ketone or the presence of any signals in the ^{1}H NMR spectra located in the vinyl region, thus eliminating the possibility of it being a cleavage product. Using the COSY spectrum it was possible to distinguish between the protons on the C1, C2 and C4 carbons, all lying in the 2.95 - 3.31 ppm range. This was indicated by a strong coupling between the downfield H3$_b$ proton (1.60 ppm) and H4 (3.18 ppm), while the upfield H3$_a$ proton (0.55 ppm) coupled strongly to H2 (2.95 ppm). Both H1 (4.26) and H4 were coupled to H9 (3.31 ppm), with H1 also showing a strong coupling to H2. The *endo*-aryl stereochemistry at C10 was determined based on the results of NOESY experiments, as shown in Figure 3.2, with correlations between H12 of the phenyl ring with H4 and H3$_b$, indicating that the phenyl group was positioned on the *endo*- face of the molecule. Additionally, correlations were observed between the proton of the hydroxyl group with H1 and H2, indicating their close spatial proximity. It is worth noting that the *endo*-aryl orientation at C10 is also the one that would be predicted for the major cyclobutanol upon photolysis, as formation of the *exo*- epimer would require a large rotation of the hydroxybenzyl portion of the biradical intermediate to occur before ring closure. This point will be discussed in more detail in the following chapters.
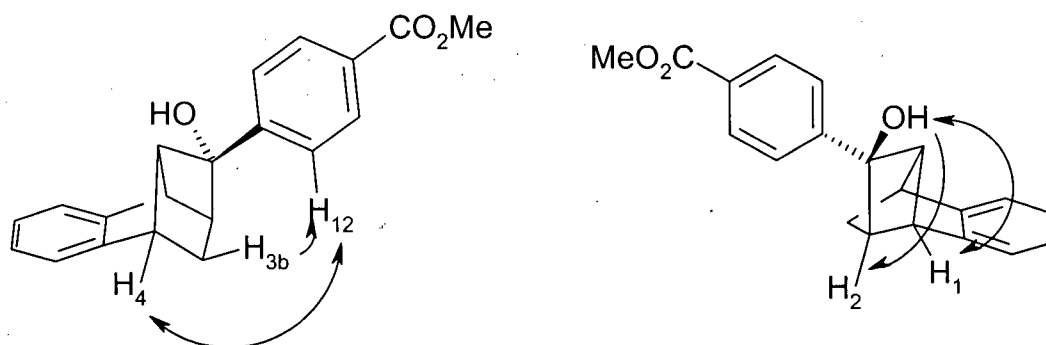
Figure 3.2 Relevant NOE correlations for the stereochemical determination of *endo*-arylcyclobutanol **65**.

Table 3.3 Comparison of NMR data for cyclobutanols **63**, **64**, and **65**.

Carbon #	63		64		65	
	^{13}C δ (ppm)	^{1}H δ (ppm)	^{13}C δ (ppm)	^{1}H δ (ppm)	^{13}C δ (ppm)	^{1}H δ (ppm)
1	48.88	4.25	48.89	4.24	48.97	4.26
2	46.32	2.94	46.44	2.91	46.51	2.95
3	32.23	0.55	32.18	0.56	32.18	0.55
		1.67		1.65		1.60
4	44.45	3.18	44.41	3.17	44.46	3.18
5a	155.35	-	155.23	-	155.19	-
5	119.56	7.18	119.58	7.19	119.65	7.17
6	126.05	7.11	126.11	7.11	126.21	7.10
7	125.73	7.11	125.78	7.11	125.87	7.10
8	123.49	7.30	123.51	7.28	123.57	7.29
8a	142.41	-	142.27	-	142.12	-
9	66.46	3.31	66.49	3.28	66.37	3.31
10	83.92	-	83.38	-	83.62	-
11	143.10	-	139.18, 139.14	-	129.89	-
12	126.33	7.30	128.29, 128.19	7.28	126.52	7.37
13	128.95	7.41	115.86, 115.57	7.11	130.27	8.05
14	127.86	7.34	164.07, 160.81	-	147.93	-
15	-	-	-	-	167.02	-
16	-	-	-	-	52.37	3.90
OH	-	2.19	-	2.24	-	2.20

3.1.2.2 Identification of Cleavage Products 69, 70 and 71

A photoproduct resulting from cleavage of the 1,4-hydroxy biradical intermediate was observed in all of the photolyses in roughly equal amounts to the *endo*-arylcyclobutanol product. Once again, elucidation of the carbon skeleton was based primarily on the NMR spectral data presented in Table 3.4 in addition to IR spectroscopy and mass spectrometry.

The ^{13}C spectra showed immediate support for a cleavage-type product, with the presence of a carbonyl signal at 199.03 ppm as well as two additional signals in the vinyl/aromatic region eventually assigned to C3 (126.95 ppm) and C4 (127.93 ppm). The absence of an alcohol and further evidence of the carbonyl group in the molecule was confirmed by IR spectroscopy. The IR spectrum did not contain any broad absorptions above 3100 cm^{-1} as would be expected for an alcohol, and did exhibit strong carbonyl stretches at 1681 cm^{-1} for the ketone and 1716 cm^{-1} for the ester. Owing to the relative simplicity of the ^{1}H NMR spectrum, assignment of the relevant peaks was trivial with the use of 2D NMR experiments. Confirmation of the structural connectivity was given by the X-ray crystal structure of cleavage product **71** as shown in Figure 3.3. The cleavage products **69** and **70** obtained from the photolysis of ketones **43** and **44** respectively gave similar spectra, with the exception of the signals due to the phenyl group, as outlined in Table 3.5.
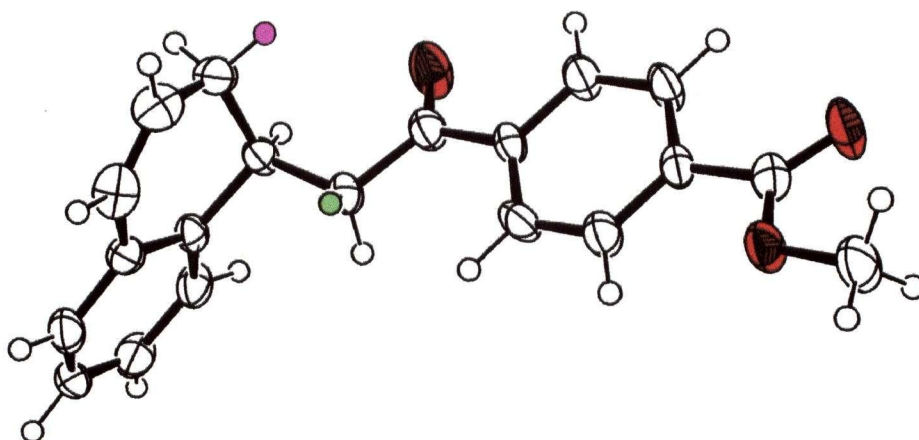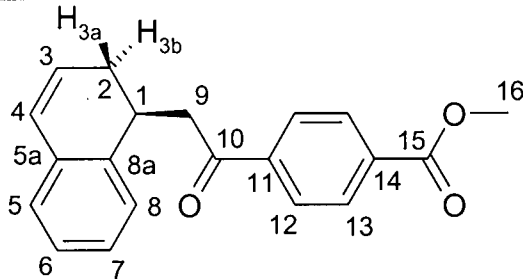
Figure 3.3 ORTEP representation of cleavage product **71**. Oxygen atoms are shown in red, the unabstracted γ-hydrogen in purple and the abstracted γ-hydrogen in green.

Table 3.4 Comprehensive NMR assignments for cleavage product **71** in CD$_2$Cl$_2$.

Carbon #	^{13}C δ (ppm)	^{1}H δ (ppm) (correlations from HMQC)	^{1}H-^{1}H COSY correlations	HMBC (long-range) ^{13}C-^{1}H correlations	^{1}H - ^{1}H NOE correlations
1	33.42	3.56 m, 1H	H2$_a$, H2$_b$, H9, H9'	H2$_a$, H3, H7, H8, H9, H9'	H2$_a$ (w), H2$_b$, H9, H9', H8, H12
2	28.81	H$_a$, 2.32 dddd, J = 17.5, 5.7, 3.5, 0.6 Hz, 1H	H1, H2$_b$, H3	H3, H4, H9, H9'	H1, H2$_b$, H3, H9'
		H$_b$, 2.58 ddt, J = 17.5, 6.9, 2.8 Hz, 1H	H1, H$_a$, H3, H4		H1, H2$_a$, H3
3	126.95	5.94 m, 1H	H2$_a$, H2$_b$, H4	H2$_a$	H2$_a$, H2$_b$ (w), H4
4	127.93	6.53 dd, J = 9.6, 2.5 Hz, 1H	H2$_b$, H3	H5	H3, H5
5a	133.77	-	-	H7/H8	-
5	126.73	7.06 br d J = 7.1 Hz, 1H	H6	H7/H8	-
6	127.70	7.16 m, 1H	H5, H7/H8	H5, H6	-
7	127.70	7.12 m, 1H	-		-

8	127.31	7.12 m, 1H	-	H2$_a$	-
8a	138.48	-	-	H1 (w), H2$_a$, H9, H9'	-
9	43.35	H9 3.13 dd, $J = 16.7, 5.6$ Hz, 1H	H1, H9'	H2$_a$	H1, H8, H9', H12
		H9' 3.33 dd, $J = 16.7, 8.3$ Hz, 1H	H1, H9		H1, H9, H12
10	199.03	-	-	H9, H9', H12	-
11	140.77	-	-	H13	-
12	128.32	7.93 dt, $J = 8.7, 1.6$, 2H	H13	H13	-
13	130.01	8.07 dt, $J = 8.7, 1.7$ Hz, 2H	H12	H12	-
14	134.22	-	-	H12, H16	-
15	166.45	-	-	H13, H16	-
16	52.70	3.91 s, 3H	-	-	-
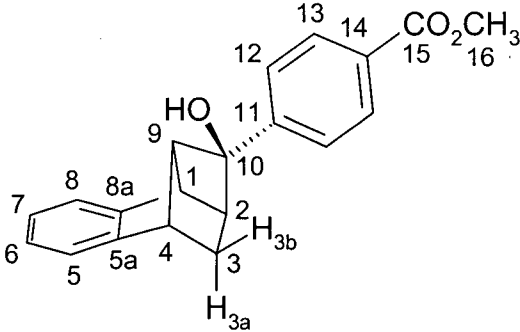
Table 3.5 Comparison of ^{1}H and ^{13}C NMR data for photoproducts **69, 70** and **71**.

Carbon #	69		70		71	
	^{13}C δ (ppm)	^{1}H δ (ppm)	^{13}C δ (ppm)	^{1}H δ (ppm)	^{13}C δ (ppm)	^{1}H δ (ppm)
1	33.03	3.58	33.09	3.56	33.42	3.56
2	28.29	2.31	28.31	2.29	28.81	2.32
		2.58		2.58		2.58
3	126.51	5.91	126.97	5.90	126.95	5.94
4	127.62	6.50	127.63	6.50	127.93	6.53
5a	133.30	-	133.24	-	133.77	-
5	126.35	7.05	126.4	7.05	126.73	7.06
6	126.89	7.16	127.4	7.15	127.70	7.16
7	127.3	7.13	127.4	7.11	127.70	7.12
8	127.3	7.13	126.4	7.11	127.31	7.12
8a	138.25	-	138.07	-	138.48	-
9	42.60	3.05	42.49	3.02	43.35	3.13
		3.34		3.27		3.33
10	199.30	-	197.75	-	199.03	-
11	137.19	-	133.63, 133.58	-	140.77	-
12	128.07	7.89	130.76, 130.63	7.89	128.32	7.93
13	128.51	7.41	115.72, 115.43	7.05	130.01	8.07
14	133.00	7.52	167.34, 163.97	-	134.22	-
15	-	-	-	-	166.45	-
16	-	-	-	-	52.70	3.91

3.1.2.3 Identification of *exo*-Aryl Cyclobutanols 66, 67 and 68

The third, and relatively minor, primary photoproduct obtained on photolysis of the ketones was an *exo*-arylcyclobutanol that is structurally identical to the epimeric *endo*-arylcyclobutanol with the only exception being the inverted stereochemistry at C10. While *exo*-aryl cyclobutanols **66** and **67** were isolated in small amounts, it was not possible to separate an appreciable amount of **68** from its epimer, **65**. However, after characterization of the epimeric *endo*-arylcyclobutanol **65**, it was possible to elucidate the structure of the *exo*- epimer based on the limited spectral data available as outlined in Table 3.6. *Exo*-aryl cyclobutanols **66** and **67** exhibited similar spectra as shown in Table 3.7.

Table 3.6 Comprehensive NMR assignments[a] for cyclobutanol **68**.

Carbon #	^{13}C δ (ppm)	^{1}H δ (ppm) (correlations from HMQC)	^{1}H-^{1}H COSY correlations
1	45.94	2.78 m, 1H	H2, H4, H9
2	46.01	3.10 m, 1H	H1, H3$_a$, H9
3	31.53	H3$_a$, 0.77 dd, J = 10.5, 2.3 Hz, 1H	H2, H3$_b$
3	31.53	H3$_b$, 2.70 dd, J = 10.5, 6.0 Hz, 1H	H3$_a$, H4
4	44.77	3.48	H1 (w), H3$_b$, H9

		m, 1H	
5a	155.12	-	-
5	119.84	7.17 m, 1H	H6
6	126.07	7.07 m, 1H	H5, H7
7	125.81	7.07 m, 1H	H6. H8
8	123.52	7.27 m, 1H	H7
8a	140.92	-	-
9	68.01	3.34 m, 1H (obscured)	H1, H2, H4
10	78.36	-	-
11	130.06	-	-
12	128.03	7.68 m, 2H	H13
13	130.10	8.07 m, 2H (obscured)	H12
14	147.67	-	-
15	167.04	-	-
16	52.41	3.91 s, 3H	-
OH	-	OH, 2.00 br s, 1H	-

[a]Peaks for this compound were assigned using spectra from a mixture of compounds **65** and **68** following assignments of peaks due to alcohol **65** from spectra of the pure compound.

Table 3.7 Comparison of NMR signals[a] for *exo*-aryl cyclobutanols **66**, **67** and **68**.

Carbon #	66		67		68	
	^{13}C δ (ppm)	^1H δ (ppm)	^{13}C δ (ppm)	^1H δ (ppm)	^{13}C δ (ppm)	^1H δ (ppm)
1	45.91	2.77	46.04	2.76	45.94	2.78
2	46.04	3.09	46.04	3.06	46.01	3.10
3	31.57	0.75	31.58	0.75	31.53	0.77
		2.69		2.68		2.70
4	44.73	3.46	44.70	3.45	44.77	3.48
5a	155.30	-	155.21	-	155.12	-
5	119.77	7.06	119.79	7.09	119.84	7.17
6	125.91	7.06	125.99	7.09	126.07	7.07
7	125.69	7.06	125.73	7.09	125.81	7.07
8	123.44	7.26	123.46	7.26	123.52	7.27
8a	141.19	-	141.02	-	140.92	-
9	68.21	3.35	68.26	3.31	68.01	3.34
10	88.13	-	78.05	-	78.36	-
11	142.72	-	138.75, 138.70	-	130.06	-
12	127.83	7.43	129.78, 129.67	7.59	128.03	7.68
13	128.94	7.61	115.75, 115.47	7.12	130.10	8.07
14	128.23	7.36	164.27, 161.01	-	147.67	-
15	-	-	-	-	167.04	-
16	-	-	-	-	52.41	3.91
OH	-	1.90	-	1.90	-	2.00

[a]NMR signals for **66** and **67** were determined from spectra composed of the pure compounds; signals for **68** were determined from spectra of a mixture of **71** and **68**.

Although the *exo-* and *endo-* cyclobutanols are structurally similar, with virtually identical coupling patterns in the ^1H NMR spectra, there are two major differences in chemical shifts due to the effects of the phenyl group as shown in Table 3.8. Most noticeable were the

shifts in H3$_b$, which lies at 1.60 ppm in the *endo*-arylcyclobutanol and 2.70 ppm in the *exo*-epimer, and in H1, which lies at 4.26 ppm in the *endo*-arylcyclobutanol and 2.78 ppm in the *exo*- epimer. This difference in chemical shift corresponds to the shielding effect of the phenyl ring upon the protons lying directly beneath it. In *endo*-arylcyclobutanol **65** the phenyl group lies over H3$_b$, while in *exo*-arylcyclobutanol **68** the phenyl ring lies over H1.

Table 3.8 Comparison of relevant NMR data for cyclobutanols **65** and **68**.

Carbon	65 (*endo*-aryl)		68 (*exo*-aryl)	
	^{13}C δ (ppm)	^{1}H δ (ppm)	^{13}C δ (ppm)	^{1}H δ (ppm)
1	48.97	**4.26**	45.94	**2.78**
2	46.54	2.95	46.01	3.10
3	32.18	0.55	31.53	0.77
		1.60		**2.70**
4	44.46	3.18	44.77	3.48
9	66.37	3.31	68.01	3.34
10	83.62	-	78.36	-
OH	-	2.20	-	2.00

3.1.3 Solid State Photolyses of Ketones 43, 44, 45 and 46

Following identification of the primary photoproducts obtained from the preparative scale solution photolyses, the reactivity of the four ketones was studied in the solid state. When conducting the solid state photolyses, 2-3 milligrams of the crystalline ketone were crushed between two glass microscope slides and sealed under a nitrogen atmosphere within a polyethylene bag. The results of the photolyses are summarized in Table 3.9 for each of the ketones, with the photoproducts from ketoacid **46** being treated with ethereal diazomethane and converted into the corresponding methyl esters (**65, 71** and **68**) for identification. Initial photolyses conducted with a 450 W light source showed melting of ketones **43** (mp = 60.5-61 °C) and **44** (mp = 83-84 °C) along with a subsequent loss in selectivity due to the breakdown of

the crystal lattice. These photolyses were attempted at reduced temperatures (0 °C), however this prevented any reaction from occurring. Additional photolyses were conducted using an 800 W light source fitted with two dichroic filters to remove >98% of the infrared light emitted, allowing for the successful photolysis of ketone **44**.

Table 3.9 Solid State photolyses of ketones **43**, **44**, **45** and **46**.[a]

Ketone	X	time (h)	Conv. (%)[b]	Products (%)[c, d]		
				63	**69**	**66**
43	H	1	2	34	53	0
		2.5	4	49	40	0
		4[e]	13	53	22	10
		3[e, f]	9	58	29	13
				64	**70**	**67**
44	F	3[e]	76	88	5	3
		3[f]	26	94	3	0
		6[f]	47	96	4	0
				65	**71**	**68**
45	CO$_2$Me	60	2	trace	0	0
		44.5[g]	trace	trace	0	0
46[h]	CO$_2$H	3[f]	28	>99	0	0
		4.5[f]	55	>99	trace	0

[a]Photolyses were conducted on 2-3 mg quantities of the ketones crushed between two microscope slides and sealed under nitrogen in a polyethylene bag. All photolyses were conducted using 450 W Pyrex filtered light (λ > 290 nm) at room temperature. [b]Percentage of total GC integral due to the disappearance of the corresponding ketone. [c]Percentage of the total GC integral of photoproducts due to the corresponding compound. [d]Any remaining products were present in minor amounts and not isolated. [e]Melting of the sample was evident. [f]Photolyses conducted at 800 W filtered through two dichroic filters, to remove >99% infrared light, and through Pyrex glass. [g]Photolysis conducted on ketones suspended in water with sodium dodecylsulphate (surfactant). [h]Following photolysis the sample is treated with ethereal diazomethane, converting the remaining ketone and any photoproducts into the corresponding methyl esters.

The data show that of the four ketones only three, **43**, **44** and **46**, may be considered reactive in the solid state. It is immediately noticed when comparing the results of the solid state photolyses for ketones **44** and **46** to those in solution that there is a large change in the product ratios; the *endo*-arylcyclobutanol makes up 95% of the product mixture with the remainder containing only small amounts of the cleavage product and none of the *exo*-aryl cyclobutanol. Due to the confines of the crystal lattice it is not at all surprising that the *exo*-aryl cyclobutanol is not present in the product mixtures, as it was present only in small amounts following photolysis in solution and the necessary rotation of the phenyl ring within the crystal lattice would be extremely hindered. The exception to this observation is that of ketone **43**, which shows relatively significant amounts of the *exo*-aryl cyclobutanol **66**. Since crystal melting was observed in this photolysis, even at low conversions, this occurrence is most likely due to a breakdown of the crystal lattice on the crystal surface. If the lattice has been destroyed then the chemical selectivity will be lost as well. Perhaps the most surprising result in the photolyses is that ketone **45** was essentially unreactive in the solid state, even upon prolonged irradiation.

Differing reactivity within the solid state photochemistry of a set of analogous phenyl ketones is known. One study by Ito and co-workers on the solid state photocyclization of *para*-substituted 2,4,6-triisopropylbenzophenones concluded that a narrow reaction cavity was responsible for an unreactive methyl ester substituted derivative.[81] As will be seen in the photochemistry of the optically active salts formed from acid **46**, the unreactivity of ester **45** in the solid state is not an isolated event, with a number of salts giving low conversions upon prolonged irradiation. A plausible explanation for the observed photoinertness will be presented following a discussion of the geometric parameters obtained from the X-ray crystal structures of the ketones. This will show that an unfavourable geometry, rather than an unfavourable reaction cavity is the likely cause.

3.2 Photochemistry of Phenyl Ketones 54, 55, 56 and 57

The photochemistry of the four phenyl ketones was studied in both solution and the solid state. As for the work described in the previous section, this serves the dual purpose of providing a point of comparison for the outcome of photolysis in the two media as well as providing a method of producing a sufficient amount of the photoproducts for characterization.

3.2.1 Solution State Photochemistry of the Phenyl Ketones

The solution state photochemistry of the three ketones (represented by **36**) proceeded to give only one photoproduct, the *endo*-arylcyclobutanol (**72**) as shown in Scheme 3.2. In no case was there any evidence of products resulting from either Norrish type II cleavage (**73**) or the diastereomeric *exo*-arylcyclobutanol (**74**), resulting from rotation in the hydroxybiradical intermediate (**75**). This observed reactivity is in stark contrast to the related system discussed in the previous section, where mixtures of photoproducts were observed. The results of the photolyses are summarized in Table 3.10.

Table 3.10 Solution photolyses of ketones **54**, **55** and **57**.[a]

Ketone	X	Time (h)	Conv. (%)[b]	Yield (%)[c]
54	F	2	>99	92 (**76**)
55	CN	2	>99	97 (**77**)
57	CO_2Me	4	>99	99 (**78**)

[a]All photolyses were conducted using 450 W Pyrex filtered light ($\lambda > 290$ nm) in acetonitrile at room temperature under a nitrogen atmosphere. [b]Percentage of total GC integral due to the disappearance of the corresponding ketone. [c]Percentage of the total GC integral of photoproducts due to the corresponding compound.
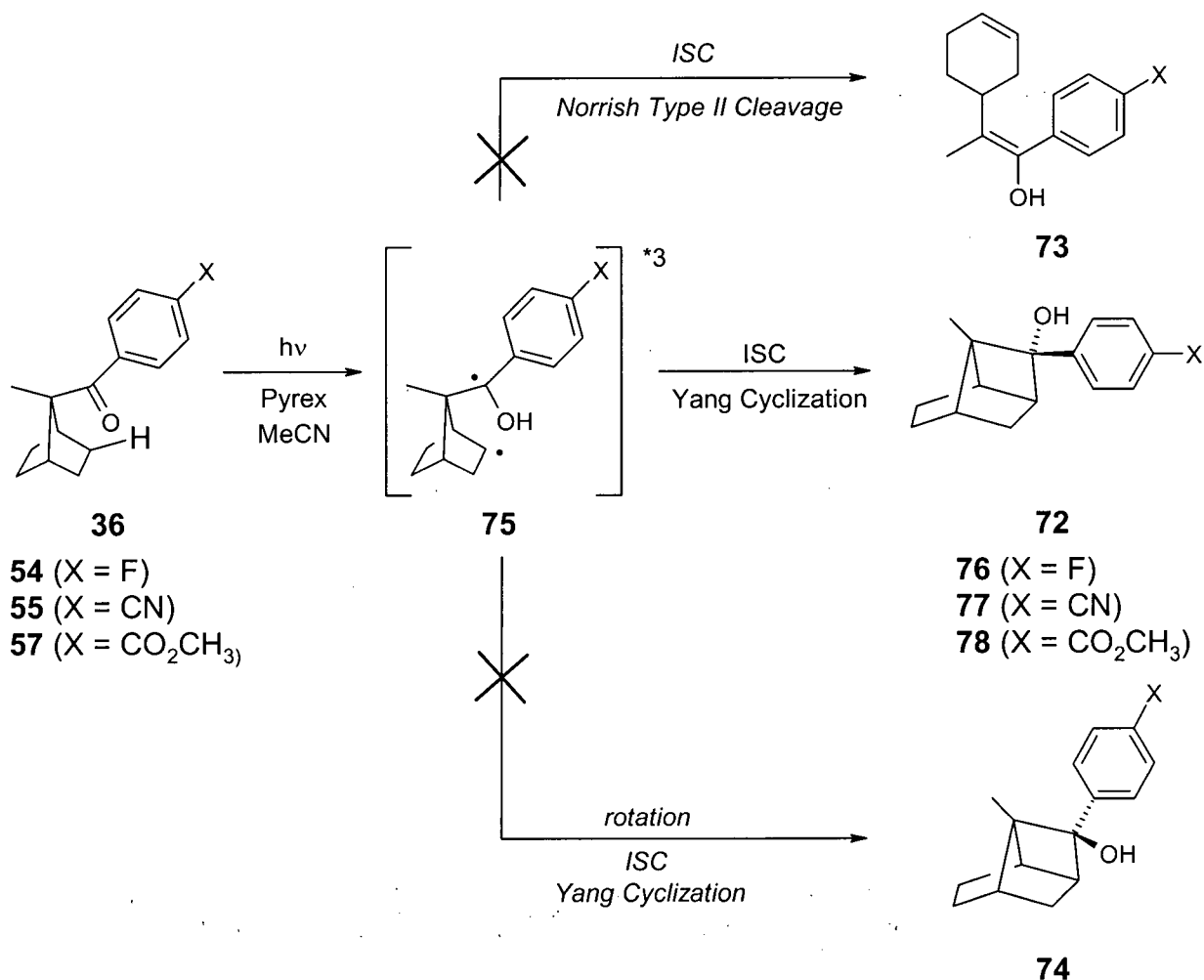
Scheme 3.2 Reaction pathways for the photolysis of phenyl ketone **36**.

3.2.2 Solid State Photochemistry of the Phenyl Ketones

As was observed in the solution reactions, the *endo*-arylcyclobutanol was the only observed product resulting from photolysis in the solid state. Once again the reaction proceeded cleanly with no evidence of the other possible photoproducts. Based on these results there is obviously no benefit to photolysing this particular system in the solid state in order to maximize the formation of one product over another, but as will be shown, the photochemistry of chiral ammonium carboxylate salts in the solid state provides an excellent method of achieving enantioselectivity in the reaction.

Table 3.11 Solid state photolysis of ketones **54**, **55**, **56**, and **57**.[a]
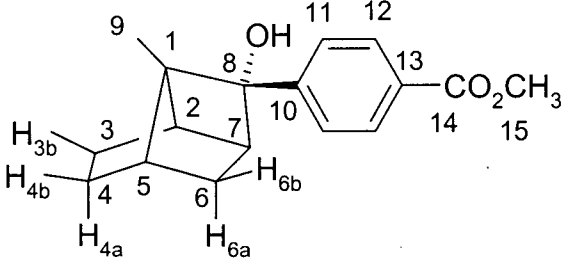
Ketone	X	Time (min.)	Conv. (%)[b]	Yield (%)[c]
54[d]	F	20	70	>99 (**76**)
55	CN	60	80	>99 (**77**)
56[e]	CO_2H	60	77	98 (**78**)
57	CO_2CH_3	60	>99	97 (**78**)

[a]Photolyses were conducted on 2-3 mg quantities of the ketones crushed between two microscope slides and sealed under nitrogen in a polyethylene bag. All photolyses were conducted using 450 W Pyrex filtered light (λ > 290 nm) at room temperature. [b]Percentage of total GC integral due to the disappearance of the corresponding ketone. [c]Percentage of the total GC integral of photoproducts due to the corresponding compound. [d]Irradiation to higher conversions led to melting of the sample. [e]Following photolysis the sample is treated with ethereal diazomethane, converting the remaining ketone and any photoproducts into the corresponding methyl esters.

3.2.3 Identification of *endo*-Aryl Cyclobutanols 76, 77 and 78

Following photolysis of each ketone in a solution of acetonitrile and subsequent purification by radial chromatography, its structure was elucidated by NMR spectroscopy. In addition to the NMR data obtained, mass spectrometry confirmed that the compound was indeed a structural isomer of the starting material, and IR spectroscopy confirmed the presence of an alcohol in the molecule with a broad absorption due to the O-H stretching vibration around 3400 cm^{-1}. The structural assignments based on NMR data are outlined for cyclobutanol **78** in Table 3.12, while Table 3.12 provides a comparison of the ^{1}H and ^{13}C NMR data for the series of analogous cyclobutanols **76**, **77**, and **78**. The structural connectivity of the cyclobutanol product was confirmed by X-ray crystal structures obtained for salts **79** and **80** (shown in Figure 3.4) that were converted into **78** upon treatment with diazomethane.

Table 3.12 Comprehensive NMR assignments for *endo*-arylcyclobutanol **78**.

Carbon #	$^{13}C\ \delta$ (ppm)	$^1H\ \delta$ (ppm) (correlations from HMQC)	^1H-^1H COSY correlations	HMBC (long-range) ^{13}C-^1H correlations	^1H-^1H NOE correlations
1	58.04	-	-	H4$_a$, H5, H6$_a$, H7	-
2	47.61	2.71 m, 1H	H3$_a$ (w), H3$_b$, H7	H4$_a$, H5, H6$_b$	H3$_a$ (w), H3$_b$, H7, H9 (w), OH (w)
3	21.89	H3$_a$, 1.50 m, 1H	H4$_a$, H3$_b$	H5	H2 (w), H3$_b$, H4$_a$, H4$_b$, H6$_a$
3	21.89	H3$_b$, 1.61 m, 1H (obscured)	H2, H3$_a$, H4$_b$	H5	H2, H3$_a$, H4$_b$
4	33.72	H4$_a$, 1.61 m, 1H (obscured)	H3$_a$, H4$_b$	H6$_a$, H6$_b$	H3$_{ax}$, H5, H6$_a$
4	33.72	H4$_b$, 1.88 m, 1H (obscured)	H3$_b$, H4$_a$, H5	H6$_a$, H6$_b$	H3$_b$, H4$_a$, H9
5	42.48	1.89 m, 1H (obscured)	H4$_b$, H6$_b$ (w)	H2, H3$_b$, H6$_a$, H6$_b$, H7, H9	H4$_a$, H4$_b$ (w), H6$_b$, H9 (w)
6	28.55	H6$_a$, 0.95 dd, J = 11.3, 2.2 Hz, 1H	H6$_b$, H7	H4$_a$, H4$_b$	H3$_a$, H4$_a$, H5, H6$_b$, H7
6	28.55	H6$_b$, 1.10 dd, J = 11.3, 6.3 Hz, 1H	H5, H6$_a$	H4$_a$, H4$_b$	H5, H6$_a$, H7, H11 (w)

7	49.04	2.62 m, 1H (obscured)	H2, H6$_a$	H3$_a$, H3$_b$, H5 H6$_a$, H6$_b$,	H2, H6$_a$ H6$_b$, H11
8	85.11	-	-	H6$_a$, H6$_b$, H9, H11	-
9	10.96	1.30 s, 3H	-	H7 (w)	H2, H5, H11, OH (w)
10	129.43	-	-	H11, H12 (w)	-
11	126.70	7.33 m, 2H	H12	H12 (w)	H5, H6$_b$ (w), H7, H9, H12
12	130.03	7.96 m, 2H	H11	-	H11
13	149.23	-	-	H12	-
14	167.09	-	-	H11 (w), H12, H15	-
15	52.29	3.87 s, 3H	-	-	H12 (w)
OH	-	2.10 br s, 1H	-	-	H2 (w)
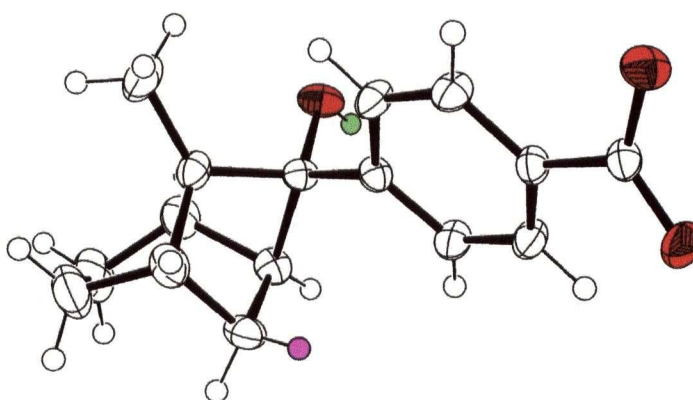
Figure 3.4 ORTEP representation of salt **80** (auxiliary removed) which, upon treatment with CH$_2$N$_2$, is converted into its methyl ester derivative **78**. Oxygen atoms are coloured red with the abstracted γ-hydrogen shown in green and the unabstracted γ-hydrogen shown in purple.

From the APT and HMQC experiments it was observed that **78** contained 10 carbon signals in the alkyl region: two methyl, three methylene, three methine and two quaternary, consistent with the proposed structure. The two geminal protons, H6$_a$ (0.95 ppm) and H6$_b$ (1.10 ppm), were easily distinguished from the other methylene groups based on their upfield shift, due to shielding from the phenyl group, and characteristic 'doublet of doublets' splitting pattern, observed in the cyclobutanols discussed in the previous section. Using data derived from a COSY experiment it was possible to assign the methine protons H7 (2.62 ppm), showing a strong coupling to H6$_a$, and H5 (1.89), showing a strong coupling to H6$_b$. The remaining methine proton was then assigned to H2 (2.71), which also exhibited a coupling to H7. C3 and C4 were distinguished through their HMBC interactions, where C4 showed a 3-bond correlation to H6$_a$ and H6$_b$, while C3 showed a 3-coupling to H5. Conversely, correlations were observed between C7 and the two H3 protons (3 bond), along with C6 and the two H4 protons (3 bonds).

As for the previous cyclobutanols, the stereochemical assignment of C8 was determined using NOE. Selective irradiation of the aromatic H11 showed correlations to H6$_b$ and H5, while the hydroxyl proton showed correlations to H2. Based on these spatial proximities the *endo*-aryl stereochemistry was assigned for the molecule. In addition to providing stereochemical information for the structure, NOE experiments were also able to help distinguish between protons on C3 and C4. Both H3$_a$ (1.50 ppm) and H4$_a$ (1.61 ppm) showed correlations when H6$_a$ was selectively irradiated in an NOE experiment. The NOE correlations that were useful in resolving the location of specific proton signals are illustrated in Figure 3.5.
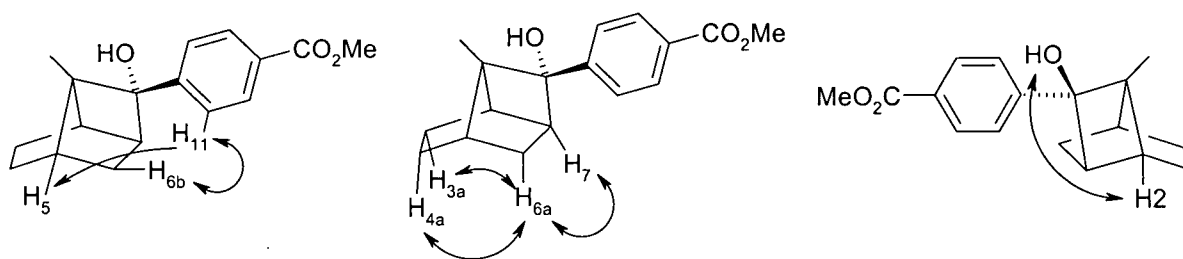
Figure 3.5 Selected NOE correlations for cyclobutanol **78**.

Table 3.13 Comparison of NMR data for cyclobutanols **78**, **76** and **77**.

Cyclobutanol	78		76		77	
Carbon #	$^{13}C\ \delta$	$^1H\ \delta$	$^{13}C\ \delta$	$^1H\ \delta$	$^{13}C\ \delta$	$^1H\ \delta$
1	58.08	-	58.00	-	58.04	-
2	47.64	2.68	47.69	2.71	47.61	2.71
3	22.00	1.49	21.82	1.62	21.89	1.50
		1.61		1.51		1.61
4	33.77	1.61	33.71	1.62	33.72	1.61
		1.87		1.89		1.88
5	42.53	1.87	42.67	1.89	42.48	1.89
6	28.63	0.95	28.47	0.97	28.55	0.95
		1.14		1.08		1.10
7	49.07	2.57	49.04	2.62	49.04	2.62
8	84.97	-	84.95	-	85.11	-
9	10.96	1.28	10.87	1.28	10.96	1.30
10	140.41	-	111.32	-	129.43	-
	140.45					
11	128.38	7.24	119.16	7.38	126.70	7.33
	128.48					
12	115.33	7.02	127.51	7.62	130.03	7.96
	115.62					
13	160.58	-	132.73	-	149.23	-
	163.83					
14	-	-	149.29	-	167.09	-
15	-	-	-	-	52.29	3.87
OH	-	2.08	-	2.22	-	2.10

67

Chapter 4 Asymmetric Induction Studies

4.1 Asymmetric Induction in the Solid State Photolysis of Benzonorbornene Derivatives

4.1.1 Formation of Chiral Salts With Achiral Ketoacid 46

Using a variety of commercially available optically pure amines, thirteen chiral salts of achiral ketoacid **46** were prepared. For each preparation, equimolar amounts of ketoacid **46** and the optically pure amine were added together in solution and allowed to precipitate gradually over a period of 1-7 days. In the cases where complete evaporation of the solvent left either an oil or oily solid, trituration with diethyl ether was used to facilitate formation of the solid. The resulting chiral salts were isolated by vacuum filtration followed by thorough washing with ether to remove any unreacted acid or amine. Attempts to recrystallize the salts from a variety of different solvent systems in order to obtain crystals suitable for X-ray diffraction studies were unsuccessful with the exception of salt **81** (Figure 4.1). This was likely due in part to the general insolubility of the salts in solvents other than dimethylsulfoxide, methanol and mixtures of ethanol and/or methanol with water. Table 4.1 shows the chiral salts formed along with the crystal morphology, solvent system used, and melting point of the isolated product.
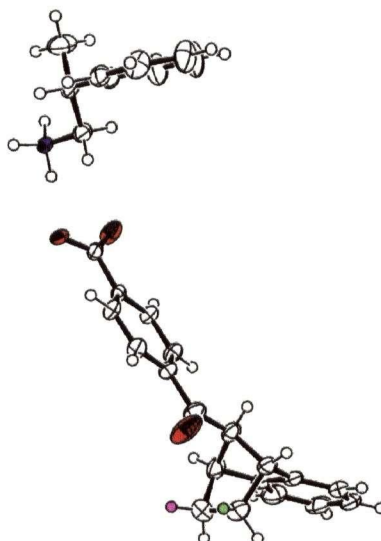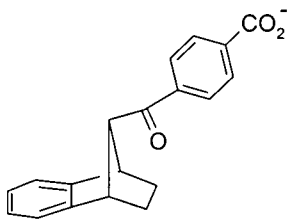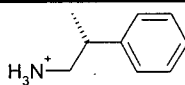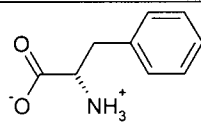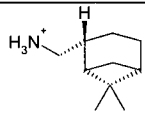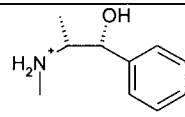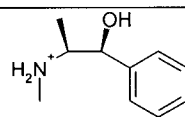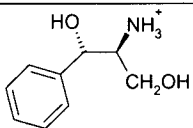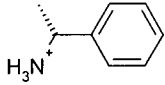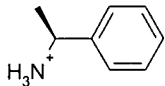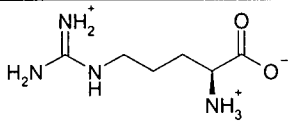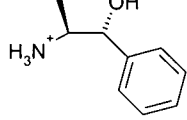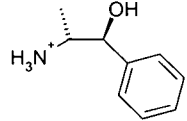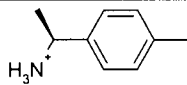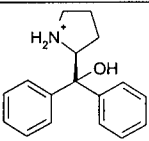
Figure 4.1 ORTEP representation of salt **81**. Oxygen atoms have been coloured red; nitrogen, blue; the γ-hydrogen favoured for abstraction, green; and the unfavoured γ-hydrogen, purple.

Table 4.1 Chiral salts prepared from achiral ketoacid **46** and optically pure amines.

Salt	Cation	Morphology (solvent)	mp (°C)
81[a]	(R)-(+)-β-methylphenylethylamine	prisms (MeOH)	156-158
82[b]	(S)-(-)-phenylalanine	fine needles (MeOH/EtOH/H$_2$O)	178-179.5
83	(-)-cis-myrtanylamine	fine needles (MeOH)	154-156
84	(1R,2R)-(+)-pseudoephedrine	powder[c] (MeOH)	131-132.5
85	(1S,2S)-(-)-pseudoephedrine	powder[c] (MeOH)	130-132
86	(1S,2S)-(+)-2-amino-1-phenyl-1,3-propanediol	plates (MeOH)	157-158

69

87	(R)-(+)-1-phenylethylamine	powder (MeOH)	178-180
88	(S)-(-)-1-phenylethylamine	powder (MeOH)	178-179.5
89	(S)-(+)-arginine	powder[c] (MeOH/H₂O)	154-156
90	(1R,2S)-(-)-norephedrine	powder[c] (MeOH)	153-154
91	(1S,2R)-(+)-norephedrine	powder[c] (MeOH)	154-156
92	(S)-(-)-α,4-dimethylbenzylamine	thin needles[c] (MeOH)	196-199
93	(S)-(-)-α,α-diphenyl-2-pyrrolidinemethanol	powder (MeOH)	224-226

[a]X-ray crystal structure obtained. [b]This compound is most likely an inclusion complex rather than an ammonium carboxylate salt; an explanation is given in the text. [c]Initially isolated oil was triturated with ether until a solid precipitate formed.

Although salt **81** will be seen to give no observable photoreaction, there are some features of the crystal structure deserving mention. From Figure 4.1 it is clearly seen that the carbonyl oxygen atom lies closer to one of the two diastereotopic γ-hydrogens (the closer has been coloured green, the further purple). It is reasonable to assume that all of the salts showing optical selectivity following solid state photolysis crystallize in a similar manner. Therefore, the observed enantioselectivity is due to a conformational effect during crystallization rather than a direct influence of the chiral auxiliary upon the reaction, or even the chiral cavity created by the neighbouring molecules. The idea that the auxiliary could indeed be uninvolved in any part of the reaction after the crystallization step is confirmed upon a closer examination of the unit cell, where it is seen that the closest auxiliary chirality centre is greater than 5 Å from the reacting γ-carbon.

The formation of an ammonium carboxylate linkage between the acid and amine was confirmed through the IR spectrum of each salt with the exception of **82**. In the IR spectrum of ketoacid **46**, the carbonyl stretch absorptions due to the ketone and carboxylic acid exist as a single, broadened band at 1680 cm^{-1} and 1675 cm^{-1} respectively. In the salts a much sharper absorption is observed at ~1680 cm^{-1} due to the ketone carbonyl stretch while new absorptions were observed for the symmetric (1370-1400 cm^{-1}) and asymmetric (1520-1546 cm^{-1}) stretches expected for a carboxylate group. Less conclusive evidence could be found in the broadening and shift of the carboxylic acid proton stretch (2500-2900 cm^{-1}) to that of an ammonium proton stretch (3300-2700 cm^{-1}). The 1:1 stoichiometry of the salts was confirmed by ^{1}H NMR spectroscopy through integration of signals representing single, isolated, protons for the acid and amine. In general, it was not possible to observe signals from ammonium or hydroxyl protons owing to deuterium exchange with the solvent. Microanalysis was used wherever possible to confirm the 1:1 composition of the salts, but this was hindered by the absorption of water during the crystallization process in many cases.

The exact nature of salt **82** is not definitively known but it has been termed a salt to avoid confusion. While the carbonyl stretching band is distinctly sharper as seen in the other salts, the strong asymmetric and symmetric absorptions of a carboxylate salt are not observed in the expected locations, although similar peaks are observed at 1500 cm^{-1} and 1294 cm^{-1}. The stretches expected for an ammonium ion are also narrower than observed for the other salts.

Unlike arginine (salt **89**), a basic amino acid, phenylalanine is a neutral amino acid and is therefore insufficiently basic to remove a proton from ketoacid **46**.

4.1.2 Photochemistry of the Chiral Ammonium Carboxylate Salts

4.1.2.1 Determination of the Enantioselectivity

Salts **81** through **93** were photolyzed in the crystalline state in the same manner as ketones **43**, **44**, **45** and **46**. For each salt a 2-3 mg sample was gently crushed between two microscope slides, sealed in a polyethylene bag under a nitrogen atmosphere, and photolyzed for various times using a Pyrex filtered ($\lambda > 290$ nm) 800 W Hg-Xe light source producing a collimated beam that was filtered through two dichroic filters to remove IR radiation. In order to achieve high conversions it was usually necessary to rotate the sample 180° midway through the reaction, exposing the rear side of the slides to the light and allowing as much of the sample as possible to react. Following photolysis the sample was dissolved in ethereal diazomethane, converting the carboxylate anions into methyl esters, and filtered through a short plug of silica gel to remove the chiral auxiliary. Due to the presence of minor impurity peaks overlapping with product peaks in the chiral analysis, isolation of each photoproduct (product peaks also overlapped each other) by preparative HPLC was required. Following purification the enantiomeric excess of each sample was determined using HPLC columns containing a chiral stationary phase; Chiralcel® OD® for cleavage product **71** and Chiralpak® AS® for cyclobutanol **65**. Details of the chromatographic separations for **65** and **71** are shown in Table 4.2. In the table, R_s refers to the chromatographic separation achieved, serving as a useful indicator of column performance, and is defined as:

$$R_s = \frac{2\left(t_{R2} - t_{R1}\right)}{W_1 + W_2}$$

where t_{r1} and t_{r2} are the retention times of the two enantiomer peaks and W_1 and W_2 are the peak widths at 0.607 of the peak height (0.5 of the base peak width). The enantiomeric excess of the photoproduct is a measure of the compound's optical purity and is defined by the equations:

(1) $\quad \%ee = \dfrac{[\alpha]_{mixture}}{[\alpha]_{pure\ enantiomer}} \times 100\% \quad or \quad$ (2) $\quad \%ee = \dfrac{[R] - [S]}{[R] + [S]} \times 100\%$

For practical purposes equation 1 was not used as it would require relatively large amounts of pure photoproduct in addition to the isolation of the photoproducts in enantiomerically pure form prior to analysis of the salts. Equation 2 on the other hand allows for the rapid analysis of small quantities of the photoproduct by HPLC or other analytical methods such as GC and NMR. Analysis of the optical purity of the compounds was indeed tested using chiral phase GC columns in the hope that the crude mixture of the photoproducts could be analyzed directly but suitable conditions were not found to resolve either compound with the available columns.

Both of the chiral stationary phase HPLC columns were obtained from Chiral Technologies Inc. The Chiralpak® AS® column is packed with amylose $tris$-((S)-α-methylbenzylcarbamate) as the chiral stationary phase on 10 μm silica gel while the Chiralcel® OD® column is packed with cellulose $tris$-(3,5-dimethylphenylcarbamate). In both cases a baseline resolution was obtained although the chromatographic resolution was significantly better for cyclobutanol **65** on the AS column (Figure 4.2a) than **71** on the OD column (Figure 4.2b).

Table 4.2 Chromatographic data for enantiomeric excess determination of **65** and **71**.

Compound	Column	HPLC Conditions			Retention Time (min.)[a]	R_s
		Solvents	Flow Rate (mL/min)	UV Detector (nm)		
65	AS[b]	95:5 hexanes:IPA	1.2	254	A: 14.2 B: 24.8	3.6
71	OD[c]	92:8 hexanes: IPA	1.2	254	A: 25.7 B: 32.3	1.7

[a]A refers to the first eluted peak, B to the second. [b]Chiralpak® AS® column (25 cm x 0.46 cm ID), Chiral Technologies Inc. [c]Chiralcel® OD® column (25 cm x 0.46 cm ID), Chiral Technologies Inc.
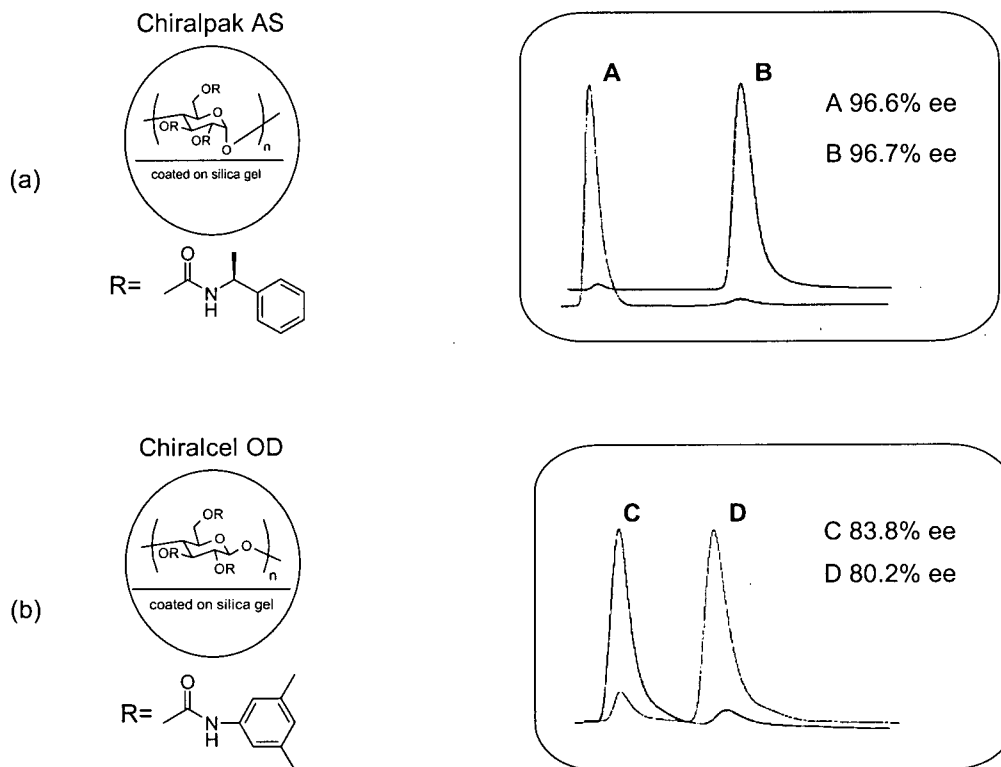
Figure 4.2 Column composition and separation for (a) *endo*-aryl cyclobutanol **65** on Chiralpak® AS®; (b) cleavage product **71** on Chiralcel® OD®.

4.1.2.2 Asymmetric Induction Results

Based on the results observed for the solid state photolyses of the 4 phenyl ketones studied (**43, 44, 45** and **46**) it is not surprising that the chiral salts of ketoacid **46** also display a varied reactivity. The salts can be roughly divided into three groups: A) (Table 4.3) salts giving primarily the *endo*-arylcyclobutanol photoproduct **65**, B) (Table 4.4) salts giving a mixture of cleavage product **71** and *endo*-arylcyclobutanol **65**, and C) (Table 4.5) salts that were essentially unreactive in the solid state. As the desired goal of the present research is to achieve both high enantio- and chemical selectivity simultaneously in the photoreaction, salts giving a single photoproduct at high conversion were of the most interest. However, in terms of understanding the observed reactivity, the two other groups become more important, especially when considering the partitioning between the two different modes of reactivity. For future work, it would be extremely desirable to determine why different reactivities are obtained for the same

substrate, as this could possibly allow for directing reactions to favour formation of one photoproduct over another through crystal engineering. An in-depth discussion of the modes of reactivity is presented in Section 5.1.

Table 4.3 Solid state photolysis of Group A[a] optically active salts of ketone **46**.

Salt	Amine	% Conversion[b]	% Yield[b]		% ee[c]	α[d]
			71	**65**		
82	(S)-(-)-phenylalanine	>99	trace	>99	86	A
		99[e]	6	94	84	
		>97[f]	6	93	88	
83	(-)-cis-myrtanylamine	>99	trace	>99	4	B
87	(R)-(+)-1-phenylethylamine	24	11	89	97	B
		66	trace	>99	92	B
88	(S)-(-)-1-phenylethylamine	17	9	91	96	A
		99	5	94	93	A
89	(l)-(S)-(+)-arginine	54	trace	>99	4	A

[a]Group A indicates salts in which there was <10% **71** in the product mixture. [b]Irradiations conducted at room temperature on ~2.5 mg crystalline sample crushed between two glass slides and sealed in a N_2 atmosphere. Conversions and yields were determined by GC following ethereal CH_2N_2 workup and filtration through silica gel. [c]Enantiomeric excesses were determined for compound **65** using a Chiralpak® AS® HPLC column. [d]A refers to the first peak eluted in the HPLC analysis as the predominant enantiomer, B to the second. [e]Reaction performed on a 10 mg scale as a suspension in hexanes. [f]Reaction performed on 250 mg scale as a suspension in hexanes.

The data in Table 4.3 show the solid state asymmetric induction study results for the 5 salts reacting to give primarily *endo*-arylcyclobutanol **65** following work-up and analysis. Although a completely clean reaction was never observed for the salts due to the presence of varying degrees of minor photoproducts formed during irradiation, the degree of selectivity observed when compared to the solution photolyses of the ketones in this system has been greatly enhanced. The most favourable results were observed for the salt formed between acid **46** and (S)-(-)-1-phenylethylamine, where an enantiomeric excess of 93% was achieved at 99% conversion of the starting material with a 94% yield of **65** for salt **88**. As expected, photolysis

of the salt composed of the opposite antipode of the chiral auxiliary, **87**, led to formation of the enantiomeric photoproduct. Acceptable enantioselectivities were also obtained for salt **82**, formed between **46** and phenylalanine, where an enantioselectivity of 86% percent was obtained at a quantitative conversion with only trace amounts of impurities. Since photolysis of salt **82** tended to be cleaner than the rest, attempts were made to increase the scale of the reaction by suspending the crystalline sample in hexanes. Although there was very little change in the enantioselectivity of the reaction, there was a larger amount of impurities observed and the chemical yield of the reaction was reduced to 93% when performed on a 250 mg scale. This is possibly due to a relaxation effect upon the lattice structure near the surface of the crystals induced by the presence of solvent in the reaction system.

The final salts in the first group, **83** and **89**, while exhibiting the same high chemical selectivity, show a disappointing enantioselectivity, both at 4%. Previous studies have shown that carrying out reactions such as this to a lower conversion often results in an increase in the observed enantioselectivity. Such a study was not undertaken for these salts since high enantioselectivities had already been achieved. While it was not possible to obtain X-ray crystal structures of either of these salts, the low enantioselectivity observed is most likely due to an effect termed *conformational enantiomerism.*[82] This occurs when both enantiomeric conformations of the achiral acid exist within the crystal lattice and is presented in further detail in Section 4.2.2.3. As each enantiomeric conformation favours abstraction of one of the two enantiotopic γ-hydrogens, the resulting photoproduct mixture contains nearly equal amounts of each enantiomer.

The second group of salts shows reactivity giving a mixture containing approximately 80% *endo*-arylcyclobutanol **65** and 20% cleavage product **71** as shown in Table 4.4. High to moderate enantioselectivities were observed for both photoproducts at low conversions; however, these values drop off at higher conversion. The loss in enantioselectivity is likely due to a breakdown in the crystal lattice over the course of the reaction. The increased conformational mobility of cleavage product **71** with respect to the more rigid cyclobutanol **65** likely plays a role in the lattice breakdown. Since two photoproducts are produced in these reactions while only one was observed previously, it is probable that the acid portions of the salts adopt a different conformation that makes the cleavage reaction more favourable. The following chapter will discuss the effects of conformational changes on reactivity.

Table 4.4 Solid state photolysis of Group B[a] optically active salts of ketone **46**.

Salt	Amine	% Conv.[b]	65		71	
			% Yield[b]	% ee[c] $(\alpha)^e$	% Yield[b]	% ee[d] $(\alpha)^e$
84	(*1R,2R*)-(-)-pseudoephedrine	22	78	96 (B)	22	84 (C)
		42	81	86 (B)	19	77 (C)
85	(*1S,2S*)-(+)-pseudoephedrine	28	80	89 (A)	20	80 (D)
		35	81	89 (A)	19	76 (D)
86	(*1S,2S*)-(+)-2-amino-1-phenyl-1,3-propandiol	21	76	12 (B)	24	63 (C)
		31	79	10 (B)	21	54 (C)

[a]Group B indicates salts in which there was ~20% **71** and 80% **65** in the product mixture. [b]Irradiations conducted at room temperature on ~2.5 mg crystalline sample crushed between two glass slides and sealed in a N_2 atmosphere. Conversions and yields were determined by GC following ethereal CH_2N_2 workup and filtration through silica gel. [c]Enantiomeric excesses were determined for compound **71** using a Chiralcel® OD® HPLC column. [d]Enantiomeric excesses were determined for compound **65** using a Chiralpak® AS® HPLC column. [e]A and C refer to the first eluted peak by HPLC as being the predominant enantiomer, B and D to the second.

The results obtained upon photolysis of salt **86** show a remarkable contrast when compared with those for salts **84** and **85**. Salts **84** and **85**, formed with (-) and (+) pseudoephedrine, show good enantioselectivity at low conversion for both photoproducts while salt **86**, formed with 2-amino-1-phenyl-1,3-propanediol, shows low enantioselectivity for cyclobutanol **65** and moderate enantioselectivity for **71**, even at low conversion. The variable enantioselectivity observed for salt **86** can be attributed in part to conformational enantiomerism since, in the crystalline state, the enantiomeric conformations exist as diastereomers and may therefore have different rates of reactivity. As illustrated in Figure 4.3, if the rates of the two cyclization reactions (k_{cy+} and k_{cy-}), producing the (+) and (-) enantiomers of the *endo*-arylcyclobutanol, occur at roughly the same rate a low enantioselectivity would be expected. However, if the corresponding rates of cleavage (k_{cl+} and k_{cl-}) are significantly different a moderate ee may be observed at low conversions within the same crystal.
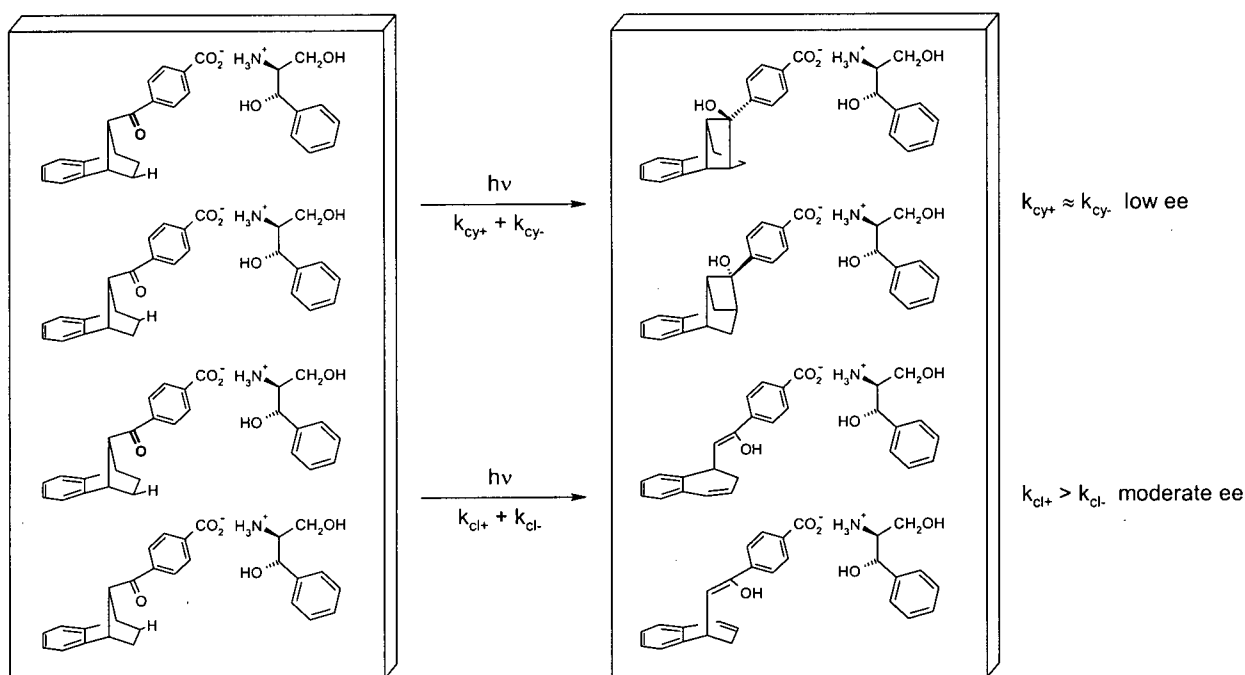
Figure 4.3 Rationale for mixed optical selectivity in the photolysis of salt **86**.

The final group of 5 salts are those that showed minimal production of photoproducts during photolysis, as was also observed for ketone **45**. A summary of the photolyses conducted is presented in Table 4.5 where it is seen that prolonged irradiation led to very low conversion of the starting material. Similar irradiation times for the salts discussed in Table 4.3 and Table 4.4 led to near quantitative conversions. Based on the crystal structure obtained for salt **81**, it seems improbable that hydrogen abstraction does not occur due to the favourable hydrogen abstraction parameters observed. For these salts it is most likely that the reverse hydrogen abstraction reaction, reforming the starting ketone, occurs rather than one proceeding to a photoproduct. A more in-depth discussion of these factors is presented in the following chapter.

Table 4.5 Solid state photolysis of Group C[a] optically active salts of ketone **46**.

Salt	Amine	Irradiation time (h)	% Conversion[b]
81	(R)-(+)-β-methylphenethylamine	24	3
90	(1R,2S)-(-)-norephedrine	24	4
91	(1S,2R)-(+)-norephedrine	3	0
92	(S)-(-)-α,4-dimethylbenzyl amine	17.5	8
93	(S)-(-)-α,α-diphenyl-2-pyrrolidemethanol	24	4

[a]Group C indicates salts in which there was <10% conversion to photoproducts upon prolonged irradiation. [b]Irradiations conducted at room temperature on ~2.5 mg crystalline sample crushed between two glass slides and sealed in a N_2 atmosphere. Conversions were determined by GC following ethereal CH_2N_2 workup and filtration through silica gel.

Photolyses of selected salts in methanol (Table 4.6) shows that the chiral crystal lattice does indeed have a profound effect on both the reactivity and enantioselectivity. Salt **82**, forming predominantly the *endo*-aryl cyclobutanol photoproduct with a high optical purity upon photolysis in the solid state, shows a nearly equal mixture of racemic cleavage and *endo*-aryl cyclobutanol when photolyzed as a methanolic solution. Similarly, salt **88**, which was virtually unreactive in the solid state also gave a racemic mixture of the two photoproducts in solution. These results are not surprising when the nature of the chiral auxiliaries is examined. Unlike traditional, covalent chiral auxiliaries that are located near the reacting centre, the ammonium carboxylate linkage involved in bonding the achiral and chiral components of the salts places the reacting centre far removed from the auxiliary. This large distance is unimportant when reactions are carried out in the solid state, as the chiral influence is exerted upon the reacting centre indirectly by the chiral crystal lattice and not by the direct chiral/steric influence of the auxiliary.

Table 4.6 Solution photolysis of selected optically active salts of ketone **46**.

Salt	Amine	% Conv.[a]	65		71	
			% Yield[a]	% ee[b]	% Yield[a]	% ee[c]
82	(S)-(-)-phenylalanine	98.1	48	4	45	2
88	(S)-(-)-1-phenylethylamine	95.7	50	1	46	3

[a]Irradiations conducted at room temperature on ~2.5 mg crystalline sample dissolved in methanol and under a N_2 atmosphere. Conversions and yields were determined by GC following removal of the solvent *in vacuo*, ethereal CH_2N_2 workup and filtration through silica gel. [b]Enantiomeric excesses were determined for compound **71** using a Chiralcel OD HPLC column. [c]Enantiomeric excesses were determined for compound **65** using a Chiralpak AS HPLC column.
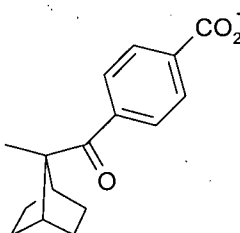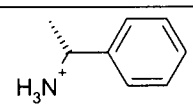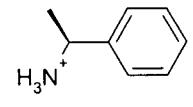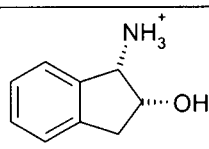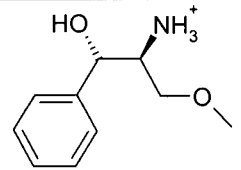
4.2 Preparation of Chiral Ammonium Carboxylate Salts With Ketoacid 56
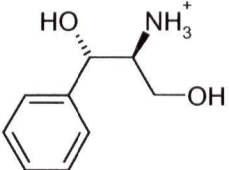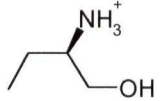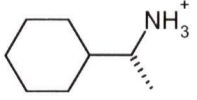
4.2.1 Formation of the Ammonium Carboxylate Salts

As for the previous enantioselectivity study discussed in Section 4.1, chiral salts of ketoacid **56** and various optically pure, commercially available amines were prepared as shown in Table 4.7. This was accomplished by dissolving ketoacid **56** in methanol and adding an equimolar amount of the amine as either the neat liquid or a methanolic solution (crystalline amines). The mixture was then allowed to crystallize over a period of days as the solvent slowly evaporated. Before the evaporation of the solvent was complete the crystallized salt was isolated by vacuum filtration and washed with ether to remove any residual acid or amine. Characterization by ^{1}H NMR spectroscopy showed that in each case the isolated salt was a 1:1 adduct of the acid and amine. Confirmation of this stoichiometry was obtained by elemental analysis where possible, although these results were also hampered by the absorption of water during the recrystallization process for many of the salts, especially for those involving hydroxyl groups on the amines. The formation of an ammonium carboxylate bond was confirmed by changes in the IR spectra for the salts when compared to the parent acid. A broad carbonyl stretch containing absorptions for the carbonyls of both the ketone and carboxylic acid is observed in ketoacid **56** at 1676 cm^{-1}. In the salts the carbonyl absorption at ~1667 cm^{-1} is much sharper suggesting that it is due only to the stretching vibration of the ketone. Asymmetric and symmetric stretches consistent with carboxylates are observed in the salts at

1540-1520 cm^{-1} and ~1395 cm^{-1} respectively. For two of the salts, **94** and **95** (Figure 4.4), crystals of X-ray quality were obtained, allowing for in-depth studies to be undertaken on the reactivity and selectivity observed in this system.

Table 4.7 Optically active salts prepared from ketone **56**.

Salt	Cation	Morphology	mp (°C)
94[a]	H_3N^+ (*R*)-(+)-1-phenylethylamine	prisms	197 - 198.5
95[a]	H_3N^+ (*S*)-(-)-1-phenylethylamine	prisms	197 - 199
96	NH_3^+ ····OH (*1S,2R*)-(-)-*cis*-1-amino-2-indanol	powder	199 (dec)
97	HO NH_3^+ O (*1S,2S*)-(+)-2-amino-3-methoxy-1-phenyl- 1-propanol	powder	162 - 163

98	HO NH$_3^+$ OH (*1R,2R*)-(-)-2-amino-1-phenyl-1,3-propanediol	powder	162 - 164
99	NH$_3^+$ OH (*R*)-(-)-2-amino-1-butanol	powder	174 - 176.5
100	NH$_3^+$ (*R*)-(-)-cyclohexylethylamine	powder	196 - 198.5

[a]X-ray crystal structure obtained.

(a)   (b)
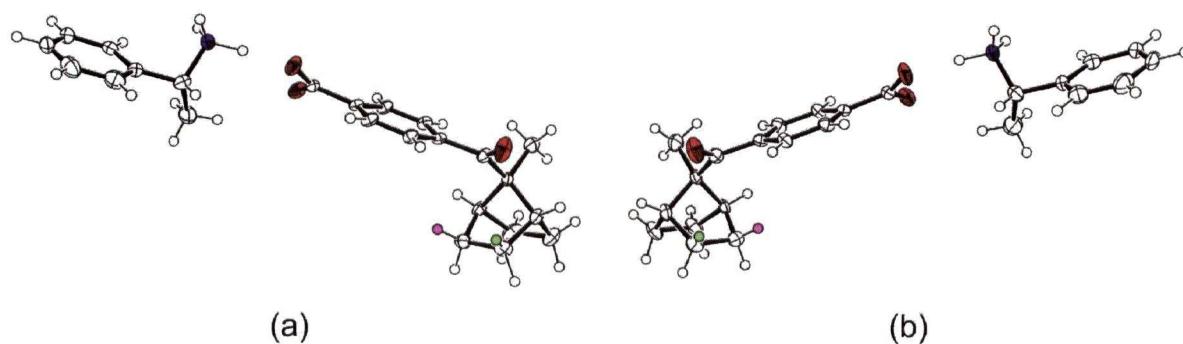
Figure 4.4 ORTEP representations of (a) salt **94** and (b) salt **95**. Oxygen atoms have been coloured red; nitrogen, blue; the γ-hydrogen most favoured for abstraction, green and less favoured, purple.

4.2.2 Photochemistry of Chiral Salts 94 to 100

4.2.2.1 Enantioselectivity Determination

Determination of the enantioselectivity was performed utilizing HPLC columns possessing a chiral stationary phase. Details of the chromatographic separation of cyclobutanol 78 are given in Table 4.8 and Figure 4.5. The Chiralcel® OC® column, from Chiral Technologies Inc. is packed with cellulose *tris*-phenylcarbamate as the chiral stationary phase on 10 μm silica. Due to the high chemical selectivity in this system it was possible to obtain sufficient amounts of each enantiomer of cyclobutanol 78 in a highly enantioenriched form, allowing for determination of the sign of the optical rotation by polarimetry at the sodium D-line.

Table 4.8 Chromatographic data for enantiomeric excess determination of cyclobutanol **78**.

Compound	Column	HPLC Conditions			Retention Time (min.)[a]	R_s
		Solvents	Flow Rate (mL/min)	UV Detector (nm)		
78	OC[b]	97:3 hexanes:IPA	0.4	254	(+): 62.2 (-): 70.0	1.92

[a](+) and (-) refers to the sign of the optical rotation of the enantiomer as determined at the sodium D-line.
[b]Chiralcel® OC® column (25 cm x 0.46 cm ID), Chiral Technologies Inc.

Chiralcel OC

R=
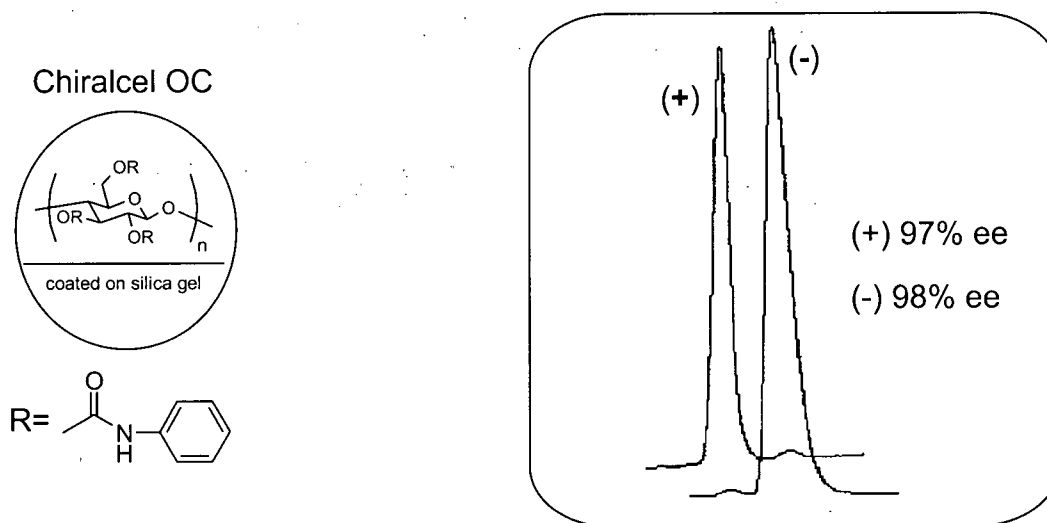
Figure 4.5 Column composition and separation for *endo*-aryl cyclobutanol **78** on Chiralcel® OC®.

4.2.2.2 Solution State Photochemistry of Salts 95 and 99

In order to confirm that the selectivity observed in the salts was indeed due to the influence of the chiral crystal lattice and not merely the presence of the optically pure amine, two of the salts, **95** and **99**, were subjected to photolysis in solution. For this the two salts were dissolved in methanol and irradiated, using Pyrex filtered light, to complete conversion. As expected both salts gave an essentially racemic mixture following conversion to cyclobutanol **78** as shown in Table 4.9.

Table 4.9 Solution state photolysis of selected optically active salts of ketone **56**.

Salt	Amine	% Conversion[a]	% ee[b]	α[c]
95	(*S*)-(-)-phenylethylamine	100	1	-
99	(*R*)-(-)-2-amino-1-butanol	100	2	-

[a]Irradiations conducted at room temperature on ~2.5 mg crystalline sample dissolved in methanol and under a N_2 atmosphere. Conversions and yields were determined by GC following removal of the solvent *in vacuo*, ethereal CH_2N_2 workup and filtration through silica gel. [b]Enantiomeric excesses were determined for compound **78** using a Chiralcel OC HPLC column. [c]Sign of the optical rotation at the sodium D-line.

4.2.2.3 Solid State Photolysis of Salts 94 through 100

Much like the solid state photolyses of the associated ketones (**54, 55, 56** and **57**), all of the salts exhibited extremely clean reactions with virtually no minor photoproducts formed. Salts were prepared for photolysis by crushing a 2-3 mg sample between 2 microscope slides and sealing under a nitrogen atmosphere in a polyethylene bag. Each sample was then irradiated using Pyrex-filtered light from a water-cooled 450 W mercury arc lamp. With the exception of the lower conversions examined for salt **100**, salts were irradiated for 40 minutes, a time found to completely convert salts **94** and **95**. Following irradiation the salts were scraped off of the microscope slides and dissolved in ethereal diazomethane. Following solvent evaporation the resulting oil was dissolved in dichloromethane and filtered through a short plug of silica gel to remove the chiral auxiliary. The enantioselectivity was then determined by HPLC.

From the results summarized in Table 4.10 it is seen that a high degree of enantioselectivity was observed for five of the seven salts, with the 1-phenylethylamine salts (**94** and **95**) reacting to give almost entirely one enantiomer (98 and 97% ee respectively) at complete conversion. As expected, by using opposite antipodes of the chiral auxiliary either enantiomer of the final product may be obtained. High selectivities were also observed for (-)-*cis*-1-amino-2-indanol (**96**, 96% ee at 94% conversion), (+)-2-amino-3-methoxy-1-phenyl-1-propanol (**97**, 96% ee at 88% conversion) and (-)-2-amino-1-butanol (**99**, 84%ee at >99% conversion). Lower selectivities were observed for (-)-2-amino-1-phenyl-1,3-propanediol (**98**, 35% ee at 98% conversion) and (-)-cyclohexylethylamine (**100**, <1% ee at >99% conversion).

Owing to the high rate of reactivity and exceptionally clean product mixtures obtained upon photolysis in this system it was decided to further examine the reactivity of salt **100**, exhibiting no selectivity at high conversion. While the reasons for low selectivity are not always known, salt **98** for example, the results obtained for salt **100** suggest the likelihood of *conformational enantiomerism* within the crystal lattice. This assumption is based on the fact that at complete conversion the observed enantioselectivity is essentially zero, indicating that there is an equal number of molecules with the (+) and (-) absolute configurations in the crystal. Since the large molecular motions required for rotations of the carbonyl are greatly hindered by the neighbouring molecules in the crystal lattice it is reasonable to assume that the unit cell of salt **100** contains an equal number of acid molecules with enantiomeric conformations (i.e. an

equal number of molecules in the pro-(+) and pro-(-) conformation) . As shown in Figure 4.6, the carbonyl group will favour abstraction of one of the two γ-hydrogens depending on its orientation in the crystal. Since the two independent molecules, **100a** and **100b**, are diastereomers in the chiral crystal lattice, they should react at different rates, k_+ and k_-, to produce the (+) and (-) enantiomers of cyclobutanol **78** following workup.

Table 4.10 Solid state photolysis of optically active salts of ketone **56**.

Salt	Amine	% Conversion[a]	% ee[b]	α[c]
94	(*R*)-(+)-phenylethylamine	>99	98	-
95	(*S*)-(-)-phenylethylamine	>99	97	+
96	(*1S,2R*)-(-)-*cis*-1-amino-2-indanol	94	96	+
97	(*1S,2S*)-(+)-2-amino-3-methoxy-1-phenyl-1-propanol	88	95	-
98	(*1R,2R*)-(-)-2-amino-1-phenyl-1,3-propanediol	98	35	-
99	(*R*)-(-)-2-amino-1-butanol	>99	84	-
100	(*R*)-(-)-cyclohexylethylamine	97[d]	2	+
		>99	<1	
		76	10	
		54	12	
		37	22	
		10	38	
		6	44	
		.4	46	

[a]Irradiations conducted at room temperature on ~2.5 mg crystalline sample crushed between two glass slides and sealed in a N_2 atmosphere. Conversions and yields were determined by GC following ethereal CH_2N_2 workup and filtration through silica gel. [b]Enantiomeric excesses for cyclobutanol **78** were determined using a Chiralcel® OC® HPLC column. [c]Signs of rotation were determined at the sodium D-line. [d]Photolysis conducted at -27°C.
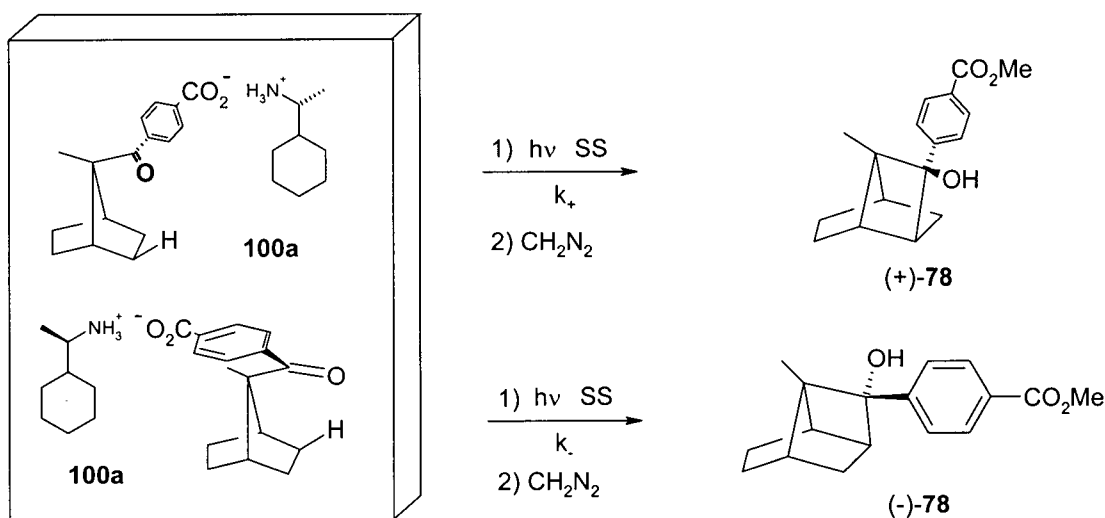
Figure 4.6 Proposed conformational enantiomerism in salt **100**.

Photolysis of salt **100** in the solid state to different degrees of conversion does indeed lead to modest enantioselectivity at low conversion. From Figure 4.7 and Figure 4.8 it is seen that at low conversion there is an appreciable amount of enantioselectivity in the crystal owing to the differing rates of reactivity for each conformer. At low conversions ees of over 40% were attainable, and while not practical in a synthetic sense, these results do demonstrate that the enantiomers are formed at different rates during the photolysis. As the ultimate amount of each enantiomer is predetermined by the conformation of the starting material, the enantioselectivity declines as the conversion increases.

Enantioselectivity at Varying Conversions for Salt 100
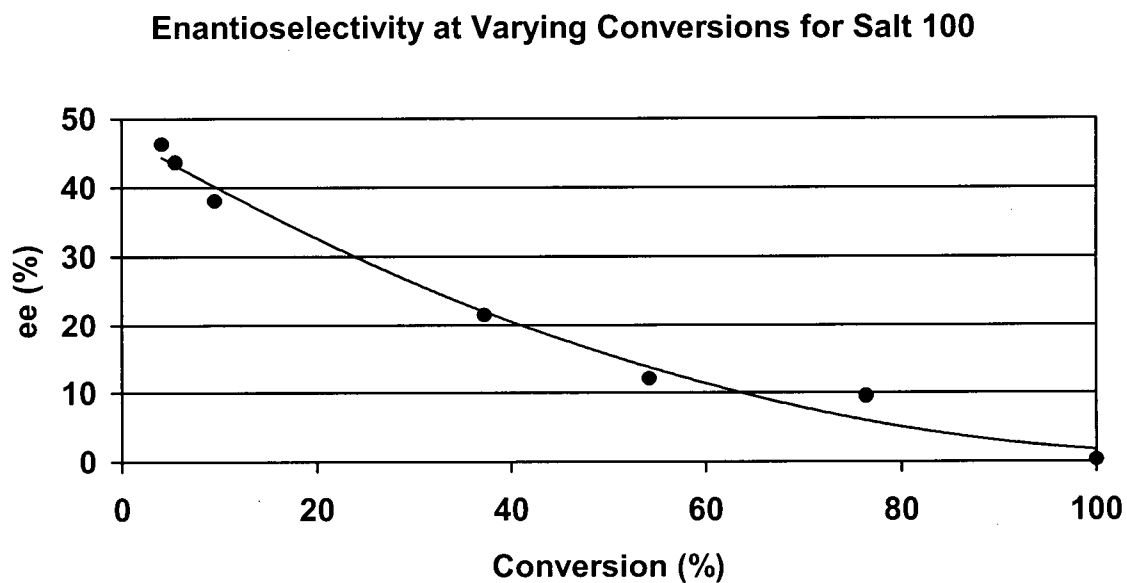
Figure 4.7 Enantioselectivity observed for salt **100** at different conversions.

Salt 100 Product Composition at Varying Conversions
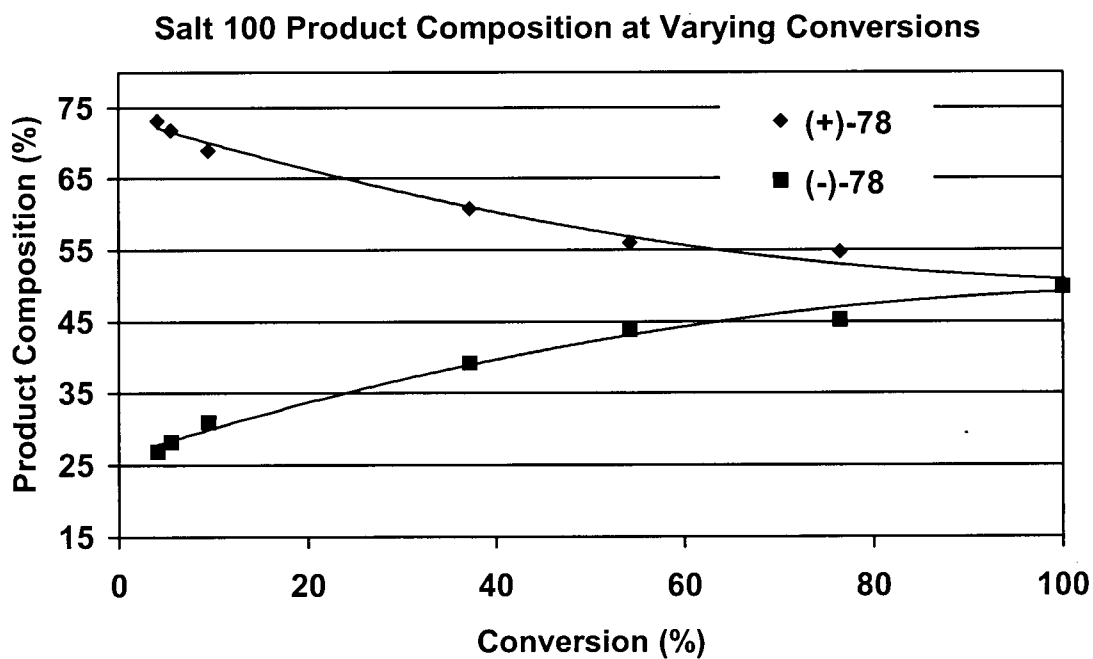
Figure 4.8 Product composition following photolysis of salt **100** at varying conversions.

Chapter 5 Crystal Structure - Reactivity Relationships

5.1 Crystal Structure - Solid State Reactivity Relationships

The ability to correlate the solid state structure of a molecule (obtained by X-ray crystallography) and its observed reactivity in the solid state is an invaluable tool for examining how and why reactions occur within crystals. This is particularly useful in the benzonorbornene system where three different types of reactivity were observed. Ester **45** and three of the salts showed little reaction after a 24 hour period, acid **46** and 5 of the salts gave primarily the *endo-*aryl cyclobutanol product, while the remaining salts consistently gave an 80:20 *endo-*aryl cyclobutanol:cleavage product mixture. From the five crystal structures obtained for ketones in this series of compounds, variations are readily seen in the ketone conformation, giving rise to the differing modes of reaction. The observed reactivity in the methylnorbornane system was much more consistent, with all ketones giving a single photoproduct. Analysis of the 6 crystal structures obtained shows that all of the ketones adopt similar solid state conformations.

5.2 Parameters for Hydrogen Abstraction

In constructing a relationship between a molecule's conformation in the crystal structure and its observed reactivity a number of different areas need to be addressed. Before trying to predict the observed outcome for a given reaction it is necessary to ascertain whether it is even possible for a reaction to occur. In studying the Norrish/Yang photochemistry of a molecule this means whether or not hydrogen abstraction is possible. Obviously, if the molecule does not lie in an orientation that would allow for abstraction to occur, it would not be expected that a product would be observed.

When examining the structure of both the benzornorbornene and norbornane derivatives it is obvious that there are more than two γ-hydrogen atoms in each molecule. In the following discussions, use of the term γ-hydrogen refers only to those two hydrogens atoms that are in a position to be intramolecularly abstracted by the carbonyl group upon photoexcitation.
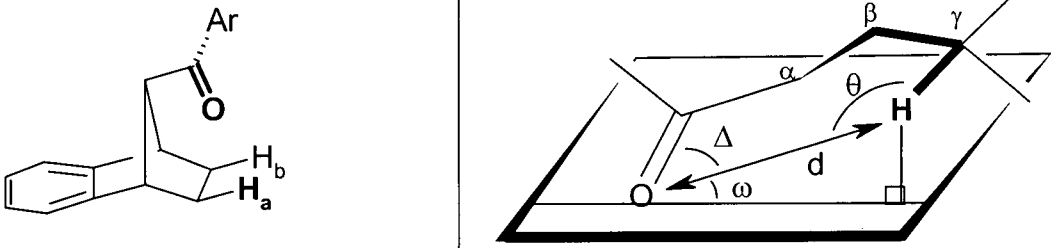
5.2.1 Benzonorbornene Derivatives

From the discussion of hydrogen abstraction parameters given in the Introduction it is seen that all of the ketones presented in Table 5.1 have parameters within favourable limits of the "ideal" values. Most notable is the differentiation between the two enantiotopic γ-hydrogens, with one, H_a (d_{avg} = 2.51 ± 0.04 Å) lying well within the ideal value of 2.74 Å, while the other, H_b (d_{avg} = 3.07 ± 0.15 Å) lies far outside. Although hydrogen abstractions have been observed at distances up to 3.15 Å,[83] studies of Norrish type II abstraction reactions have shown that a difference in the distances of only 0.27 Å will lead to the exclusive abstraction of one hydrogen over the other.[84] Values observed for the parameter θ (109 ± 0.5°), representing the alignment of the C-H bond orbitals with the oxygen atom, all lie outside the ideal value of 180° but this has not been found to preclude reactivity. Although 180° does represent a perfect alignment, obtaining this value would put the molecule into an extremely strained conformation. Values for Δ are well within acceptable abstraction parameters, and while the average value of 97 ± 4° may tend to suggest support for the carbonyl group model proposed by Kasha,[53a] knowing that variations from the ideal are acceptable and will still lead to reactivity, such a statement is not supported by the current data. Deviations from the ideal value are also commonly seen for ω (33 ± 12°) as is observed for all of the ketones. It has been suggested that the rate of hydrogen abstraction is proportional to the angle ω, and is governed by a $\cos^2\omega$ dependence based on the electron density function of a p-orbital.[85] Therefore, an ω value of 33° would be expected to retain 72% of the reactivity observed for a ketone possessing the ideal value of 0°.

While the data do point toward all of the ketones being able to undergo hydrogen abstraction in the solid state, there is a suggestion that differing conformations are indeed responsible for changes in the observed reactivity for some of the ketones, particularly unreactivity. For ketones **45** and **81**, both unreactive in the solid state, Δ is ~10° higher and ω is ~25° lower than the corresponding values for the reactive ketones **44** and **46**. The fact that these abstraction parameters are closer to the ideal make it likely that abstraction does indeed occur but that the biradical intermediate undergoes the reverse abstraction reaction at a faster rate than the cleavage or cyclization reactions. Unfortunately, there is not a reliable method for detecting

the formation of biradical intermediates in the solid state, since trapping with an external reagent is not possible while maintaining crystal lattice integrity.[86]

Table 5.1 Hydrogen abstraction parameters for the phenyl ketones in the solid state.

		d (Å)	θ (°)	Δ (°)	ω (°)
Ideal		< 2.72	< 180	90-120	0
43	H_a	2.54	109	96	36
	H_b	3.05	98	65	59
44	H_a	2.55	109	92	44
	H_b	3.23	95	59	56
45	H_a	2.48	108	101	21
	H_b	2.94	99	78	58
46	H_a	2.55	108	92	47
	H_b	3.25	94	58	55
81	H_a	2.44	109	102	17
	H_b	2.88	100	76	57
Average (H_a)		2.51 ± 0.04	108.6 ± 0.5	96.6 ± 4	33 ± 12

*H_a (highlighted in bold) denotes the γ-hydrogen with the most favourable abstraction parameters.

5.2.2 Norbornane Derivatives

A summary of the hydrogen abstraction data for 6 norbornane derivatives is summarized in Table 5.2. It is not surprising that all of the ketones exhibit similar hydrogen abstraction parameters since all of the compounds in this series underwent a very clean photoreaction in the

Table 5.2 Abstraction parameters derived from X-ray crystallography.[a]

		d (Å)	θ (°)	Δ (°)	ω (°)
Ideal		< 2.72	< 180	90-120	0
54[b]	H_a	2.62	108	83	60
	H_b	3.41	92	48	48
	$H_{a'}$	2.63	107	83	60
	$H_{b'}$	3.42	92	47	47
55	H_a	2.75	106	79	62
	H_b	3.46	93	43	43
56	H_a	2.65	108	91	62
	H_b	3.43	92	46	45
57	H_a	2.73	105	79	63
	H_b	3.45	92	44	44
94	H_a	2.70	105	80	64
	H_b	3.47	92	43	43
95	H_a	2.70	104	80	64
	H_b	3.43	94	43	43
Average (H_a)		2.68 ± 0.05	106 ± 1.5	82 ± 4	62 ± 1.5

[a]H_a denotes the γ-hydrogen most likely to be abstracted. [b]Two independent molecules were present in the unit cell.

solid state to yield a cyclobutanol. Once again, a large difference in the abstraction values for the two γ-hydrogen atoms is found, with the abstracted hydrogen distance (d_{avg} = 2.68 ±0.05 Å) being 0.76 Å shorter than the non-abstracted hydrogen (d_{avg} = 3.44 ± 0.02 Å). This difference will lead to exclusive abstraction of H_a over H_b. As expected, the observed values for θ (θ_{avg} = 106 ± 1.5°) lie well outside the ideal value of 180°, but unlike the benzonorbornenyl ketones there are deviations for Δ (Δ_{avg} = 82 ± 4°). Although outside of the ideal range (90-120°) there was no observable effect on the outcome of the reaction. Similarly, values obtained for ω (ω_{avg} = 62 ± 1.5°) are well outside the ideal value, significantly more so than was seen for the benzonorbornene system. In the following discussion on cyclization parameters it will be seen

that large variations from the ideal ω value actually give a more favourable alignment for cyclization.

5.3 Cleavage Parameters

After determining whether or not hydrogen abstraction may occur, the parameters governing the cleavage and cyclization reactions may be examined. Cleavage is only possible when there exists a suitable overlap in the biradical intermediate between the p-orbital of the carbonyl carbon (C_1) with the C_2-C_3 (C_α-C_β) σ-bond, designated φ_1, and between the p-orbital of the γ-carbon (C_4) with the C_2-C_3 (C_α-C_β) σ-bond, designated φ_4, as shown in Figure 5.1.[54,56] A third torsion angle, φ, shows the overlap between the C_1-C_2 and C_3-C_4 sigma bonds. This angle does not directly affect the cleavage process but is given to show consistency in the carbon skeleton between the compounds in a series.
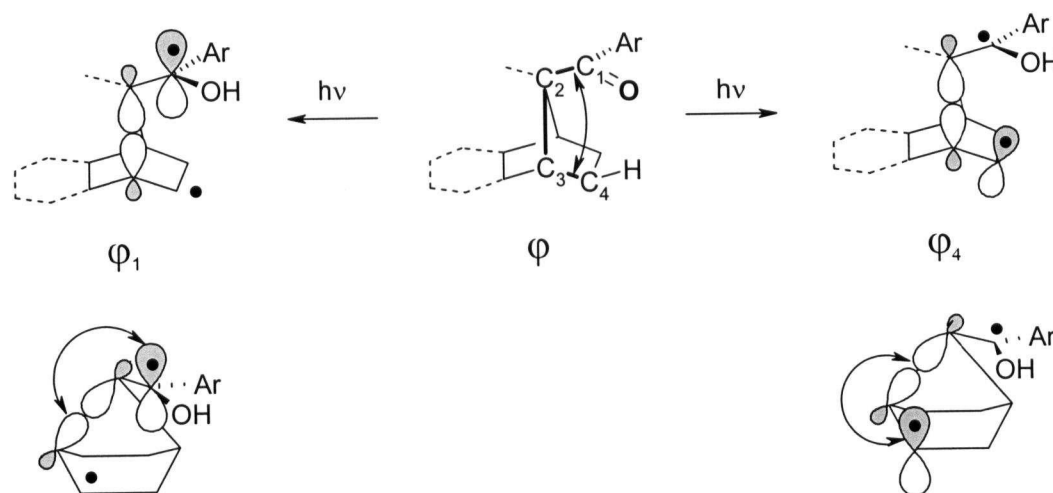
Figure 5.1 Orbital overlaps required for cleavage reactions.

Since the ground state structures of these molecules are being used to predict or explain their behaviour in the excited state some assumptions have to be made. When considering the cleavage parameters of a molecule these are that: 1) the hydroxybiradical intermediate formed

upon hydrogen abstraction maintains the same structure as the ketone, and 2) the radical centres (carbonyl carbon and γ-hydrogen) are sp^2 hybridized.

5.3.1 Benzonorbornene Derivatives

Table 5.3 lists the torsion angles φ_1, φ_4, and φ for the five ketones characterized by crystallography. As expected, the angle φ_4 (φ_{4avg} = -57°) is similar for all of the compounds since this angle is held constant by the rigid structure of the molecular skeleton and is not subject to conformational changes through bond rotation. Similarly, the values of φ are also fairly consistent (φ_{avg} = 67.5 ± 1°) for the same reasons. Values of φ_1, however, show a large fluctuation owing to rotation of the C_1-C_2 bond, with the reactive ketones (Yang cyclization) possessing a negative torsion angle (φ_{1avg} = -82 ± 3°) and the unreactive ketones (reverse hydrogen transfer) possessing a positive angle (φ_{1avg} = 76.5 ± 2°). This represents a 25° range in which the carbonyl group may lie. Interestingly, even though there is a large difference in the carbonyl position for the reactive and unreactive ketones, there is little difference in the suitability of the biradical for cleavage. This is due to the $\cos\varphi_1$ relationship (φ_4 also shows a cos dependence) for the overlapping orbitals.[87] Thus, when there is maximum overlap between the p-orbital of C_1 and the C_2-C_3 σ-bond, φ_1 will be 0° and $\cos\varphi_1$ will be 1, representing 100% orbital overlap. Alternatively, if the p-orbital of C_1 is perpendicular to the C_2-C_3 σ-bond, φ_1 will be 90° and $\cos\varphi_1$ will be 0, representing 0% orbital overlap. The data show that while the carbonyl does not lie in a position favouring cleavage, with φ_1 showing only 17% overlap of the orbitals, φ_4 has a moderately favourable overlap of 55%. With the large variations in φ_1 values obtained it does not seem unreasonable to assume that other values may be possible for the ketones that did not give crystals of suitable quality for X-ray diffraction. The prime candidates here would be salts **84**, **85**, and **86**, all giving both cleavage and cyclization products in their solid state photochemistry (see Table 4.4). For example, a 10° difference in the φ_1 value (φ_1 = -68°, $\cos\varphi_1$ = 0.37) would increase the orbital overlap by 80%, making the cleavage reaction much more competitive than in ketoacid **46** ($\cos\varphi_1$ = 0.21), where no cleavage was observed. It seems unlikely that this factor alone would lead to the observation of a cleavage reaction product unless the competing cyclization reaction also faced a conformational barrier.

Table 5.3 Geometric parameters[a] for biradical intermediates derived from the phenyl ketones.

	φ_1 (°)	$\cos(\varphi_1)$	φ_4 (°)	$\cos(\varphi_4)$	φ (°)
Ideal[b]	0	1	0	1	-
43	-87	0.05	-57	0.54	66
44	-81	0.16	-57	0.54	68
45	78	0.21	-57	0.54	69
46	-78	0.21	-57	0.54	68
81	75	0.26	-57	0.54	67
Average	-82 ± 3 (cyclization) / 76.5 ± 2 (RHT[c])	0.18 ± 0.1	-57	0.54	67.5 ± 1

[a]Parameters are given for the hydrogen atoms having favourable abstraction parameters only. [b]These values represent the ideal values giving the most favourable orbital overlap for a cleavage reaction to occur. [c]Reverse hydrogen transfer.

5.3.2 Norbornane Derivatives

The cleavage parameters obtained from the 6 crystal structures in the 7-methylnorbornane series (see Table 5.4) are much more consistent than those of the benzonorbornene derivatives. Once again, values obtained for φ_4 (φ_{4avg} = -56.5 ± 1°) and φ (φ_{avg} = 63.5 ± 1°) are relatively constant owing to the nature of the conformationally locked bicyclic skeleton. The φ_1 values (φ_{1avg} = -56.5 ± 3°) are also consistent despite the ability of the carbonyl to rotate about the C_1-C_2 bond. This behaviour was not observed for the benzonorbornene derivatives and can probably be attributed to the presence of the 7-methyl substituent, which provides a steric barrier through interactions with the aryl group. When considering the cosine relationship of the orbital overlap it is seen that both φ_1 (($\cos\varphi_1$)$_{avg}$ = 0.55 ± 0.05) and φ_4 (($\cos\varphi_4$)$_{avg}$ = 0.55 ± 0.01) have values that do not exclude the possibility of a cleavage reaction. Recalling that all of the ketones reacted exclusively in the solid state to give a cyclobutanol product (see Table 3.11), the question can be raised as to why a single type of

photoproduct is observed if the cleavage parameters are not unfavourable. The most reasonable answer is that although the cleavage reaction is not disfavoured, the cyclization reaction is more favoured to occur based on orbital overlap between C_1 and C_4.

Table 5.4 Geometric parameters[a] for the Norrish type II cleavage reaction.

	φ_1 (°)	$\cos(\varphi_1)$	φ_4 (°)	$\cos(\varphi_4)$	φ (°)
Ideal	0	1	0	1	-
54[b]	-61	0.48	-56	0.56	64
	-60	0.50	-57	0.54	65
55	-55	0.57	-57	0.54	64
56	-56	0.56	-55	0.57	62
57	-55	0.57	-57	0.54	63
94	-54	0.59	-57	0.54	63
95[c]	54	0.59	56	0.56	-63
Average	-56.5 ± 3	0.55 ± 0.05	-56.5 ± 1	0.55 ± 0.01	63.5 ± 1

[a]Parameters are only given for the hydrogen atom favoured for abstraction. [b]Two independent molecules were present in the unit cell. [c]The values of φ_1, φ_4, and φ have the negative values of those for the related salt **94** since the ketoacid portions of the salts are enantiomeric conformations of each other. When obtaining averages the absolute value of the angles were used.

5.4 Cyclization Parameters

The final parameters of interest in examining the Norrish/Yang reactivity of ketones are those necessary for cyclization, the predominant process observed in the solid state. Once again, the effects of a molecule's conformation can play a large role in determining its reactivity, since even if hydrogen abstraction occurs and cleavage is unfavourable, cyclization may not be geometrically possible. This would lead to reverse hydrogen transfer as the predominant reaction pathway. In order for cyclization to occur from the biradical intermediate formed upon hydrogen abstraction it is necessary for: (1) the p-orbitals on the γ-carbon and carbonyl carbon to be directed towards each other (Figure 5.2b), and (2) the carbonyl and γ-carbons to be within a suitable distance for ring closure to occur (Figure 5.2a). The ideal distance (D) is <3.40 Å, the

sum of the van der Waals radii for two carbon atoms,[51] and the ideal value for β is $0°$, representing perfect alignment of the two orbitals.

(a)   (b)
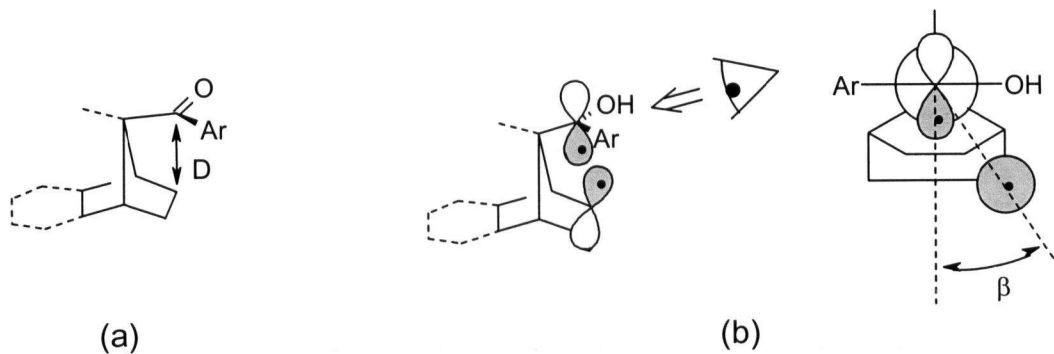
Figure 5.2 Cyclization parameters: (a) carbon-carbon distance D; (b) orbital alignment angle β.

The data presented in Table 5.5 for the benzonorbornene derivatives show that while all values of D are favourable ($D_{avg} = 3.01 \pm 0.03$ Å), the values of β lie far outside the ideal angle of $0°$. Of particular interest is that the two ketones found to undergo reverse hydrogen transfer in the solid state, **45** and **81**, have much higher values of β, $66°$ and $70°$ respectively, than the reactive (Yang cyclization) ketones ($\beta_{avg} = 49.5 \pm 5°$). This difference is the most likely reason for a lack of cyclization product in the solid state reaction of **45** and **81**. It is reasonable to assume that β will follow a cosine dependence as seen for the torsion angles described for the cleavage process, with $\cos\beta = 1$ representing maximum overlap at $0°$ and $\cos\beta = 0$ when the orbitals are poorly aligned at $90°$.[88] Examination of the $\cos\beta$ values shows that the average value for the unreactive ketones is indeed much lower (0.38 ± 0.05) than that for the reactive ketones (0.65 ± 0.1), indicating that the orbital overlap is significantly decreased for the unreactive ketones.

The cyclization parameters observed for the 7-methylnorbornane derivatives (Table 5.6) show that the β angle is much more favourable than those for the benzonorbornene ketones. The average value of $22 \pm 3°$ gives an orbital overlap that is approximately 93% of the ideal. Having an extremely favourable orientation for cyclization is the most likely reason for the complete absence of a cleavage product in the photoreaction; recall that both φ_1 and φ_4 showed

only moderate orbital overlap for this reaction (Table 5.4). Methyl substitution in this case plays a very important role because it forces the carbonyl group to adopt a conformation that is much more favourable for cyclization. Steric interactions between the α-methyl group and the aryl ring are obviously much greater than those observed between a hydrogen atom and an aryl group as seen in the benzonorbornenyl system, where these two groups nearly eclipse each other.

Table 5.5 Cyclization parameters[a] for the benzonorbornene derivatives.

	D (Å)	β (°)	cosβ
Ideal	< 3.40	0	1
43	3.01	51	0.63
44	2.99	55	0.57
45	3.04	66	0.41
46	2.96	42	0.74
81	3.03	70	0.34
Average	3.01 ± 0.03	49.5 ± 5 (cyclization)	0.65 ± 0.1
		68 ± 2 (RHT[b])	0.38 ± 0.05

[a]Data is given only for the hydrogen atom most likely to be abstracted. [b]Reverse hydrogen transfer.

The differences in p-orbital direction for the benzonorbornene and 7-methylnorbornane derivatives are shown in Figure 5.3. These values range from 70° for the unreactive benzonorbornenyl salt **81** to 21° for the reactive norbornyl ketoester **57**. Benzonorbornenyl ketoacid **46**, which gives a Yang cyclization product upon photolysis in the solid state lies between the two with a β angle of 42°. Unfortunately, with only five crystal structures available for the benzonorbornene derivatives, there is not enough data to obtain a more certain β cut-off angle, past which cyclization cannot occur. This cut-off presumably lies between 55°, the β value for the reactive **44**, and 66°, the β value for the unreactive **45**.

Table 5.6 Cyclization parameters[a] for the 7-methylnorbornane derivatives.

	D (Å)	β (°)	cosβ
Ideal	< 3.40	0	1
54[b]	2.89	27	0.89
	2.88	26	0.90
55	2.89	20	0.94
56	2.87	23	0.92
57	2.87	21	0.93
94	2.88	20	0.94
95	2.86	20	0.94
Average	2.88 ± 0.01	22 ± 3	0.92 ± 0.05

[a]Parameters are given only for the hydrogen atom most likely to be abstracted.

[b]Two independent molecules were present in the unit cell.

β = 70°   β = 42°   β = 21°

(a)   (b)   (c)
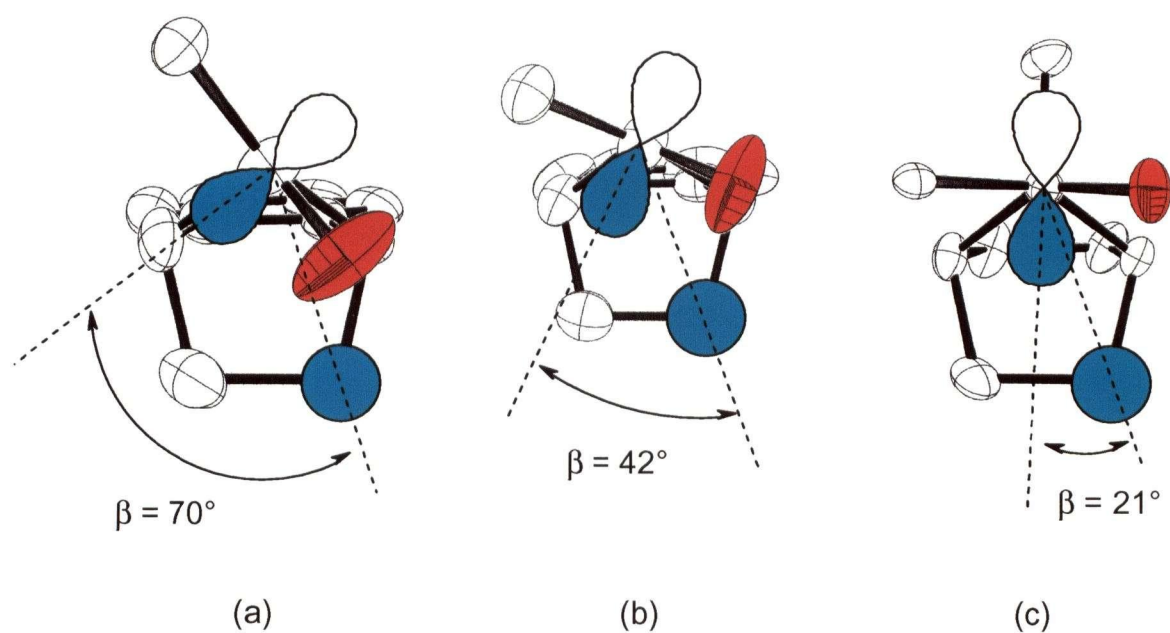
Figure 5.3 Cyclization orbital orientations for (a) salt **81**, (b) ketoacid **46**, and (c) ketoester **57**. Oxygen atoms have been coloured red and the hydrogen atoms and phenyl rings have been removed for clarity.

The final remaining question as to the unreactivity of benzonorbornenyl ketoester **45** and salt **81** is whether the lack of observed reactivity is due to the poor cyclization parameters or a restrictive reaction cavity. Examination of the respective crystal lattices shows that it is most likely a combination of the two factors. Within the crystal lattice of ketoacid **46**, which is reactive in the solid state, parallel planes of phenyl rings are spaced 3.39 Å apart. In the unreactive ketoester **45** and salt **81**, these rings are 3.06 Å and 2.30 Å apart respectively. As well, there is a difference in the number of close contacts (intermolecular contacts less than the sum of the van der Waals radii of the two nearest atoms) within the unit cells. The reactive ketoacid **46** has 11 close contacts, five of which are centered about the carboxylic acid, while the unreactive ketoester has 15 close contacts and salt **81** has 18. This combined data indicates that there seems to be a denser packing involved in the two crystals that are unreactive in the solid state. The single crystal-to-single crystal reactivity studies performed on salts **94** and **95**, discussed in Section 5.6, show that the Yang cyclization reaction will occur with a minimum amount of atomic movement; only two atoms show significant motion, with virtually no movement in the phenyl group or chiral auxiliary. Therefore, for a molecule with favourable abstraction and cyclization parameters, a narrow or densely packed reaction cavity would be of little consequence. On the other hand, molecules with poor cyclization and cleavage parameters, as seen for ketoester **45** and salt **81**, will not be able to undergo a reaction if a significant rearrangement is required in the small available space. Even if a larger reaction cavity were available to salt **81**, it is unlikely that a reaction would be possible with the same unfavourable cyclization parameters, since the ionic bonding between the chiral auxiliaries (each carboxylic acid is bonded to three neighbouring amines) will make the necessary rotation to improve the β angle next to impossible.

5.5 Transition State Geometry

It is generally thought that systems adopting a six-membered transition state during a reactive process occupy a chair-like conformation, as it would be of lower energy than the alternative boat-like conformation.[89] Initially it was thought that a 1,5 hydrogen transfer (γ abstraction) would follow this trend,[40] however, crystallographic studies by Scheffer *et al.* later showed that a boat-like transition state is preferred.[90] In terms of a hydrogen abstraction

process, whether a molecule adopts a chair or boat conformation should have little bearing on the ability of the molecule to undergo a reaction. In either conformation all of the abstraction and cyclization parameters would be unaffected. What would change, however, is the stereochemistry of the photoproduct. Figure 5.4 illustrates the differences that would arise from photolysis of a chair or boat conformation that undergoes least-motion ring closure to form a cyclobutanol. Ketone **101** (chair conformation) would form biradical **102** upon photolysis and ring close to give cyclobutanol **103**. Ketone **104**, which has a boat-like conformation, would form biradical **105** following hydrogen abstraction and give cyclobutanol **106** as the photoproduct. Therefore, depending on the conformation adopted, either of the diastereomeric cyclobutanols could be obtained.
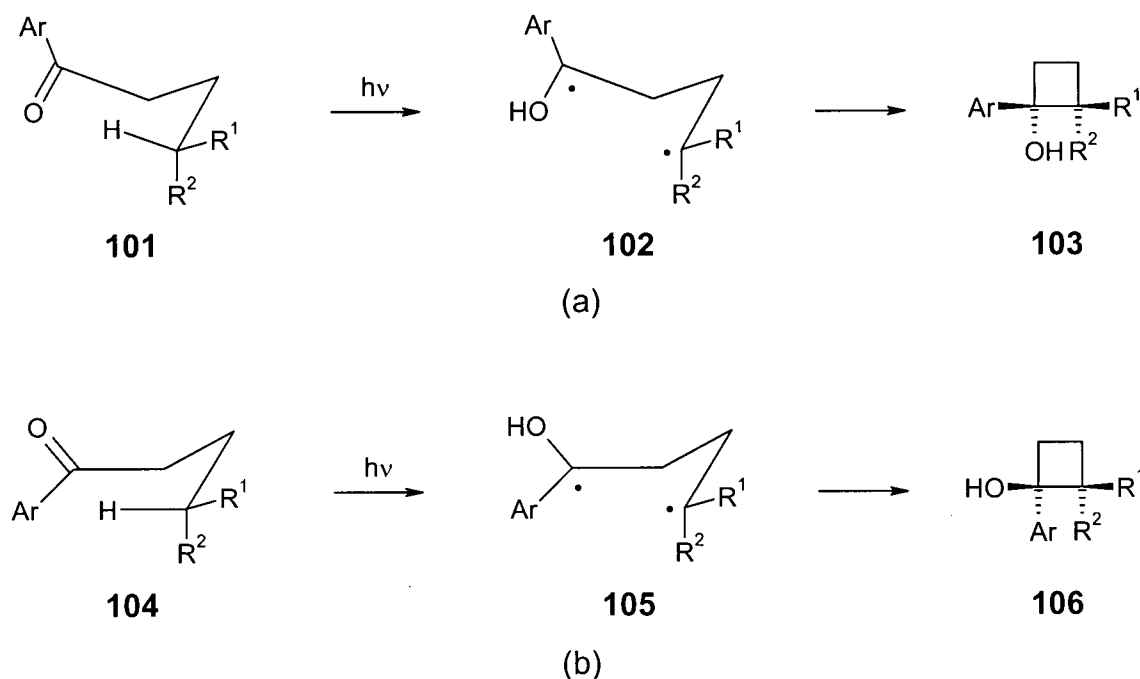
Figure 5.4 Cyclobutanol obtained from least-motion ring closure of (a) a chair-like transition state; (b) a boat-like transition state.

Despite the findings of Scheffer, there is still a strong belief that Norrish type II hydrogen abstraction occurs from a chair-like transition state, based mainly on the results of theoretical calculations.[91] For the chair-like abstraction geometry a three-step reaction has been proposed by Griesbeck in order to give the correct stereochemistry of the product.[92] The three

step process (abstraction, biradical equilibration, cyclization/cleavage), shown in Figure 5.5, proposes γ-hydrogen abstraction in tolylketone **107** from a chair-like conformation (**108**) followed by rotation of the C_1-C_2 bond of the intermediate, hydroxybiradical **109**, into hydroxybiradical **110**, which then undergoes ring closure to give cyclobutanol **111** or further rotations followed by cleavage. Direct, least-motion ring closure of biradical **109**, with a chair-like conformation, to give cyclobutanol **112** was not observed. The rationale given for the observed selectivity in the cyclobutanol formation is that there is hydrogen bonding present between the hydroxyl group and acylamino carbonyl oxygen. While these conclusions are conceivable, it is instructive to comment that abstraction from a boat-like conformation would give cyclobutanol **111** directly from biradical **110**.
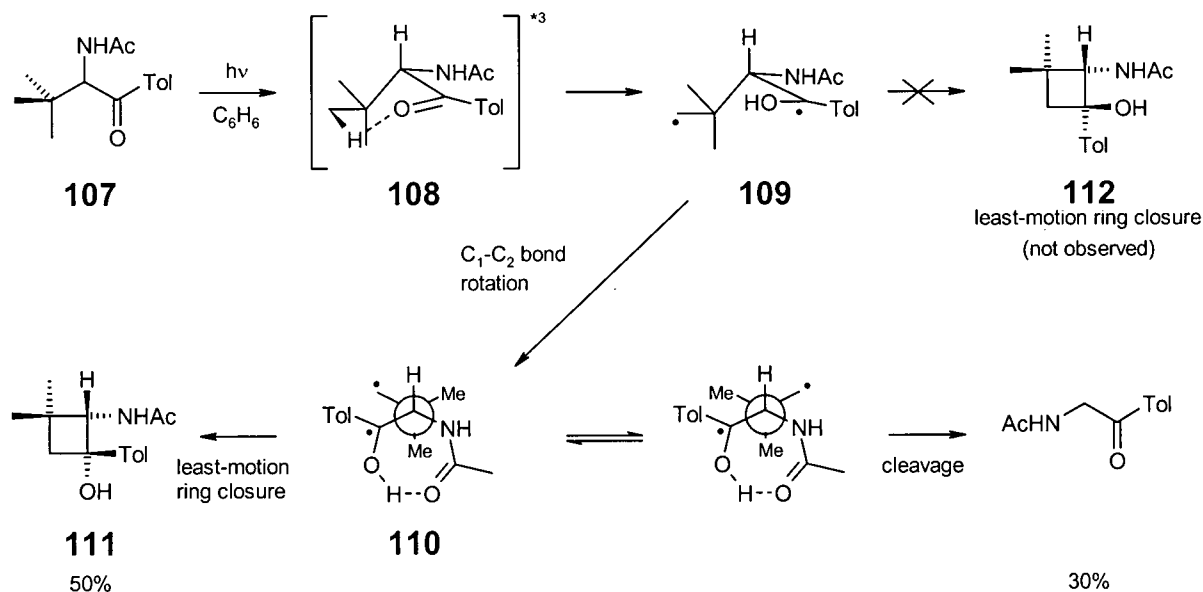
Figure 5.5 Griesbeck's proposed three-step reaction protocol for Norrish/Yang photochemistry.

From the crystal structure of ketoacid **46** shown in Figure 5.8 it is seen that a boat-like conformation of the reacting functional groups is adopted. Similarly, the crystal structure of ketoacid **56** (Figure 5.9) also shows a boat-like conformation. Since the molecules in the crystal can be considered confined to these conformations, all of the ketones studied will have cyclized from a boat-like transition state to give the predicted *endo*-aryl cyclobutanol. Upon photolysis

the *endo*-aryl cyclobutanols that would be predicted based on the molecular conformations in the solid state are indeed the ones found. If it were possible for any of the ketones to cyclize from a chair conformation this would lead to the formation of the *exo*-aryl cyclobutanol as the major product. This type of photoproduct was isolated as a minor product in the solution photolysis of the benzonorbornene derivatives and not observed at all in the solid state. Since the *exo*-aryl cyclobutanol was only present as a minor photoproduct it is reasonable to assume that a boat-like conformation is the preferred conformation from which the ketones react in solution as well. A second factor to consider for the present molecules is that abstraction from a chair-like conformation is unlikely to occur due to the nature of the carbon skeleton. Rotation of the carbonyl group into a chair-like conformation for H_a will simultaneously place it in a boat-like conformation for the neighbouring H_b as shown in Figure 5.6.

boat-like conformation   chair-like conformation

R = H, CH$_3$

boat-like conformation   chair-like conformation   boat-like conformation

(a)   (b)

Figure 5.6 Newman projections showing: (a) boat-like conformation for H_a, (b) chair-like conformation for H_a that is equivalent to a boat-like conformation for H_b.

Preference for a boat-like conformation/transition state in the solid state seems to be a general trend, having been observed for a number of systems studied in the solid state.[93] To rationalize why this may occur so frequently it is important to remember that the eclipsing 'bowsprit-flagpole' steric interactions present in boat cyclohexane do not exist for the ketones since the 'bow' of the boat is the carbonyl oxygen and does not possess a substituent (bowsprit). More importantly, positioning of the phenyl group in the boat conformation lessens the steric interactions between the phenyl group and the α-substituent as shown in Figure 5.7. Interestingly, a theoretical study by Houk and Dorigo on the intramolecular hydrogen abstraction of an alkoxy radical, predicts a chair-like transition state.[48,52] Unlike the phenyl ketones used in the present work, the butoxy radical used in the calculations would be more similar to cyclohexane in structure and therefore have more steric interactions in the boat form.

R = H, CH₃

boat-like conformation

low R-Ar steric repulsion

(a)

chair-like conformation

high R-Ar steric repulsion

(b)
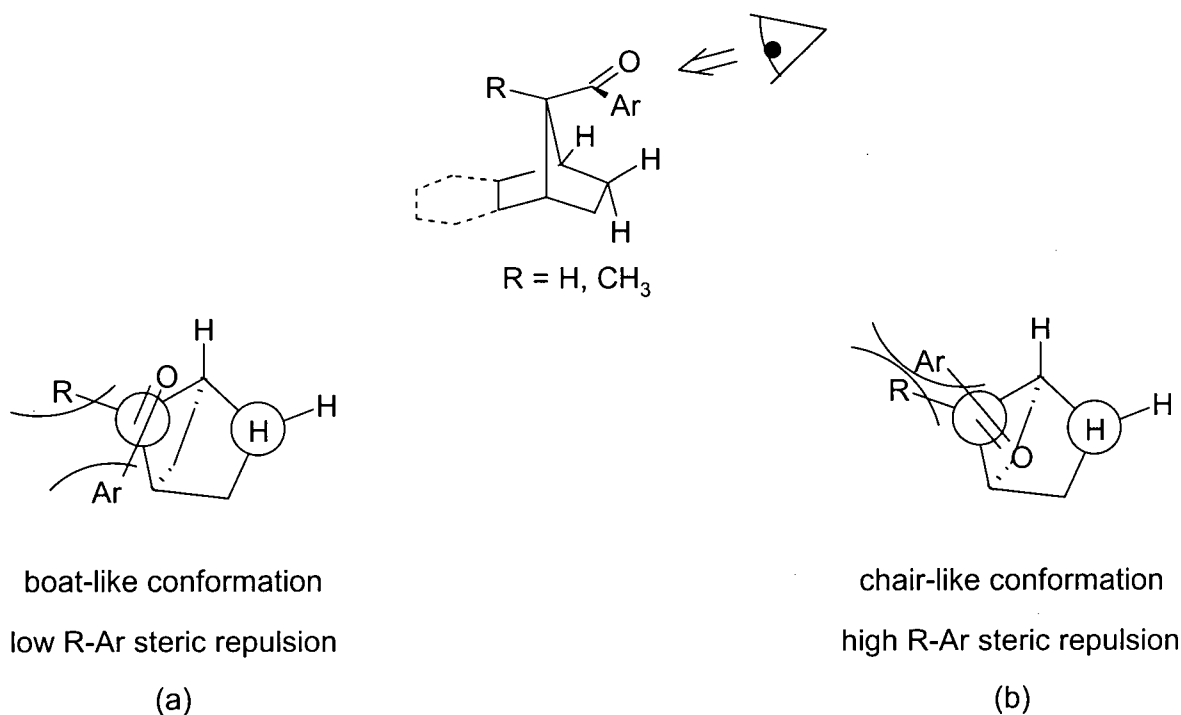
Figure 5.7 Newman projections of (a) boat-like conformation and (b) chair-like conformation.
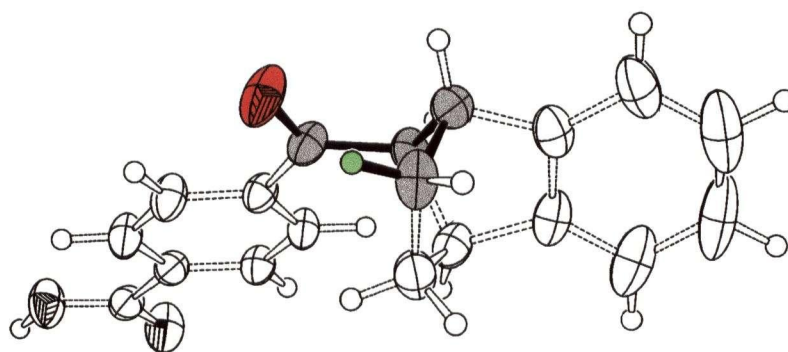
Figure 5.8 Boat-like conformation of ketoacid **46**. The oxygen atom is coloured red, abstracted hydrogen green and carbon atoms in the 6-membered transition state grey. Atoms and bonds not directly involved in the formation of the "boat" have been left uncoloured.
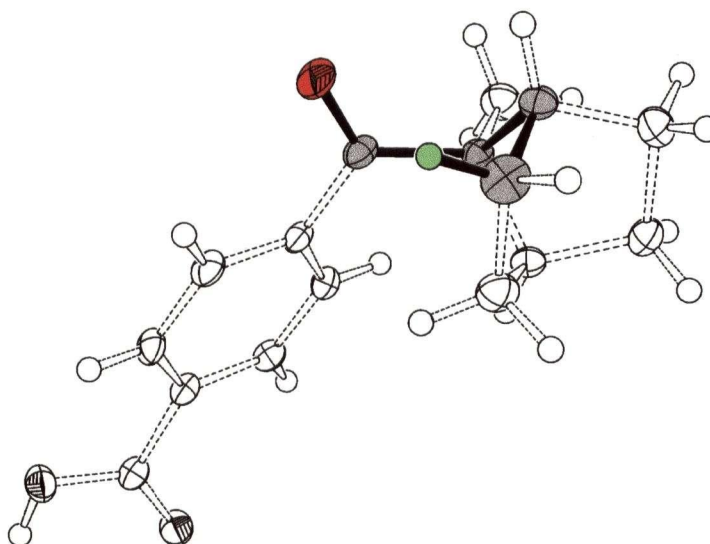
Figure 5.9 Boat-like conformation of ketoacid **56**. The oxygen atom is coloured red, abstracted hydrogen green and carbon atoms in the 6-membered transition state grey. Atoms and bonds not directly involved in the formation of the "boat" have been left uncoloured.

5.6 Single-Crystal to Single-Crystal Reactivity

The ultimate way in which to test the validity of crystal structure-solid state reactivity relationships is to monitor the reaction as it occurs within the crystal. This can be accomplished through X-ray crystallography and allows for a definitive mapping of the reaction as it progresses through various stages. Unfortunately, this is also a challenging endeavour because the vast majority of crystalline state reactions do not proceed topochemically, an essential requirement where crystallography is concerned. As has been shown however, high quality crystals are not a requirement for success in solid state studies, where samples of poor quality routinely give high chemical and optical selectivity. When conducting the photolyses of salts **94** and **95** it was noticed that the crystals did not show any signs of degradation (i.e. cracking, shattering, opaqueness) that are often associated with changes in the crystal lattice over the course of a reaction. Therefore, photolysis of single crystals suitable for X-ray diffraction were studied as shown in Figure 5.10. After obtaining the initial crystal structure it was left upon its mounting and sealed within a polyethylene tent under a N_2 atmosphere. Following photolysis to an intermediate conversion, the crystal structure of the mixed crystal was obtained (**95a**) and the photolysis procedure repeated to obtain a final structure (**95b**).
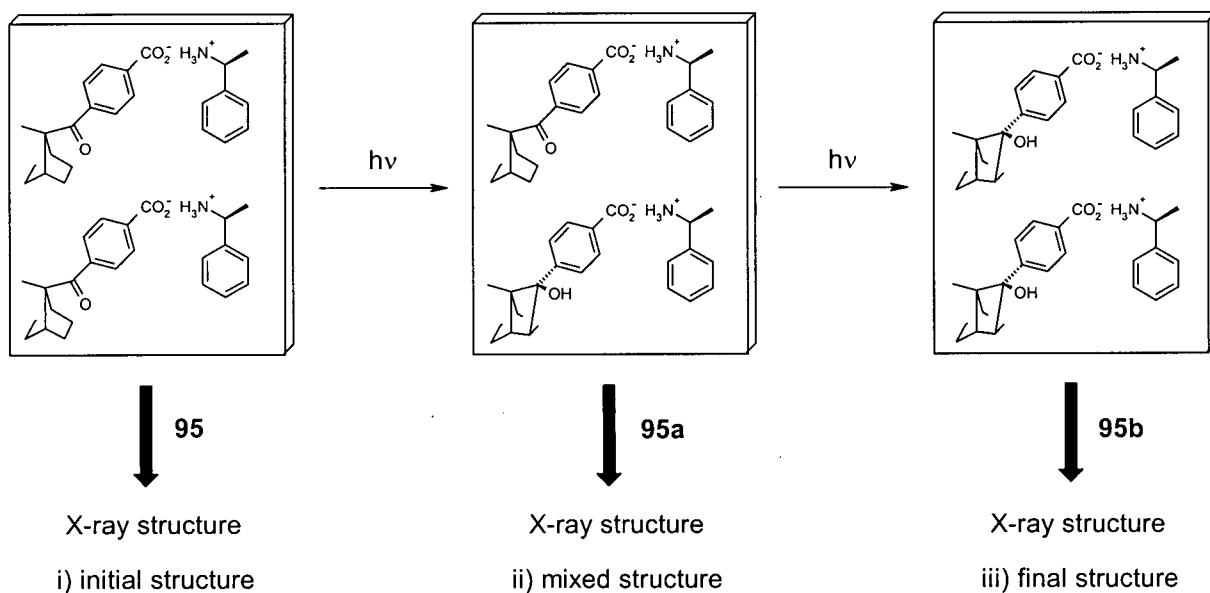
Figure 5.10 Representation of the single crystal to single crystal X-ray diffraction study for salt **95**.

5.6.1 Single Crystal-to-Single Crystal Photolysis of Salt 95

For the single crystal-to-single crystal reactivity study of salt **95** a single crystal was chosen and subjected to X-ray crystallographic analysis. Following data collection the crystal was photolyzed for 10 minutes at which time a second crystallographic data set was obtained. On solving this structure it was determined that the crystal had been photolyzed to 70% conversion. This value was in close agreement with an estimated value obtained through GC analysis of a separate sample irradiated alongside the single crystal. The single crystal was irradiated for an additional two hours before collecting a final data set, showing that the reaction had halted at 93% conversion (determined crystallographically). The X-ray structures displayed in Figure 5.11 show the structure salt **95** at 0%, 70% and 93% conversion; unit cell parameters for the crystal are given in Table 5.7.

Examination of the structures shown in Figure 5.11 show that there is minimal movement of the atoms within the molecule in accordance with topochemical principles. The only atoms showing significant motion are the abstracted γ-hydrogen, the carbonyl/hydroxyl oxygen atom and the γ-carbon atom. During the course of the reaction the oxygen atom shifts 0.101 Å as the carbonyl carbon atom changes hybridization from sp^2 (carbonyl) to sp^3 (quaternary centre). Similarly, the γ-carbon moves 0.153 Å to facilitate closure of the 1,4-hydroxybiradical as it changes from a secondary carbon in salt **95** to a tertiary carbon in salt **79**. That the carbonyl carbon does not undergo a similar movement during ring closure is not totally unexpected since it would not have the same freedom of motion due to the attached phenyl ring and bicyclic skeleton. Movement of either of these two appendages will be severely restricted by neighbouring molecules within the crystal lattice. The γ-carbon, however, will have a limited range of motion in which to move.

107

Table 5.7 Crystallographic details for photolysis of salt **95**.

	95	**95-70**[a]	**95-93**[b]	% change[c]	**79**[d]
Space Group	$P2_12_12_1$	$P2_12_12_1$	$P2_12_12_1$		$P2_1$
a (Å)	6.165(2)	6.1726(5)	6.1652(18)	+0.00	12.2580(13)
b (Å)	7.090(2)	7.0973(6)	7.0925(14)	+0.04	6.9904(5)
c (Å)	45.81(2)	46.391(4)	46.969(9)	+2.53	12.6647(14)
β (°)	90[e]	90[e]	90[e]		105.865(5)
V (Å³)	2002(1)	2032.3(3)	2053.8(7)	+2.59	1053.88(18)
Z	4	4	4		2
D_{calc} (g cm⁻³)	1.259	1.224	1.227	-2.54	1.207
R (%)	0.038	0.053	0.050		0.0406

[a]Single crystal of **95** photolyzed to 70% conversion. [b]Single crystal of **95** photolyzed to 93% conversion. [c]Percent change in parameters between **95** and **95-93**. [d]Recrystallized product following complete photolysis. [e]This is the default value for an orthorhombic cell.

Although the photoproduct, salt **79**, produced upon photolysis of salt **95** may exist in the same space group as the original salt, it is not necessarily the compound's native environment. Indeed, following a quantitative photolysis of salt **95** into **79**, and recrystallization from methanol, salt **79** was found to exist in a different space group ($P2_1$ rather than $P2_12_12_1$). Examination of the crystal structures of both the native and non-native forms of the salt shows that the molecule packs in a monoclinic arrangement rather than an orthorhombic arrangement, as well as adopting a different conformation. In the native form of the crystal the phenyl ring has undergone a 32° rotation, causing a similar reorientation of the chiral auxiliary. Obviously such a massive reorganization would be topochemically forbidden in the single crystal-to-single crystal reaction. The two crystal forms of salt **79** are illustrated in Figure 5.12. As expected for polymorphic crystal forms, the IR spectra of salt **79** in the native (Figure 5.13b) and non-native (Figure 5.13a) crystals show minor differences. Most notable is the broadening and shift observed for the hydroxyl stretch following recrystallization from methanol. Additional differences are observable in the fingerprint region of the spectra.
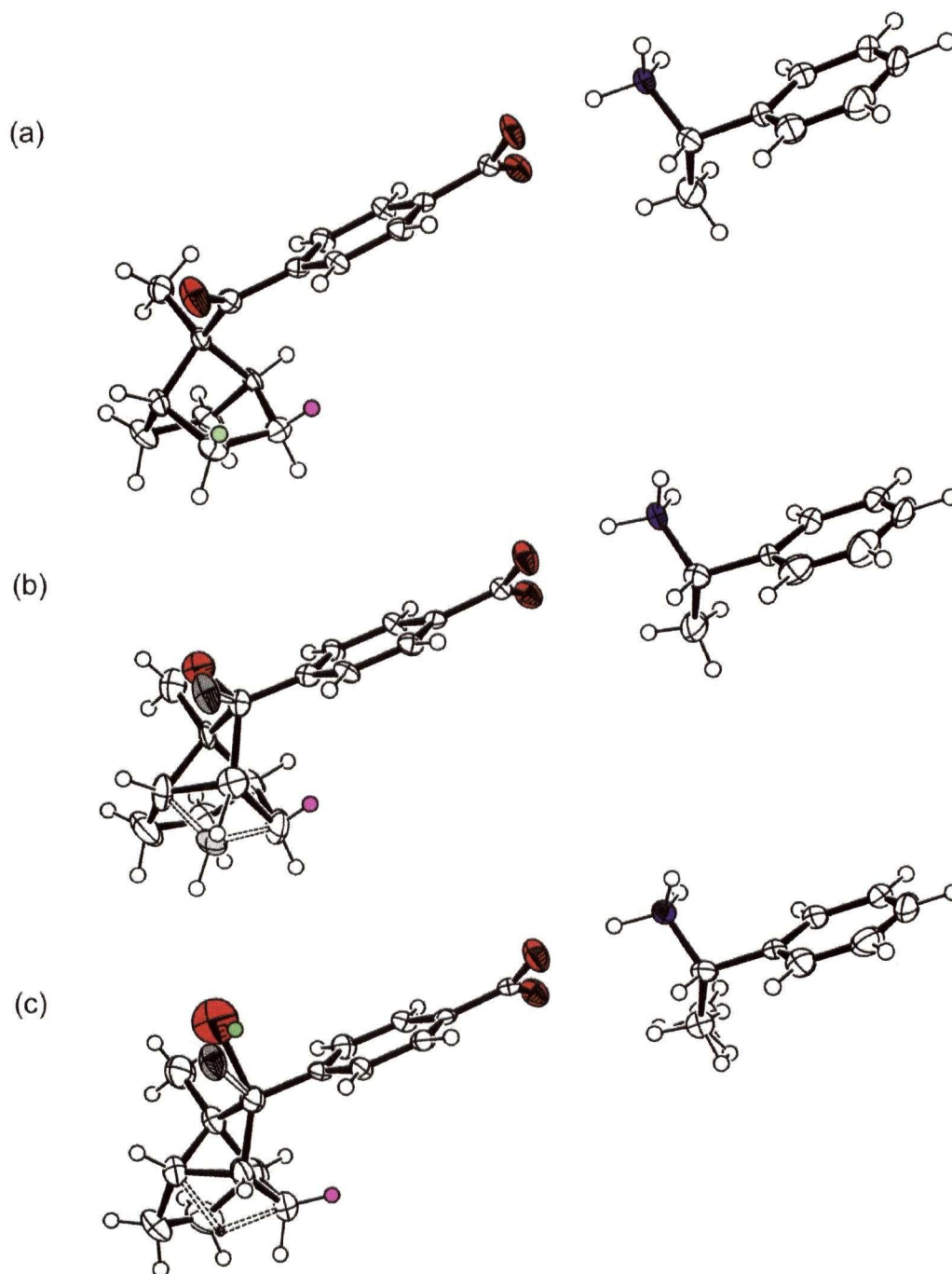
Figure 5.11 ORTEP representations of the single crystal-to-single crystal transformation of salt **95**. (a) unreacted salt **95**, (b) mixed crystal **95-70** (70% **79** and 30% **95**), (c) mixed crystal **95-93** (93% **79** and 7% **95**). Oxygen atoms are coloured red, nitrogen atoms blue, the abstracted hydrogen atom green and unabstracted purple. In mixed crystals the residual atoms from **95** have been coloured grey.
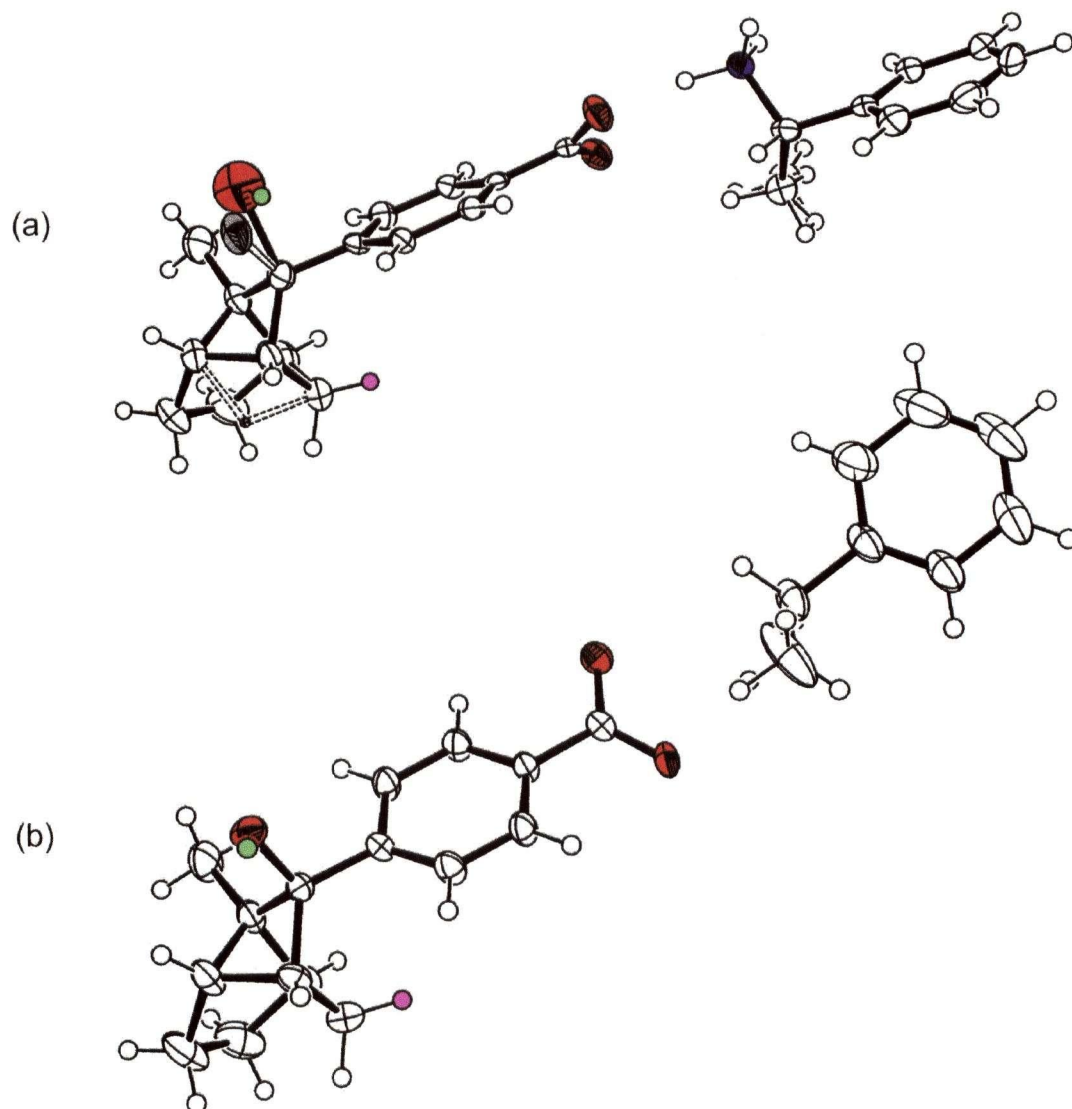
Figure 5.12 ORTEP representations of (a) the mixed crystal containing 93% **79** and 7% **95** from the single crystal-to-single crystal reaction; (b) salt **79** following recrystallization from methanol. The oxygen atoms have been coloured red, nitrogen atoms blue, abstracted hydrogen atom green, and unabstracted hydrogen atom purple. In the mixed crystal, residual atoms of **95** have been coloured grey.
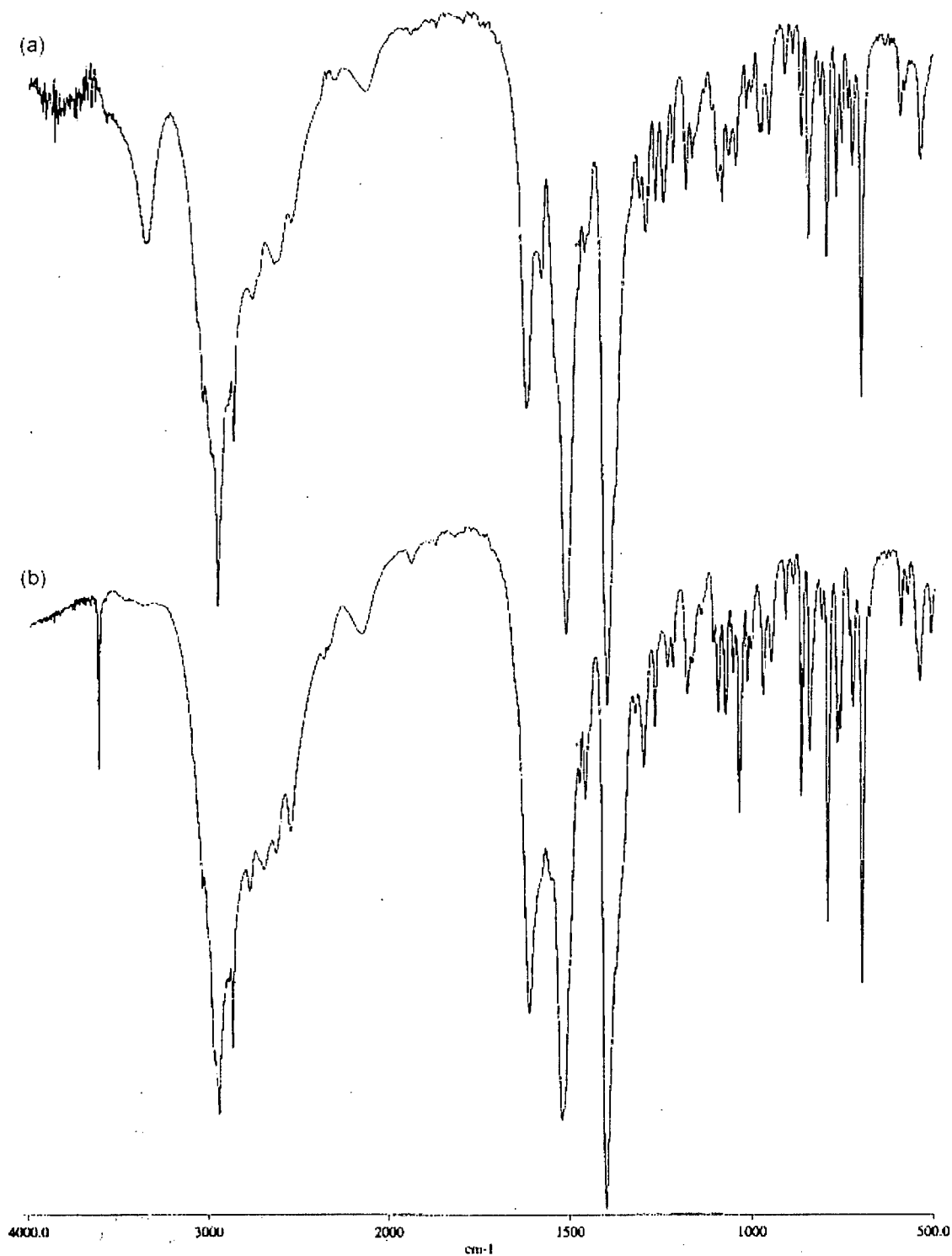
Figure 5.13 IR spectra (from KBr pellets) of (a) salt **79** following recrystallization from methanol (native form, space group P2$_1$); (b) salt **79** following formation in the solid state (non-native form, space group P2$_1$2$_1$2$_1$).

5.6.2 Single Crystal Photolysis of Salt 94

The single crystal-to-single crystal reaction of salt **94** was also studied in an analogous fashion to salt **95**. Crystallographic details of the study are given in Table 5.8 with ORTEP drawings of the individual crystal structures given in Figure 5.14. A comparison of the data between the studies for salts **94** and **95** shows very little overall difference, as would be expected for two enantiomers. Both show an increase in the length of the c axis of over 2% and an accompanying increase in the overall cell volume and decrease in the calculated density. Once again it is seen that following recrystallization of the photoproduct from methanol there is a reorganization of the molecule as it changes from its non-native to native environments. This includes both a change in the packing arrangement from the orthorhombic $P2_12_12_1$ (Figure 5.14b) to the monoclinic $P2_1$ (Figure 5.14c) and conformational change with a rotation of the phenyl group in the cyclobutanol by 32°. As observed for the photolysis of salt **95**, preparative photolysis of salt **94** to complete conversion followed by recrystallization from methanol gave crystals of salt **80** that exists in the space group $P2_1$ rather than the space group $P2_12_12_1$.

Table 5.8 Single Crystal Reaction data for salt **94**.

	94	**94-100**[a]	% Change[b]	**80**[c]
Space Group	$P2_12_12_1$	$P2_12_12_1$		$P2_1$
a (Å)	6.1899(7)	6.1661(7)	-0.38	12.2557(9)
b (Å)	7.1181(8)	7.0930(8)	-0.35	6.9907(4)
c (Å)	46.012(5)	46.980(5)	+2.10	12.6665(9)
β (°)	90[d]	90[d]		105.869(3)
V (Å^3)	2027.3(4)	2054.7(4)	+1.35	1043.9(1)
Z	4	4		2
D_{calc} (g cm^{-3})	1.243	1.227	-1.29	1.207
R (%)	0.0864	0.0948		0.064

[a]Single crystal of **94** photolyzed to 100% conversion (salt **80**). [b]Percent change in the cell parameters of **94** and **94-100**. [c]Salt **94-100** following recrystallization from methanol. [d]This is the default value for β in an orthorhombic system.

(a)

(b)

(c)
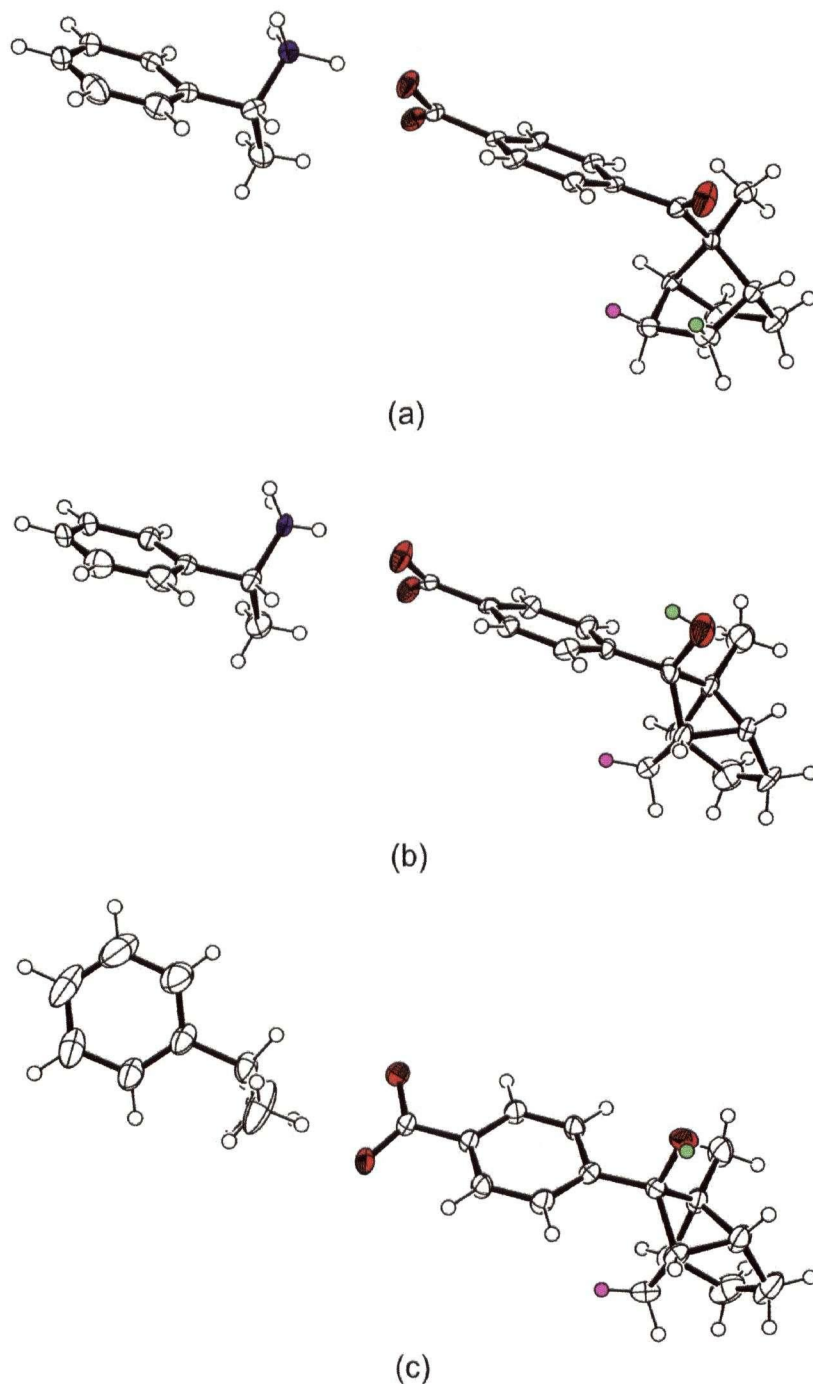
Figure 5.14 ORTEP representations of the single crystal-to-single crystal photolysis of salt **94**. (a) salt **94** before photolysis, (b) 100% conversion of salt **94** into salt **80** (salt **94-100**), (c) salt **80** following recrystallization from methanol. Oxygen atoms have been coloured red, nitrogen atoms blue, the abstracted hydrogen green and the unabstracted hydrogen purple.

In addition to showing that the two enantiomeric crystal forms react in the same manner, the crystallographic studies undertaken show conclusively that: 1) the hydrogen atom with the most favourable abstraction parameters is the hydrogen actually abstracted, 2) the achiral acid adopts a chiral conformation upon crystallization with an optically pure amine and favours abstraction of one of the two enantiotopic γ-hydrogens depending on its chirality, and 3) although the reaction occurs in the crystal lattice with minimal atomic movement, the photoproduct does not have to be formed in its lowest energy conformation in order for the reaction to proceed topotactically.

5.6.3 Absolute Configuration Determination

Determining the absolute configuration of a chiral molecule such as *endo*-aryl cyclobutanol **78** can be problematic since there is no element of known chirality or a suitably heavy atom present in achiral ketoester **57**. With the presence of an element of chirality in the molecule X-ray crystallography could be used directly since the problems associated with the Bijvoet method,[94] in the absence of a heavy atom such as sulphur, would not be present.[95] However, a direct correlation may be made from the related chiral salts **94** and **95**, and/or their photoproducts **80** and **79**, allowing for a crystallographic determination of the absolute configuration of **78**, formed upon treatment of **80** and **79** with diazomethane.[96]

Crystal structures obtained for salts **94** and **95** both show the absolute configuration of the molecule within the unit cell because the chiral auxiliary used, (*R*)- or (*S*)-1-phenylethylamine, is known. Since the absolute configuration of the starting material is known the absolute configuration of the final product may be predicted for the solid state photolysis. This type of prediction is only valid because: 1) one γ-hydrogen is clearly favoured for abstraction over the other, and 2) the chiral conformation of the achiral starting material is not in a rapid conformational equilibrium. If either of these requirements were not met for the present system then a prediction of the absolute configuration could not be made. Similarly, the absolute configurations of the photoproducts may be determined through their crystal structures either in a single crystal-to-single crystal reaction or upon recrystallization of a larger sample. The latter method is obviously a more general approach since the percentage of compounds that

are able to undergo single crystal-to-single crystal reactions is quite small. Once the absolute configuration is determined from a chiral salt, this can then be correlated to the methyl ester.

Figure 5.15 illustrates the procedure used in determining the absolute configuration of *endo*-aryl cyclobutanol **78**. Since an element of known chirality is required, ketoacid **56** is used to form chiral salts with an optically pure amine; (*R*)-1-phenylethylamine to form salt **94** or (*S*)-1-phenylethylamine to form salt **95**. From the X-ray crystal structures of the salts it could be determined that in salt **94** the ketone has a pro-(*R*) configuration (*i.e.* upon photolysis it would give a cyclobutanol with (*R*) chirality about the alcohol carbon). This prediction was confirmed upon determining the crystal structure of salt **80**, formed upon photolysis of salt **94**, where it is seen that the chirality about the hydroxyl carbon is indeed (*R*). Since esterification with diazomethane does not affect any of the chirality centres, (-)-**78** must have the same absolute configuration as salt **94**.[*] As expected, the use of the opposite antipode of the chiral auxiliary, (*S*)-1-phenylethylamine, gives the opposite result. The crystal structure of salt **95** was found to have the ketone lying in a pro-(*S*) configuration and to form a cyclobutanol with an (*S*)-configuration about the hydroxyl carbon in salt **79**. Esterification of salt **79** then forms (+)-**78** with an (*S*) configuration about the hydroxyl carbon.

Crystallographic alternatives to this method would be to either perform a transesterification of **78** with an optically pure alcohol, or derivatize the hydroxyl group with a chiral acid or other suitable molecule. Alternatively, formation of clathrates with an optically pure chiral host could be attempted. The only requirement for any of these approaches to be successful is that crystals suitable for X-ray diffraction studies can be grown.

---

[*] The sign of the optical rotation was determined by polarimetry.
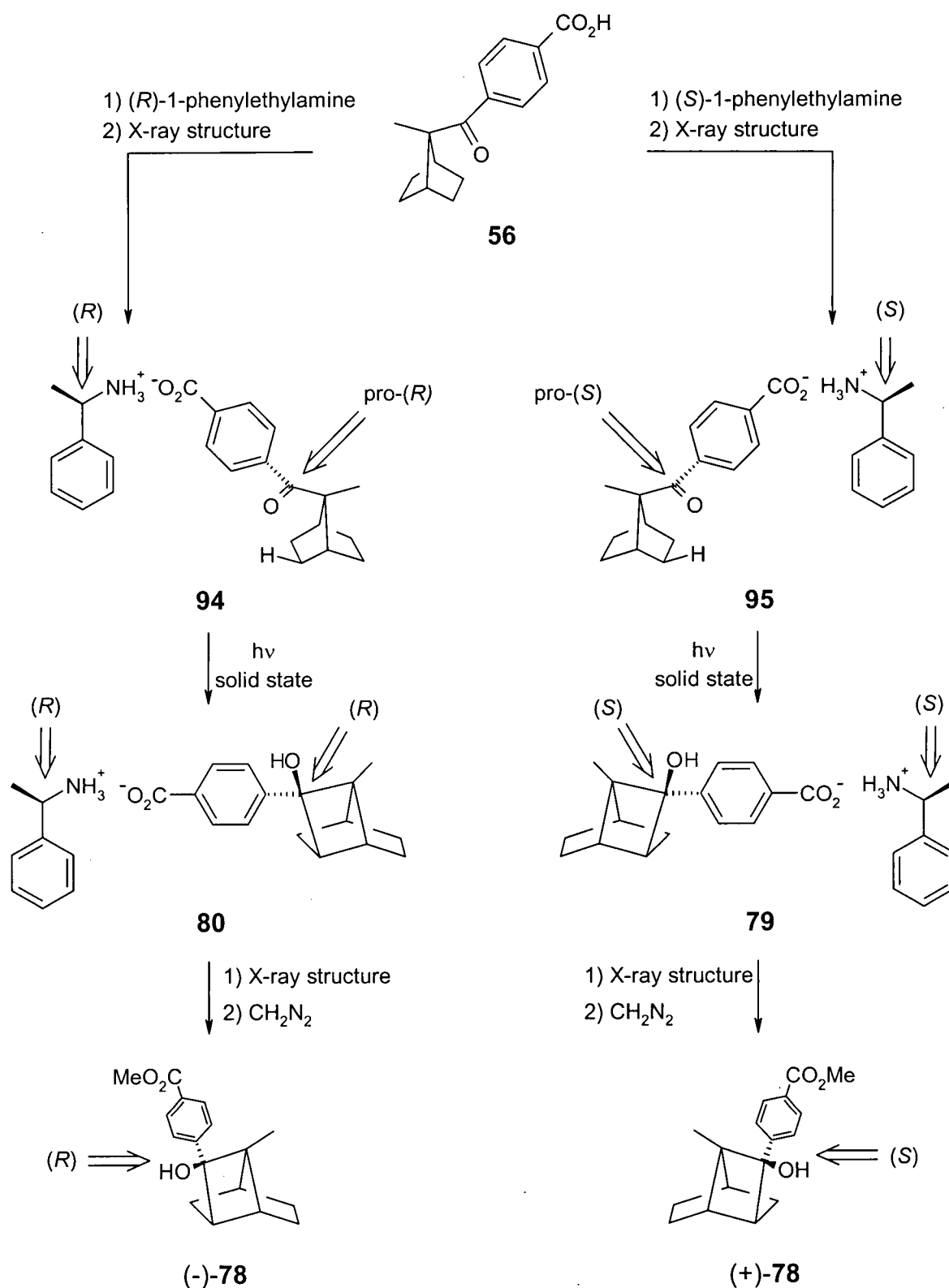
Figure 5.15 Absolute configuration prediction and determination of cyclobutanol **78** through X-ray crystallography of salts **94** and **95**.

5.7 Comparison of the Geometric Parameters for Different Systems

As stated earlier, the present research was conducted as part of continuing studies on the Norrish/Yang photochemistry of ketones in the solid state. In this section, the current data involving conformationally locked norbornane (bicyclo[2.2.1]heptane) derivatives are compared to previous studies involving conformationally locked six-membered rings (*tert*-butylcyclohexane and adamantane (tricyclo[3.3.1.1^{3,7}]decane)), as well as a concurrent study involving spiro- derivatives of the norbornane system. Analogous studies within our research group are currently being conducted on bicyclo[3.3.1]nonane and bicyclo[2.1.1]hexane derivatives.

5.7.1 Norbornane Derivatives: Abstraction From Five-Membered Ring Systems

The two systems discussed in this thesis have dealt with Norrish/Yang photochemistry within the conformationally locked five-membered ring system of a norbornane skeleton, where it was found that addition of a methyl group to the bridge position (α to the carbonyl) drastically altered the observed reactivity. Changes in the reactivity were not unexpected since addition of methyl substituents to the α-carbon of ketones has long been known to affect photochemical behaviour as shown by Lewis and co-workers in their studies of substituted butyrophenones.[97] In these studies it was found that valerophenone (butylphenylketone), with an unsubstituted α-carbon, underwent primarily the Norrish type II cleavage reaction, with only 22% Yang cyclization observed. Methyl and dimethyl substitution at the α-carbon increased the amount of cyclization product observed to 43% and 84% respectively. Methyl substitution effects in the norbornane system were previously observed by Lewis and co-workers in their study of 2-benzoyl substituted norbornanes as shown in Figure 5.16.[71] Photolysis of *exo*-2-benzoylnorbornane (**113**) in benzene gave only cleavage product **114**, which underwent a secondary photoreaction to give acetophenone (**115**). Although still photochemically reactive, *exo*-2-benzoyl-2-methylnorbornane (**116**) gave only benzaldehyde (**117**), along with a number of unidentified products resulting from the Norrish type I (α-cleavage) products **118** and **119**; no Yang cyclization was observed. While addition of a α-methyl substituent did not lead to an increase in the amount of Yang cyclization product, there is still a dramatic change in the

observed reactivity. Unfortunately, these molecules have not been studied in the solid state and therefore a comparison of the geometries involved cannot be made.
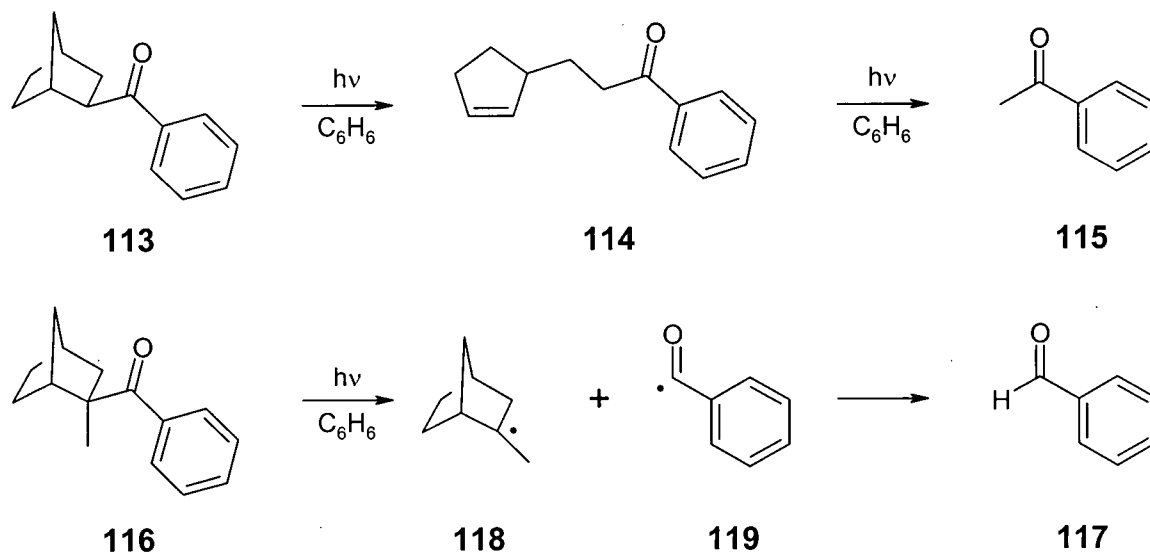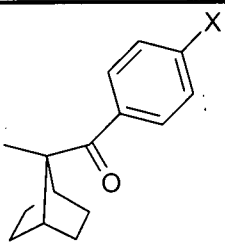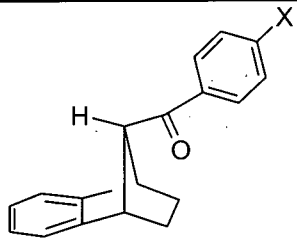
Figure 5.16 Solution photochemistry of 2-benzoylnorbornane derivatives.

A comparison of the crystallographically determined geometric parameters for hydrogen abstraction in the benzonorbornene (**35**) and 7-methylnorbornane (**36**) systems is presented in Table 5.9. The first major difference noticed between the two systems is the hydrogen abstraction distance, d (ideal value is 2.72 Å), which has a value of 2.68 ± 0.05 Å for the 7-methylnorbornanes and 2.51 ± 0.04 Å for the benzonorbornenes. Since the norbornane derivatives reacted more efficiently in the solid state than the benzonorbornene ketones (based on the time required to achieve full conversion in the solid state, not a measured quantum yield), a larger abstraction distance (0.17 Å) seems to have no effect on the overall efficiency of the reaction. This agrees with hydrogen abstraction being a reversible process, a fact that has been demonstrated previously through the use of deuterium exchange in deuterated solvents,[98] and as being independent of quantum yield.[55a] The second major difference in the hydrogen abstraction parameters is found in the angle ω (ideal value is 0°), where even though the unreactive benzonorbornene derivatives have an almost ideal value (19 ± 2°), the more reactive 7-methylnorbornanes possess a value that is well removed from the ideal (62 ± 1.5°). Although

Table 5.9 Comparison of methyl and non-methylated five membered ring systems.

System	36	35	
	$X^a = F, CN, CO_2H,$ $CO_2CH_3, CO_2^- {}^+PEA^b$	$X^c = H, F, CO_2H$	$X^d = CO_2CH_3, CO_2^- {}^+MPA^e$
Reaction	cyclization	cyclization[f]	RHT[g]
d (Å)	2.68 ± 0.05	2.55 ± 0.01	2.46 ± 0.02
θ (°)	106 ± 1.5	109 ± 0.5	108.5 ± 0.5
Δ (°)	82 ± 4	93 ± 2	101.5 ± 0.5
ω (°)	62 ± 1.5	42 ± 7	19 ± 2
φ_1 (°)	-56.5 ± 3	-82 ± 3	76.5 ± 2
φ_4 (°)	-56.5 ± 1	-57	-57
φ (°)	63.5 ± 1	67 ± 1	68 ± 1
D (Å)	2.88 ± 0.01	2.99 ± 0.02	3.04 ± 0.01
β (°)	22 ± 3	49.5 ± 5	68 ± 2

[a]Ketones **54**, **55**, **56**, **57**, and salts **94** and **95**. [b]PEA = (R)- or (S)-1-phenylethylamine. [c]Ketones **43**, **44**, and **46**. [d]Ketone **45** and salt **81**. [e]MPA = (R)-β-methylphenethylamine. [f]Crystal structures were not obtained for salts **84**, **85**, or **86**, which gave cyclization and cleavage products. [g]Reverse hydrogen transfer.

these latter values of ω likely border on the upper limits of an acceptable value,[99] and likely lead to a decrease in the rate of hydrogen abstraction, this is compensated for by the high rate of the favourable Yang cyclization process. While there is not a significant difference in the values obtained for the angle θ, there was a variance in the observed values for the C=O···H$_\gamma$ angle Δ. In the 7-methylnorbornane derivatives (**36**), the angle Δ (ideal value is 90-120°) possessed a value of 82 ± 4°, reactive benzonorbornenes (**35**, X = H, F, CO$_2$H) possessed a value of 93 ± 2°,

and the unreactive benzonorbornenes (**35**, X = CO_2CH_3, CO_2^- $^+$MPA) an even higher value of $101.5 \pm 0.5°$. While there is an obvious trend in the Δ angle, with lower values favouring Yang cyclization and higher ones favouring reverse hydrogen transfer, there is not sufficient data to support a generalization that low Δ is a requirement for cyclization to occur. A generalization of this nature may in fact be true however, since the majority of Δ values reported are in the 80-90° range.[93]

As expected, values obtained for the cleavage parameters φ_4 and φ are nearly identical in both systems since they are based on the same bicyclic skeleton. For all of the ketones studied, φ_4, representing the dihedral angle formed between the C_4 (γ-carbon) and the C_2-C_3 σ-bond, lies in the range of -57°. Through the $\cos\varphi$ relationship discussed in Section 5.3 this equates to an orbital overlap of 55%, the ideal being 100% when φ_4 is 0° (*i.e.* the C_4 p-orbital and C_2-C_3 σ-bond are eclipsed). From the photochemical studies of the benzonorbornene derivatives **35** in solution (see Table 3.1), where a cleavage product was always produced, these φ_4 values obviously permit sufficient orbital overlap for the cleavage reaction to occur from within the bicyclic skeleton. For φ_1, the dihedral angle between the C_1 p-orbital and the C_2-C_3 σ-bond, however, large differences are seen, reflecting changes in the carbonyl group conformation. The φ_1 angles for ketoacids **46** and **56**, both reacting to give cyclobutanols in the solid state, are depicted in Figure 5.17. Figure 5.17a, shows that in ketoacid **46** the p-orbital of the C_1 carbon is nearly perpendicular to the C_2-C_3 bond. The φ_1 value of -78°, giving 21% of the ideal orbital overlap, indicates that cleavage from this conformation will be unfavourable (the ideal value of φ_1 is 0°, representing 100% orbital overlap). Owing to the steric repulsions between the α-methyl group and aromatic ring in ketoacid **56**, the carbonyl group adopts a conformation in which the φ_1 dihedral angle is -56.5°, representing a 56% orbital overlap between the C_1 p-orbital and the C_2-C_3 σ-bond. Although the orbital overlap from this conformation makes a cleavage reaction more favourable, it is not able to compete with the cyclization reaction that produces the observed photoproduct.

$\varphi_1 = -78°$ $\varphi_1 = -56°$

(a)   (b)
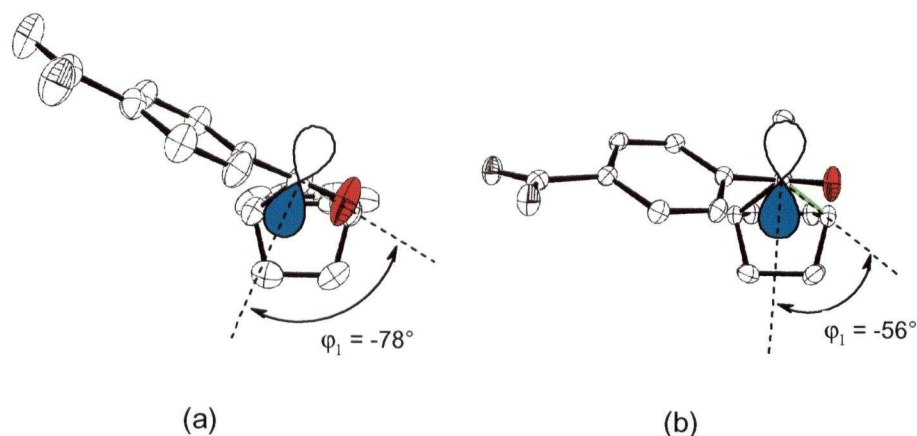
Figure 5.17 ORTEP representations of (a) ketoacid **46** and (b) ketoacid **56,** viewed down the C_1-C_2 σ-bond with p-orbitals superimposed, showing the φ_1 angle. The carbonyl oxygen has been coloured red and the C_1-C_2 bond green.

The final parameters to be compared for the norbornane derivatives are those regarding the cyclization process. Both the 7-methylnorbornanes (**36**) and benzonorbornenes (**35**) have carbon-carbon distances (D) well within the ideal value of 3.40 Å to allow for ring closure of the 1,4-hydroxybiradical intermediate produced upon hydrogen abstraction (see Table 5.9). The more important factor in gauging the ability of a ketone to undergo cyclization is the angle β, representing the dihedral angle formed between the C_1 p-orbital and the C_2-C_4 vector (see Figure 5.2). When β is 0° the C_1 p-orbital will be directed towards the C_4 p-orbital, a conformation favourable for cyclization. However, when β is 90°, the C_1 p-orbital will be directed away from the C_4 p-orbital and in the least favourable conformation for cyclization. In the benzonorbornene derivatives **35** there were two conformations found; one with a β value of 49.5 ± 5° that gave only cyclization in the solid state, and the other with a β value of 68 ± 2° that underwent reverse hydrogen transfer. The 7-methylnorbornane derivatives (**36**) possessed a β value of 22 ± 3°, making cyclization a much more favourable process, and this is most likely why the cleavage reaction is not able to compete in the solid state.

Ongoing studies within our research group have focused on the effects of systematically varying the carbonyl group conformation within the same system through the use of spirocyclic rings of varying size.[57,100] Photochemical studies of the four spiroketones illustrated in Figure 5.18 show that reactivity varies depending on the spirocyclic ring size. Ketone **120**, with a five-

membered spirocyclic ring, undergoes Norrish type II cleavage to form alkene **121**,[101] ketone **122** (6-membered spirocyclic ring) undergoes reverse hydrogen transfer and gives no observable product, while ketones **123** and **124** (seven and eight-membered spirocyclic rings) react to give Yang cyclobutanols **125** and **126** respectively. The data presented in Table 5.10 shows the hydrogen abstraction, cleavage and cyclization parameters for norbornane derivatives with 5, 6, 7, and 8 carbon spirocyclic rings at the α-carbon. In addition to the spiroketones shown in Table 5.10, similar spiroketone systems have been studied based on the adamantyl system shown in Table 5.12 and a bicyclo[3.3.1]nonane system analogous to the norbornane system. All three spirocyclic systems show a remarkable similarity in the observed reactivity and geometric parameters for each ring size.
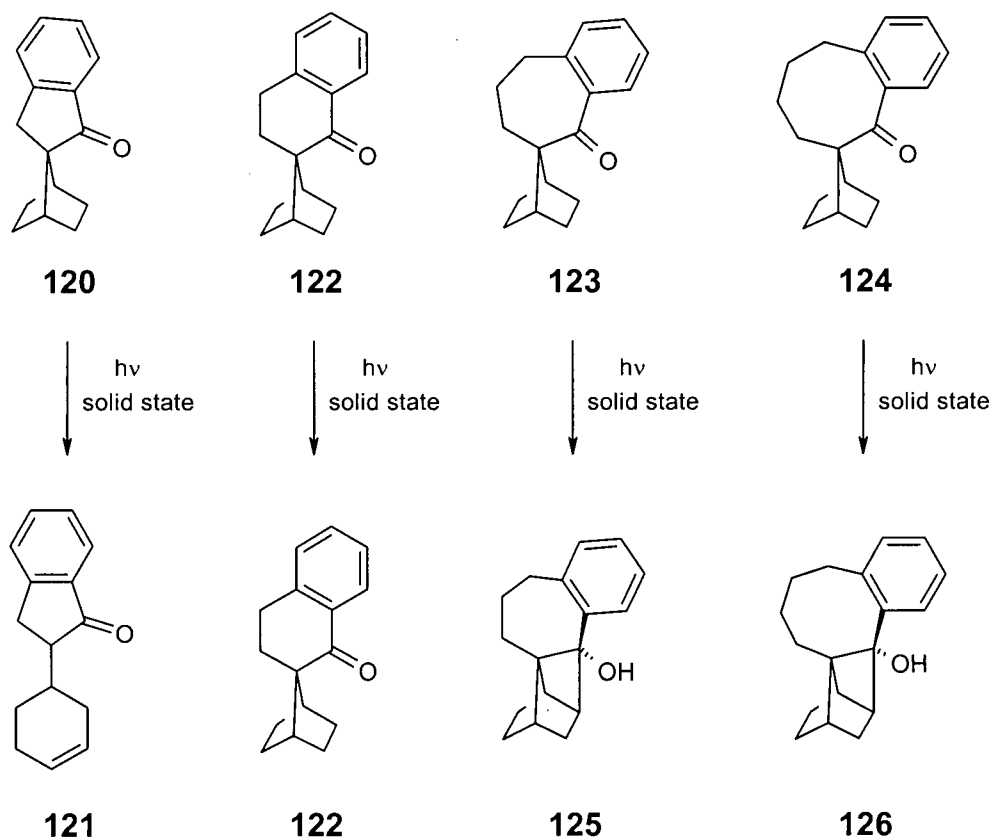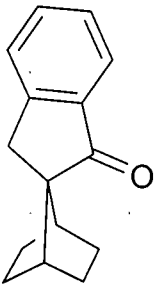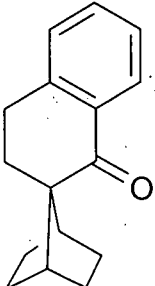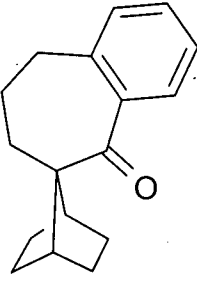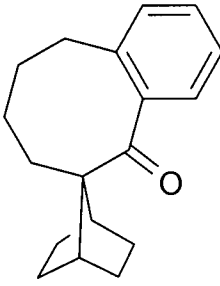
Figure 5.18 Photochemistry of spiroketones **120**, **122**, **123**, and **124**.

A comparison of the results obtained for the benzonorbornene derivatives **35** (Table 5.9) shows that the ketones exhibiting reverse hydrogen transfer (*i.e.* those that give no observable reaction) have carbonyl group geometries most similar to spirocyclic ketone **122**. The major

difference between the geometries of these molecules is the angle β (~15° greater for 35) and torsion angle φ_1 (~22° difference between 122 and 35). The higher β value observed for the benzonorbornenes actually makes these compounds less likely to undergo cyclization since the C_1 p-orbital is directed further away from the C_4 p-orbital. Although it is possible that the absence of a cyclization product for spiroketone 122 is due to the ring strain associated with the resulting fused ring system (the closely related 124 gives only cyclization, resulting in a less strained fused ring system), the increase in β for the benzonorbornenes seems to be enough to make cyclization unfavourable. Even though there is a ~22° difference in the φ_1 values this difference can be deceiving because the carbonyl group in these molecules lies on the opposite side of the C_2-C_3 σ-bond. In actuality, spiroketone 122 has a carbonyl group geometry that is much less favoured to undergo a cleavage reaction, with a φ_1 value of -86° (7% orbital overlap), than the benzonorbornenes with a φ_1 value of 76.5 ± 2° (23% orbital overlap). Spirocyclic ketone 120, which undergoes a cleavage reaction possesses a φ_1 value of 45 ± 9°, along with a very unfavourable β angle of 79°, suggesting that the minimal φ_1 value that will give cleavage in the solid state is between 45 and 77°, corresponding to an orbital overlap of 71 to 22 % for the C_1 p-orbital and the C_2-C_3 bond.

The three reactive ketones among the benzonorbornene derivatives (35) possess geometric parameters similar to those observed for spiroketone 124 and show the same solid state reactivity, undergoing Yang cyclization upon photolysis. The differences between these ketones are much smaller than those for spiroketone 122 and the benzonorbornene derivatives that undergo reverse hydrogen transfer. In fact, the parameters are remarkably similar in most respects, the only major difference being the hydrogen abstraction distance d, which is 0.07 Å shorter in spiroketone 124. The φ_1 values for both ketones is -82°, corresponding to an orbital overlap of only 14% between the C_1 p-orbital and C_2-C_3 σ-bond. Therefore it is not surprising that a cleavage reaction is not observed. The ketones also share a similar β angle of ~49°, well within the highest value of β observed for the derivatives studied of 55° for ketone 44. While this value of β is presumably approaching the upper limit of an acceptable value, it evidently provides sufficient orbital overlap between the C_1 p-orbital and the C_4 p-orbital for cyclization to be a competitive process with reverse hydrogen transfer.

Table 5.10 Geometric parameters for norbornyl spirocyclic ketones.[a]

	120[b]	122	123	124
Reaction	cleavage	RHT[c]	cyclization	cyclization
Similar to:	-	35 (RHT)	36	35 (cyclization)
d (Å)	2.47 ± 0.02	2.45	2.66	2.48
θ (°)	108 ± 0	110	107	109
Δ (°)	97 ± 2	97	84	95
ω (°)	19 ± 2	34	57	39
φ_1 (°)	45 ± 9	-86	-62	-82
φ_4 (°)	-56 ± 1	-58	-58	-58
φ (°)	65 ± 1	63	63	64
D (Å)	3.00 ± 0.01	2.95	2.91	2.94
β (°)	79 ± 9	53	29	48

[a]Data shown for the hydrogen atom with the most favourable abstraction parameters. [b]Four molecules in the asymmetric unit; average values given. [c]Reverse hydrogen transfer.

The 7-methylnorbornane derivatives **36** (Table 5.9) show a very close relationship with spiroketone **123** in geometry and reactivity; both giving exclusive cyclobutanol formation in the solid state and solution. Differences in the geometric parameters are observed for ω where the average value for the 7-methylnorbornanes (62 ± 1.5°) is 5° greater than spiroketone **123** (57°), φ_1, where the 7-methylnorbornane value is -56.5 ± 3 compared to -62° for spiroketone **123** and β, 22 ± 3° for ketone **36** and 29° for spiroketone **123**. Although the φ_1 values correspond to an orbital overlap of 47-55% between the C_1 p-orbital and the C_2-C_3 bond, and match the orbital overlap represented by φ_4 (~-57°, 54% overlap between the C_4 p-orbital and the C_2-C_3 bond), a

value known to allow cleavage (spiroketone **120**), cyclization is the only observed photoprocess. In both ketone **36** and **123**, this is likely due to the low β angles, showing excellent alignment between the C_1 and C_4 p-orbitals, a crucial factor for cyclization to occur. Spiroketone **120**, on the other hand, possesses a very unfavourable β angle of ~79°, precluding cyclization.

Unfortunately, these results still leave unresolved the question of the carbonyl conformation for the benzonorbornene salts exhibiting a cleavage product (see Table 4.4). There is, however, a possible explanation based on the acquired data. If a carbonyl group adopted a conformation intermediate between those of spiroketones **123** and **124**, then it may lie in an orientation that would allow cleavage to compete with the cyclization reaction. In such a conformation there would be sufficient orbital overlap (the φ_1 value), greater than that observed for **124**, making cleavage more favourable, and higher β value than observed for **123**, indicating that the C_1 p-orbital is directed further away from the C_4 p-orbital, making cyclization less favourable.
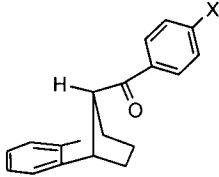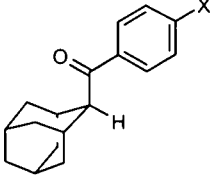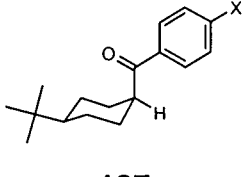
5.7.2 Five and Six-membered Ring Systems: Norbornane and Adamantane

Studies by Leibovitch on the solid state photochemistry of *tert*-butylcyclohexyl (**127**) and adamantyl (**128**) phenyl ketones, where the γ-hydrogen is abstracted from within a conformationally locked six-membered ring, were the focus of previous work within our research group.[56] Although the three ketones examined were unreactive in the solid state (solution photolysis of **127** gave a Norrish type II cleavage product exclusively while **128** was unreactive), they do provide a point of comparison to the present work (**35**) in terms of the conformational differences between the five and six membered ring systems. Since the data summarized in Table 5.11 for **128** and **127** represent only unreactive ketones, the data from **35** has been divided into the 3 reactive and 2 unreactive ketones for a more meaningful comparison.

The most notable similarities are observed for the angles β and ω. The reactive ketones of **35** have a β angle that is 12-18° less than the unreactive ketones, once again showing the importance of seemingly small changes in the carbonyl geometry on the observed reactivity. Similarly, the angle ω is 10-20° larger for the reactive ketones. This is not surprising when the inverse relationship between ω and β is considered, since ω approaches 0° as β approaches 90°. In terms of a cleavage reaction, all of the systems have similarly poor φ_1 values in the solid state

125

and this is likely the reason why a cleavage product was not observed for **35** or **127** in the solid state, even though they have been shown to undergo cleavage in solution.

Table 5.11 Comparison of geometric parameters for 5 and 6-membered ring systems.
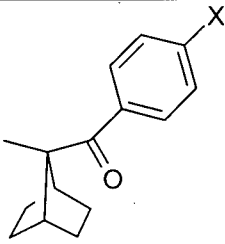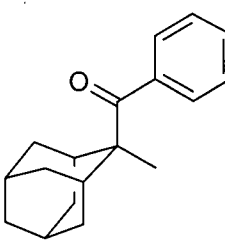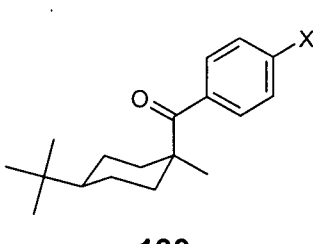
System				
	35		**128**	**127**
	X^a = H, F, CO_2H	X^b = CO_2CH_3, $CO_2^{-\ +}$MPA^c	X = H	X = H, F
Reaction	cyclization^d	RHT^e	RHT^f	RHT
d (Å)	2.55 ± 0.01	2.46 ± 0.02	2.47	2.60 ± 0.01
θ (°)	109 ± 0.5	108.5 ± 0.5	117	116 ± 0.5
Δ (°)	93 ± 2	101.5 ± 0.5	98	95.5 ± 0.5
ω (°)	42 ± 7	19 ± 2	29	32 ± 0.5
φ_1 (°)	-82 ± 3	76.5 ± 2	82	85 ± 0.5
φ_4 (°)	-57	-57 ± 0.5	31	36 ± 0.5
φ (°)	67 ± 1	68 ± 1	70	75 ± 0.5
D (Å)	2.99 ± 0.02	3.04 ± 0.01	3.17	3.23 ± 0.0
β (°)	49.5 ± 5	68 ± 2	64	62 ± 0.3

[a]Ketones **43**, **44**, and **46**. [b]Ketone **45** and salt **81**. [c]MPA = (R)-β-methylphenethylamine. [d]Crystal structures were not obtained for salts **84**, **85**, or **86**, which gave cyclization and cleavage products. [e]Reverse hydrogen transfer. [f]Ketone **128** was also found to be unreactive in solution.

What is less clear is why the solution photochemistry of the three sets of ketones is so different. While ketone **128** remained unreactive in solution, attempts were made by Leibovitch to show that hydrogen abstraction did indeed occur though trapping of the hydroxybiradical intermediate with thiols.[70] Unfortunately these experiments were unsuccessful, leading to the conclusion that the reverse hydrogen abstraction reaction most likely occurred at a faster rate than other reaction pathways, including H-D exchange. In any case, such a trapping experiment

is not easily accomplished in the solid state, making it difficult to ascertain whether hydrogen abstraction actually occurs in that medium.

Table 5.12 Comparison of geometric parameters for methylated five and six-membered ring systems.

System	36	129	130
	X^a = F, CN, CO_2H, CO_2CH_3, CO_2^- $^+PEA^b$	X = H, F, CO_2CH_3, CO_2^- $^+PEA^b$, CO_2^- $^+NE^c$	X = H, CH_3, OCH_3, CO_2H, CO_2^- $^+PA^d$
Reaction^e	cyclization	cyclization	cyclization
d (Å)	2.68 ± 0.05	2.57 ± 0.04	2.62 ± 0.05
θ (°)	106 ± 1.5	115 ± 1	113 ± 1
Δ (°)	82 ± 4	79 ± 3	83 ± 3
ω (°)	62 ± 1.5	60 ± 2	56 ± 2
φ_1 (°)	-56.5 ± 3	60 ± 3	65 ± 5
φ_4 (°)	-56.5 ± 1	32 ± 4	34 ± 1
φ (°)	63.5 ± 1	64 ± 1	70 ± 1
D (Å)	2.88 ± 0.01	2.99 ± 0.03	3.10 ± 0.02
β (°)	22 ± 3	29 ± 4	35 ± 4

^{a}Ketones **54**, **55**, **56**, **57**, and salts **94** and **95**. ^{b}PEA = (*R*)- or (*S*)-1-phenylethylamine. ^{c}NE = (*1R,2S*)-norephedrine. ^{d}PA = (*S*)-prolinamide. ^{e}All systems give exclusive formation of an *endo*-aryl cyclobutanol upon photolysis in the solid state and solution.

Similar comparisons may be made between the derivatives of the three systems possessing a methyl substituent at the bridge position (**36**, **129**, **130**), whose parameters are summarized in Table 5.12. Despite the differences imposed by the ring systems, the geometric

parameters are surprisingly similar. Most notable are the large values for ω and small values for β, indicating that these compounds are all well aligned for a cyclization reaction to occur. Indeed this is the only reaction occurring in both the solid state and solution for all of the ketones. The only significant difference in the parameters is for φ_4 as would be expected when comparing five - and six-membered rings.

5.8 Application of Molecular Modeling in Predicting Solid State Geometries

As has been shown in the work presented in this chapter, differences in the conformation of a molecule can have dramatic effects on reactivity. With the benzonorbornenyl system this was aptly illustrated with crystals reacting to give primarily an *endo*-aryl cyclobutanol, crystals reacting to give a mixture of *endo*-aryl cyclobutanol and cleavage product, and crystals giving no observable reaction. While this reactivity has been explained through the development of crystal structure-reactivity relationships, their construct requires prior synthesis of the ketones and the growth of crystals suitable for X-ray diffraction. Since there is no way of knowing in advance whether, or how, a given molecule will react in the solid state, this presents an obvious problem: is it worth going through a multi-step synthesis not knowing if a solid state reaction is possible? In terms of studying the geometric requirements of reactions in the crystalline state, the answer, of course, is yes. Even if a series of molecules is prepared and found to be unreactive in the solid state, just as much, or perhaps even more, information is gained from the structure-reactivity relationships. In terms of using the crystalline state to control the chemical selectivity of a reaction, as part of a larger synthetic scheme, there is a much greater risk involved. While it is not possible to answer definitively whether or not a reaction will occur, it is desirable, at a minimum, to be able to ascertain whether or not the reaction is likely. The obvious method for making this type of prediction would be through molecular modeling as advances in computing have now made available low-cost (both in terms of money and computing time) molecular modeling packages such as Hyperchem.[102] For the present work the MM+ force field of Hyperchem was used to conduct conformational searches on the ketones.*

---

* MM+ is a general method for molecular mechanics calculations, principally for organic molecules and is an extension of the MM2™ force field.

There are of course a number of differences between computer-generated models and the actual conformations of molecules, most notably that 'simple' computer models perform calculations on molecules in the gas state, without taking into account their environment. More complex calculations and simulations of molecules in the solid state have been carried out but these require prior knowledge of the crystal lattice of a molecule, which in turn requires its prior synthesis.[103] These studies generally use a mini-lattice of atoms around a central molecule to mimic a full crystal lattice. Reasonably accurate calculations may nevertheless be carried out using the general gaseous state calculations by performing a conformational search to ensure that the low-energy conformation found lies at the global, and not a local, minimum. This simpler approach will generally give a decent approximation of a molecule's conformation within a crystal lattice since compounds tend to crystallize in their lowest energy conformations.[104]

Presented in Table 5.13 and Table 5.14 are comparisons of the geometric parameters obtained from molecular modeling and X-ray crystallography for the norbornane systems studied. The results obtained for the benzonorbornene derivatives in Table 5.13 show very good agreement for all of the parameters with no deviations that would dispute the methods used. Comparison of the data obtained for the 7-methylnorbornane derivatives in Table 5.14 also shows a reasonable agreement between the predicted and actual values although there are larger deviations for some parameters. The most significant differences are observed for d (0.18 Å, 6.7%), and β (10°, 43.5%) which both had much lower deviations for the benzonorbornenes. Even with the larger differences, there is an adequate agreement between the predicted and observed values. Based on the comparison of the actual geometric parameters obtained from crystallography, and those obtained through molecular modeling, the conclusion can be drawn that this is an effective method to predict reactivity.

Table 5.13 Comparison of geometric parameters[a] for the benzonorbornene derivatives.

Ketone	Method	d (Å)	θ (°)	Δ (°)	ω (°)	φ_1	φ_4	D (Å)	β (°)
43	X-ray	2.54	109	96	36	-87	-57	3.01	51
	MM+	2.50	104	102	36	-88	-58	3.05	52
44	X-ray	2.55	109	92	44	-81	-57	2.99	55
	MM+	2.50	104	102	36	-88	-58	3.05	52
45	X-ray	2.48	108	101	21	78[b]	-57	3.04	66
	MM+	2.50	104	102	36	-88	-58	3.05	52
46	X-ray	2.55	108	92	47	-78	-57	2.96	42
	MM+	2.50	104	102	36	-88	-58	3.05	52
Avg.	X-ray	2.53 ± 0.03	108.5 ± 0.5	95 ± 4	37 ± 10	-82[c] ± 4	-57 ± 0.5	3.00 ± 0.03	53.5 ± 9
	MM+	2.50	104	102	36	-88	-58	3.05	52
Difference (%)		1.2	0.04	-7.4	2.7	7.3	1.8	-1.7	2.8

[a]Only parameters for the abstracted γ-hydrogen are shown. Conformational search performed using the MM+ force field. The lowest energy conformation is shown. [b]The carbonyl group in **57** lies on the opposite side of the C_2-C_3 bond than the other ketones and therefore has a dihedral angle of the opposite sign. [c]Average does not include the value for **45**.

Table 5.14 Comparison of geometric parameters[a] for the 7-methylnorboanane derivatives.

Ketone	Method	d (Å)	θ (°)	Δ (°)	ω (°)	φ_1	φ_4	D (Å)	β (°)
54	X-ray	2.62	108	83	60	-61	-56	2.89	27
		2.63	107	83	60	-60	-57	2.88	26
	MM+	2.50	104	92	58	-66	-56	2.92	33
55	X-ray	2.75	106	79	62	-55	-57	2.89	20
	MM+	2.50	104	92	58	-66	-56	2.92	33
56	X-ray	2.65	108	81	62	-56	-55	2.87	23
	MM+	2.50	104	92	58	-66	-56	2.92	33
57	X-ray	2.70	104	80	64	-55	-57	2.87	21
	MM+	2.50	104	92	58	-66	-56	2.92	33

		2.68 ± 0.05	107 ± 1	83 ± 4	61 ± 1	-57.5 ± 3	-56.5 ± 1	2.88 ± 0.01	23 ± 3
Avg.	X-ray								
	MM+	2.50	104	92	58	-66	-56	2.92	33
difference (%)		6.7	2.8	10.8	4.9	14.8	0.8	1.4	43.5

[a]Only parameters for the abstracted γ-hydrogen are shown. Conformational search performed using the MM+ force field. The lowest energy conformation is shown.

Chapter 6 Summary and Conclusions

6.1 Photochemistry in the Solid State and Solution

In the photochemical studies of 7-benzoylbenzonorbornene derivatives, photolysis in the solid state was seen to have a profound effect on the outcome of the reaction. When photolyzed in solution ketones **43**, **44**, and **45** all gave a mixture of three photoproducts composed of an *endo*-arylcyclobutanol and cleavage product, making up the majority of the photoproduct mixture, along with an *exo*-arylcyclobutanol, present in minor amounts (see Table 3.1). Although irradiation of ketone **43** (and ketone **44** upon prolonged irradiation) in the solid state led to melting of the crystals, photolysis of ketones **44** (at low conversions) and **46** gave preferential formation of their respective *endo*-aryl cyclobutanols (see Table 3.9). Irradiation of ketoester **45**, on the other hand, caused reverse hydrogen transfer, exhibiting only minor amounts of product formation after prolonged irradiation. Photolysis of thirteen chiral salts, formed between optically pure amines and ketoacid **46**, in the solid state also showed differing reactivity when compared to the same reactions in solution. Salts irradiated in methanol gave a roughly equal mixture of cyclization and cleavage products; however, when irradiated in the solid state three different types of reactivity were observed. Five of the salts formed primarily the *endo*-arylcyclobutanol, three gave a mixture composed of 80% cyclization and 20% cleavage product, and five underwent reverse hydrogen transfer (see Section 4.1.2.2). Based on correlations between the solid state structures of the molecules, the observed reaction in the solid state was rationalized as summarized in Section 6.3

Unlike the benzonorbornene derivatives, photochemical studies of 7-methylnorbornane derivatives in the solid state and solution showed that the outcome of the reaction was not medium dependant, both giving exclusive formation of an *endo*-arylcyclobutanol photoproduct.

6.2 Asymmetric Induction Studies

The ionic chiral auxiliary approach to asymmetric induction has once again proven to be a highly successful method for achieving optical selectivity in photochemical reactions. Utilizing a series of chiral ammonium carboxylate salts formed between optically pure amines and achiral ketoacid **46**, enantiomeric excesses of 93% at 99% conversion were obtained for the

photoproduct *endo*-arylcyclobutanol **65** following irradiation in the solid state and diazomethane work-up (see Section 4.1.2.2). An analogous series of chiral salts formed with achiral ketoacid **56** was able to form *endo*-arylcyclobutanol **78** with 99% ee at 99% conversion (see Section 4.2.2.3). In both series of salts it was found that use of the opposite optical antipode of the chiral auxiliary could selectively form the opposite enantiomer of the photoproduct, an important property when considering this method for further use in organic synthesis. As well, it was found that for both series of salts, irradiation in solution led to a racemic mixture of the photoproduct, highlighting the critical role played by the chiral crystal lattice in the reaction.

Although it was possible to achieve high enantioselectivity for both sets of salts studied, the results obtained show the need for a 'trial and error' approach to selecting the appropriate auxiliary. Of the ten amines used to form salts with benzonorbornene ketoacid **46**, only two gave high chemical and optical selectivity, **82** (phenylalanine) and **87/88** (1-phenylethylamine). The other eight amines gave either low optical selectivity with high chemical selectivity (**83** and **89**), low chemical selectivity, or underwent reverse hydrogen transfer. While salts formed with 7-methylnorbornane ketoacid **56** all gave high chemical selectivity, the enantioselectivities obtained were also varied. Of the six amines used, four gave enantioselectivities greater than 90% at high conversions, with **94/95** (1-phenylethylamine) giving a nearly quantitative enantioselectivity at complete conversion. It is important to note however, that in both cases it was possible to find at least one amine that would give high optical selectivity.

While it would be desirable to have every auxiliary used give high enantioselectivity, the ability to test a large number of potential chiral inductors also has advantages from a crystal engineering standpoint. This was clearly seen for the benzonorbornene salts, which showed a number of different types of reactivity in the solid state depending on the chiral amine used and similar effects may be seen for other substrates, where small conformational changes can lead to alterations in the product ratios. Typically the chiral salts have been prepared on the 75-100 mg scale, an amount sufficient for characterization and enantioselectivity studies, however, for the wide-scale testing of auxiliaries a much smaller amount (1-3 mg) of each salt could be prepared and tested for potential use. Any salts formed that showed high chemical and enantioselectivity could then be prepared in larger amounts.

Examination of the crystal structures for three chiral salts (**81**, **94** and **95**) was able to show that the enantioselectivity observed in the photoproducts was due to the adoption of a

chiral conformation during the crystallization process. In the chiral conformation, one of the two diastereotopic γ-hydrogens was clearly favoured for abstraction over the other. Photolysis of the salts in solution allowed for interconversion of the two chiral diastereomeric conformations through rotation of the carbonyl, an act that is topochemically disfavoured in the solid state, leading to a racemic photoproduct. Salts that showed no optical selectivity following photolysis in the solid state are believed to posses two independent molecules within the unit cell (conformational enantiomerism), each favouring abstraction of a different γ-hydrogen.

The substrates discussed within this thesis were specifically chosen because of their structural features, such as a phenyl ketone, guaranteeing triplet state reactivity for the Norrish/Yang reaction and likely assisting in the formation of solids through the π-stacking of adjacent molecules, and a p-carboxylic acid group on the phenyl ring that was used to form salts with the amine auxiliaries. While a binding site for the auxiliary will remain an essential component of any substrate, it may be located on any portion of the molecule; the location used within this study was chosen for its ease of addition and for symmetry considerations. As mentioned in the Introduction, carboxylic acids are not the only molecules that can be used in this manner so the formation of chiral salts between achiral amines and optically pure carboxylic acids is an equally valid approach, allowing for a wider range of molecules that can be used in this technique.[105] Previous studies have also shown that it is possible to incorporate triplet sensitizers into the chiral auxiliary, allowing for a much wider range of reactions that may be attempted.[106] This is an area that may be further exploited in future studies where a sensitizer is required for a reaction to occur, or in the case of Norrish/Yang photochemistry, where reactivity may occur from either a singlet or triplet excited state and preferential reaction from the triplet state is desired.

Future use of the ionic chiral auxiliary approach to asymmetric induction is being planned for both thermal and other excited state reactions. Other planned extensions of this work include using optically pure photoproducts produced using the ionic chiral auxiliary approach in the construction of synthons for use in natural product synthesis. Further asymmetric induction studies are also currently being conducted on the benzonorbornene and 7-methylnorbornane derivatives within the confined environments of zeolites by the Ramamurthy group at Tulane University.[107]

6.3 Crystal Structure-Solid State Reactivity Relationships

Through the use of X-ray crystallography it was possible to obtain solid-state structures for five benzonorbornene and six 7-methylnorbornane ketones, allowing for the development of structure-reactivity relationships based on the observed reactivity of the molecules within the crystalline state. These relationships were particularly valuable in understanding the reactivity of the benzonorbornene derivatives, which showed different types of reactivity in the crystalline state. Two of the molecules for which crystal structures were obtained, ketones **45** and **81**, proved to be unreactive in the solid state even though examination of the hydrogen abstraction parameters (see Table 5.1) indicated that a reaction was probable. Further examination of the structures showed that there was both poor orbital overlap for a cleavage reaction (Table 5.3) and poor orbital alignment for a Yang cyclization reaction (Table 5.5). Therefore, the only topochemically favourable reaction pathway left available to the biradical intermediates was reverse hydrogen abstraction, a degenerate reaction that would reform the starting material. The remaining structures obtained for the benzonorbornene derivatives shared a common structure that gave a more favourable positioning of the carbonyl group, allowing a cyclization reaction to form an *endo*-arylcyclobutanol. Based on the fact that differences of 22° in φ_1 and 19° in β were observed between ketones exhibiting reverse hydrogen transfer (*i.e.* they exhibit no observable reaction) and those giving exclusive formation of a cyclobutanol, it was proposed that the three salts (**84**, **85**, and **86**) showing a significant amount of cleavage product in addition to a cyclobutanol (20% cleavage, 80% cyclobutanol) had a carbonyl group conformation intermediate between the two extremes. In such a conformation the carbonyl geometry would strongly favour neither reverse hydrogen abstraction or cyclization, allowing for the cleavage reaction to become competitive.

Owing to the presence of the α-methyl substituent, structures obtained for the 7-methyl-7-benzoylnorbornane derivatives showed a different carbonyl group geometry than the benzonorbornene derivatives. For these substrates it was found that although the cleavage parameters were more favourable than for the benzonorbornenes (see Table 5.9), the cleavage reaction was not able to compete due to an extremely favourable orbital alignment for cyclization. By monitoring the photolysis of salts **94** and **95** crystallographically as single crystal-to-single crystal reactions, it was possible to confirm a number of assumptions made in the structure-reactivity relationships based on the starting ketones, as well as predict and

confirm the absolute structure of the photoproduct obtained. Of particular interest was the confirmation that the γ-hydrogen predicted to be abstracted, from a boat-like conformation, was indeed involved in the reaction. Also shown through the single crystal transformations was the fact that the photoproduct does not have to exist naturally in the same space group as the starting material. Upon recrystallization of salts **79** and **80** following irradiation in the solid state it was found that there was a change in the molecular conformation accompanied by a changes in crystal packing and space group from $P2_12_12_1$ to $P2_1$.

6.4 Future Outlook: Applications of Solid State Photochemistry in Synthesis

In the Introduction, Paquette's synthesis of Punctatin A (**25**), involving a Yang cyclization in the photochemical key step, was mentioned. The photochemical step in this case produced only a 49% yield of the desired cyclobutanol **27**, with the remainder of the reaction mixture containing 23% of cleavage product **28** and 28% unidentified material. Although successful in constructing the desired ring system and the correct stereochemistry, it would be desirable to find ways in which to maximize the yield of the desired product. Through the use of solid state techniques it may be possible to increase the chemical selectivity of this, and similar reactions with minor alterations to the synthetic scheme. Such changes would include changing protecting groups to allow for formation of solids or the attachment of auxiliaries. Where possible, ionic auxiliaries, such as the ammonium carboxylate salts formed in Chapter 4 would be ideal, whether they were chiral or achiral. Not only would they give the prerequisite high-melting solids essential for solid state reactions, but, in addition to allowing for high stereoselectivity, they could also allow for the rapid assessment of small conformational changes within the crystallized structures as observed for the benzonorbornene derivatives. In the benzonorbornene derivatives, positioning of the carbonyl group was found to favour different modes of reactivity and in such cases the ability to steer the outcome of the reaction is crucial from a synthetic point of view.

Since it is has been shown that solid state techniques are easily scalable by suspension of the crystalline material in an appropriate liquid (one that will not act as a solvent and dissolve the crystals),[69] the only limitations facing further synthetic developments will be due to the suitability of the reaction. While topochemical factors will exclude some reactions, benefits

may be seen in many unimolecular reactions that are subject to conformational changes leading to different photoproducts but do not require large molecular motions during the reaction.

6.5 Conclusions

The work presented in this thesis has shown that conducting photochemical reactions in the solid state can allow for excellent control of both the chemical and enantioselectivity of a molecule. Enantioselectivity was achieved using the ionic chiral auxiliary concept, with the presence of optically pure auxiliaries ensuring the crystallization of achiral molecules in chiral space groups. During crystallization, the achiral molecules adopted chiral conformations in which one of two enantiotopic hydrogens was able to be abstracted preferentially in a Norrish type II photoprocess. Unlike solid state reactions, where rapid equilibration between the two chiral conformations is highly disfavoured by the restrictive reaction cavity formed by neighbouring molecules, solution reactions of the same compounds led to racemic mixtures owing to the absence of topochemical control. Similarly, chemical reactivity was also found to be directly related to molecular conformation. Through the use of X-ray crystallography, crystal structure-solid state reactivity relationships were developed in order to gain a greater understanding of how changes in molecular conformation can affect chemical reactivity. In terms of the Norrish/Yang photochemistry of ketones it was found that while hydrogen abstraction was likely to occur for all of the ketones that were characterized by crystallography, changes in the geometry of the carbonyl group had a large effect on the observed reaction pathway (cyclization, cleavage or reverse hydrogen abstraction). Combination of the present work with previous Norrish/Yang studies is being used to create a database of parameters to gain a greater understanding of the geometric requirements for reactivity. This would allow for the potential to gauge the likely success of hypothetical reactions, based on molecular modeling, prior to the lengthy synthesis starting materials.

The results of the present work, in conjunction with previous work from our laboratory, have shown that the ionic chiral auxiliary approach to asymmetric photochemistry is a reliable method of achieving enantioselectivity in a variety of different photochemical reactions. By screening a variety of different auxiliaries for a given molecule it is possible to engineer crystals

that will give the desired photoproduct in high chemical yield, high optical yield, and of the correct absolute configuration. While the use of this methodology will always be limited to molecules possessing acidic or basic functional groups that are able to undergo unimolecular rearrangements with a minimum of molecular movement, applications in constructing optically pure synthons for use in natural product synthesis are an obvious area of future research. As a reliable, controllable, easily scalable methodology, this would have the potential of allowing for the greater use of photochemistry in synthetic chemistry.

EXPERIMENTAL

Chapter 7 Preparation of Substrates

7.1 General Considerations

<u>Infrared Spectra (IR)</u>

Infrared spectra were recorded on a Perkin-Elmer model 1710 Fourier transform spectrometer. Liquid samples were analyzed neat, as thin films, or as CCl_4 solutions between two sodium chloride plates. Solid samples (~1 mg) were ground with IR grade KBr (100-200 mg) in an agate mortar and pressed into a disc (1 cm diameter) using an evacuated die (Perkin-Elmer 186-0002) with a laboratory press (Carver, model B) at 17,000 psi. The positions of selected absorption maxima (ν_{max}) are reported in units of cm^{-1}.

<u>Melting Points (mp)</u>

Melting points were determined on a Fisher-Johns hot stage melting point apparatus and are uncorrected. When recrystallized samples were analyzed, the solvent of recrystallization is given in parenthesis.

<u>Nuclear Magnetic Resonance (NMR) Spectra</u>

Proton nuclear magnetic resonance (^1H NMR) spectra were recorded in deuterated solvents as noted. Data were collected on the following instruments: Bruker AC-200 (200 MHz), Varian XL-300 (300 MHz), Bruker WH-400 (400 MHz), Bruker AV-400 (400 MHz) and Bruker AMX-500 (500 MHz). Chemical shifts (δ) are measured in parts per million (ppm) of the spectrometer base frequency, and are referenced to the chemical shift of the residual ^1H solvent signals, with tetramethylsilane (δ 0.00) as an external standard: chloroform (7.24 ppm), acetone (2.04 ppm), methanol (3.30 ppm), methylene chloride (5.32 ppm) and dimethylsulfoxide (2.49 ppm). The signal multiplicity, coupling constants, and number of hydrogen atoms are given in parentheses following the signal position. Multiplicities are abbreviated as follows: multiplet (m), singlet (s), doublet (d), triplet (t), quartet (q), quintet (quint), and broad (br). Nuclear Overhauser Enhancement (NOE) spectra were acquired on the Bruker WH-400 and Bruker Avance 400 spectrometers. ^1H-^1H correlation spectroscopy

(COSY) was conducted on the Bruker AC-200, Bruker WH-400, Bruker AMX-500 or Bruker AV-400 spectrometers. Two-dimensional Nuclear Overhauser Spectroscopy (NOESY) was conducted on the Bruker AV-400 spectrometer.

Carbon nuclear magnetic resonance (^{13}C NMR) spectra were recorded on the following instruments: Bruker AC-200 (50.3 MHz), Varian XL-300 (75.4 MHz), Bruker AM-400 (100.5 MHz) and Bruker AV-300 (75.4 MHz). All experiments were conducted using broadband ^{1}H decoupling. Chemical shifts (δ) are reported in ppm and are referenced to the centre of the solvent multiplet, with tetramethylsilane (δ 0.00) as an external reference: chloroform (77.0 ppm), acetone (20.8 ppm), methanol (49.0 ppm), methylene chloride (53.8 ppm) and dimethylsulfoxide (39.5 ppm). Some spectra are supported by data from the Attached Proton Test (APT). Where these are given, (-) denotes a negative APT peak corresponding to a methine (CH) or methyl (CH$_3$) carbon centre while (+) corresponds to a quaternary (C) or methylene (CH$_2$) carbon centre.

Two-dimensional ^{13}C-^{1}H correlation spectra were obtained on the Bruker AM-400, Bruker AMX-500 and Bruker AV-400 spectrometers using the Heteronuclear Multiple Quantum Coherence (HMQC) experiment for one-bond correlations and the Heteronuclear Multiple Bond Connectivity (HMBC) experiment for long-range (2,3 bond) connectivities.

Mass Spectra

Low and high resolution mass spectra (LRMS) and (HRMS) were recorded on a Kratos MS 50 instrument using electron impact (EI) ionization at 70 eV, a Kratos MS 80 spectrometer using desorption chemical ionization (DCI) with the ionizing gas noted; a Kratos Concept IIHQ hybrid spectrometer using liquid secondary ionization (LSIMS), or a Bruker Esquire~LC (low resolution) or Micromass LCT (high resolution) spectrometer using electrospray ionization (ESI). GC/MS analyses of photoproduct mixtures were recorded on a Kratos MS 80 spectrometer. Analyses were performed by in-house technicians under the supervision of Dr. G. Eigendorf or Dr. Yun Ling.

Low resolution mass spectra and GC/MS data were also recorded on an Agilent 5973N mass selective detector, attached to an Agilent 6890+ gas chromatograph, using electron impact (EI) ionization at 70 eV.

Mass to charge ratios (m/e) are given, with relative intensities in parentheses, where applicable. Molecular ions are designated as M^+.

Ultraviolet - Visible Spectra (UV/VIS)

Electronic absorption spectra were recorded on a Perkin-Elmer Lambda-4B UV/Vis spectrometer in the solvents and concentrations indicated using spectral grade solvents. Absorption maxima (λ_{max}) are reported in nanometers (nm), with molar extinction coefficients (ε) reported in parenthesis in units of $M^{-1}cm^{-1}$.

Microanalysis (anal.)

Elemental analyses were obtained for new compounds when possible. These were performed either in-house by Mr. Peter Borda or Minaz Lakha, under the supervision of Dr. Yun Ling, on a Carlo Erba CHN Model 1106 analyzer or by Canadian Microanalytical Services Ltd. of Delta, BC.

Crystallography

Single crystal X-ray diffraction analysis was performed in-house on either a Rigaku AFC6S four-circle diffractometer (Cu-Kα or Mo-Kα radiation) or a Rigaku AFC7 four-circle diffractometer equipped with a DSC Quantum CCD detector (Mo-Kα radiation). Data collection and structural refinements were conducted by Eugene Cheung, under the supervision of Dr. James Trotter, or by Dr. Brian Patrick. Some structures were refined by Charles Scott, under the supervision of Dr. Brian Patrick. Structures are represented as ORTEP drawings at the 50% probability level.

Optical Rotations

Optical rotation data were recorded on a Jasco P-1010 polarimeter at room temperature at the sodium D-line (589.3 nm).

Gas Chromatography (GC)

Gas chromatographic analyses in a helium carrier gas were performed on a Hewlett-Packard 5890A gas chromatograph equipped with a flame ionization detector, or on an Agilent

6890 gas chromatograph, equipped with an Agilent 5970N mass selective detector. Data were collected on a Hewlett-Packard 3392A integrator (5890) or using Agilent's Chemstation software (6890). The following Hewlett-Packard fused silica capillary columns were used: HP-5 (30m x 0.25 mm x 0.25 μm ID) (5890A), HP-5MS (30m x 0.25 mm x 0.25 μm ID) (5890A and 6890) and HP-35 (15m x 0.25 mm x 0.25 μm ID) (5890A). Analyses were run with split injection ports (split ratios between 25:1 and 100:1) and column head pressures ranging from 100 kPa to 250 kPa.

High Performance Liquid Chromatography (HPLC)

HPLC analyses were performed on a Waters 600E system coupled to either a Waters 486 tunable UV detector or a Waters 994 photodiode array detector under the conditions indicated. Preparative separations were conducted using a Waters Radialpak™ μPorasil™ preparative column (25 mm x 100 mm) with a hexanes:EtOAc eluent. Enantiomeric excesses (ee) were determined using a Chiralcel™ OD™, Chiralcel™ OC™ or Chiralpak™ AS™ column (250 mm x 4.6 mm ID), from Chiral Technologies Inc., with a hexanes:IPA eluent. Data were collected using the Waters Maxima software package.

Silica Gel Chromatography

Analytical thin layer chromatography (TLC) was performed on commercial pre-coated (silica gel on aluminum) plates (E. Merck, type 5554). Preparative chromatography was performed using either the flash column method with Merck 9385 or Silicycle silica gel (particle size 230-400 mesh), or by radial elution chromatography on a Chromatatron (Harrison Research) using plates of 1 or 2 mm thickness prepared from EM Science silica gel 60 PF254 with gypsum (7749-3).

Solvents and Reagents

Tetrahydrofuran (THF) was refluxed over the sodium ketyl of benzophenone under an atmosphere of argon and distilled prior to use. Anhydrous dichloromethane and benzene were obtained by refluxing over calcium hydride under an atmosphere of argon or nitrogen and distilling prior to use. All other solvents and reagents were used without purification unless

noted otherwise. Unless otherwise noted, all reactions were conducted under an atmosphere of dry nitrogen in oven or flame-dried glassware.

7.2 Synthesis of Benzonorbornene Derivatives 43, 44, 45, and 46

7.2.1 Preparation of Benzonorbornene Derivative 43

1,4-Dihydro-1,4-methanonaphthalene (47)
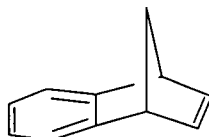
47

Following the procedure of Wittig et al.,[108] a solution of freshly cracked cyclopentadiene (9.4 mL, 114 mmol) and o-bromofluorobenzene (13.4 mL, 114 mmol) in THF (70 mL) was cooled in an ice bath and added dropwise to magnesium shavings (3.0 g, 123 mmol) in THF (25 mL). After the initial vigorous reaction subsided, the addition was continued at a rate that maintained a constant rate of reflux. After 2 h the solution was filtered to remove the magnesium residue and the THF was removed in vacuo giving a black oil. The oil was extracted with a saturated solution of NH_4Cl and ether (3 x 100 mL), with the combined organic extracts then being washed with water (3 x 100 mL) before drying over $MgSO_4$. The ether was removed in vacuo to give a brown oil (12.63 g, 77.6%), used without further purification. This product gave spectra in agreement with those previously obtained within our laboratory[75] and from the literature.[108]

^{1}H NMR (200 MHz, $CDCl_3$): δ 2.40 (br dt, J = 7.1, 1.5 Hz, 1H), 2.48 (dt, J = 7.1, J = 1.5 Hz, 1H), 4.03 (quint, J = 1.7 Hz, 2H), 6.94 (t, J = 1.9 Hz, 2H), 7.09 (dd, J = 5.1, 3.1 Hz, 2H), 7.38 (dd, J = 5.1, 3.1 Hz, 2H).

IR (neat) v_{max}: 3067, 2983, 2935, 1455, 758 cm^{-1}.

<u>*exo*-2-*anti*-9-Dibromo-1,2,3,4-tetrahydro-1,4-methanonaphthalene (**48**)</u>

48
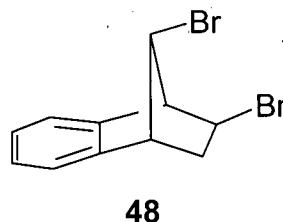
Following the procedures of Cristol *et al.*[109] and Wilt *et al.*,[110] a solution of bromine (5 mL, 92 mmol) in CCl$_4$ (65 mL) was added dropwise to a solution of compound **47** (12.63 g, 88.8 mmol) in CCl$_4$ (50 mL) that had been cooled in an ice bath. After the addition was complete the ice bath was removed and the reaction mixture was stirred at room temperature for 3 h. The residual bromine was removed by extraction with a saturated solution of sodium thiosulphate (3 x 100 mL) and the organic layer was then washed with water (3 x 100 mL) before being dried with MgSO$_4$. Removal of the solvent *in vacuo* gave a red-brown oil that was purified by column chromatography (80:20 petroleum ether:methylene chloride) to give **48** as an off-white solid (15.36 g, 57%). The spectral data obtained was in accordance with those previously recorded[75] and literature values.[110]

mp: 78.0-78.5 °C (lit.[110] 76-77 °C).

^{1}H NMR (300 MHz, CDCl$_3$): δ 2.20 (dd, *J* = 13.2, 7.8, 1H), 2.85 (dt, *J* = 13.5, 4.2 Hz, 1H), 3.50 (t, *J* = 1.8 Hz, 1H), 3.74 (s, 1H), 3.78 (ddd, *J* = 8.1, 4.5 Hz, 1H), 4.13 (t, *J* = 1.4 Hz, 2H), 7.17 (m, 4H).

^{13}C NMR (75 MHz, CDCl$_3$): δ 143.51, 142.89, 127.80, 127.28, 121.77, 121.30, 56.42, 55.55, 51.04, 45.00, 36.57.

anti-9-Bromo-1,4-dihydro-1,4-methanonaphthalene (**49**)
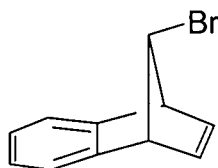
49

Following the procedure of Janz,[75] diisopropylamine (19.0 mL, 136 mmol) was added to a suspension of KH (6.02 g, 150 mmol) in THF (150 mL) and stirred for 15 min. Dibromide **48** (15.36 g, 50.9 mmol) in THF (150 mL) was added dropwise over 20 min and the resulting mixture was refluxed for 5 h. After cooling, the reaction was quenched by the slow addition of a saturated NH_4Cl solution (150 mL). The resulting mixture was extracted with ether (3 x 100 mL) and the combined organic fractions were then washed with 5% HCl (2 x 50 mL) and water (until neutral). After drying over $MgSO_4$ the solvent was removed *in vacuo* to give a dark oil that was purified by column chromatography (80% petroleum ether : 20% CH_2Cl_2) to give the desired product as a pale yellow solid (8.51 g, 75.7%). The spectral data obtained were in accordance with those previously reported by Wilt *et al.*[110]

mp: 50.5 – 52.0 °C (lit.[110] 53-54 °C).

^{1}H NMR (300 MHz, $CDCl_3$): δ 4.10 (m, 2H), 4.40 (m, 1H), 6.74 (m, 2H), 7.04 (dd, J = 5.4, 3.0 Hz, 2H), 7.26 (dd, J = 5.3, 3.2 Hz, 2H).

^{13}C NMR (75 MHz, $CDCl_3$): δ 57.27, 74.23, 122.02, 125.61, 139.50, 147.04.

IR (KBr) v_{max}: 1647, 1542, 1508, 777, 724 cm^{-1}.

1,4-Dihydro-1,4-methanonaphthalene-*anti*-9-carboxylic acid (**37**)

37
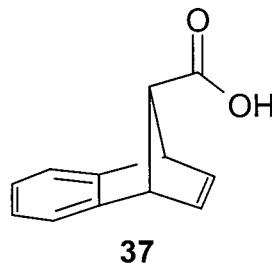
Following the procedure of Buske *et al.*,[72] ^{t}BuLi (46 mL, 78.2 mmol) was added to THF (100 mL) at -78 °C (dry ice / acetone bath) and stirred for 15 min. A solution of bromide **49** (8.51 g, 38.5 mmol) in THF (350 mL) at -78 °C was slowly added and then stirred for 45 min at which time dry CO_2 was sublimed into the solution. The reaction mixture was then allowed to warm to room temperature and, after CO_2 evolution ceased, was acidified with 5% HCl. After removal of the THF *in vacuo* the resulting suspension was extracted with ether (3 x 100 mL) and the combined organic layers were washed with 10% NaOH (2 x 50 mL). The combined aqueous layers were cooled in an ice bath and acidified with conc. HCl, causing a white precipitate to fall out of solution. The solution was stored in a refrigerator overnight before the solid was removed by suction filtration and washed with 5% HCl. After recrystallization of the solid from chloroform the desired product was obtained as a colourless solid (6.22 g, 87%). The physical and spectral data obtained for this compound matched those previously noted.[75,72]

mp: 204.5–205 °C (lit.[72] 198–200 °C).

^{1}H NMR (200 MHz, acetone-d_6): δ 3.2 (m, 1H), 4.1 (m, 2H), 6.7 (m, 2H), 6.9 (dd, J = 5.2, 3.1 Hz, 2H), 7.1 (dd, J = 5.2, 3.1 Hz, 2H), 10.8 (br, 1H).

^{13}C NMR (75 MHz): δ 53.17, 82.19, 122.56, 125.72, 141.76, 151.37, 174.17.

<u>1,2,3,4-Tetrahydro-1,4-methanonaphthalene-*anti*-9-carboxylic acid (**50**)</u>

50
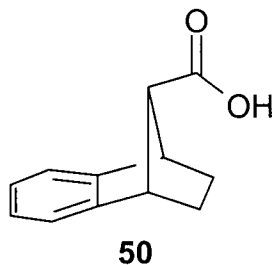
Acid **37** (6.22 g, 33.4 mmol) was dissolved in EtOAc (50 mL) followed by the addition of Pd/C (380 mg). The reaction vessel was placed on a hydrogenation apparatus and, after evacuation of the system, H_2 (800 mL, 35.7 mmol) was introduced. Once gas uptake had ceased Celite (2 g) was added and the reaction mixture was filtered through a bed of Celite to remove the Pd catalyst. Removal of the solvent *in vacuo* gave a colourless solid (6.04 g, 96%), which was used without further purification.

mp: 154 – 156 °C (methanol)

^{1}H NMR (400 MHz, $CDCl_3$): δ 1.21 (m, 2H), 2.11 (m, 2H), 2.82 (m, 1H), 3.60 (m, 2H), 7.09 (m, 2H), 7.17 (m, 2H), 11.1 (br, 2H).

^{13}C NMR (75 MHz, $CDCl_3$): δ 25.13 (+), 45.22 (-), 61.79 (-), 120.57 (-), 126.00 (-), 146.62 (+), 177.97 (+).

IR (KBr) v_{max}: 3350-2900 (br), 2977, 1695, 1469, 1456, 1408, 1151, 1108, 1017, 923, 873, 747, 714 cm^{-1}.

UV/Vis (MeOH): 202.4 (4,391), 264.2 (438), 270.8 (450) nm ($M^{-1}cm^{-1}$).

LRMS (EI): 188 (54, M^+), 160 (47), 143 (33), 142 (16), 141 (16), 129 (20), 128 (65), 127 (11), 117 (16), 116 (100), 115 (93), 89 (13), 63 (20), 51 (11), 39 (11).

HRMS (EI) calcd for $C_{12}H_{12}O_2$: 188.0837, found 188.0875.

Anal. Calcd for $C_{12}H_{12}O_2$: C, 76.57; H, 6.43. Found: C, 76.29; H, 6.44.

Phenyl(1,2,3,4-tetrahydro-1,4-methanonaphthalen-*anti*-9-yl)methanone (**43**)
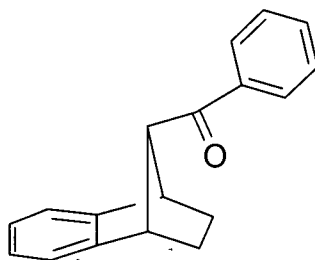
43

Acid **50** (1.11 g, 5.9 mmol) was dissolved in thionyl chloride (9.0 mL, 125 mmol) and refluxed for 2 h. Residual thionyl chloride was removed by vacuum distillation to leave a light brown oil, which was washed with ether (2 x 10 mL) and removed *in vacuo* to give the acid chloride of acid **50** as an off-white solid (1.21 g, 99%). The acid chloride (1.21 g, 5.9 mmol) was dissolved in benzene (10 mL) and added dropwise to a solution of AlCl$_3$ (2.12 g, 15.9 mmol) in benzene (10 mL). After stirring for 3 h the black solution was quenched with water (5 mL) and extracted with ether (2 x 15 mL). The combined ethereal fractions were then washed with water (3 x 10 mL) before drying over MgSO$_4$. Removal of the solvent *in vacuo* gave a viscous brown oil that was purified by chromatography (5% ether in pet. ether) to give a yellow oil. Following trituration of the yellow oil with pentanes, ketone **43** was obtained as a colourless solid (0.39 g, 27%).

mp: 60.5-61 °C (methanol/water).

^{1}H NMR (400 MHz, CDCl$_3$): δ 1.16 (m, 2H), 2.05 (m, 2H), 3.49 (t, *J* = 1.3 Hz, 1H), 3.66 (m, 2H), 7.12 (m, 2H), 7.19 (m, 2H), 7.45 (m, 2H), 7.55 (tt, *J* = 7.4, 1.3 Hz, 1H), 7.95 (m, 2H).

^{13}C NMR (75 MHz, CDCl$_3$): δ 24.95 (+), 46.41 (-), 66.22 (-), 120.50 (-), 125.91 (-), 128.26 (-), 128.53 (-), 132.90 (+), 136.32 (+), 147.26 (+), 198.94 (+).

IR (KBr) ν$_{max}$: 3050, 3001, 2981, 2963, 2949, 2872, 1678, 1595, 1577, 1467, 1446, 1361, 1306, 1279, 1243, 1221, 1183, 1112, 1044, 1020, 1000, 989, 884, 836, 820, 790, 773, 747, 717, 697, 672, 637, 568, 508, 446 cm^{-1}.

UV/VIS (hexanes, 9.67 x 10^{-5} M): 240 (11,325), 272 (1354), 336 (19) nm (M^{-1}cm^{-1}).

LRMS (EI): 249 (2), 248 (9, M$^+$), 143 (10), 128 (64), 115 (19), 105 (100), 77 (48.34).

HRMS (EI) calcd for $C_{18}H_{16}O$: 248.1201; found: 248.1205.

Anal. Calcd for $C_{18}H_{16}O$: C 87.05; H 6.50. Found C 86.76; H 6.53.

This structure was confirmed by X-ray crystallographic analysis:

Habit	colourless prisms
Space Group	*P*bca
a, Å	27.107(3)
b, Å	11.790(1)
c, Å	8.617(2)
α (°)	90
β (°)	90
γ (°)	90
Z	8
R	0.045

7.2.2 Preparation of Benzonorbornene Derivative 44

N-Methoxy-*N*-methyl-1,2,3,4-tetrahydro-1,4-methanonaphthalen-*anti*-9-carboxamide (**52**)
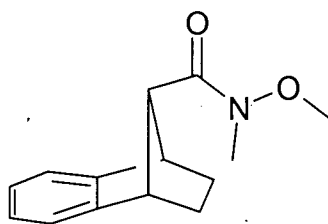
52

Based on a procedure by Jones *et al.* for the formation of Weinreb amides[76,77] acid **50** (2.52 g, 11.5 mmol) was dissolved in CH_2Cl_2 (75 mL) and cooled in an ice bath. Carbonyldiimidazole (2.77 g, 17.1 mmol) was added and the mixture was stirred for 30 min after which time Me$_2$ONH·HCl (3.27 g, 33.5 mmol) was added. The resulting mixture was stirred overnight with the resulting precipitate being removed by filtration. The filtrate was

washed with 10% NaOH (2 x 25 mL) and water (4 x 25 mL) before being dried over $MgSO_4$. Removal of the solvent gave the desired amide as a colourless solid (2.36 g, 76.4%), which was used without further purification.

mp: 58.5 – 59.5 °C

^{1}H NMR (400 MHz, $CDCl_3$): δ 1.14 (m, 2H), 2.19 (m, 2H), 2.86 (br, 1H), 3.17 (s, 3H), 3.56 (m, 2H), 3.65 (s, 3H), 7.08 (m, 2H), 7.16 (m, 2H).

^{13}C NMR (100 MHz, $CDCl_3$): δ 25.45 (+), 32.33 , 45.86 (-), 60.28 (-), 60.98 (-), 120.29 (-), 125.65 (-), 147.47 (+), 171.87 (+).

IR (KBr) v_{max}: 3044, 3000, 2979, 2960, 2937, 2869, 1655, 1460, 1385, 1320, 1279, 1184, 1154, 1110, 1012, 988, 964, 862, 835, 750, 574 cm^{-1}.

LRMS (EI): 232 (5, M^+), 171 (16), 144 (12), 143 (100), 129 (14), 128 (22), 116 (22), 115 (42).

HRMS (EI) calcd for $C_{14}H_{17}O_2N$: 231.1259, found: 231.1256.

Anal. Calcd for $C_{14}H_{17}O_2N$: C, 72.70; H, 7.41; N, 6.06. Found: C 72.48; H, 7.38; N, 5.97.

4-(Fluorophenyl)(1,2,3,4-tetrahydro-1,4-methanonaphthalen-*anti*-9-yl)methanone (44)
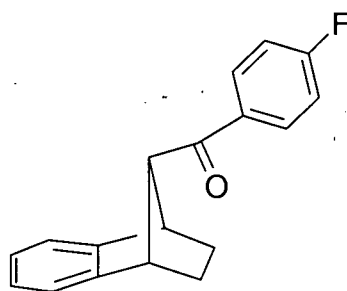
44

Amide **52** (4.80 g, 20.8 mmol) in THF (200 mL) was cooled in an ice bath and *p*-FPhMgBr (17 mL, 34.0 mmol) was added dropwise. After stirring for 1 h the temperature was allowed to rise to room temperature for an additional 4 h. A saturated solution of ammonium chloride (50 mL) was added and followed by the removal of THF *in vacuo*. The resulting oily solid was taken up in ether (100 mL) and washed with 10% HCl (2 x 50 mL) and water (3 x 50 mL) then dried over $MgSO_4$. Removal of the solvent gave a yellow solid that was

purified by column chromatography (5% ether/petroleum ether) to give a **44** as a colourless solid (4.98 g, 90.2%).

mp: 83 – 84 °C (hexanes).

^{1}H NMR (400 MHz, CDCl$_3$): δ 1.16 (m, 2H), 2.04 (m, 2H), 3.44 (m, 1H), 3.63 (m, 2H), 7.12 (m, 4H), 7.20 (m, 2H), 7.98 (m, 2H).

^{13}C NMR (75 MHz, CDCl$_3$): δ 24.94 (+), 46.45 (-), 66.04 (-), 115.49 and 115.78 (-, $^2J_{C-F}$ = 22 Hz), 120.51 (-), 125.97 (-), 130.81 and 130.93 (-, $^3J_{C-F}$ = 9 Hz), 132.65 and 132.69 (+, $^4J_{C-F}$ = 4 Hz), 147.11 (+), 163.88 and 167.26 (+, $^1J_{C-F}$ = 255 Hz), 197.22 (+).

IR (KBr) v_{max}: 3068, 3022, 2989, 2976, 2875, 1667, 1597, 1504, 1459, 1346, 1225, 1154, 750 cm^{-1}.

UV/VIS (hexanes, 1.65 x 10^{-4} M): 244 (14,972), 271 (1560), 332 (23) nm (M^{-1}cm^{-1}).

LRMS (EI): 266 (15, M$^+$), 151 (17), 143 (23), 129 (13), 128 (100), 123 (99.9), 115 (25), 95 (38), 75 (11).

HRMS (EI) calcd for C$_{18}$H$_{15}$OF: 266.1107, found: 266.1108.

Anal. Calcd for C$_{18}$H$_{15}$OF: C, 81.18; H, 5.68. Found: C, 80.92; H, 5.64.

This structure was confirmed by X-ray crystallographic analysis:

Habit	colourless prisms
Space Group	P$\bar{1}$
a, Å	9.0169(1)
b, Å	10.906(1)
c, Å	6.8869(7)
α (°)	92.340(8)
β (°)	90.63(1)
γ (°)	81.735(9)
Z	2
R	0.044

7.2.3 Preparation of Benzonorbornene Derivative 45

<u>Methyl 4-(1,2,3,4-tetrahydro-1,4-methanonaphthalen-*anti*-9-ylcarbonyl)benzoate (45)</u>

45
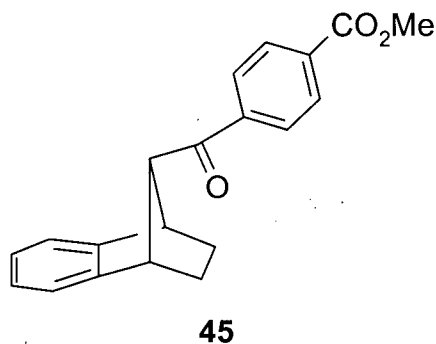
Using a modification of the procedure by Knochel *et al.* for the preparation of substituted aryl Grignard reagents,[78] *p*-iodobenzoic acid methyl ester (2.25 g, 8.6 mmol) was dissolved in THF (35 mL) and cooled to –40 °C. Isopropylmagnesiumchloride (4.8 mL, 2 M, 9.6 mmol) was added and the solution was stirred for 1 h. A solution of amide **52** (1.64 g, 7.01 mmol) in THF (15 mL) was added and the solution was stirred for 2 h, then gradually warmed to –20°C, stirred for 2 h, and finally stirred overnight at room temperature. The reaction was quenched by addition of a saturated solution of ammonium chloride (50 mL), followed by removal of the THF *in vacuo* and its replacement with diethyl ether (100 mL). The ethereal solution was washed 10% HCl (2 x 30 mL) and water (3 x 30 mL) before being dried over MgSO$_4$. Removal of the solvent gave a yellow oil which was purified by chromatography (10% ether/pet. ether) to give a colourless solid (1.41 g, 63%)

mp: 89 – 89.5 °C (ether/pet. ether).

^{1}H NMR (400 MHz, CDCl$_3$): δ 1.17 (m, 2H), 2.02 (m, 2H), 3.49 (t, *J* = 1Hz, 1H), 3.65 (m, 2H), 3.94 (s, 3H), 7.12 (m, 2H), 7.20 (m, 2H), 7.98 (m, 2H), 8.11 (m, 2H).

^{13}C NMR (75 MHz, CDCl$_3$): δ 24.86 (+), 46.25 (-), 52.42 (-), 66.32 (-), 120.51 (-), 125.98 (-), 128.10 (-), 129.75 (-), 133.66 (+), 139.55 (+), 146.94 (+), 155.15 (+), 198.49 (+).

IR (KBr) ν$_{max}$: 2959, 2865, 1718, 1681, 1569, 1435, 1274, 1213, 1105, 813, 754 cm^{-1}.

UV/VIS (methanol, 1.57 x 10^{-4} M): 214 (9580), 254 (16, 094), 288 (sh) (2953), 330 (206) nm (M^{-1}cm^{-1}).

LRMS (EI): 306 (20, M$^+$), 191 (12), 163 (74), 143 (28), 142 (11), 135 (14), 129 (14), 128 (100), 115 (30), 103 (10), 76 (10).

HRMS (EI) calcd for $C_{20}H_{18}O_3$: 306.1256, found: 306.1257.

Anal. Calcd for $C_{20}H_{18}O_3$: C, 78.41; H, 5.92. Found: C, 78.40; H, 5.88.

This structure was confirmed by X-ray crystallographic analysis:

Habit	colourless prisms
Space Group	$P2_12_12_1$
a, Å	13.693(4)
b, Å	19.066(8)
c, Å	5.947(3)
α (°)	90
β (°)	90
γ (°)	90
Z	4
R	0.037

7.2.4 Preparation of Benzonorbornene Derivative 46

4-(1,2,3,4-tetrahydro-1,4-methanonaphthalen-*anti*-9-ylcarbonyl)benzoic acid **(46)**
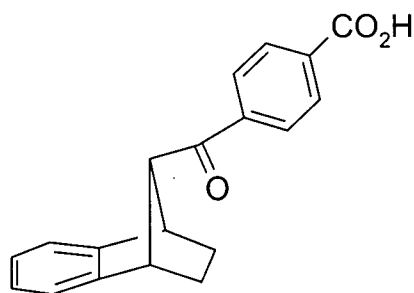
46

Using an extension of the technique by Knochel *et al.* for the synthesis of substituted aryl Grignard reagents,[78] *p*-iodobenzoic acid (1.60 g, 6.45 mmol) was dissolved in THF (25 mL)

under N_2 and cooled to $-30°C$. Isopropylmagnesiumchloride (6.45 mL, 2 M, 12.9 mmol) was added dropwise and the resulting solution was stirred for 45 min. On addition of the second Grignard equivalent, a light brown precipitate began to form. Amide **52** (1.0 g, 4.32 mmol) in THF (5 mL) was added dropwise and the resulting mixture was gradually warmed to $-20°C$ and stirred for 4 h during which time the precipitate dissolved. The reaction was allowed to stir at room temperature overnight and then quenched with saturated ammonium chloride. After acidification with 10% HCl the THF was replaced by ether and extracted with 10% HCl and water. The organic layer was then washed with saturated sodium bicarbonate (3 x 50 mL) and the combined aqueous portions were acidified with conc. HCl causing acid **46** to precipitate. The suspended precipitate was washed with ether (2 x 50 mL) and the organic portions were washed with water (3 x 50 mL) before being dried over magnesium sulphate. Removal of the solvent gave an off-white solid composed of the desired acid and its unwanted epimer in a 9:1 ratio. The unwanted epimer was removed by recrystallization from ethanol. The filtrate was then concentrated by removal of the solvent and the resulting solid was fractionally crystallized from methanol to give **46** as a colourless solid (0.84 g, 66%).

mp: 225 – 226 °C (methanol).

^{1}H NMR (400 MHz, CD_3OD): δ 1.11 (m, 2H), 1.98 (m, 2H), 3.57 (m, 1H), 3.63 (m, 2H), 7.09 (m, 2H), 7.19 (m, 2H), 8.03 (m, 2H), 8.13 (m, 2H).

^{13}C NMR (100 MHz, CD_3OD): δ 25.91 (+), 47.55 (-), 67.67 (-), 121.49 (-), 127.11 (-), 129.31 (-), 130.97 (-), 135.77 (+), 141.02 (+), 148.37 (+), 166.74 (+), 200.51 (+).

IR (KBr) v_{max}: 2980, 2955, 2900 – 2500 (br), 1685, 1675, 1504, 1419, 1282, 1216, 745 cm^{-1}.

UV/VIS (methanol, 1.51 x 10^{-4} M): 216 (9604), 256 (16470), 290 (sh) (2065), 328 (187) nm ($M^{-1}cm^{-1}$).

LRMS (EI): 293 (8, M^+), 292 (38), 177 (12), 149 (89), 143 (41), 142 (12), 129 (14), 128 (100), 115 (24), 65 (14).

HRMS (EI) calcd for $C_{19}H_{16}O_3$: 292.1099. found : 292.1101.

This structure was confirmed by X-ray crystallographic analysis:

Habit	colourless blocks
Space Group	$P2_1/a$
a, Å	11.8667(6)
b, Å	9.1837(6)
c, Å	13.992(1)
α (°)	90
β (°)	98.081(2)
γ (°)	90
Z	4
R	0.069

7.2.5 Preparation of *anti*-9-(*p*-Carboxybenzoyl)benzonorbornene (46) Salts

(*R*)-(+)-2-Phenylpropylammonium 4-(1,2,3,4-tetrahydro-1,4-methanonaphthalen-*anti*-9-ylcarbonyl)benzoate (81)

81
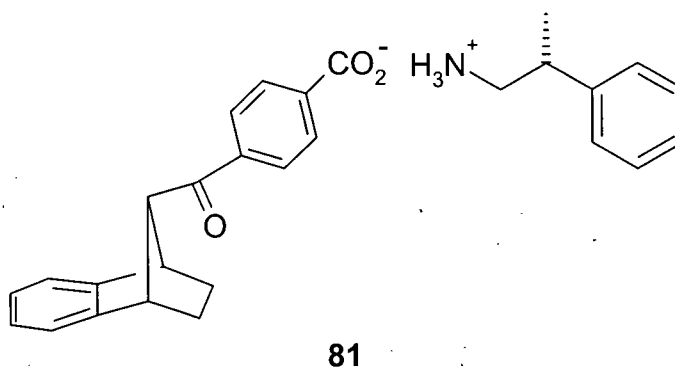
(*R*)-(+)-β-Methylphenethylamine (40 µL, 0.28 mmol) was added to a solution of acid **46** (74 mg, 0.25 mmol) in methanol (5 mL). Upon standing a white precipitate formed, which was isolated by filtration to give salt **81** (59 mg, 55%) as a colourless solid.

mp: 156 - 158 °C (methanol)

¹H NMR (400 MHz, DMSO): δ 1.02 (m, 2H), 1.24 (d, J = 6.6 Hz, 3H), 1.89 (m, 2H), 2.94 (m, 3H), 3.60 (br s, 3H), 7.09 (dd, J = 5.3, 3.1 Hz, 2H), 7.23 (dd, J = 5.3, 3.1 Hz, 2H), 7.25 (m, 1H), 7.26 (m, 2H), 7.33 (m, 2H), 7.91 (dm, J = 8.4 Hz, 2H), 7.97 (dm, J = 8.4 Hz, 2H).

¹³C NMR (75 MHz, DMSO): δ 19.23 (-), 24.71 (+), 38.43 (-), 45.59 (+), 54.92 (+), 65.92 (-), 120.49 (-), 125.74 (-), 126.68 (-), 127.14 (-), 127.65 (-), 128.58 (-), 129.12 (-), 136.77 (+), 141.75 (+), 143.58 (+), 147.00 (+), 168.03 (+), 198.81 (+).

IR (KBr) ν_{max}: 3200-2700 (br), 2961, 1674, 1583, 1531, 1377, 1243, 1215, 1015, 813, 755, 698 cm^{-1}.

HRMS (ESI, +, 0.1% HCO$_2$H in MeOH) calcd for C$_{28}$H$_{30}$O$_3$N (M+1): 428.2226, found: 428.2234.

Anal. Calcd for C$_{28}$H$_{29}$O$_3$N : C, 78.66; H, 6.84; N, 3.28. Found: C, 78.50; H, 6.82; N, 3.20.

This structure was confirmed by X-ray crystallographic analysis:

Habit	colourless prisms
Space Group	$C2$
a, Å	24.770(3)
b, Å	6.2560(6)
c, Å	15.702(2)
α (°)	90
β (°)	104.503(6)
γ (°)	90
Z	4
R	0.0495

[(*S*)-(-)-2-Ammonio-3-phenylpropanoate]-[4-(1,2,3,4-tetrahydro-1,4-methanonaphthalen-*anti*-9-ylcarbonyl)benzoic acid] **(82)**
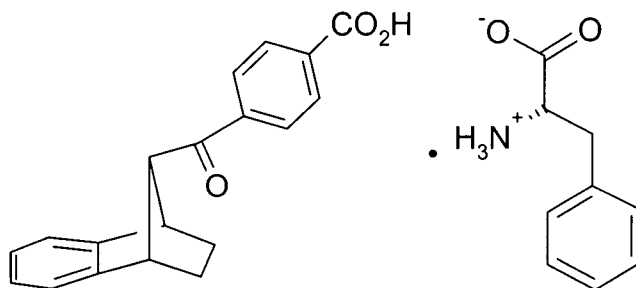
82

(*S*)-(-)-Phenylalanine (42 mg, 0.26 mmol) was dissolved in a 1:1 ethanol:water mixture (3 mL) and added to a solution of acid **46** (72 mg, 0.25 mmol) in methanol (6 mL). Upon prolonged standing a white precipitate began to fall out of solution, which was collected by suction filtration to give salt **82** (113 mg, 67%).

mp: 178 - 179.5 °C (methanol)

¹H NMR (400 MHz, DMSO): δ 1.03 (m, 2H), 1.88 (br d, *J* = 7 Hz, 2H), 2.85 (dd, *J* = 14.3, 8.3 Hz, 1H), 3.14 (dd, *J* = 14.3, 4.5 Hz, 1H), 3.36 (br), 3.44 (dd, *J* = 8.3, 4.5 Hz, 1H), 3.61 (m, 2H), 3.65 (s, 1H), 7.10 (dd, *J* = 5.3, 3.1 Hz, 2H), 7.23 (dd, *J* = 5.3, 3.1 Hz, 2H), 7.26 (m, 5H), 8.04 (m, 4H).

¹³C NMR (75 MHz, DMSO): δ 24.69 (+), 36.91 (+), 45.89 (-), 55.37 (+), 65.95 (-)120.54 (-), 125.81 (-), 126.46 (-), 128.30 (-), 129.36 (-), 129.54 (-), 135.01 (+), 137.46 (+), 138.96 (+), 146.90 (+), 166.33 (+), 169.38 (+), 172.09 (+), 198.81 (+).

IR (KBr) v_{max}: 3300-3600 (br), 2994, 2967, 2867, 1683, 1637, 1604, 1458, 1450, 1408, 1364, 1294, 1240, 1213, 1108, 754, 696 cm⁻¹.

HRMS (ESI, -ve, Methanol) calcd for $C_{28}H_{26}O_5N$ (M-1): 456.1811, found: 456.1802.

Anal. Calcd for $C_{28}H_{27}O_5N \cdot \frac{1}{4}H_2O$: C, 72.79; H, 6.00; N, 3.03. Found: 72.99; H, 5.87; N, 3.03

        (Calcd for $C_{28}H_{27}O_5N$: C, 73.51; H, 5.95; N, 3.06)

(-)-[(*1S,2R,5S*)-6,6-dimethylbicyclo[3.1.1]hept-2-yl]methylammonium 4-(1,2,3,4-tetrahydro-1,4-methanonaphthalen-*anti*-9-ylcarbonyl)benzoate (**83**)
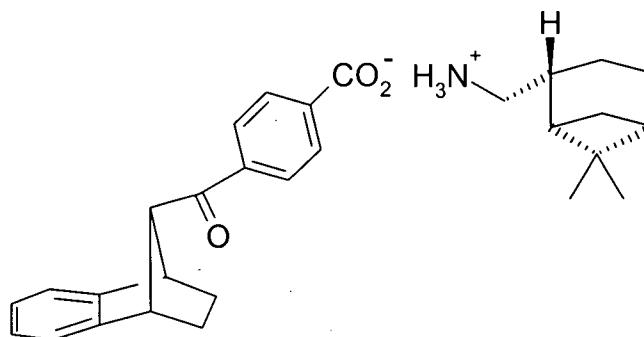
83

Acid **46** (77 mg, 0.26 mmol) was dissolved in methanol (5 mL) followed by the addition of (-)-cis-myrtanylamine (44 μL, 0.27 mmol). Upon prolonged standing the resulting salt precipitated and was collected by suction filtration followed by thorough washing with ether to give salt **83** (87 mg, 73.5%).

mp: 154 - 155 °C (methanol)

^{1}H NMR (400 MHz, DMSO): δ 0.86 (d, J = 9.4 Hz, 1H), 0.95 (s, 3H), 1.02 (m, 2H), 1.15 (s, 3H), 1.48 (m, 1H), 1.89 (br m, 6H), 2.00 (m, 1H), 2.25 (m, 1H), 2.39 (m, 1H), 2.76 (m, 2H), 3.35 (br), 3.59 (br s, 1H), 3.60 (br s, 2H), 7.09 (dd, J = 5.3, 3.1 Hz, 2H), 7.23 (dd, J = 5.3, 3.1 Hz, 2H), 7.88 (d, J = 8.3 Hz, 2H), 7.95 (d, J = 8.3 Hz, 2H).

^{13}C NMR (75 MHz, DMSO): δ 18.91 (+), 22.76 (-), 24.72 (+), 25.42 (+), 27.50 (-), 32.32 (+), 38.12 (-), 40.50 (-), 42.48 (-), 44.14 (+), 45.60 (-), 54.91 (+), 65.91 (-), 120.48 (-), 125.73 (-), 127.52 (-), 129.02 (-), 136.35 (+), 143.00 (+), 147.021 (+), 168.23 (+), 198.81 (+).

IR (KBr) v_{max}: 3200-2600 (br), 2943, 1673, 1582, 1538, 1469, 1376, 1248, 1218, 1012, 813, 783, 751 cm^{-1}.

HRMS (LSIMS, +ve, glycerol) calcd for $C_{29}H_{36}O_3N$ (M+1): 446.2695, found: 446.2694.

Anal. Calcd for $C_{29}H_{35}O_3N \cdot \frac{1}{4}H_2O$: C, 77.39; H, 7.95; N, 3.11. Found: C, 77.18; H, 7.89; N, 3.12.

(Calcd for $C_{29}H_{35}O_3N$: C, 78.17; H, 7.92; N, 3.14)

(*1R,2R*)-(-)-1-Hydroxy-*N*-methyl-1-phenyl-2-propylammonium 4-(1,2,3,4-tetrahydro-1,4-methanonaphthalen-*anti*-9-ylcarbonyl)benzoate (**84**)

84
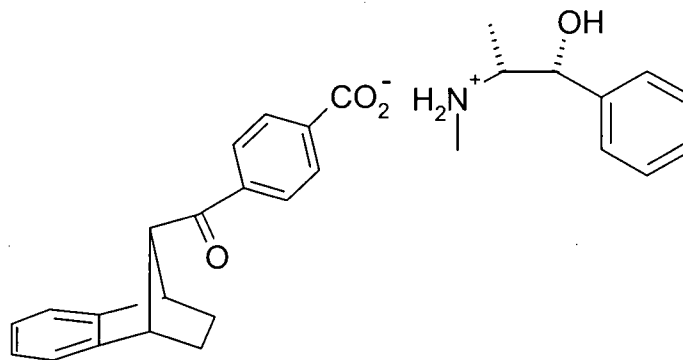
(*1R,2R*)-(-)-Pseudoephedrine (42 mg, 0.26 mmol) was dissolved in methanol (5 mL) and added to a solution of acid **46** (72 mg, 0.24 mmol) in methanol (5 mL). Upon evaporation of the solvent the resulting oil was triturated with ether giving salt **84** (79 mg, 70%) as a white powder.

mp: 131 - 132.5 °C (methanol)

^{1}H NMR (400 MHz, DMSO): δ 0.87 (d, *J* = 6.6 Hz, 3H), 1.02 (m, 2H), 1.89 (m, 2H), 2.50 (s, 3H), 3.04 (m, 1H), 3.4 (br), 3.61 (m, 3H), 4.46 (d, *J* = 8.8 Hz), 7.09 (dd *J* = 5.3, 3.1 Hz, 2H), 7.23 (dd, *J* = 5.3, 3.1 Hz, 2H), 7.29 (m, 1H), 7.35 (m, 2H), 7.36 (m, 2H), 7.93 (d, *J* = 8.4 Hz, 2H), 8.00 (d, *J* = 8.4 Hz, 2H).

^{13}C NMR (75 MHz, DMSO): δ 13.15 (-), 24.76 (+), 30.63 (-), 45.64 (-), 59.58 (-), 65.98 (-), 74.41 (-), 120.55 (-), 125.80 (-), 127.18 (-), 127.75 (-), 128.26 (-), 128.26 (-), 129.24 (-), 137.00 (+), 141.34 (+), 142.27 (+), 147.05 (+), 168.39 (+), 198.87 (+).

IR (KBr) v_{max}: 3350-2700 (br), 3278, 2981, 2866, 1684, 1587, 1546, 1457, 1373, 1240, 1217, 1044, 1013, 813, 783, 763, 750, 705 cm^{-1}.

HRMS (LSIMS, +ve, glycerol) calcd for $C_{29}H_{32}O_4N$ (M+1): 458.2332, found: 458.2332.

Anal. Calcd for $C_{29}H_{31}O_4N\cdot\frac{1}{4}H_2O$: C, 75.34; H, 6.87; N, 3.03. Found: C, 75.10; H, 6.65; N, 3.05.

(Calcd for $C_{29}H_{31}O_4N$: C, 76.12; H, 6.83; N, 3.06)

(*1S,2S*)-(+)-1-Hydroxy-*N*-methyl-1-phenyl-2-propylammonium 4-(1,2,3,4-tetrahydro-1,4-methanonaphthalen-*anti*-9-ylcarbonyl)benzoate (**85**)

85
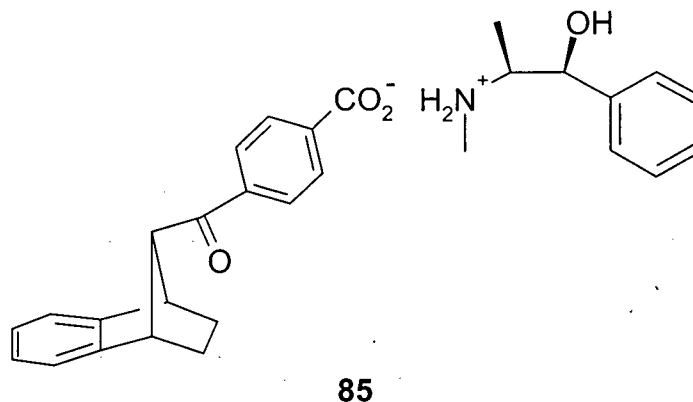
(*1S,2S*)-(+)-Pseudoephedrine (42 mg, 0.25 mmol) was dissolved in methanol (5 mL) and added to a solution of acid **46** (70 mg, 0.24 mmol) in methanol (5 mL). Upon evaporation of the solvent the resulting oil was triturated with ether giving salt **85** (74 mg, 68%) as a white powder.

mp: 130 - 132 °C (methanol)

^{1}H NMR (400 MHz, DMSO): δ 0.87 (d, J = 6.6 Hz, 3H), 1.03 (m, 2H), 1.89 (m, 2H), 2.50 (s, 3H), 3.04 (m, 1H), 3.4 (br), 3.61 (m, 3H), 4.46 (d, J = 8.8 Hz, 1H), 7.10 (dd, J = 5.3, 3.1 Hz, 2H), 7.24 (dd, J = 5.3, 3.1 Hz, 2H), 7.30 (m, 1H), 7.35 (m, 2H), 7.36 (m, 2H), 7.93 (d, J = 8.4 Hz, 2H), 8.00 (d, J = 8.4 Hz, 2H).

^{13}C NMR (75 MHz, DMSO): δ 24.80 (+), 30.69 (-), 45.69 (-), 59.62 (-), 66.01 (-), 74.45 (-), 120.58 (-), 125.84 (-), 127.22 (-), 127.78 (-), 128.29 (-), 129.28 (-), 137.04 (+), 141.31 (+), 142.30 (+), 147.08 (+), 168.37 (+), 198.90 (+).

IR (KBr) ν_{max}: 3350-2700 (br), 3259, 2981, 2866, 1684, 1587, 1546, 1457, 1373, 1240, 1217, 1044, 1014, 813, 783, 763, 750, 704 cm^{-1}.

HRMS (ESI, +, 0.1% HCO_2H in MeOH) calcd for $C_{10}H_{16}ON$ (M+1, amine): 166.1232, found: 166.1227

(ESI, -, MeOH) calcd for $C_{19}H_{15}O_3$ (M-1, acid): 291.1021, found: 291.1022.

Anal. Calcd for $C_{29}H_{31}O_4N\cdot\frac{1}{2}H_2O$: C, 74.65; H, 6.91; N, 3.00. Found: C, 74.30; H, 6.72; N, 3.00.

(Calcd for $C_{29}H_{31}O_4N$: C, 76.12; H, 6.83; N, 3.06)

<u>(*1S,2S*)-(+)-1,3-Dihydroxy-1-phenyl-2-propylammonium 4-(1,2,3,4-tetrahydro-1,4-methanonaphthalen-*anti*-9-ylcarbonyl)benzoate (**86**)</u>

86
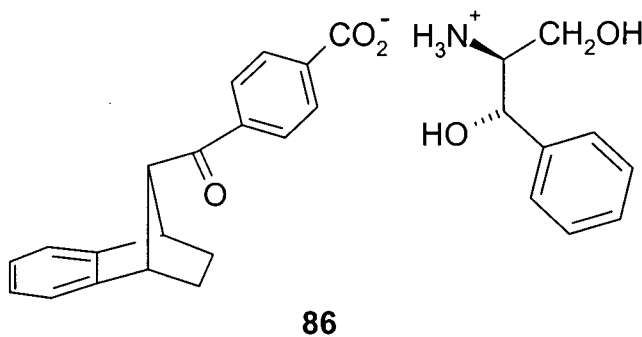
(*1S,2S*)-(+)-2-Amino-1-phenyl-1,3-propanediol (42 mg, 0.25 mmol) was dissolved in methanol (5 mL) and added to a solution of acid **46** (72 mg, 0.25 mmol) in methanol (5 mL). Evaporation of the solvent caused precipitation of plate-like crystals which were triturated with ether and filtered to give salt **86** (101 mg, 89%) as colourless plates.

mp: 157 - 158 °C (methanol)

^{1}H NMR (400 MHz, DMSO): δ 1.03 (m, 2H), 1.89 (m, 2H), 3.03 (m, 1H), 3.21 (dd, *J* = 11.6, 5.8 Hz, 1H), 3.3 (br), 3.38 (dd, *J* = 11.6, 3.7 Hz, 1H), 3.61 (m, 3H), 4.62 (d, *J* = 8.2 Hz, 1H), 7.09 (dd, *J* = 5.3, 3.1 Hz, 2H), 7.23 (dd, *J* = 5.3, 3.1 Hz, 2H), 7.29 (m, 1H), 7.35 (m, 2H), 7.37 (m, 2H), 7.93 (d, *J* = 8.4 Hz, 2H), 8.00 (d, *J* = 8.4 Hz, 2H).

^{13}C NMR (75 MHz, DMSO): δ 24.74 (+), 45.61 (-), 58.61 (-), 59.41 (+), 65.95 (-), 71.11 (-), 120.53 (-), 125.78 (-), 126.86 (-), 127.84 (-), 127.72 (-), 128.24 (-), 129.23 (-), 136.94 (+), 141.47 (+), 142.35 (+), 147.03 (+), 168.79 (+), 198.85 (+).

IR (KBr) v_{max}: 3300-2700 (br), 3279 (br), 2977, 1682, 1602, 1543, 1402, 1353, 1243, 1222, 1047, 1015, 815, 785, 769, 746, 723 cm^{-1}.

HRMS (ESI, +, 0.1% HCO_2H in MeOH) calcd for $C_9H_{14}O_2N$ (M+1, amine): 168.1025, found: 168.1024

(ESI, -, MeOH) calcd for $C_{19}H_{15}O_3$ (M-1, acid): 292.1021, found: 292.1028.

Anal. Calcd for $C_{28}H_{29}O_5N \cdot H_2O$: C, 70.42; H, 6.54; N, 2.93. Found: C, 70.19; H, 6.43; N, 2.97.

(Calcd for $C_{28}H_{29}O_5N$: C, 73.18; H, 6.36; N, 3.05)

(R)-(+)-1-Phenylethylammonium 4-(1,2,3,4-tetrahydro-1,4-methanonaphthalen-*anti*-9-ylcarbonyl)benzoate (87)

87
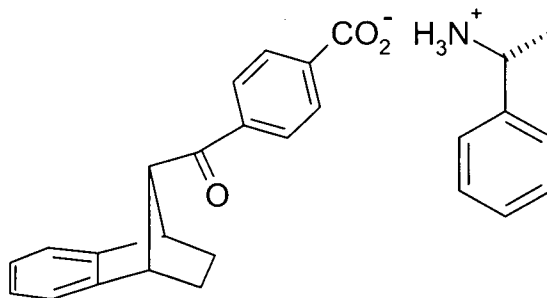
(R)-(+)-1-Phenylethylamine (35 μL, 0.27 mmol) was added to a solution of acid **46** (74 mg, 0.25 mmol) in methanol (6 mL). Upon standing a white precipitate formed, which was removed by filtration to give salt **87** (75 mg, 71%) as a white powder.

mp: 178 - 180 °C (methanol)

¹H NMR (400 MHz, DMSO): δ 1.02 (m, 2H), 1.44 (d, J = 6.8 Hz, 3H), 1.89 (m, 2H), 3.4 (br), 3.60 (br s, 3H), 4.29 (q, J = 6.7 Hz, 1H), 7.09 (dd, J = 5.3, 3.1 Hz, 2H), 7.23 (dd, J = 5.3, 3.1 Hz), 7.29 (tt J = 7.3, 1.2 Hz, 1H), 7.37 (m, 2H), 7.47 (m, 2H), 7.91 (d, J = 8.4 Hz, 2H), 7.98 (d, J = 8.4 Hz, 2H).

¹³C NMR (75 MHz, DMSO): δ 22.21 (-), 24.71 (+), 45.59 (-), 49.94 (-), 65.92 (-), 120.49 (-), 125.74 (-), 126.51 (-), 127.62 (-), 127.71 (-), 128.49 (-), 129.10 (-), 136.68 (+), 142.08 (+), 147.01 (+), 153.54 (+), 168.11 (+), 198.82 (+).

IR (KBr) ν_{max}: 3200 - 2700 (br), 2972, 2872, 2539, 1683, 1614, 1520, 1402, 1344, 1217, 757m
748, 695 cm^{-1}.

HRMS (ESI, +, 0.1% HCO$_2$H in MeOH) calcd for C$_{27}$H$_{28}$O$_3$N (M+1): 414.2069, found:
414.2065.

Anal. Calcd for C$_{27}$H$_{27}$O$_3$N·¾H$_2$O: C, 75.94; H, 6.67; N, 3.28. Found: C, 75.78; H, 6.42; N,
3.34.

(Calcd for C$_{27}$H$_{27}$O$_3$N: C, 78.42; H, 6.58; N, 3.39)

(*S*)-(-)-1-Phenylethylammonium 4-(1,2,3,4-tetrahydro-1,4-methanonaphthalen-*anti*-9-ylcarbonyl)benzoate **(88)**

88
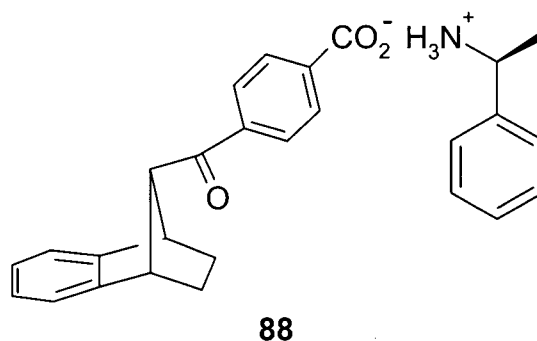
(*S*)-(-)-1-Phenylethylamine (34 µL, 0.26 mmol) was added to a solution of acid **46**
(73 mg, 0.25 mmol) in methanol (6 mL). Upon standing a white precipitate formed, which was
removed by filtration to give salt **88** (77 mg, 75%) as a white powder.

mp: 178 - 179.5 °C (methanol)

^{1}H NMR (400 MHz, DMSO): δ 1.02 (m, 2H), 1.43 (d, *J* = 6.8 Hz, 3H), 1.89 (m, 2H), 3.4 (br),
3.60 (br s, 3H), 4.28 (q, *J* = 6.7 Hz, 1H), 7.09 (dd, *J* = 5.3, 3.1 Hz, 2H), 7.23 (dd, *J* =
5.3, 3.1 Hz, 2H), 7.30 (tt, *J* = 7.3, 1.2 Hz, 1H), 7.37 (m, 2H), 7.46 (m, 2H), 7.92
(d, *J* = 8.4 Hz, 2H), 7.98 (d, *J* = 8.4 Hz, 2H).

^{13}C NMR (75 MHz, DMSO): δ 22.34 (-), 24.70 (+), 45.58 (-), 49.98 (-), 65.91 (-), 120.48 (-),
125.74 (-), 126.47 (-), 127.65 (-, 2C), 128.47 (-), 129.11 (-), 136.75 (+), 142.19 (+),
147.00 (+), 153.53 (+), 167.94 (+), 198.81 (+).

IR (KBr) v_{max}: 3200-2700 (br), 2972, 1683, 1614, 1520, 1402, 1345, 1218, 816, 784, 757, 749, 695 cm^{-1}.

HRMS (ESI, +, 0.1% HCO$_2$H in MeOH) calcd for C$_{27}$H$_{28}$O$_3$N (M+1): 414.2069, found: 414.2078.

Anal. Calcd for C$_{27}$H$_{27}$O$_3$N : C, 78.42; H, 6.58; N, 3.39. Found: C, 78.44; H, 6.56; N, 3.45.

(*S*)-(+)-Amino[(4-ammonio-4-butylcarboxylate)amino]methyliminium 4-(1,2,3,4-tetrahydro-1,4-methanonaphthalen-*anti*-9-ylcarbonyl)benzoate (**89**)

89
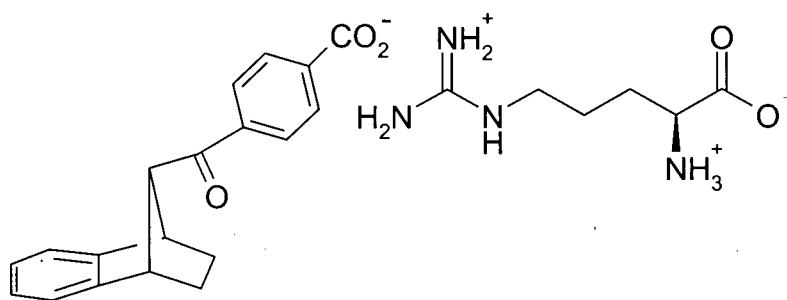
(*1S*)-(+)-Arginine (46 mg, 0.26 mmol) was dissolved in water (1 mL) and added to a solution of acid **46** (72 mg, 0.25 mmol) in methanol (6 mL). Upon evaporation of the solvent the resulting oily film was triturated with ether to give a colourless solid. Following filtration of the solid, salt **89** (87 mg, 76%) was obtained as a white powder.

mp: 154 - 156 °C (methanol/water)

^{1}**H NMR** (400 MHz, DMSO): δ 1.02 (m, 2H), 1.6-1.8 (m, 4H), 1.89 (m, 2H), 3.10 (m, 1H), 3.36 (br m, 2H), 3.59 (s, 1H), 3.60 (br s, 2H), 7.09 (dd, J = 5.3, 3.1 Hz, 2H), 7.23 (dd, J = 5.3, 3.1 Hz, 2H), 7.88 (d, J = 8.4 Hz, 2H), 7.95 (d, J = 8.4 Hz, 2H), 8.1 (br)

^{13}**C NMR** (75 MHz, DMSO): δ 24.69 (+), 24.80 (+), 28.09 (+), 45.57 (-), 53.43 (-), 65.88 (-), 120.46 (-), 125.70 (-), 127.50 (-), 129.02 (-), 136.36 (+), 143.08 (+), 146.99 (+), 157.63 (+), 169.21 (+), 171.40 (+), 198.78 (+).

IR (KBr) v_{max}: 3500-2700 (br), 3354, 1674, 1622, 1531, 1470, 1371, 1247, 1219, 813, 747 cm^{-1}.

HRMS (LSIMS, -ve, glycerol) calcd for C$_{25}$H$_{29}$O$_5$N$_4$ (M-1): 465.2138, found: 465.2138.

Anal. Calcd for $C_{25}H_{30}O_5N_4 \cdot \frac{1}{4}H_2O$: C, 63.75; H, 6.53; N, 11.89. Found: C, 63.65; H, 6.56; N, 11.55.

(Calcd for $C_{25}H_{30}O_5N_4$: C, 64.36; H, 6.48; N, 12.01)

(*1R,2S*)-(-)-1-Hydroxy-1-phenyl-2-propylammonium 4-(1,2,3,4-tetrahydro-1,4-methanonaphthalen-*anti*-9-ylcarbonyl)benzoate (**90**)

90
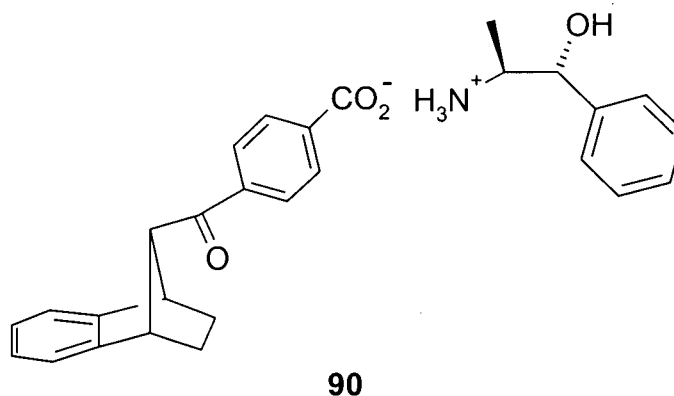
(*1R,2S*)-(-)-Norephedrine (38 mg, 0.25 mmol) was dissolved in methanol (1 mL) and added to a solution of acid **46** (73 mg, 0.25 mmol) in methanol (5 mL). After the solvent had evaporated the resulting solid was triturated with ether and filtered to give salt **90** (88 mg, 79%) as a white powder.

mp: 153 - 154 °C (methanol)

¹H NMR (400 MHz, DMSO): δ 0.90 (d, *J* = 6.7 Hz, 3H), 1.02 (m, 2H), 1.89 (m, 2H), 3.35 (br), 3.36 (m, 1H), 3.60 (br s, 3H), 4.91 (d, *J* = 3.0 Hz, 1H), 7.09 (dd, *J* = 5.3, 3.1 Hz, 2H), 7.23 (dd, *J* = 5.3, 3.1 Hz, 2H), 7.25 (m, 1H), 7.36 (m, 4H), 7.91 (d, *J* = 8.4 Hz, 2H), 7.99 (d, *J* = 8.4 Hz, 2H).

¹³C NMR (75 MHz, DMSO): δ 12.56 (-), 24.80 (+), 45.68 (-), 51.86 (-), 61.00 (-), 72.10 (-), 120.58 (-), 125.83 (-), 126.05 (-), 127.11 (-), 127.70 (-), 128.11 (-), 129.21 (-), 136.34 (+), 141.95 (+), 142.36 (+), 147.10 (+), 168.76 (+), 198.90 (+).

IR (KBr) ν_{max}: 3300-2700 (br), 2981, 2873, 1681, 1582, 1549, 1469, 1453, 1392, 1242, 1218, 1049, 814, 758, 703 cm⁻¹.

HRMS (ESI, +, 0.1% HCO_2H in MeOH) calcd for $C_{28}H_{30}O_4N$ (M+1): 444.2175, found: 444.2179.

Anal. Calcd for $C_{28}H_{29}O_4N\cdot\frac{1}{4}H_2O$: C, 75.06; H, 6.64; N, 3.13. Found: C, 75.02; H, 6.62; N, 3.17.

(Calcd for $C_{28}H_{29}O_4N$: C, 75.82; H, 6.59; N, 3.16)

(1S,2R)-(+)-1-Hydroxy-1-phenyl-2-propylammonium 4-(1,2,3,4-tetrahydro-1,4-methanonaphthalen-*anti*-9-ylcarbonyl)benzoate (**91**)

91
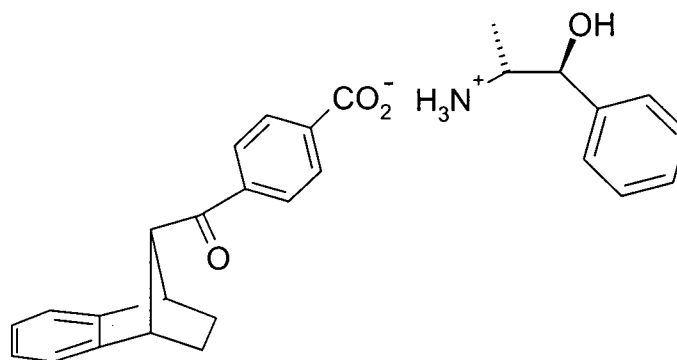
(1S,2R)-(+)-Norephedrine (45 mg, 0.29 mmol) was dissolved in methanol (1 mL) and added to a solution of acid **46** (77 mg, 0.26 mmol) in methanol (5 mL). After the solvent had evaporated the resulting solid was triturated with ether and filtered to give salt **91** (91 mg, 78%) as a white powder.

mp: 154 - 156 °C (methanol)

¹H NMR (400 MHz, DMSO): δ 0.90 (d, *J* = 6.7 Hz, 3H), 1.02 (m, 2H), 1.89 (m, 2H), 3.35 (br), 3.36 (m, 1H), 3.60 (br s, 3H), 4.91 (d, *J* = 3.0 Hz, 1H), 7.09 (dd, *J* = 5.3, 3.1 Hz, 2H), 7.23 (dd, *J* = 5.3, 3.1 Hz, 2H), 7.25 (m, 1H), 7.36 (m, 4H), 7.91 (d, *J* = 8.4 Hz, 2H), 7.99 (d, *J* = 8.4 Hz, 2H).

¹³C NMR (75 MHz, DMSO): δ 12.37 (-), 24.72 (+), 45.59 (-), 51.77 (-), 65.92 (-), 71.90 (-), 120.49 (-), 125.74 (-), 125.95 (-), 127.02 (-), 127.62 (-), 128.03 (-), 129.13 (-), 136.65 (+), 141.84 (+), 142.28 (+), 147.01 (+), 168.72 (+), 198.82 (+).

IR (KBr) v_{max}: 3300-2700 (br), 2981, 1681, 1583, 1549, 1453, 1392, 1243, 1218, 1049, 814, 757, 703 cm^{-1}.

HRMS (LSIMS, +ve, glycerol) calcd for $C_{28}H_{30}O_4N$ (M+1): 444.2175, found: 444.2174.

Anal. Calcd for $C_{28}H_{29}O_4N \cdot \frac{1}{4}H_2O$: C, 75.06; H, 6.64; N, 3.13.   Found: C, 74.89; H, 6.51; N, 3.14.

(Calcd for $C_{28}H_{29}O_4N$: C, 75.82; H, 6.59; N, 3.16)

(*S*)-(-)-1-(4-Methylphenyl)ethylammonium 4-(1,2,3,4-tetrahydro-1,4-methanonaphthalen-*anti*-9-ylcarbonyl)benzoate **(92)**
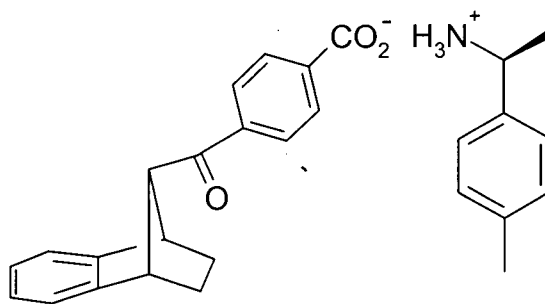
92

(*S*)-(-)-*p*-Tolylethylamine (39 µL, 0.26 mmol) was added to a solution of acid **46** (72 mg, 0.25 mmol) in methanol (10 mL).   Evaporation of the solvent left an oily residue that was triturated with ether causing a white precipitate to form.   Filtration of the solid gave salt **92** (82 mg, 77%) as a white powder.

mp: 196 - 199 °C (methanol)

^{1}H NMR (400 MHz, DMSO): δ 1.08 (m, 2H), 1.41 (d, J = 6.7 Hz, 3H), 1.89 (m, 2H), 2.27 (s, 3H), 3.60 (br s, 3H), 4.25 (q, J = 6.7 Hz), 7.09 (dd, J = 5.3, 3.1 Hz, 2H), 7.16 (d, J = 7.9 Hz, 2H), 7.23 (dd, J = 5.3, 3.1 Hz, 2H), 7.34 (d, J = 8.0 Hz, 2H), 7.90 (d, J = 8.4 Hz, 2H), 7.96 (d, J = 8.4 Hz, 2H).

^{13}C NMR (75 MHz, DMSO): δ 20.70 (-), 22.16 (-), 24.74 (+), 45.62 (-), 49.70 (-), 65.95 (-), 120.52 (-), 125.78 (-), 126.47 (-), 127.64 (-), 129.03 (-), 129.12 (-), 136.67 (+), 136.98 (+), 138.81 (+), 142.23 (+), 147.04 (+), 168.04 (+), 198.84 (+).

IR (KBr) v_{max}: 3200-2700 (br), 2976, 1681, 1613, 1526, 1467, 1397, 1240, 1217, 1109, 830, 816, 783, 759, 749cm^{-1}.

HRMS (ESI, +, 0.1% HCO$_2$H in MeOH) calcd for C$_{28}$H$_{30}$O$_3$N (M+1): 428.2226, found: 428.2222.

Anal. Calcd for C$_{28}$H$_{29}$O$_3$N: C, 78.66; H, 6.84; N, 3.28. Found: C, 78.95; H, 6.84; N, 3.22.

(*S*)-(-)-2-[Hydroxy(diphenyl)methyl]pyrrolidinium 4-(1,2,3,4-tetrahydro-1,4-methanonaphthalen-*anti*-9-ylcarbonyl)benzoate (**93**)

93
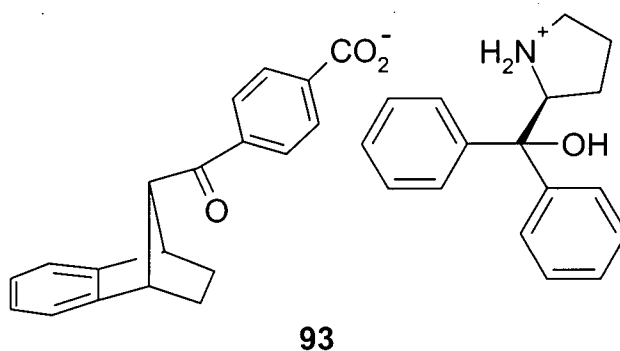
(*S*)-(-)-α,α-Diphenyl-2-pyrrolidemethanol (67 mg, 0.26 mmol) was dissolved in methanol (1ml) and added to a solution of acid **46** (72 mg, 0.25 mmol) in methanol (5 mL). Upon addition a white precipitate began to fall out of solution and after standing overnight was filtered to give salt **93** (87 mg, 64%) as a white powder.

mp: 224 - 226 °C (methanol)

^{1}H NMR (400 MHz, DMSO): δ 1.03 (m, 2H), 1.58 (m, 1H), 1.73 (m, 3H), 1.89 (m, 2H), 3.03 (t, *J* = 6.4 Hz, 2H), 3.4 (br), 3.61 (br s, 3H), 4.68 (m, 1H), 7.10 (dd, *J* = 5.3, 3.1 Hz, 2H), 7.16 (m, 2H), 7.21-7.29 (m, 6H), 7.49 (dm, *J* = 7.2 Hz, 2H), 7.61 (dm, *J* = 7.3 Hz, 2H), 7.95 (m, 4H).

^{13}C NMR (75 MHz, DMSO): δ 24.75 (+), 26.38 (+), 38.44 (+), 45.61 (-), 46.76 (+), 64.27 (-), 65.97 (-), 77.22 (+), 120.55 (-), 125.39 (-), 125.81 (-), 126.06 (-), 126.48 (-), 126.69 (-), 127.81 (-), 128.04 (-), 128.09 (-), 129.27 (-), 137.30 (+), 140.20 (+), 146.04 (+), 146.20 (+), 147.03 (+), 168.10 (+), 198.86 (+).

IR (KBr) v_{max}: 3250-2400 (br), 3191, 3022, 2977, 2716, 1672, 1645, 1582, 1544, 1449, 1397, 1217, 762, 745, 698 cm^{-1}.

HRMS (LSIMS, +, thioglycerol) calcd for $C_{17}H_{20}ON$ (M+1, amine): 254.1545, found: 254.4540.

(LSIMS, -, glycerol) calcd for $C_{19}H_{15}O_3$ (M-1, acid): 291.1021, found: 291.1022.

7.3 Preparation of 7-Methylnorbornane Derivatives 54, 55, 56 and 57

7.3.1 Preparation of 7-Methylnorbornane Derivative 54

Exo-2,*syn*-7-dibromobicyclo[2.2.1]heptane (**58**)

58
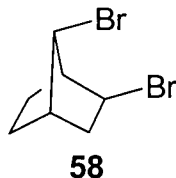
Following the procedure of Kwart and Kaplan,[74] norbornene (59 g, 0.62 mol) was dissolved in CCl$_4$ (200 mL) and pyridine (50 mL, 0.62 mol) was added before the system was placed under a N$_2$ atmosphere and cooled to 0 °C in an ice bath. A solution of bromine (31.7 mL, 0.62 mol) in CCl$_4$ (30 mL) was added dropwise via an addition funnel over a period of 3 h, during which time pyridinium bromide precipitated as a yellow-orange solid. Upon completion of the bromine addition, the reaction was stirred for an additional 30 minutes when the solid was removed by suction filtration and thoroughly washed with CCl$_4$. The resulting filtrate was washed with 10% HCl (50 mL x 3), saturated sodium thiosulphate (50 mL x 2) and water until neutral. After drying over MgSO$_4$ the solvent was removed *in vacuo* to give a pale yellow oil. Dibromide **58** was isolated as a colourless liquid (50 g, 32 %) following vacuum distillation. The IR spectral data obtained were in agreement with those previously published.[74]

bp: 102 °C @ 2.5 mmHg (lit.[74] 74 °C @ 0.3 mmHg)

¹H NMR (400 MHz, CDCl₃): δ 1.31 (m, 2H), 1.67 (m, 2H), 2.22 (dd, J = 13.6, 8.1 Hz, 1H), 2.43 (t, J = 4 Hz, 1H), 2.64 (m, 1H), 2.69 (d, J = 3.9 Hz, 1H), 3.95 (m !H), 3.97 (m, 1H).

¹³C NMR (75 MHz, CDCl₃): δ 25.14 (+), 28.36 (+), 41.95 (+), 44.43 (-), 48.06 (-), 50.26 (-), 53.64 (-).

IR (neat) ν_{max}: 2970, 2876, 1467, 1150, 1309, 1246, 1135, 897, 987, 940, 878, 810, 782, 765, 743, 612 cm⁻¹.

LRMS (EI): 256 (1, M⁺ {⁸¹Br,⁸¹Br}), 254 (1, M⁺ {⁸¹Br,⁷⁹Br}), 252 (1, M⁺ {⁷⁹Br,⁷⁹Br}), 175 (73), 94 (13), 93 (100), 91 (52), 79 (10), 77 (37), 67 (27), 66 (22), 65 (28).

HRMS (EI) calcd for C₇H₁₀Br₂: 255.9108 {⁸¹Br,⁸¹Br}, 253.9129 {⁸¹Br,⁷⁹Br}, 251.9149 {⁷⁹Br,⁷⁹Br}, found: 255.9111, 253.9130, 251.9147.

Syn-7-bromobicyclo[2.2.1]hept-2-ene **(59)**
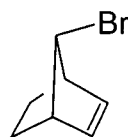
59

Following the procedure of Shultz *et al.*,[79] dibromide **58** (50 g, 0.20 mol) was added to DMSO (250 mL) under a N₂ atmosphere. KOʳBu (39 g, 0.35 mol) was added and the solution was heated to 80 °C for 18 h during which time the colour of the solution became dark brown. Upon cooling, water (100 mL) was slowly added and the mixture was extracted with ether (100 mL x 3). The combined ethereal fractions were combined and washed with water (50 mL), 10% HCl (50 mL) and water (3 x 50 mL) followed by drying over MgSO₄. After removal of the ether *in vacuo* a brown oil was obtained and purified by distillation at reduced pressure to give monobromide **59** as a colourless oil (32 g, 93%). The IR spectral data were in agreement with those previously published.[74]

bp: 58 °C @ 10 mmHg (lit.[74] 68 - 70 °C @ 13 mmHg)

171

^{1}H NMR (400 MHz, CDCl$_3$): δ 1.10 (m, 2H), 1.75 (m, 2H), 3.02 (m, 2H), 3.86 (s, 1H), 6.02 (s, 2H).

^{13}C NMR (75 MHz, CDCl$_3$): δ 22.59 (+), 49.31 (-), 66.14 (-), 132.86 (-).

IR (neat) ν$_{max}$: 3069, 2973, 2947, 2874, 1718, 1616, 1576, 1468, 1447, 1338, 1297, 1286, 1267, 1227, 1196, 1123, 1069, 929, 852, 810, 707 cm^{-1}.

LRMS (EI): 174 (8, M$^+$ {^{81}Br}), 172 (9, M$^+$ {^{79}Br}), 146 (62), 144 (65), 93 (76), 91 (68), 78 (13), 77 (49), 66 (11), 65 (100), 63 (20), 51 (17).

HRMS (EI) calcd for C$_7$H$_9$Br: 174.9945 {^{81}Br}, 172.9966 {^{79}Br}, found: 174.9953, 172.9970.

Bicyclo[2.2.1]hept-2-ene-*syn*-7-carboxylic acid (**60**)

60
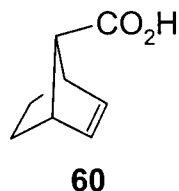
^{t}BuLi (94 mL, 1.7 M in hexanes, 0.16 mol) was added to THF (100 mL) under a N$_2$ atmosphere at -78 °C. After stirring for 15 min a solution of bromide **59** (14 g, 78 mmol) in THF (50 mL) was added dropwise over a period of 20 min and stirred for 2 h. Dry gaseous CO$_2$ was introduced (sublimed dry ice passed through a CaSO$_4$ drying tube) and the mixture was gradually allowed to warm to room temperature during which time a white precipitate fell out of solution. Water (100 mL) was added and the THF was removed *in vacuo*. After extracting the aqueous solution with ether (3 x 50 mL) the combined organic fractions were washed with NaOH (2 x 50 mL). The basic aqueous fractions were acidified with conc. HCl and washed with ether (3 x 50 mL). The combined organic fractions were washed with water (3 x 50 mL) and dried over MgSO$_4$. Removal of the solvent *in vacuo* followed by recrystallization from methanol/water gave acid **60** as a colourless solid (9.4 g, 87%).

mp: 98 - 99 °C (methanol/water) (lit.[111] 91-95 °C, sub.)

^{1}H NMR (400 MHz, CDCl$_3$): δ 1.01 (m, 2H), 1.74 (m, 2H), 2.39 (s, 2H), 3.14 (m, 2H), 6.00 (s, 2H).

^{13}**C NMR** (75 MHz, CDCl$_3$): δ 24.67 (+), 43.98 (-), 62.44 (-), 133.36 (-), 178.97 (+).

IR (KBr) v_{max}: 3200-2500 (br), 2992, 1707, 1417, 1335, 1298, 1252, 1130m 951, 873, 860, 712, 519 cm^{-1}.

LRMS (EI): 139 (5, M+1), 138 (40, M$^+$), 110 (100), 93 (19), 91 (21), 85 (56), 77 (20), 66 (80), 65 (29), 51 (10).

HRMS (EI) calcd for C$_8$H$_{10}$O$_2$: 138.0681, found: 138.0683.

Bicyclo[2.2.1]heptane-7-carboxylic acid (**41**)

41
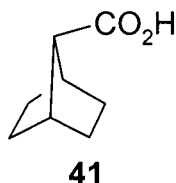
Acid **60** (7.4 g, 53 mmol) was dissolved in EtOAc (100 mL) containing Pd/C (75 mg). The solution was placed under a H$_2$ atmosphere via a balloon and kept under a positive pressure until the reaction was completed (monitored by GC/MS). Celite (2 g) was added and the mixture was filtered through a Celite bed to remove the palladium catalyst. Following removal of the solvent *in vacuo*, acid **41** was obtained as a colourless solid (6.7 g, 89%), which was used without further purification. The IR spectral data were in agreement with those previously published.[74]

bp: 75 - 76 °C (methanol) (lit.[74] 77.5 - 78.5 °C)

^{1}**H NMR** (400 MHz, CDCl$_3$): δ 1.24 (m, 4H), 1.61 (m, 2H), 1.81 (m, 2H), 2.46 (m, 3H).

^{13}**C NMR** (75 MHz, CDCl$_3$): δ 27.94 (+), 29.83 (+), 39.15 (-), 53.63 (-), 179.84 (+).

IR (KBr) v_{max}: 3200-2600 (br), 2963, 1695, 1419, 1302, 951, 731 cm^{-1}.

LRMS (EI): 140 (7, M+), 122 (19), 97 (12), 95 (15), 86 (100), 80 (40), 67 (23), 55 (12).

HRMS (EI) calcd for C$_8$H$_{12}$O$_2$: 140.0838, found: 140.0837.

Methyl bicyclo[2.2.1]heptane-7-carboxylate (**61**)

61
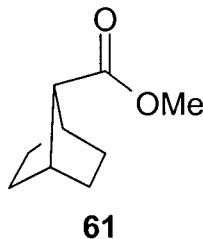
Acid **41** (2.4 g, 17 mmol) was dissolved in CH_2Cl_2 (50 mL) along with DMF (5 μL) under a N_2 atmosphere. Upon addition of $(COCl)_2$ (3 mL, 35 mmol) gas evolution from the solution was observed and the mixture was stirred for 45 min. The solvent was removed *in vacuo* and replaced with fresh CH_2Cl_2 (25 mL). After removal of the fresh solvent *in vacuo* and repetition of this process two more times in order to ensure complete removal of any residual oxalyl chloride, CH_2Cl_2 (25 mL) was added and the system was placed under a N_2 atmosphere. MeOH (10 mL) was added and the solution stirred for 4 h. Following removal of the solvent *in vacuo* the resulting yellow oil was taken up in ether (50 mL) and washed with saturated $NaHCO_3$ (3 x 25 mL) followed by water (3 x 25 mL) before drying over $MgSO_4$. Removal of the solvent and vacuum distillation gave ester **61** (2.2 g, 81%) as a colourless oil.

bp: 65 °C @ 7.5 mmHg

^{1}H NMR (400 MHz, $CDCl_3$): δ 1.22 (m, 4H), 1.59 (m, 2H), 1.75 (m, 2H), 2.41 (s, 1H), 2.44 (m, 2H), 3.63 (s, 3H).

^{13}C NMR (75 MHz, $CDCl_3$): δ 28.02 (+), 29.80 (+), 39.15 (-), 51.31 (-, br), 53.71 (-), 173.83 (+).

IR (KBr) ν_{max}: 2953, 2874, 1736, 1436, 1366, 1300, 1214, 1175, 1145, 1043 cm^{-1}.

LRMS (EI): 154 (4, M$^+$), 123 (13), 122 (22), 100 (100), 95 (20), 94 (12), 80 (13), 67 (20).

HRMS (EI) calcd for $C_9H_{14}O_2$: 154.0994, found: 154.0993.

Methyl 7-methylbicyclo[2.2.1]heptane-7-carboxylate (**62**)

62
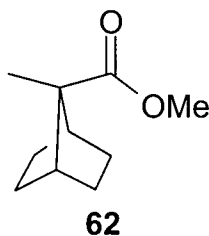
     LDA was prepared by adding *n*-BuLi (9.3 mL, 1.6 M, 15 mmol) to a solution of diisopropylamine (2.2 mL, 16 mmol) in THF (50 mL) at -78 °C under a N_2 atmosphere. After stirring for 45 min, DMPU (1.9 mL, 16 mmol) was added and stirring was continued for a further 15 min during which time the solution became opaque white in colour. Ester **61** (1.9 g, 12 mmol) in THF (10 mL) was added dropwise and stirred for 4 h at which time CH_3I (3.1 mL, 50 mmol) was added and the reaction mixture was allowed to warm to room temperature. Following the addition of water (25 mL) the THF was removed *in vacuo* and replaced with ether (50 mL). Following extraction with ether (2 x 25 mL) the combined organic fractions were washed with 10% HCl (2 x 25 mL) and water (3 x 25 mL) before drying over anhydrous $MgSO_4$. Removal of the solvent *in vacuo* gave ester **62** as a yellow oil (1.9 g, 89%).

^{1}H NMR (400 MHz, $CDCl_3$): δ 1.21 (s, 3H), 1.21 (m, 2H), 1.68 (m, 2H), 1.75 (m, 2H), 2.11 (m, 2H), 3.64 (s, 3H).

^{13}C NMR (75 MHz, $CDCl_3$): δ 17.02 (-), 27.72 (+), 29.34 (+), 47.75 (-), 51.39 (-), 58.29 (+), 177.33 (+).

IR (KBr) v_{max}: 2963, 2880, 1733, 1456, 1279, 1252, 1205, 1161, 1116, 1096 cm^{-1}.

LRMS (EI): 169 (5, M+1), 168 (41, M$^+$), 136 (17), 125 (47), 114 (100), 109 (46), 108 (15), 93 (11), 88 (23), 83 (11), 82 (22), 81 (31), 80 (12), 79 (27), 77 (13), 67 (30), 55 (16), 53 (12).

HRMS (EI) calcd for $C_{10}H_{16}O_2$: 168.1150, found: 168.1154.

Anal. Calcd for $C_{10}H_{16}O_2$: C, 71.39; H, 9.59. Found: C, 71.47; H, 9.52.

7-Methylbicyclo[2.2.1]heptane-7-carboxylic acid (40)

40
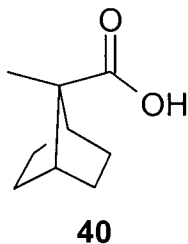
Based on the procedure of Olah *et al.* for the hydrolysis of esters,[80] ester **62** (1.9 g, 11 mmol) was dissolved in MeCN (50 mL) under a N_2 atmosphere. Following the addition of NaI (3.5 g, 23 mmol) and Me_3SiCl (3.0 mL, 24 mmol), the solution was heated to reflux for a period of 3 days. After cooling the dark brown reaction mixture to room temperature, water (50 mL) was added to the mixture dropwise until all of the suspended solid present had dissolved. The resulting solution was thoroughly extracted with ether (4 x 50 mL). The combined ethereal fractions were washed with water (1 x 50 mL), saturated sodium thiosulphate (1 x 50 mL) and water (3 x 50 mL). The acid was then isolated from unreacted starting material, which could be recycled, by washing the organic fraction with 10% NaOH (2 x 50 mL) and acidifying the aqueous extract with concentrated HCl. Upon acidification a white precipitate was formed, which was isolated by extraction with ether (2 x 50 mL). Following washing with water (3 x 50 mL), drying over $MgSO_4$, and removal of the solvent *in vacuo*, acid **40** was obtained as a colourless solid (0.95 g, 56%).

mp: 140 - 141 °C (acetonitrile) (lit.[73,112] 194 - 195 °C)

^{1}H NMR (400 MHz, $CDCl_3$): δ 1.25 (m, 4H), 1.25 (s, 3H), 1.80 (m, 4H), 2.05 (m, 2H).

^{13}C NMR (75 MHz, $CDCl_3$): δ 17.60 (-), 28.67 (+), 30.34 (+), 42.88 (-), 59.46 (+), 180.88 (+).

IR (KBr) v_{max}: 3200-2500 (br), 2960, 2881, 2815, 2658, 2574, 1694, 1411, 1325, 13125, 1299, 1172, 955, 725 cm^{-1}.

LRMS (EI): 155 (5, M+1), 154 (47, M$^+$), 136 (14), 112 (12), 111 (61), 109 (25), 100 (100), 87 (20), 82 (15), 81 (60 , 80 (19), 79 (19), 68 (16), 67 (33), 55 (24), 53 (12).

HRMS (EI) calcd for $C_9H_{14}O_2$: 154.0994, found: 154.0994.

(4-Fluorophenyl)(7-methylbicyclo[2.2.1]hept-7-yl)methanone (**54**)
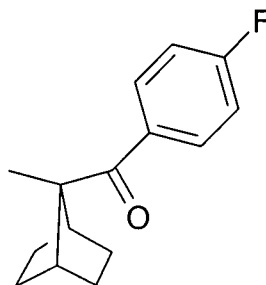
54

Acid **40** (0.65 g, 4.2 mmol) was converted into its corresponding acid chloride by treatment with $(COCl)_2$ (3.0 mL, 35 mmol) and DMF (2 μL) in CH_2Cl_2 (50 mL). After 3 h the solvent and residual oxalyl chloride were removed *in vacuo* and replaced with fresh CH_2Cl_2 (25 mL). The fresh solvent was removed *in vacuo*, then replaced and removed one final time to ensure complete removal of any residual oxalyl chloride. The resulting yellow oil was then ·taken up in THF (50 mL), placed under a N_2 atmosphere and cooled to 0 °C in an ice bath. *p*-Fluorophenylmagnesiumbromide (5.0 mL, 1.0 M in THF, 5.0 mmol) was added dropwise and the solution stirred for 3 h at which time the reaction was warmed to room temperature and stirred overnight. Following quenching of the mixture with saturated aqueous NH_4Cl (20 mL) the mixture was extracted with ether (2 x 25 mL). The combined organic fractions were washed with 10% NaOH (2 x 25 mL) and water (3 x 25 mL) before being dried over $MgSO_4$. Removal of the solvent *in vacuo* yielded a yellow oil that was purified by column chromatography (2% ether/pet. ether) to give ketone **54** as a colourless solid (0.42 g, 43%).

mp: 80 - 81 °C (hexanes)

¹H NMR (400 MHz, $CDCl_3$): δ 1.17 (m, 2H), 1.29 (m, 2H), 1.38 (s, 3H), 1.49 (m, 2H), 1.86 (m, 2H), 2.41 (m, 2H), 7.06 (m, 2H), 7.69 (m, 2H).

¹³C NMR (75 MHz, $CDCl_3$): δ 17.50 (-), 27.93 (+), 28.72 (+), 42.90 (-), 62.65 (+), 115.05 and 115.33 (-, $^2J_{C-F}$ = 21.5 Hz), 131.12 and 131.00 (-, $^3J_{C-F}$ = 8.9 Hz), 133.27 and 133.23 (+, $^4J_{C-F}$ = 2.7 Hz), 166.59 and 163.23 (+, $^1J_{C-F}$ = 251.9 Hz), 203.54 (+).

IR (KBr) v_{max}: 2952, 2868, 1666, 1599, 1503, 1278, 1227, 1158, 972, 844, 767, 615 cm⁻¹.

UV/VIS (methanol, 1.55×10^{-4} M): 212 (8239), 246 (12,583), 322 (114) nm ($M^{-1}cm^{-1}$).

LRMS (EI) 232 (16, M^+), 178 (34), 177 (13), 163 (13), 151 (30), 123 (100), 109 (73), 95 (53), 94 (11), 81 (25), 79 (14), 75 (14), 67 (59), 55 (17).

HRMS (EI): calcd for $C_{15}H_{17}OF$: 232.1263, found: 232.1263.

Anal. Calcd for $C_{15}H_{17}OF$: C, 77.56; H, 7.38. Found: C, 77.95; H, 7.43.

This structure was confirmed by X-ray crystallographic analysis:

Habit	colourless prisms
Space Group	$P2_1/n$
a, Å	12.3873(7)
b, Å	10.1085(5)
c, Å	18.9261(9)
α (°)	90
β (°)	91.546(4)
γ (°)	90
Z	4
R	0.0449

7.3.2 Preparation of 7-Methylnorbornane Derivative 55

4-[(7-Methylbicyclo[2.2.1]hept-7-yl)carbonyl]benzonitrile (55)

55
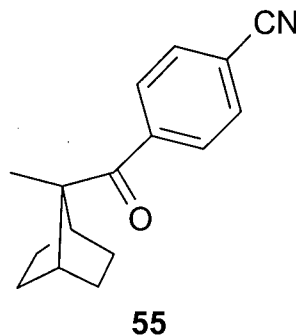
Ketone **54** (0.42 g, 1.8 mmol) was dissolved in DMSO (50 mL) with KCN (0.24 g, 4 mmol) and placed under a N_2 atmosphere. The solution was then heated for 16 h at 85 °C. After cooling to room temperature, water (10 mL) was slowly added and the mixture was extracted with ether (3 x 20 mL). The combined ethereal fractions were washed with water (3 x 25 mL) and dried over $MgSO_4$. Removal of the solvent *in vacuo* yielded an off-white solid that was purified by column chromatography (10% ether/pet. ether) to give ketone **55** as a colourless solid (0.40 g, 93%).

mp: 125 - 126 °C (hexanes)

^{1}H NMR (400 MHz, CDCl$_3$): δ 1.17 (m, 2H), 1.29 (m, 2H), 1.37 (s, 3H), 1.42 (m, 2H), 1.85 (m, 2H), 2.37 (m, 2H), 7.69 (dt, J = 8.7, 1.9 Hz, 2H), 7.97 (dt, J = 8.7, 1.9 Hz, 2H).

^{13}C NMR (75 MHz, CDCl$_3$): δ 17.30 (-), 27.83 (+), 28.59 (+), 42.70 (-), 62.82 (+), 115.26 (+), 117.96 (+), 128.72 (-), 132.04 (-), 146.49 (+), 203.98 (+).

IR (KBr) ν_{max}: 2961, 2876, 2229, 1672, 1462, 1273, 1164, 971, 849, 768 cm^{-1}.

UV/VIS (methanol, 1.67 x 10^{-4} M): 214 (8322), 244 (14362), 288 (2350), 332 (114) nm (M^{-1}cm^{-1}).

LRMS (EI): 239 (13, M$^+$), 197 (12), 196 (10), 185 (38), 184 (10), 170 (16), 130 (32), 109 (100), 102 (44), 94 (11), 81 (48), 80 (11), 79 (17), 67 (72), 55 (20), 53 (12).

HRMS (EI) calcd for $C_{16}H_{17}ON$: 239.1310, found: 239.1312.

Anal. Calcd for $C_{16}H_{17}ON$: C, 80.30; H, 7.16; N, 5.85. Found: C, 80.20; H, 7.25; N, 5.86.

This structure was confirmed by X-ray crystallographic analysis:

Habit	colourless prisms
Space Group	$P2_1/c$
a, Å	10.0204(8)
b, Å	11.4091(7)
c, Å	11.7125(11)
α (°)	90
β (°)	107.014(4)
γ (°)	90
Z	4
R	0.0416

7.3.3 Preparation of 7-Methylnorbornane Derivative 56

4-[(7-Methylbicyclo[2.2.1]hept-7-yl)carbonyl]benzoic acid (**56**)

56
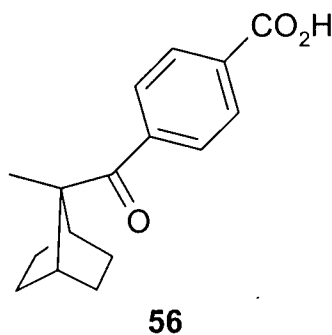
Ketone **55** (0.40 g, 1.7 mmol) was suspended is a solution of water (75 mL) and ethanol (15 mL) containing KOH (13.5 g, 241 mmol). The solution was heated to reflux for 18 h before being allowed to cool to room temperature and acidified with conc. HCl. The white precipitate formed upon acidification was removed by extraction with ether (3 x 25 mL) and the combined organic fractions were washed with water (3 x 25 mL) and dried over MgSO$_4$. Removal of the solvent *in vacuo* gave a yellow solid that was purified by recrystallization from methanol to give ketone **56** as a colourless solid (0.42 g, 98%).

mp: 215 - 217 °C (methanol)

^{1}H NMR (400 MHz, DMSO): δ 1.14 (m, 2H), 1.24 (m, 2H), 1.34 (m, 2H), 1.36 (s, 3H), 1.85 (m, 2H), 2.36 (br s, 2H), 7.99 (m, 2H), 8.02 (m, 2H).

^{13}C NMR (75 MHz, DMSO): δ 16.94 (-), 27.45 (+), 28.20 (+), 42.06 (-), 62.47 (+), 128.20 (-), 139.34 (-), 133.69 (+), 139.93 (+), 166.59 (+), 204.49 (+).

IR (KBr) v_{max}: 3200-2500 (br), 2957, 2872, 2554, 1676, 1430, 1319, 1295, 1272, 1250, 969, 930, 864, 736 cm^{-1}.

UV/VIS (methanol, 1.24 x 10^{-4} M): 210 (7662), 252 (15,984), 290 (sh) (1677), 332 (sh) (159) nm (M^{-1}cm^{-1}).

LRMS (EI): 259 (3, M+!), 258 (13, M$^+$), 213 (23), 204 (28), 177 (10), 159 (16), 150 (21), 149 (32), 109 (100), 94 (11), 81 (26), 67 (46), 65 (23), 53 (15).

HRMS (EI) calcd for $C_{16}H_{18}O_3$: 258.1256, found: 258.1255.

**Anal.** Calcd for $C_{16}H_{18}O_3$: C, 74.40; H, 7.02. Found: C, 74.40; H, 7.03.

This structure was confirmed by X-ray crystallographic analysis:

Habit	colourless prisms
Space Group	$C2/c$
a, Å	35.986(5)
b, Å	6.4522(7)
c, Å	11.113(2)
α (°)	90
β (°)	96.05(6)
γ (°)	90
Z	8
R	0.051

7.3.4 Preparation of 7-Methylnorbornane Derivative 57

Methyl 4-[(7-methylbicyclo[2.2.1]hept-7-yl)carbonyl]benzoate (57)
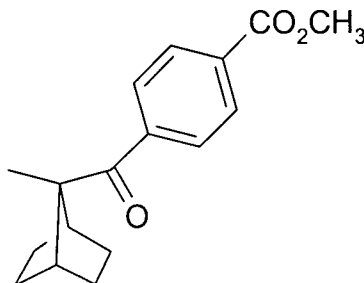
57

Acid **56** (0.42 g, 1.6 mmol) was dissolved in CH_2Cl_2 (25 mL) under a N_2 atmosphere. Oxalyl chloride (0.42 mL, 4.8 mmol) and DMF (2 μL) were added, with the addition of the latter causing gas evolution, and the mixture was stirred for 2 h. The solvent was removed *in vacuo* and replaced with fresh CH_2Cl_2 (20 mL). This process was repeated two more times before the system was again placed under a N_2 atmosphere and methanol (5 mL) was added and the solution stirred for 1 h. The solution was then extracted with CH_2Cl_2 (2 x 20 mL) and washed with water (20 mL), saturated $NaHCO_3$ (2 x 25 mL) and water (3 x 20 mL) before being dried over $MgSO_4$. Removal of the solvent gave a yellowish solid that was purified by column chromatography (10% ether/pet. ether) to yield ketone **57** as a colourless solid (0.35 g, 78%).

mp: 132 - 133 °C (hexanes)

^{1}H NMR (400 MHz, $CDCl_3$): δ 1.16 (m, 2H), 1.28 (m, 2H), 1.40 (s, 3H), 1.46 (m, 2H), 1.86 (m, 2H), 2.40 (m, 2H), 3.91 (s, 3H), 7.93 (m, 2H), 8.05 (m, 2H).

^{13}C NMR (75 MHz, $CDCl_3$): δ 17.44 (-), 27.92 (+), 28.67 (+), 42.72 (-), 52.31 (-), 62.94 (+), 128.18 (-), 129.39 (-), 132.82 (+), 140.86 (+), 166.26 (+), 205.08 (+).

IR (KBr) ν_{max}: 2978, 2959, 2920, 2877, 1718, 1670, 1439, 1279, 1252, 1107, 971, 736 cm^{-1}.

UV/VIS (methanol, 1.76 x 10^{-4} M): 210 (6582), 254 (14,407), 288 (1828), 332 (sh) (142) nm (M^{-1}cm^{-1}).

LRMS (EI): 272 (7, M$^+$), 241 (14), 218 (32), 213 (43), 192 (13), 191 (22), 164 (31), 163 (100), 184 (33), 136 (14), 135 (18), 109 (94), 104 (16), 103 (15), 94 (12), 81 (28), 79 (15), 77 (17), 76 (16), 67 (65), 56 (17).

HRMS (EI) calcd for $C_{17}H_{20}O_3$: 272.1412, found: 272.1406.

Anal. Calcd for $C_{17}H_{20}O_3$: C, 74.97; H, 7.40. Found: C, 74.88; H, 7.10.

This structure was confirmed by X-ray crystallographic analysis:

Habit	colourless needles
Space Group	$P\bar{1}$
a, Å	6.1735(3)
b, Å	10.8013(1)
c, Å	11.4558(2)
α (°)	71.660(8)
β (°)	83.760(10)
γ (°)	78.360(10)
Z	2
R	0.041

7.3.5 Preparation of 7-(*p*-Carboxybenzoyl)-7-methylnorbornane (56) Salts

(*R*)-(+)-1-Phenylethylammonium 4-[(7-methylbicyclo[2.2.1]hept-7-yl)carbonyl]benzoate (94)

94
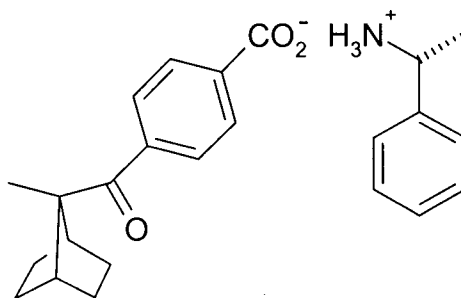
(*R*)-(+)-Phenylethylamine (42 µL, 0.33 mmol) was added to a solution of acid **56** (81 mg, 0.31 mmol) in methanol (5 mL). Upon standing a precipitate formed that was isolated by suction filtration to give salt **94** (105 mg, 88%) as colourless prisms.

mp: 197 - 198.5 °C (methanol)

^{1}H NMR (400 MHz, DMSO): δ 1.14 (m, 2H), 1.25 (m, 2H), 1.37 (m, 2H), 1.37 (s, 3H), 1.48 (d, *J* = 7.2 Hz, 3H), 1.86 (m, 2H), 2.38 (m, 2H), 4.34 (q, *J* = 7 Hz, 1H), 7.30 (t, *J* = 7.2 Hz, 1H), 7.37 (t, *J* = 7.2 Hz, 2H), 7.50 (d, *J* = 7.2 Hz, 2H), 7.88 (d, 8.0 Hz, 2H), 7.95 (d, *J* = 8.4 Hz, 2H), 8.0 - 8.8 (br).

^{13}C NMR (75 MHz, DMSO, 70 °C): δ 16.69, 22.87, 27.19, 27.99, 41.93, 49.87, 62.16, 125.89, 126.80, 127.19, 127.92, 128.57, 138.09, 139.08, 143.65, 167.46, 204.20.

IR (KBr) v_{max}: 3200-2600 (br), 2964, 1667, 1618, 1521, 1457, 1396, 1273, 1254, 969, 818, 762, 745, 695 cm^{-1}.

HRMS (LSIMS, +, glycerol) calcd for $C_{34}H_{30}O_3N$ (M+1): 380.2226, found: 380.2227.

Anal. Calcd for $C_{34}H_{29}O_3N$: C, 75.96; H, 7.70; N, 3.69. Found: C, 75.55; H, 7.67; N, 3.65.

This structure was confirmed by X-ray crystallographic analysis:

Habit	colourless prisms
Space Group	$P2_12_12_1$
a, Å	6.1899(7)
b, Å	7.1181(8)
c, Å	46.012(5)
α (°)	90
β (°)	90
γ (°)	90
Z	4
R	0.0864

(S)-(-)-1-Phenylethylammonium 4-[(7-methylbicyclo[2.2.1]hept-7-yl)carbonyl]benzoate (95)

95
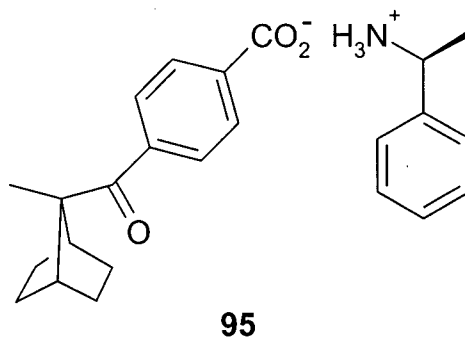
(S)-(-)-1-phenylethylamine (37.7 μL, 0.29 mmol) was added to a solution of acid **56** (73 mg, 0.28 mmol) in methanol (5 mL). Upon standing a precipitate formed that was isolated by suction filtration to give salt **95** (84 mg, 79%) as colourless prisms.

mp: 197 - 199 °C (methanol)

^{1}H NMR (400 MHz, DMSO): δ 1.14 (m, 2H), 1.25 (m, 2H), 1.37 (m, 2H), 1.37 (s, 3H), 1.47 (d, J = 6.5 Hz, 3H), 1.87 (m, 2H), 2.38 (m, 2H), 4.32 (q, J = 6.5 Hz, 1H), 7.30 (m, 1H),

7.37 (m, 2H), 7.49 (d, J = 7.2 Hz, 2H), 7.88 (d, J = 8 Hz, 2H), 7.94 (d, J = 8 Hz), 8.0 - 8.8 (br).

^{13}C NMR (75 MHz, DMSO): δ 17.53, 22.69, 27.94, 28.72, 42.59, 50.39, 62.84, 126.94, 128.00, 128.68, 128.89, 129.31, 137.88, 141.73, 142.57, 168.72, 205.00.

IR (KBr) ν_{max}: 3200-2600 (br), 2963, 1667, 1618, 1573, 1521, 1396, 1973, 1256, 969, 818, 762, 745, 695 cm^{-1}.

HRMS (ESI, +, 0.1% HCO$_2$H in MeOH) calcd for C$_{34}$H$_{30}$O$_3$N (M+1): 380.2226, found: 380.2220.

Anal. Calcd for C$_{24}$H$_{29}$O$_3$N: C, 75.96; H, 7.70; N, 3.69. Found: C, 76.23; H, 7.57; N, 3.67.

This structure was confirmed by X-ray crystallographic analysis:

Habit	colourless prisms
Space Group	$P2_12_12_1$
a, Å	6.165(2)
b, Å	7.090(2)
c, Å	45.81(2)
α (°)	90
β (°)	90
γ (°)	90
Z	4
R	0.038

<u>(*1S,2R*)-(-)-2-Hydroxyindan-1-ammonium 4-[(7-methylbicyclo[2.2.1]hept-7-yl)carbonyl]benzoate (**96**)</u>

96
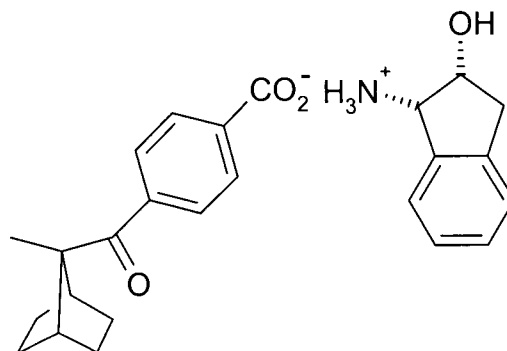
(*1S,2R*)-(-)-*cis*-1-Amino-2-indanol (47 mg, 0.31 mmol) in methanol (3 mL) was added to a solution of acid **56** (81 mg, 0.31 mmol) in methanol (5 mL). Upon standing a precipitate formed that was collected by suction filtration to give salt **96** (100 mg, 78%) as a colourless powder.

mp: 199 °C (dec) (methanol)

^{1}H NMR (400 MHz, DMSO): δ 1.15 (m, 2H), 1.25 (m, 2H), 1.37 (m, 2H), 1.37 (s, 3H), 1.87 (m, 2H), 2.38 (m, 2H), 2.91 (dd, J = 16, 3 Hz, 1H), 3.10 (dd, J = 16, 6 Hz, 1H), 4.44 (d, J = 5.2 Hz, 1H), 4.47 (m, 1H), 7.26 (m, 3H), 7.46 (d, J = 1.8 Hz, 1H), 7.90 (d, J = 8.4 Hz, 2H), 7.97 (d, J = 8.0 Hz, 2H), 7.6-8.4 (br).

^{13}C NMR (75 MHz, DMSO): δ 17.07, 27.48, 28.26, 39.09, 42.12, 57.10, 62.40, 70.90, 124.89, 125.06, 126.49, 127.63, 128.36, 128.98, 137.77, 139.56, 140.35, 141.37, 169.02, 204.54.

IR (KBr) v_{max}: 3300-2600 (br), 2960, 1669, 1581, 1538, 1398, 1273, 1087, 974, 742 cm^{-1}.

HRMS (LSIMS, +, glycerol) calcd for $C_{25}H_{30}O_4N$ (M+1): 408.2175, found: 408.2173.

Anal. Calcd for $C_{25}H_{29}O_4N$: C, 73.69; H, 7.17; N, 3.44. Found: C, 73.47; H, 7.14; N, 3.44.

(*1S,2S*)-(+)-1-Hydroxy-3-methoxy-1-phenylpropylammonium 4-[7-methylbicyclo[2.2.1]hept-7-yl)carbonyl]benzoate (**97**)

97
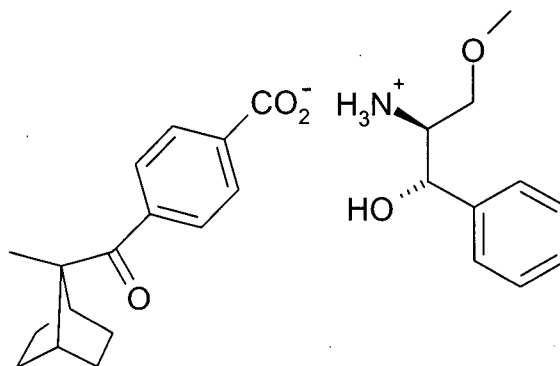
(*1S,2S*)-(+)-2-Amino-3-methoxy-1-phenyl-1-propanol (52 mg, 0.29 mmol) was dissolved in methanol (3 mL) and added to a solution of acid **56** (74 mg, 0.28 mmol) in methanol (5 mL). Upon standing a precipitate formed and was isolated by filtration to give salt **97** (92 mg, 74%) as a colourless powder.

mp: 162 - 163 °C (methanol)

^{1}H NMR (400 MHz, DMSO): δ 1.14 (m, 2H), 1.25 (m, 2H), 1.37 (m, 2H), 1.37 (s, 3H), 1.86 (m, 2H), 2.38 (m, 2H), 3.10 (dd, J = 10.0, 5.5 Hz, 1H), 3.19 (m, 1H), 3.19 (s, 3H), 3.27 (dd, J = 10.0, 3.5 Hz, 1H), 4.63 (d, J = 8.0 Hz, 1H), 7.30 (m, 1H), 7.36 (m, 4H), 7.90 (d, J = 8.4 Hz, 2H), 7.98 (d, J = 8.4 Hz, 2H).

^{13}C NMR (75 MHz, DMSO): δ 17.04, 27.47, 28.24, 42.11, 56.48, 58.36, 62.39, 70.98, 71.44, 126.66, 127.48, 127.63, 128.15, 128.98, 137.87, 139.99, 142.29, 168.55, 204.55.

IR (KBr) v_{max}: 3300-2600 (br), 2968, 1672, 1581, 1557, 1523, 1389, 1274, 1119, 1048, 972, 743, 702 cm^{-1}.

HRMS (LSIMS, +, glycerol) calcd for $C_{26}H_{34}O_5N$ (M+1): 440.2437, found: 440.2437.

Anal. Calcd $C_{26}H_{33}O_5N$: C, 71.05; H, 7.57; N, 3.19. Found: C, 71.03; H, 7.62; N, 3.03.

(*1R,2R*)-(-)-1,3-Dihydroxy-1-phenylpropylammonium 4-[(7-methylbicyclo[2.2.1]hept-7-yl)carbonyl]benzoate (**98**)

98
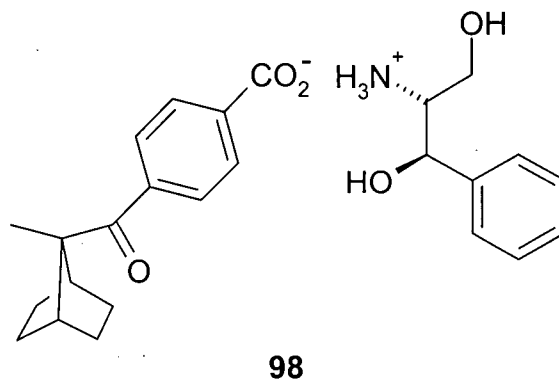
(*1R,2R*)-(-)-2-Amino-1-phenyl-1,3-propanediol (49 mg, 0.29 mmol) was dissolved in methanol (3 mL) and added to a solution of acid **56** (75 mg, 0.29 mmol) in methanol (5 mL). Upon standing a precipitate formed that was isolated by suction filtration to give salt **98** (101 mg, 82%) as a colourless powder.

mp: 162 - 164 °C (methanol)

^{1}H NMR (400 MHz, DMSO): δ 1.14 (m, 2H), 1.25 (m, 2H), 1.37 (m, 2H), 1.37 (s, 3H), 1.87 (m, 2H), 2.38 (m, 2H), 3.08 (m, 1H), 3.23 (dd, J = 11.6, 5.6 Hz, 1H), 3.41 (dd, J = 11.6, 3.6 Hz, 1H), 4.65 (d, J = 8.4 Hz, 1H), 6.6-7.8 (br), 7.29 (m, 1H), 7.38 (m, 4H), 7.89 (d, J = 8.0 Hz, 2H), 7.97 (d, J = 8.0 Hz, 2H)

^{13}C NMR (75 MHz, DMSO): δ 17.08, 27.48, 28.26, 42.13, 58.62, 59.30, 62.40, 71.03, 126.82, 127.58, 127.58, 128.18, 128.96, 137.62, 140.82, 142.29, 169.17, 204.58.

IR (KBr) v_{max}: 3300-2700 (br), 2960, 1670, 1585, 1423, 1392, 1275, 1041, 970, 945, 701 cm^{-1}.

HRMS (ESI, +, 0.1% HCO_2H in MeOH) Calcd for $C_{25}H_{32}O_5$: 426.2280, found: 426.2288.

Anal. Calcd for $C_{25}H_{31}O_5N\cdot\frac{1}{4}H_2O$: C, 69.83; H, 7.38; N, 3.26. Found: C, 69.87; H, 7.38; N, 3.25.

(Calcd for $C_{25}H_{31}O_5N$: C, 70.57; H, 7.34; N, 3.29)

(*R*)-(-)-1-Hydroxy-2-butylammonium 4-[(7-methylbicyclo[2.2.1]hept-7-yl)carbonyl]benzoate (**99**)

99
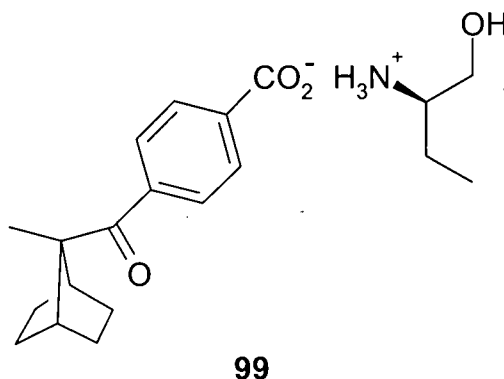
(*R*)-(-)-2-Amino-1-butanol (29 µL, 0.31 mmol) was added to a solution of acid **56** (77 mg, 0.30 mmol) in methanol (5mL). A precipitate formed on standing that was isolated by suction filtration to give salt **99** (63 mg, 61%) as a white powder.

mp: 174 - 176.5 °C (methanol)

^{1}H NMR (400 MHz, DMSO): δ 0.91 (t, *J* 7.5 Hz, 3H), 1.14 (m, 2H), 1.25 (m, 2H), 1.36 (m, 2H), 1.36 (s, 3H), 1.54 (m, 2H), 1.86 (m, 2H), 2.37 (m, 2H), 2.96 (m, 1H), 3.45 (dd, *J* = 12, 6 Hz, 1H), 3.61 (dd, *J* - 12, 3.6 Hz, 1H), 7.4-8.2 (br), 7.86 (d, 8.4 Hz, 2H), 7.93 (d, *J* = 8.0 Hz, 2H)

^{13}C NMR (75 MHz, DMSO): δ 9.85, 17.07, 22.73, 27.47, 28.25, 42.12, 53.85, 60.97, 52.36, 127.46, 128.82, 137.21, 141.93, 169.01, 204.53.

IR (KBr) v_{max}: 3400-2700 (br), 2963, 1668, 1584, 1525, 1392, 1275, 972, 744 cm^{-1}.

HRMS (LSIMS, +, glycerol) calcd for $C_{20}H_{30}O_4N$ (M+1): 348.2174, found: 348.2174.

Anal. Calcd for $C_{20}H_{29}O_4N \cdot \frac{1}{4}H_2O$: C, 68.25; H, 8.44; N, 3.98. Found: C, 68.53; H, 8.26; N, 4.10.

(Calcd for $C_{20}H_{29}O_4N$: C, 69.14; H, 6.41; N, 4.03)

<u>(*R*)-(-)-1-Cyclohexylethylammonium 4-[(7-methylbicyclo[2.2.1]hept-7-yl)carbonyl]benzoate (**100**)</u>
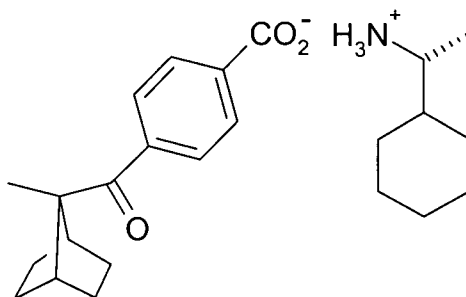
100

(*R*)-(-)-1-Cyclohexylethylamine (45 µL, 0.30 mmol) was added to a solution of acid **56** (75 mg, 0.29 mmol) in methanol (5 mL). Upon standing a precipitate formed that was removed by suction filtration to give salt **100** (102 mg, 91%) as a white powder.

mp: 196 - 198.5 °C (methanol)

^{1}H NMR (400 MHz, DMSO): δ 0.97 (m, 2H), 1.13 (m, 8H), 1.24 (m, 2H), 1.36 (m, 2H), 1.36 (s, 3H), 1.45 (m, 1H), 1.60 (m, 1H), 1.70 (m, 2H), 1.86 (m, 2H), 2.37 (m, 2H), 2.96 (m, 1H), 7.8-8.6 (br), 7.85 (d, *J* 8.0 Hz, 2H), 7.92 (d, *J* = 8 Hz, 2H).

^{13}C NMR (75 MHz, DMSO, 70 °C): δ 16.60 (br), 16.72, 25.26, 25.33, 25.51, 27.20, 27.99, 28.23, 41.71, 41.94, 50.60, 62.14, 127.02, 128.44, 137.43, 140.99, 167.68, 204.21.

IR (KBr) v_{max}: 3200-3700 (br), 1666, 1584, 1542, 1388, 1273, 971, 815, 746 cm^{-1}.

HRMS (ESI, +, 0.1% HCO_2H in MeOH): calcd for $C_{24}H_{36}O_3N$: 386.2695, found: 386.2696.

Anal. Calcd for $C_{24}H_{35}O_3N$: C, 74.77; H, 9.15; N, 3.63. Found: C, 74.55; H, 8.90; N, 3.46.

Chapter 8 Photochemical Studies

8.1 General Considerations

<u>Light Sources and Filters</u>

Irradiations were performed using either a 450 W Hanovia medium-pressure mercury arc lamp in a water cooled immersion well, or a 1000 W Advanced Radiation Corporation (ARC) high-pressure Hg-Xe arc lamp in a Sciencetech model 201 air cooled arc lamp housing controlled with a 500-1k power supply operating at 800 W. Light emitted from the Hanovia lamp was filtered through Pyrex (transmits $\lambda \geq 290$ nm). Light emitted from the ARC lamp was filtered through two dichroic filters (transmits λ 200 - 320 nm) and Pyrex (transmits $\lambda \geq 290$ nm).

<u>Solution State Photolyses</u>

HPLC grade or spectral grade (Fisher Chemical) solvents were used for all solution state photochemical reactions. Reaction solutions were purged by bubbling nitrogen through the solution for at least 15 minutes prior to irradiation. During irradiations the reaction vessel was either sealed (small scale reaction, <5 mg ketone) or under a positive pressure of nitrogen (large scale reaction, 200-300 mg). Reactions were monitored by GC and/or TLC until a high conversion was reached or until the relative amounts of the major photoproducts decreased due to the emergence of minor or secondary photoproducts.

<u>Analytical Solid State Photolyses</u>

The solid material (~2 mg), either as ground single crystals or in polycrystalline form (powder), was sandwiched between two microscope slides (Pyrex equivalent) and spread out to cover a surface area of approximately 2 cm^2. The plates were fastened together with tape at the top and bottom edge before the assembly was heat-sealed in a polyethylene bag under a nitrogen atmosphere. Following irradiation, the sample was quantitatively washed from the plates with an appropriate solvent, and concentrated under a nitrogen gas stream. For neutral molecules, the sample was analyzed directly by gas chromatography. For salts or free acids, the sample was converted to the corresponding methyl ester with an ethereal solution of diazomethane, and in

the case of salts, filtered through silica gel to remove the amine, before being analyzed by gas chromatography and/or high performance liquid chromatography.

Preparative Scale Solid State Photolyses

The solid material was suspended in HPLC grade hexanes or distilled water (containing sufficient sodium dodecylsulfonate to ensure that the material was evenly distributed throughout the solution), purged with nitrogen for 15 minutes prior to irradiation, and kept under a positive pressure of nitrogen during the reaction. Following irradiation the solvent was removed by filtration and the solid dissolved in an appropriate solvent before being prepared for analysis as previously described.

Low-Temperature Photolyses

A low temperature ethanol bath contained in an unsilvered Dewar vessel (Pyrex) was maintained by a Cryocool CC-100 II Immersion Cooling System (Neslab Instrument Inc.). Samples sealed in polyethylene bags were suspended in the cold liquid and irradiated through the transparent walls of the Dewar vessel.

Reaction Conversion and Yield Determinations

Yields for preparative scale photolyses were calculated based on the mass of the isolated, purified products. Conversions for preparative scale photolyses were based on the results of GC integration. Yields and conversions for analytical photolyses were determined based on the results of GC analysis. The difference in GC detector response for a particular starting material and its reaction products was found to be negligible (all are structural isomers in most cases) and thus no corrections were applied to the integration data. The overall precision of the reported results is estimated to be ± 1%.

8.2 Photolysis of Benzonorbornene Phenyl Ketones

8.2.1 Preparative Photolysis of Phenyl Ketone 43
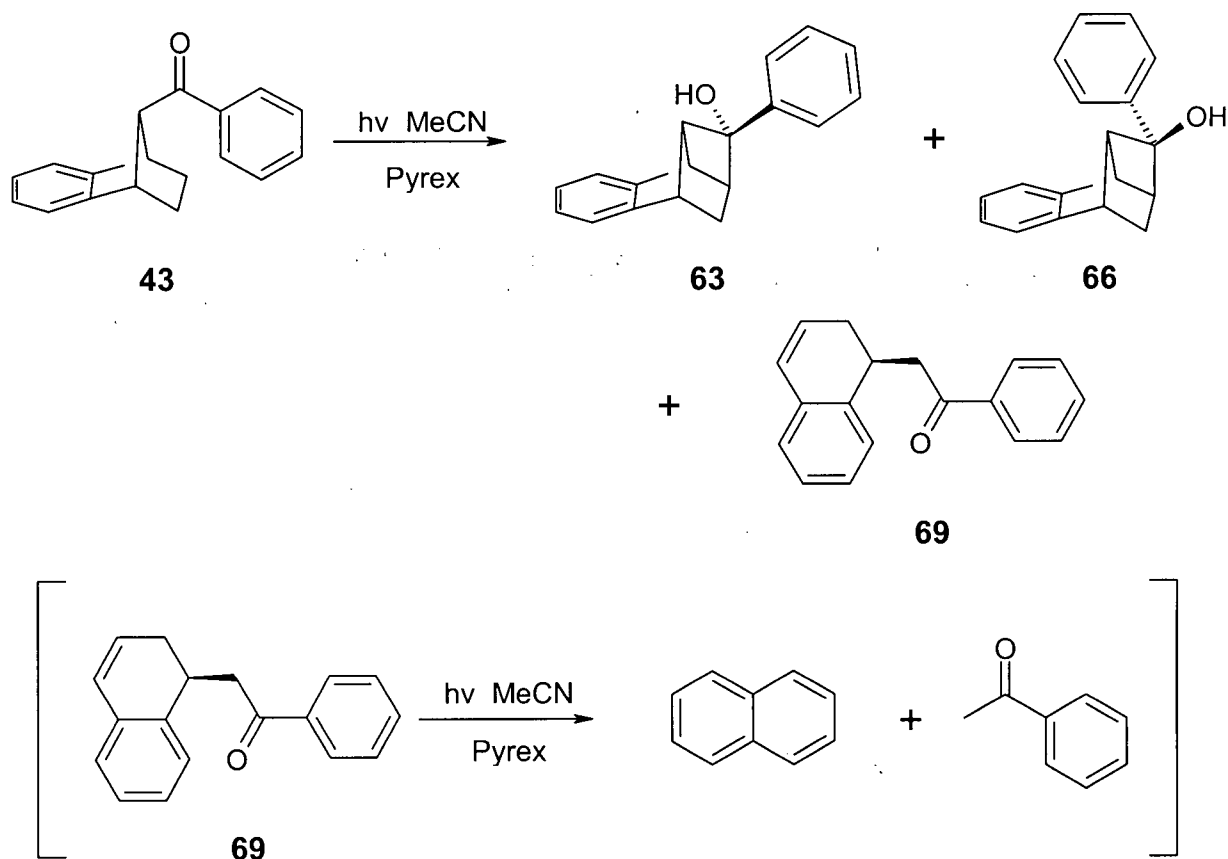
A solution of ketone **43** (300 mg, 1.21 mmol) in acetonitrile (45 mL) was purged with N_2 and irradiated (Pyrex filter, 450 W Hanovia lamp) for 6 hours and forty-five minutes. Analysis of the mixture following photolysis by gas chromatography indicated that the reaction had proceeded to 91% conversion, producing three primary photoproducts: **63** (60%), **66** (7.6%) and **69** (19%). Further analysis by gas chromatography with a mass selective detector confirmed the presence of small amounts of naphthalene and acetophenone, resulting from Norrish type II cleavage of ketone **69** in a secondary photoreaction. Mass spectral fragmentation patterns and gas chromatograph retention times matched those of authentic samples. Due to the volatility of both of these compounds under the reaction conditions a quantitative analysis was not possible.

The solvent was removed *in vacuo* and the residue purified by repeated radial chromatography (12% ether/petroleum ether) to yield *endo*-aryl cyclobutanol **63** (47.2 mg, 15.7%), *exo*-aryl cyclobutanol **66** (1.2 mg, 0.4%), and ketone **69** (45.5 mg, 15.2%) as colourless oils   The remaining mass was due to starting material, the secondary photoproducts mentioned, minor photoproducts (<5% of total in reaction mixture) and a mixture of cyclobutanols **63** and **66**.

(*1R*,2S*,4S*,9R*,10R**)-1α,2β,4α-Ethano-1,2,3,4-tetrahydro-10-phenylnaphthalen-10-ol (63)

^{1}H NMR (400 MHz, CD$_2$Cl$_2$): δ 0.55 (dd, J = 11.0, 2.4 Hz, 1H), 1.67 (dd, J = 11.0, 5.9 Hz, 1H), 2.19 (br s, 1H), 2.94 (m, 1H), 3.18 (d, J = 5.8 Hz), 3.31 (m, 1H), 4.25 (br s, 1H), 7.11 (m, 2H), 7.18 (m, 1H), 7.30 (m, 2H), 7.34 (m, 2H), 7.41 (m, 2H).

^{13}C NMR (75 MHz, CD$_2$Cl$_2$): δ 32.23 (+), 44.45 (-), 46.32 (-), 48.88 (-), 66.46 (-), 83.92 (+), 119.56 (-), 123.49 (-), 125.73 (-), 126.05 (-), 126.33 (-), 127.86 (-), 128.95 (-), 142.41 (+), 143.09 (+), 155.35 (+).

IR (CCl$_4$) v_{max}: 3412 (br), 3061, 3025, 2976, 2889, 1460, 1448, 1364, 1269, 1188, 1060, 1050, 1014, 974, 912, 566, 521 cm^{-1}.

LRMS (EI): 248 (2, M$^+$), 230 (7), 134 (10), 133 (100), 129 (5), 128 (28), 116 (12), 115 (12), 105 (19), 88 (8), 84 (72), 77 (8), 55 (9), 51 (13).

HRMS (EI) calcd for C$_{18}$H$_{16}$O: 248.1201, found: 248.1200.

(*1R*,2S*,4S*,9R*,10S**)-1α,2β,4α-Ethano-1,2,3,4-tetrahydro-10-phenylnaphthalen-10-ol (66)

^{1}H NMR (400 MHz, CD$_2$Cl$_2$): δ 0.75 (dd, J = 10.4, 2.0 Hz, 1H), 1.90 (br s, 1H), 2.69 (dd, J = 10.4, 6.0 Hz, 1H), 2.77 (m, 1H), 3.09 (m, 1H), 3.35 (m, 1H), 3.46 (m, 1H), 7.06 (m, 3H), 7.26 (m, 1H), 7.36 (m, 1H), 7.43 (m, 2H), 7.61 (m, 2H).

^{13}C NMR (75 MHz, CD$_2$Cl$_2$): δ 31.57 (+), 44.73 (-), 45.91 (-), 46.04 (-), 68.21 (-), 88.13 (+), 119.77 (-), 123.44 (-), 125.68 (-), 125.91 (-), 127.83 (-), 128.23 (-), 128.94 (-), 141.19 (+), 142.72 (+), 155.30 (+).

LRMS (EI): 248 (3, M$^+$), 134 (10), 133 (100), 129 (5), 128 (27), 116 (9), 115 (12), 105 (18), 84 (6), 77 (8), 55 (9).

HRMS (EI) calcd for C$_{18}$H$_{16}$O: 248.1201, found: 248.1200.

2-[(*1S**)-1,2-Dihydronaphthalen-1-yl]-1-phenylethanone (69)

¹H NMR (400 MHz, CDCl₃): δ 2.31 (m, 1H), 2.58 (ddt, J = 17.5, 6.8, 3.2 Hz, 1H), 3.05 (dd, J = 16.5, 5.1 Hz, 1H), 3.34 (dd, J = 16.5, 8.9 Hz, 1H), 3.58 (m, 1H), 5.91 (m, 1H), 6.50 (dd, J = 9.6, 2.7 Hz, 1H), 7.05 (d, J = 6.2 Hz, 1H), 7.14 (m, 3H), 7.41 (m, 2H), 7.52 (tt, J = 7.4, 1.3 Hz, 1H), 7.89 (m, 2H). ·

¹³C NMR (75 MHz, CDCl₃): δ 28.29 (+), 33.03 (-), 42.60 (+), 126.35 (-), 126.51 (-), 126.89 (-), 127.32 (-), 127.37 (-), 127.62 (-), 128.07 (-), 128.51 (-), 133.00 (-), 133.30 (+), 137.17 (+), 138.25 (+), 199.30 (+).

IR (neat) ν$_{max}$: 3060, 3032, 2928, 2877, 1684, 1597, 1487, 1448, 1357, 1284, 1208, 997, 784, 749, 690, 520 cm⁻¹.

LRMS (EI): 248 (0.5, M⁺), 129 (14), 128 (100), 127 (6), 115 (6), 105 (12), 78 (5), 77 (18), 51 (7).

HRMS (EI) calcd for C₁₈H₁₆O: 248.1201, found: 248.1200.

8.2.2 Preparative Photolysis of Phenyl Ketone 44
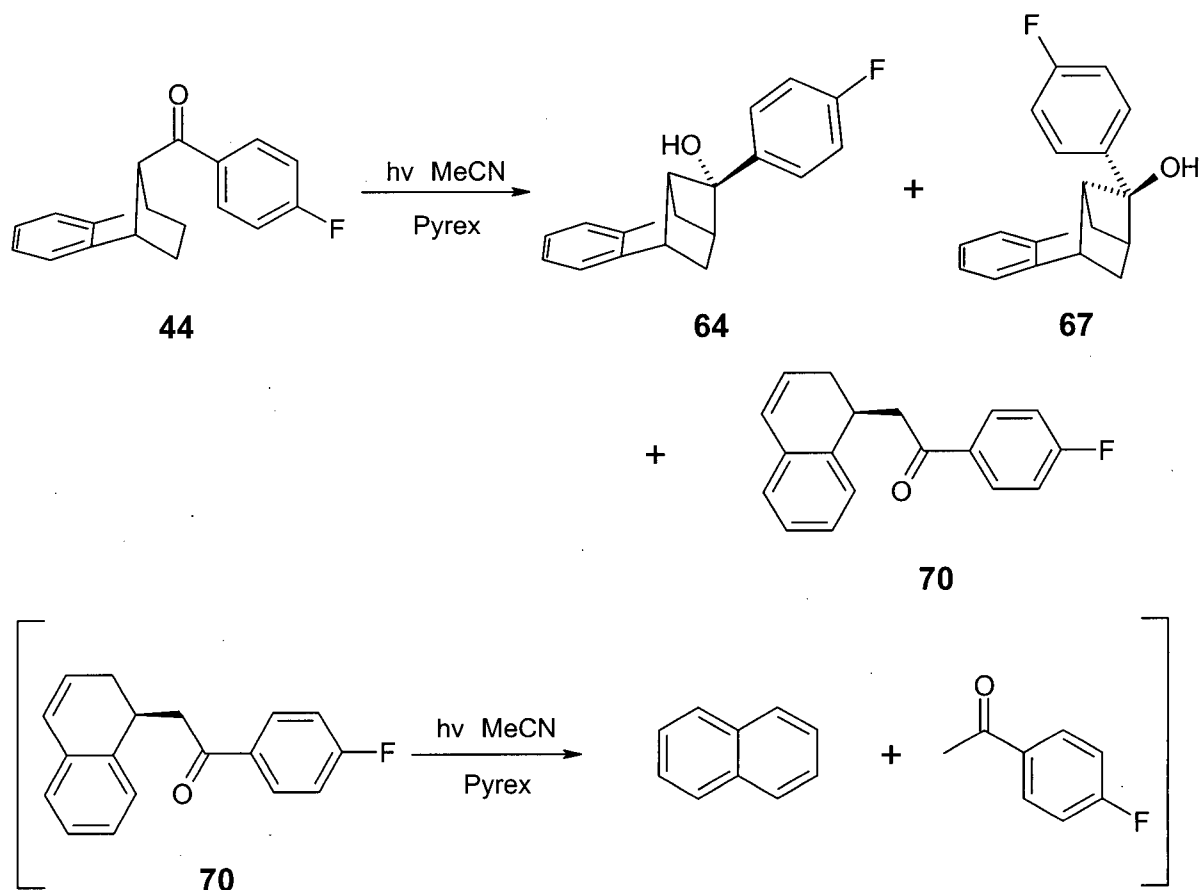
A solution of ketone **44** (272 mg, 1.10 mmol) in acetonitrile (200 mL) was purged with N_2 and irradiated (Pyrex filter, 450 W Hanovia lamp) for 4 hours. Analysis of the mixture after photolysis by gas chromatography indicated that the reaction had proceeded to 93% conversion, producing three primary photoproducts: **64** (57%), **67** (5.2%) and **70** (31%). Analysis by gas chromatography with a mass selective detector confirmed the presence of small amounts of naphthalene and *p*-fluoroacetophenone, resulting from Norrish type II cleavage of ketone **70** in a secondary photoreaction. Mass spectral fragmentation patterns and retention times were identical to those of authentic samples. Due to the volatility of both of these compounds under the reaction conditions a quantitative analysis of these products was not possible. The solvent was removed *in vacuo* and the residue purified by repeated radial chromatography (7% ether/petroleum ether) to yield *endo*-aryl cyclobutanol **64** (75 mg, 27.6%) as a colourless solid

and *exo*-aryl cyclobutanol **67** (6 mg, 2.2%) and ketone **70** (45.5 mg, 16.7%) as colourless oils. The remainder of the material consisted of unreacted ketone **44**, secondary photoproducts, unisolated minor photoproducts (<5% in reaction mixture) and a mixture of cyclobutanols **64** and **67**.

(1R*,2S*,4S*,9R*,10R*)-1α,2β,4α-Ethano-1,2,3,4-tetrahydro-10-(4-fluorophenyl)naphthalen-10-ol **(64)**

mp: 128.5-130 °C (10% ether / petroleum ether)

^{1}H NMR (400 MHz, CD_2Cl_2): δ 0.56 (dd, J = 11.0, 2.4 Hz, 1H), 1.65 (dd, J = 11.0, 5.9 Hz, 1H), 2.24 (br s, 1H), 2.91 (m, 1H), 3.17 (br d, J = 5.8 Hz), 3.28 (m, 1H), 4.24 (br s, 1H), 7.11 (m, 4H), 7.19 (m, 1H), 7.28 (m, 3H).

^{13}C NMR (75 MHz, CD_2Cl_2): δ 32.18 (+), 44.41 (-), 46.44 (-), 48.89 (-), 66.49 (-), 83.38 (+), 115.57 and 115.86 (-, $^2J_{C-F}$ = 21 Hz), 119.58 (-), 123.51 (-), 125.78 (-), 126.11 (-), 128.19 and 128.29 (-, $^3J_{C-F}$ = 8 Hz), 139.14 and 139.18 (+, $^4J_{C-F}$ = 3 Hz), 142.27 (+), 155.23 (+), 160.81 and 164.06 (+, $^1J_{C-F}$ = 244 Hz).

IR (KBr) v_{max}: 3550, 3067, 2975, 1602, 1509, 1459, 1333, 1263, 1214, 1162, 1069, 1049, 1009, 926, 852, 769, 761, 611, 575, 528 cm^{-1}.

LRMS (EI): 266 (5, M$^+$), 248 (11), 247 (6), 152 (11), 151 (100), 128 (23), 123 (18), 116 (16), 115 (9), 95 (6).

HRMS (EI) calcd for $C_{18}H_{15}OF$: 266.1107, found: 266.1107.

Anal. Calcd for $C_{18}H_{15}OF$: C, 81.18; H, 5.68. Found: C, 81.25; H, 5.82.

This structure was confirmed by X-ray crystallographic analysis:

Habit	colourless needles
Space Group	P2$_1$/n
a, Å	7.018(3)
b, Å	11.604(6)
c, Å	16.799(5)
α (°)	90
β (°)	98.10(1)
γ (°)	90
Z	4
R	0.051

(1R*,2S*,4S*,9R*,10S*)-1α,2β,4α-Ethano-1,2,3,4-tetrahydro-10-(4-fluorophenyl)naphthalen-10-ol (67)

^{1}H NMR (400 MHz, CD$_2$Cl$_2$): δ 0.75 (dd, J = 10.5, 2.3 Hz, 1H), 1.90 (br s, 1H), 2.68 (dd, J = 10.5, 6.0 Hz, 1H), 2.76 (m, 1H), 3.06 (dt, J = 6.3, 2.5 Hz, 1H), 3.31 (dt, J = 6.3, 2.6 Hz, 1H), 3.46 (m, 1H), 7.09 (m, 3H), 7.12 (m, 2H), 7.26 (m, 1H), 7.59 (m, 2H).

^{13}C NMR (75 MHz, CD$_2$Cl$_2$): δ 31.58 (+), 44.70 (-), 46.04 (-. 2C), 68.26 (-), 78.05 (+), 115.47 and 115.75 (-, $^2J_{C-F}$ = 21 Hz), 119.79 (-), 123.46 (-), 125.73 (-), 125.99 (-), 129.67 and 129.78 (-, $^3J_{C-F}$ = 8 Hz), 138.70 and 138.75 (+, $^4J_{C-F}$ = 3 Hz), 141.02 (+), 155.21 (+), 161.01 and 164.27 (+, $^1J_{C-F}$ = 244 Hz).

LRMS (EI): 266 (3, M$^+$), 152 (11), 151 (100), 143 (6), 129 (5), 128 (32), 123 (20), 116 (9), 115 (8), 95 (7), 84 (6), 55(6).

HRMS (EI) calcd for C$_{18}$H$_{15}$OF: 266.1107, found: 266.1107.

2-[(1S*)-1,2-Dihydronaphthalen-1yl]-1-(4-fluorophenyl)ethanone (70)

^{1}H NMR (400 MHz, CDCl$_3$): δ 2.29 (m, 1H), 2.58 (ddt, J = 17.5, 6.9, 2.9 Hz, 1H), 3.02 (dd, J = 16.4, 5.3 Hz, 1H), 3.27 (dd, J = 16.4, 8.7 Hz, 1H), 3.56 (m, 1H), 5.90 (m, 1H), 6.50 (dd, J = 9.6, 2.7 Hz, 1H), 7.05 (m, 2H), 7.11 (m, 3H), 7.15 (m, 1H), 7.89 (m, 2H).

¹³C NMR (75 MHz, CDCl₃): δ 28.31 (+), 33.09 (-), 42.49 (+), 115.72 and 115.43 (-, $^2J_{C-F}$ = 22 Hz), 126.39 (-), 126.44 (-), 126.97 (-), 127.35 (-), 127.39 (-), 127.63 (-), 130.63 and 130.76 (-, $^3J_{C-F}$ = 9 Hz), 133.24 (+), 133.58 and 133.63 (+, $^4J_{C-F}$ = 4 Hz), 138.07 (+), 163.97and 167.34 (+, $^1J_{C-F}$ = 253 Hz), 197.75 (+).

IR (CCl₄) v_{max}: 3065, 3034, 2928, 1684, 1598, 1506, 1458, 1408, 1356, 1284, 1231, 1156, 996, 592 cm⁻¹.

LRMS (DCI+, NH₃): 268 (7), 267 (35, M+1), 129 (16), 128 (100), 123 (14).

HRMS (DCI+, NH₃) calcd for $C_{18}H_{16}OF$ (M+1): 267.1185, found: 267.1183.

8.2.3 Preparative Photolysis of Phenyl Ketone 45
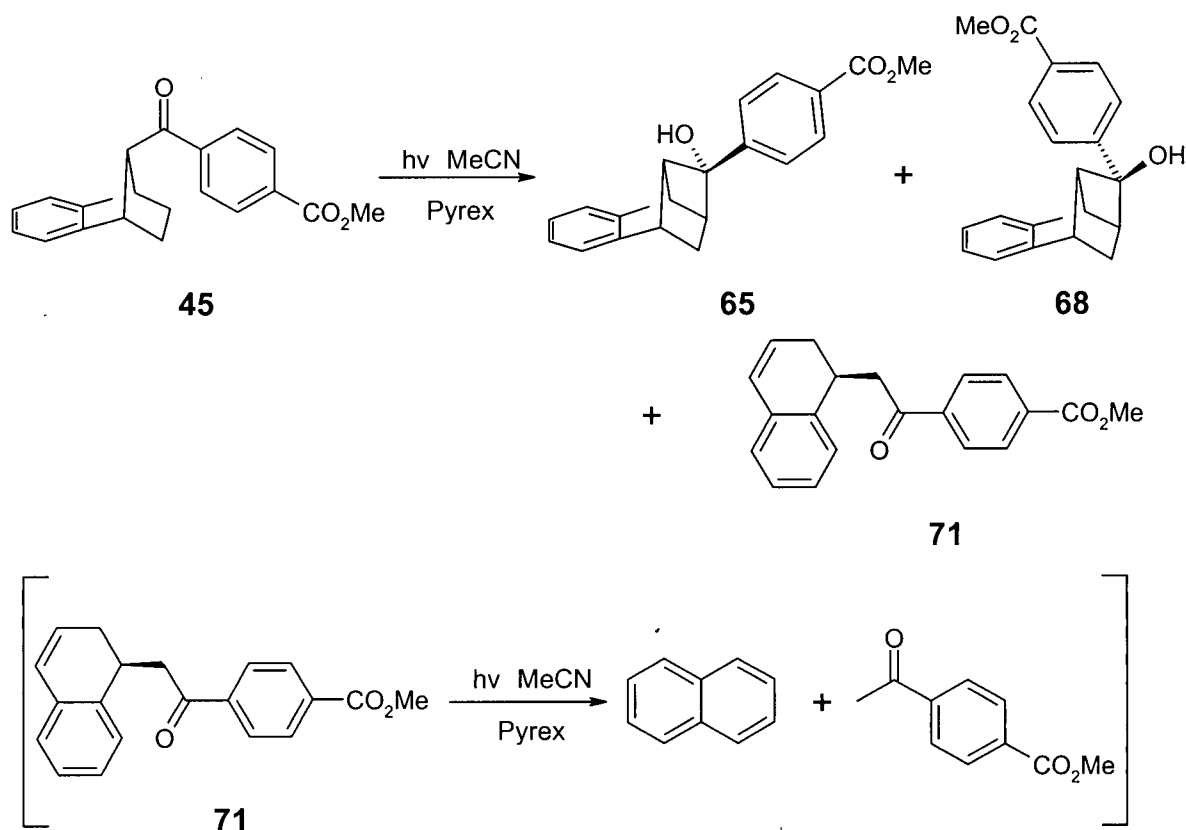
A solution of ketone **45** (267 mg, 0.87 mmol) in acetonitrile (40 mL) was purged with N₂ and irradiated (Pyrex filter, 450 W Hanovia lamp) for 4.5 hours. Analysis of the mixture after photolysis by gas chromatography indicated that the reaction had proceeded to 91% conversion,

producing three primary photoproducts: **65** (46%), **68** (1.9%) and **71** (52%). Analysis by gas chromatography with a mass selective detector confirmed the presence of small amounts of naphthalene and *p*-carboxymethylacetophenone resulting from Norrish type II cleavage of ketone **71** in a secondary photoreaction. Mass spectral fragmentation patterns and gas chromatograph retention times matched those of authentic samples. The solvent was removed *in vacuo* and the residue purified by radial chromatography (2.5% EtOAc/pet. ether) to give ketone **71** (93 mg, 35%) as a colourless solid and a mixture of two cyclobutanols **65** and **68**. *Endo*-aryl cyclobutanol **65** (55 mg, 21%) was isolated by purification from preparative HPLC (6% ethyl acetate / 94% hexanes). *Exo*-aryl cyclobutanol **68** was partially characterized by nmr spectroscopy of the crude mixture and comparison to the analagous *endo*-arylcyclobutanls **66** and **67**. The remaining mass in the reaction mixture was due to ketone **45**, the cyclobutanol **65/68** mixture, secondary photoproducts and unisolated minor photoproducts (<5% of total mass).

Methyl 4-[(*1R*,2S*,4S*,9R*,10R**)-1α,2β,4α-ethano-1,2,3,4-tetrahydro-10-hydroxynamhthalene-10-yl]benzoate (65)

mp: 175 - 176 °C (hexanes/ether)

^{1}H NMR (400 MHz, CD_2Cl_2): δ 0.55 (dd, *J* = 11.2, 2.4 Hz, 1H), 1.60 (dd, *J* = 11.2, 5.9 Hz, 1H), 2.20 (s, 1H), 2.95 (m, 1H), 3.17 (br d, *J* = 5.8 Hz), 3.31 (m, 1H), 3.90 (s, 3H), 4.26 (m, 1H), 7.10 (m, 2H), 7.17 (m, 1H), 7.29 (m, 1H), 7.37 (m, 2H), 8.05 (m, 2H).

^{13}C NMR (100 MHz, CD_2Cl_2): δ 32.19 (+), 44.49 (-), 46.53 (-), 49.01 (-), 52.39 (-), 66.39 (-), 83.61 (+), 119.67 (-), 123.59 (-), 125.90 (-), 126.23 (-), 126.54 (-), 129.89 (+), 142.15 (+), 147.98 (+), 155.32 (+), 167.07 (+).

IR (KBr) v_{max}: 3476, 2983. 1702, 1611, 1459, 1436, 1409, 1295, 1188, 1109, 1066, 1016, 976, 933, 860, 780, 760, 711 cm^{-1}

LRMS (EI): 306 (2, M$^+$), 288 (6), 192 (12), 191 (100), 163 (21), 159 (19), 143 (8), 141 (7), 132 (10), 131 (11), 129 (14), 128 (58), 116 (33), 115 (17), 103 (7), qq (7), 59 (13), 55 (35).

HRMS (EI) calcd for $C_{20}H_{18}O_3$: 306.1256, found: 306.1253.

Anal. Calcd for $C_{20}H_{18}O_3$: C, 78.41; H, 5.92. Found: C, 78.40; H, 6.01.

Methyl 4-[(*1R*,2S*,4S*,9R*,10S**)-1α,2β,4α-ethano-1,2,3,4-tetrahydro-10-hydroxynamhthalene-10-yl]benzoate (**68**)

¹H NMR (400 MHz, CD₂Cl₂): δ 0.76 (dd, *J* = 10.5, 2.3 Hz, 1H), 2.00 (br s, 1H), 2.70 (dd, *J* = 10.5, 6.0 Hz, 1H), 2.78 (m, 1H), 3.10 (m, 1H), 3.34 (m, 1H), 3.47 (m, 1H), 3.91 (s, 3H), 7.07 (m, 2H), 7.17 (m, 1H), 7.27 (m, 1H), 7.68 (m, 2H), 8.07 (m, 2H).

¹³C NMR (125 MHz, CD₂Cl₂): δ 31.53 (+), 44.77 (-), 45.94 (-), 46.01 (-), 52.41 (-), 66.01 (-), 78.36 (+), 119.84 (-), 123.52 (-), 125.81 (-), 126.07 (-), 128.03 (-), 130.06 (+), 130.10 (-), 140.92 (+), 147.67 (+), 155.12 (+). 167.04 (+),

Methyl 4-[(*1S**)-1,2-dihydronaphthalen-1-ylacetyl]benzoate (**71**)

mp: 109 - 110 °C (hexanes)

¹H NMR (400 MHz, CD₂Cl₂): δ 2.32 (, *J* = , 1H), 2.58 (ddt, *J* = 17.5, 6.9, 2.8 Hz, 1H), 3.13 (dd, *J* = 16.7, 5.6 Hz, 1H), 3.33 (dd, *J* = 16.7, 8.4 Hz, 1H), 3.56 (m, 1H), 5.94 (m, 1H), 6.53 (dd, *J* = 9.6, 2.5 Hz, 1H), 7.06 (br d, *J* = 7.1 Hz, 1H), 7.12 (m, 2H), 7.16 (m, 1H), 7.93 (dt, *J* = 8.7, 1.5 Hz, 2H), 8.07 (dt, *J* = 8.7, 1.5 Hz, 2H).

¹³C NMR (75 MHz, CD₂Cl₂): δ 28.81 (+), 33.42 (-), 43.35 (+), 52.70 (-), 126.73 (-), 126.95 (-, 2C), 127.31 (-), 127.70 (-), 129.93 (-), 128.32 (-), 130.01 (-), 133.77 (+), 134.22 (+), 138.48 (+), 140.77 (+), 166.45 (+), 199.03 (+).

IR (KBr) ν$_{max}$: 3044, 2942, 2886, 1716, 1681, 1572, 1564, 1488, 1408, 1359, 1279, 1224, 1209, 1193, 1112, 1017, 996, 960, 865, 783, 756, 695, 608, 532 cm⁻¹

LRMS (EI): 306 (0.4, M⁺), 275 (4), 178 (4), 163 (6), 129 (15), 128 (100), 127 (5), 115 (2).

HRMS (EI) calcd for C₂₀H₁₈O₃: 306.1256, found: 306.1252.

Anal. Calcd for C₂₀H₁₈O₃: C, 78.41; H, 5.92. Found: C, 78.10; H, 5.91.

This structure was confirmed by X-ray crystallographic analysis:

Habit	colourless platelets
Space Group	P$\bar{1}$
a, Å	6.0581(7)
b, Å	15.025(2)
c, Å	19.094(2)
α (°)	112.22(1)
β (°)	98.750(7)
γ (°)	91.477(5)
Z	4
R	0.113

8.3 Photolysis of 7-Methylnorbornyl Phenyl Ketones 54, 55 and 57

8.3.1 Preparative Photolysis of Phenyl Ketone 54
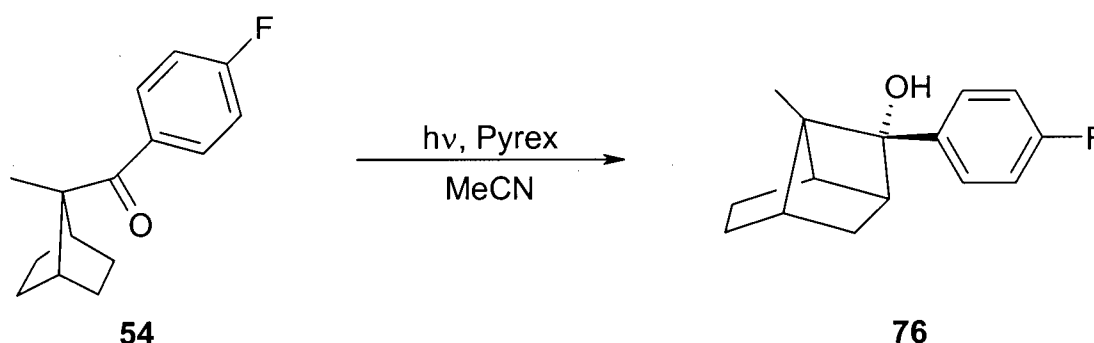
Ketone **54** (94 mg, 0.41 mmol) was dissolved in acetonitrile (10 mL) in a Pyrex photolysis tube. After purging the system with N_2 for 15 min, the solution was photolysed for 2 h resulting in complete reaction of the starting material. Following removal of the solvent *in vacuo* and purification by radial chromatography (5% ether/pet. ether), cyclobutanol **76** was obtained as a colourless solid (85 mg, 90%).

(*1R*,*2R*,*5S*,*7S*,*8R**)-8-(4-Fluorophenyl)-1-methyltricyclo[3.3.0.0^{2,7}]octan-8-ol (**76**)

mp: 52 - 53 °C (hexanes)

¹H NMR (400 MHz, CD₂Cl₂): δ 0.95 (m, 1H), 1.14 (m, 1H), 1.28 (s, 3H), 1.49 (m, 1H), 1.61 (m, 2H), 1.87 (m, 2H), 2.08 (s, 1H), 2.57 (m, 1H), 2.68 (br s, 1H), 7.02 (m, 2H), 7.24 (m, 2H).

¹³C NMR (75 MHz, CD₂Cl₂): δ 10.96 (-), 22.00 (+), 28.63 (+), 33.77 (+), 42.53 (-), 47.64 (-), 49.07 (-), 58.08 (+), 84.97 (+), 115.33 and 115.62 (-, $^{2}J_{C-F}$ = 21.1 Hz), 128.38 and 128.48 (-, $^{3}J_{C-F}$ = 7.9 Hz), 140.41 and 140.45 (+, $^{4}J_{C-F}$ = 3.2 Hz), 160.58 and 163.83 (+, $^{1}J_{C-F}$ = 243.2 Hz).

IR (KBr) ν$_{max}$: 3368 (br), 2949, 2867, 1606, 1508, 1221, 1042, 843 cm⁻¹.

LRMS (EI): 232 (7, M⁺), 214 (26), 188 (15), 186 (22), 185 (27), 183 (10), 178 (41), 177 (20), 173 (16), 165 (12), 163 (31), 152 (19)151 (100), 146 (10), 133 (19), 123 (49), 109 (25), 95 (27), 81 (18), 79 (13), 67 (11), 55 (16).

HRMS (EI) calcd for C₁₅H₁₇OF: 232.1263, found: 232.1264.

Anal. Calcd: C, 77.56; H, 7.38. Found: C, 77.53; H, 7.44.

8.3.2 Preparative Photolysis of Phenyl Ketone 55

55   **77**
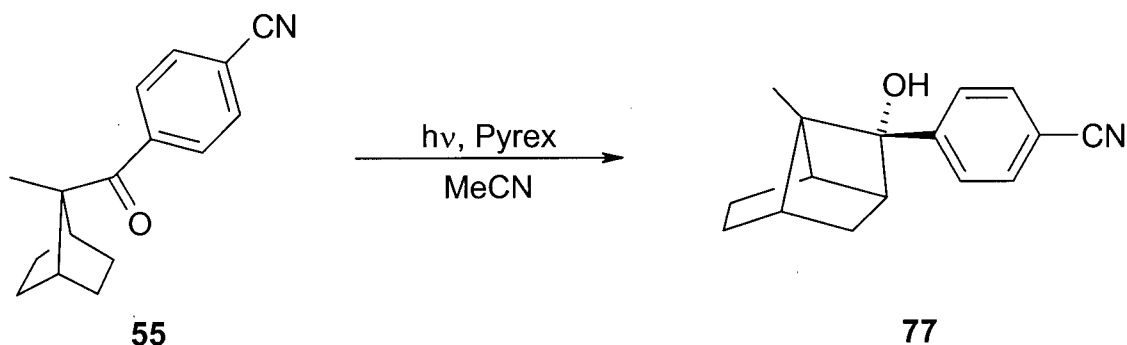
Ketone **55** (56 mg, 0.23 mmol) was dissolved in acetonitrile (20 mL) in a Pyrex photolysis tube. After purging with N₂ for 20 min the solution was photolysed for 2 h resulting in complete conversion of the starting material. Following removal of the solvent *in vacuo* and purification by radial chromatography (15% ether/pet. ether), cyclobutanol **77** was obtained as a colourless solid (51 mg, 91%).

4-[(*1R*,2R*,5S*,7R*,8S**)-8-hydroxy-1-methyltricyclo[3.3.0.0^{2,7}]oct-8-yl)benzonitrile (**77**)

mp: 118- 119 °C (hexanes)

^{1}**H NMR** (400 MHz, CD$_2$Cl$_2$): δ 0.97 (dd, J = 11.5, 2.2 Hz, 1H), 1.08 (m, 1H), 1.28 (s, 3H), 1.51 (m, 1H), 1.62 (m, 2H), 1.89 (m, 2H), 2.22 (s, 1H), 2.62 (m, 1H), 2.71 (m, 1H), 7.38 (dt, J = 8.5, 1.9 Hz, 2H), 7.62 (dt, J = 8.5, 1.9 Hz, 2H).

^{13}**C NMR** (75 MHz, CD$_2$Cl$_2$): δ 10.87 (-), 21.82 (+), 28.47 (+), 33.71 (+), 42.67 (-), 47.69 (-), 49.04 (-), 58.00 (+), 84.95 (+), 111.32 (+), 119.16 (+), 127.51 (-), 132.73 (-), 149.29 (+).

IR (KBr) ν$_{max}$: 3464, 2993, 2950, 2867, 2236, 1604, 1476, 1380, 1292, 1084, 1056, 954, 856, 839, 583 cm^{-1}.

LRMS (EI): 239 (4, M$^+$), 221 (40), 206 (11), 193 (50), 192 (45), 191 (11), 190 (18), 185 (57), 184 (25), 180 (26), 179 (11), 178 (14), 171 (28), 170 (47), 166 (13), 165 (17), 159 (17), 158 (33), 153 (12), 152 (??), 140 (18), 130 (35), 109 (21), 103 (10), 102 (35), 94 (13), 91 (11), 82 (14), 81 (100), 80 (13), 79 (28), 77 (20), 67 (12), 55 (13), 53 (11).

HRMS (EI) calcd for C$_{16}$H$_{17}$ON: 239.1310, found: 239.1312.

Anal. Calcd: C, 80.30; H, 7.16; N, 5.85. Found: C, 80.05; H, 7.11; N, 5.76.

8.3.3 Preparative Photolysis of Phenyl Ketone 57
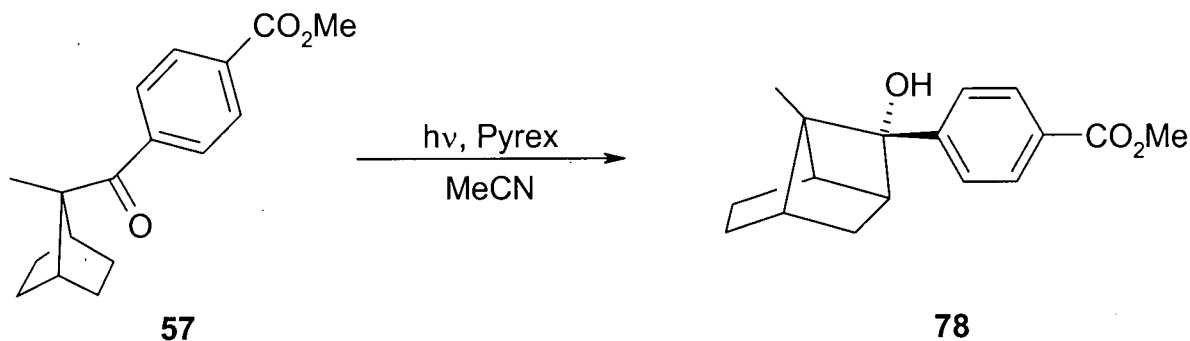
Ketone **57** (179 mg, 0.66 mmol) was dissolved in acetonitrile (40 mL) in a Pyrex photolysis tube. After purging with N$_2$ for 15 min the solution was photolysed for 4 h resulting

in complete conversion of the starting material. Following removal of the solvent *in vacuo* and purification by radial chromatography (10% ether/pet. ether), cyclobutanol **78** was obtained as a colourless solid (169 mg, 94%).

Methyl 4-[(*1R*,2R*,5S*,7R*,8S**)-8-hydroxy-1-methyltricyclo[3.3.0.0^{2,7}]oct-8-yl]benzoate (**78**)

mp: 125.5 - 127 °C (hexanes)

^{1}H NMR (400 MHz, CD$_2$Cl$_2$): δ 0.95 (dd, J = 11.3, 2.2 Hz, 1H), 1.10 (dd, J = 11.2, 6.3 Hz, 1H), 1.30 (s, 3H), 1.50 (m, 1H), 1.61 (m, 2H), 1.88 (m, 1H), 1.89 (m, 1H), 2.11 (br s, 1H), 2.62 (m, 1H), 2.71 (m, 1H), 3.87 (s, 3H), 7.35 (m, 2H), 7.96 (m, 2H).

^{13}C NMR (75 MHz, CD$_2$Cl$_2$): δ 10.96 (-), 21.89 (+), 28.55 (+), 33.72 (+), 42.48 (-), 47.61 (-), 49.04 (-), 52.29 (-), 58.04 (+), 85.11 (+), 126.70 (-), 129.43 (+), 130.03 (-), 149.23 (+), 167.09 (+).

IR (KBr) v_{max}: 3480, 3365, 2953, 2865, 1709, 1610, 1437, 1278, 1105, 1057, 777 cm^{-1}.

LRMS (EI): 272 (2, M$^+$), 254 (41), 226 (20), 225 (14), 218 (22), 213 (16), 195 (34), 192 (17), 191 (45), 181 (12), 168 (16), 167 (100), 166 (22), 165 (47), 163 (32), 157 (55), 154 (11), 153 (20), 152 (28), 141 (13), 132 (11), 131 (16), 128 (13), 122 (13), 115 (21), 109 (14), 91 (16), 81 (23), 55 (11).

HRMS (EI) calcd for C$_{17}$H$_{20}$O$_3$: 272.1412, found: 272.1414.

Anal. Calcd: C, 74.97; H, 7.40. Found: C, 75.05; H, 7.29.

8.3.4 Single Crystal Photolysis of Salt 95

95   **79**
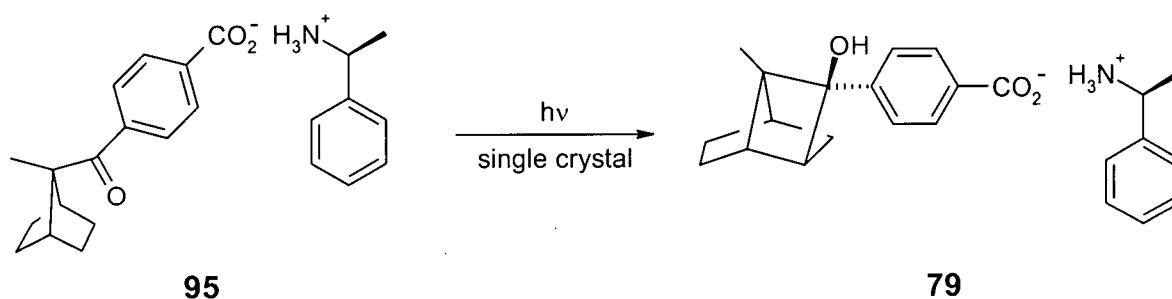
After obtaining the crystal structure of salt **95**, it was left mounted for diffraction and sealed in a polyethylene bag under a N_2 atmosphere. After irradiation (Pyrex filter, 450 W) for 10 min, a second crystal structure was obtained of the mixed crystal. The percent conversion (70%) of the starting material was estimated by both X-ray crystallographic data and by gas chromatographic analysis of a sample, which was photolysed concurrently with the single crystal. The photolysis procedure was repeated for another 3 h followed by X-ray crystallographic analysis of the single crystal irradiated to 93% conversion (determined from X-ray crystallographic data) to salt **79**.

These structures were confirmed by X-ray crystallographic analysis:

	0% Conversion	70% Conversion	93% Conversion
Habit	colourless needle	colourless needle	colourless needle
Space Group	$P2_12_12_1$	$P2_12_12_1$	$P2_12_12_1$
a, Å	6.165(2)	6.1726(5)	6.1652(18)
b, Å	7.090(2)	7.0973(6)	7.0925(14)
c, Å	45.81(2)	46.391(4)	46.969(9)
α (°)	90	90	90
β (°)	90	90	90
γ (°)	90	90	90
Z	4	4	4
R	0.038	0.053	0.050

8.3.5 Single Crystal Photolysis of Salt 94

94   **80**

After obtaining the crystal structure of salt **94**, it was left mounted for diffraction and sealed in a polyethylene bag under a N_2 atmosphere. After irradiation (Pyrex filter, 450 W) for 2 h, a second crystal structure was obtained. The percent conversion 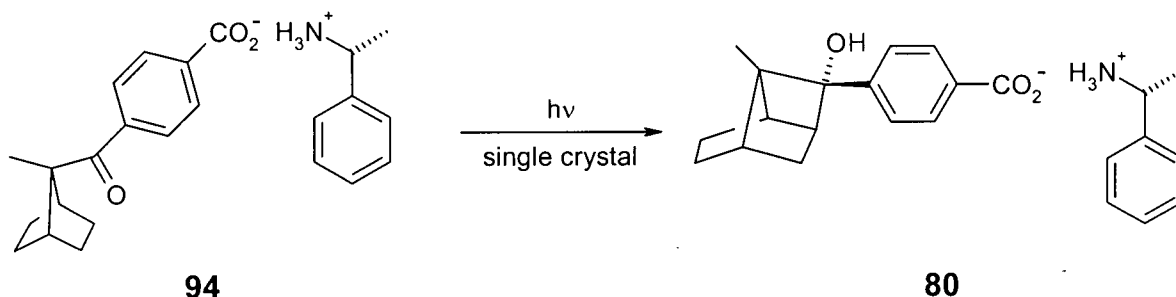(100%) of the starting material to salt **80** was determined by the X-ray crystallographic data, which showed no sign of residual starting material within the crystal lattice.

This structure was confirmed by X-ray crystallographic analysis:

	0% Conversion	100% Conversion
Habit	colourless needle	colourless needle
Space Group	$P2_12_12_1$	$P2_12_12_1$
a, Å	6.1899(7)	6.1661(7)
b, Å	7.1181(8)	7.0930(8)
c, Å	46.012(5)	46.980(5)
α (°)	90	90
β (°)	90	90
γ (°)	90	90
Z	4	4
R	0.0864	0.0948

8.3.6 Preparative Solid State Photolysis of Salt 94
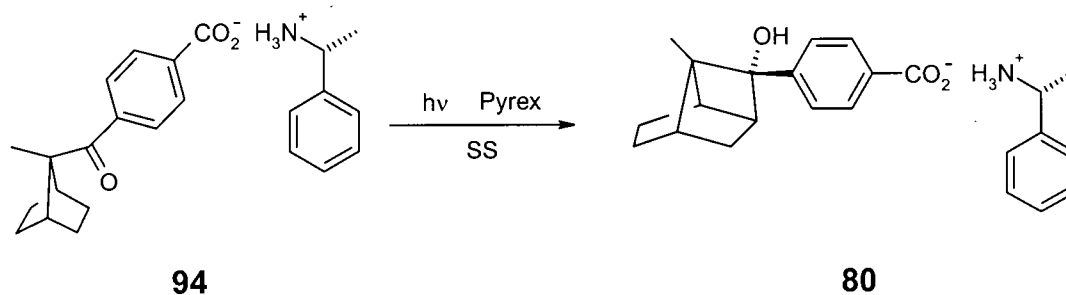
Salt **94** (20 mg, 0.053 mmol) was crushed between two microscope slides (Pyrex equivalent) and sealed in a polyethylene bag under a positive pressure of N_2. The sample was irradiated (Pyrex filter, 450 W) for 40 min, when analysis by gas chromatography of the methyl ester, obtained after treatment of the salt with CH_2N_2, showed that 100% conversion to salt **80** had occurred. After obtaining the melting point and IR spectrum of salt **80**, the remaining product was recrystallized from methanol to give colourless prisms (12 mg, 60%).

(R)-(+)-1-Phenylethylammonium 4-((1*R*,2*R*,5*S*,7*S*,8*R*)-8-hydroxy-1-methyl-tricyclo[3.3.0.0^{2,7}]oct-8-yl)benzoate **(80)**

mp: 161 - 162.5 °C (non-recrystallized)

mp: 163 - 165 °C (methanol)

¹H NMR (400 MHz, CD_2Cl_2): δ 0.84 (dd, *J* = 10.8, 1.8 Hz, 1H), 0.99 (dd, *J* = 10.5, 6.6 Hz, 1H), 1.23 (s, 3H), 1.36 (d, *J* = 6.7 Hz, 3H), 1.41 (m, 1H), 1.53 (m, 2H), 1.79 (m, 2H), 2.51 (m, 1H), 2.63 (m, 1H), 4.16 (q, *J* = 6.6 Hz, 1H), 5.28 (br s, 1H), 7.21 (m, 2H), 7.25 (m, 1H), 7.33 (m, 1H), 7.42 (m, 1H), 7.83 (m, 2H).

¹³C NMR (75 MHz, DMSO): δ 10.87 (-), 21.23 (+), 24.01 (-), 28.01 (+), 33.12 (+), 41.36 (-), 46.46 (-), 47.92 (-), 50.19 (-), 57.29 (+), 83.14 (+), 125.74 (-), 126.09 (-), 126.89 (-), 128.19 (-), 129.91 (-), 132.65 (+), 145.11 (+), 147.75 (+), 168.17 (+).

IR (KBr) v_{max}: 3608, 3200-2500 (br), 2940, 2866, 2543, 1612, 1522, 1398, 1035, 791, 696 cm^{-1}.

IR (recrystallized from methanol) (KBr) v_{max}: 3340 (br), 3200-2500 (br), 2950, 2863, 1618, 1510, 1396, 854, 794, 697 cm^{-1}.

HRMS (ESI, 0.1% HCO_2H in MeOH) calcd for $C_{24}H_{30}O_3N$ (M+1): 380.2226, found: 380.2226.

This structure was confirmed by X-ray crystallographic analysis:

Habit	colourless prism
Space Group	*P2₁*
a, Å	12.2557(9)
b, Å	6.9907(4)
c, Å	12.6665(9)
α (°)	90
β (°)	105.869(3)
γ (°)	90
Z	2
R	0.035

8.3.7 Preparative Solid State Photolysis of Salt 95

95   **79**
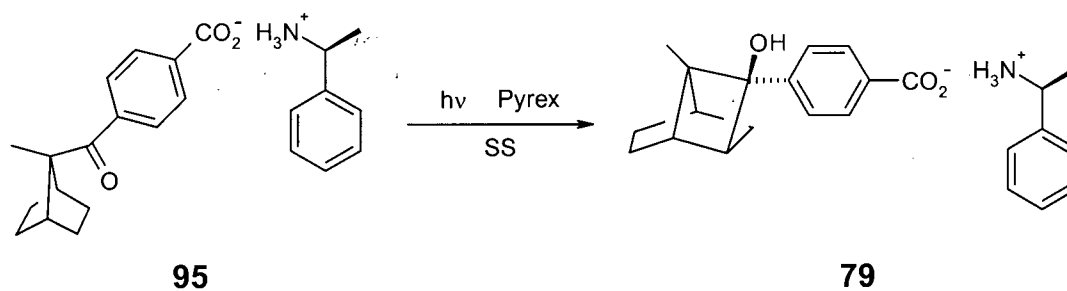
Salt **95** (25 mg, 0.066 mmol) was crushed between two microscope slides (Pyrex equivalent) and sealed in a polyethylene bag under a positive pressure of N_2. The sample was irradiated (Pyrex filter, 450 W) for 60 min, when analysis by gas chromatography of the methyl ester, obtained after treatment of the salt with CH_2N_2, showed that 100% conversion to salt **79** had occurred. After obtaining the melting point and IR spectrum of salt **79**, the remaining product was recrystallized from methanol to give colourless prisms (18 mg, 72%).

(S)-(-)-1-Phenylethylammonium 4-((1S,2S,5R,7R,8S)-1-methyltricyclo[3.3.0.0^{2,7}]oct-8-yl)benzoate (**79**)

mp: 162 - 163 °C (non-recrystallized)

mp: 160 - 162 °C (methanol)

^{1}H NMR (400 MHz, CD$_2$Cl$_2$): δ 0.84 (dd, J = 10.7, 1.8 Hz, 1H), 0.99 (dd, J = 10.5, 6.7 Hz, 1H), 1.23 (s, 3H), 1.36 (d, J = 6.7 Hz, 3H), 1.41 (m, 1H), 1.53 (m, 2H), 1.79 (m, 2H), 2.51 (m, 1H), 2.63 (m, 1H), 4.16 (m, 1H), 5.28 (br s, 1H), 7.21 (m, 2H), 7.24 (m, 1H), 7.33 (m, 1H), 7.42 (m, 1H), 7.83 (m, 2H).

^{13}C NMR (75 MHz, DMSO): δ 10.87, 21.23, 24.01, 28.01, 33.12, 41.36, 46.46, 47.92, 50.19, 57.29, 83.14, 125.76, 126.09, 126.88, 128.19, 128.92, 132.51, 145.20, 147.80, 168.12.

IR (KBr) ν$_{max}$: 3607, 3250-2500 (br), 2940, 2865, 2543, 1612, 1523, 1455, 1397, 1296, 1035, 864, 841, 792, 696 cm^{-1}.

IR (recrystallized from methanol) (KBr) ν$_{max}$: 3348 (br), 3200-2500 (br), 2951, 2864, 1619, 1509, 1396, 854, 795, 697 cm^{-1}.

HRMS (ESI, 0.1% HCO$_2$H in MeOH) calcd for C$_{24}$H$_{30}$O$_3$N (M+1): 380.2226, found: 380.2222.

This structure was confirmed by X-ray crystallographic analysis:

Habit	colourless prism
Space Group	*P2$_1$*
a, Å	12.2580(13)
b, Å	6.9904(5)
c, Å	12.6647(14)
α (°)	90
β (°)	105.865(5)
γ (°)	90
Z	2
R	0.0406

References

[1] Wöhler, F. *Ann. Phys. Chem.* **1828**, *12*, 253.

[2] Trommsdorff, H. *Ann. Chem. Pharm.* **1834**, *11*, 190.

[3] (a) Desiraju, G. R. *Crystal Engineering: The design of Organic Solids*: Elsevier: Amsterdam. 1989. (b) Braga, D.; Maini, L.; Polito, M.; Grepioni, F. In *Strength from Weakness: Structural Consequences of Weak Interactions in Molecules, Supermolecules and Crystals. NATO Science Series. II, Mathematics, Physics and Chemistry Vol. 68*; Domenicano, A., Hargittai, I., Eds.; Kluwer Academic Publishers: Amsterdam. 2002. Chapter 18. (c) Hollingsworth, M. D. *Science* **2002**, *295*, 2410. (d) Irie, M.; Kobatake, S.; Horichi, M. *Science* **2001**, *291*, 1769. (e) Scheffer, J. R.; Scott, C. *Science* **2001**, 291, *1712*.

[4] Byrn, S. R. *Solid-State Chemistry of Drugs*; Academic Press: New York. 1982. Chapter 4.

[5] Cushny, A. R. *The Biological Relations of Optically Isomeric Substances*; Williams Wilkins: Baltimore. 1926.

[6] Blaschke, G.; Kraft, H. P.; Markgraf, H. *Chem. Ber.* **1980**, *113*, 2318.

[7] Draber, W.; Stetter, J. In *Chemistry and Agriculture*; Spec. Publ. No. 36; The Chemical Society: London. 1979; p. 128.

[8] Brudvig, G. W.; Thorp, H. H.; Crabtree, R. W. *Acc. Chem. Res.* **1991**, *24*, 311 and references cited therein.

[9] Margulis, L.; Walker, J. C. G.; Rambler, M. *Nature (London)* **1976**, *263*, 620.

[10] For a review article on the history of organic, and some early inorganic, photochemistry see: Roth, H. D. *Angew. Chem. Int. Ed. Engl.* **1989**, *28*, 1193.

[11] Rothenberg, G.; Downie, A. P.; Raston, C. L.; Scott, J. L. *J. Am. Chem. Soc.* **2001**, *123*, 8701.

[12] Desiraju, G. R. *Solid State Ionics*, **1997**, *101-103*, 839.

[13] Cohen, M. D.; Schmidt, G. M. J. *J. Chem. Soc.* **1964**, 1996.

[14] Cohen, M. D.; Green, B. S. *Chem. Br.* **1973**, *9*, 490.

[15] Some examples of latent reactivity found in crystals include: (a) Heggie, W.; Sutherland, J. K. *Chem. Commun.* **1972**, 957. (b) Ariel, S.; Askari, S.; Scheffer, J. R.; Trotter, J. *J. Org.*

Chem., **1989**, *54*, 4324. (c) Pokkuluri, P. R.; Scheffer, J. R.; Trotter, J.; Yap, M. *J. Org. Chem.* **1992**, *57*, 1486. (d) Cheung, E.; Kang, T.; Scheffer, J. R.; Trotter, J. *Chem. Commun.* **2000**, 2309. (e) Kang, T.; Scheffer, J. R. *Org. Lett.* **2001**, *3*, 3361.

[16] Quinkert, G.; Tabata, T.; Hickman, E. A. J.; Dobrat, W. *Angew. Chem. Int. Ed.* **1971**, *10*, 199.

[17] Some examples of solvent/waste-free reactions inlcude: (a) Kaupp, G.; Herrmann, A.; Schmeyers, J. *Chem. Eur. J.* **2002**, *8*, 1395. (b) Kaupp, G.; Schmeyers, J.; Boy, J. *Chemosphere*, **2001**, *43*, 55. (c) Kaupp, G.; Schmeyers, J.; Naimi-Jamal, M. R.; Zoz, H. Ren, H. *Chem. Eng. Sci.* **2002**, *57*, 763. (d) Toda, F. *Acc. Chem. Res.* **1995**, *28*, 480.

[18] Engler, C.; Dorant, K. *Chem. Ber.* **1895**, *28*, 2497.

[19] Schmitt, R. *J. Prakt. Chem.* **1885**, *31*, 397.

[20] Kohlshutter, H. W. *Z. Anorg. Allg. Chem.* **1919**, *105*, 1.

[21] (a) Cohen, M. D.; Schmidt, G. M. J.; Sonntag, F. I.; *J. Chem. Soc.* **1964**, 2000. (b) Schmidt, G. M. J. *J. Chem. Soc.* **1964**, 2014. (c) Schmidt, G. M. J. *Pure. Appl. Chem.* **1971**, *27*, 647.

[22] (a) Libermann, C. *Chem. Ber.* **1889**, *22*, 124. (b) Libermann, C. *Chem. Ber.* **1889**, *22*, 782.

[23] (a) de Jong, A. W. K. *Chem. Ber.* **1922**, *55*, 463. (b) de Jong, A. W. K. *Chem. Ber.* **1923**, *56*, 818.

[24] (a) Stobbe, H. *Chem. Ber.*, **1922**, *55*, 2225. (b) Stobbe, H. *Chem. Ber.* **1925**, *58*, 2415.

[25] Bernstein, H. I.; Quimby, W. C. *J. Am. Chem. Soc.* **1943**, *65*, 1845.

[26] Cohen, M. D. *Angew. Chem. Intl. Ed.* **1975**, *14*, 386.

[27] Weiss, R. G.; Ramamurthy, V.; Hammond, G. S. *Acc. Chem. Res.* **1993**, *26*, 530.

[28] Nakanishi, H.; Jones, W.; Thomas, J. M.; Hursthouse, M. B.; Motevalli, M. *Chem. Commun.* **1980**, 611.

[29] A further discussion of classes of solid state reactivity can be found in: Keating, A. E.; Garcia-Garibay, M. A. In *Molecular and Supramolecular Photochemistry*; Ramamurthy, V., Schanze, K. S., Eds.; Marcel Dekker: New York. 1998; Volume 2; Chapter 5.

[30] (a) Jones, W.; Nakanishi, H.; Theocharis, C. R.; Thomas, J. M. *Chem. Commun.* **1980**, 610. (b) Nakanishi, H.; Jones, W.; Thomas, J. M. *Chem. Phys. Lett.* **1980**, *71*, 44. (c) Jones, W.; Theocharis, C. R. *J. Cryst. Spec. Res.* **1984**, *14*, 447. (d) Theocharis, C. R.; Desiraju,

G. R.; Jones, W. *J. Am. Chem. Soc.* **1984**, *106*, 3606. (e) Feeder, N.; Honda, K. *Mol. Cryst. Liq. Cryst.* **1998**, *313*, 327. (f) Honda, K.; Nakanishi, F.; Feeder, N. *J. Am. Chem. Soc.* **1999**, *121*, 8246.

[31] This temperature is calculated using the Böltzman distribution where N_e and N_g are the relative populations of the excited and ground states, (E_e-E_g) is the difference in energy between the excited and ground states. To achieve a 1% population of the excited state equal to excitation by 320 nm light a temperature of 9737 K would be required.

$$\frac{N_e}{N_g} = e^{-\frac{(E_e - E_g)}{RT}} \Rightarrow T = -\frac{(E_e - E_g)}{R\ln(\frac{N_e}{N_g})} = -\frac{372.8 \times 10^3 \, J\,mol^{-1}}{(8.314\,J\,K^{-1}\,mol^{-1})(\ln(0.01))} = 9737\,K$$

[32] A more complete explanation of photoexcitation and the associated decay processes may be found in: (a) Lowry, T. H.; Richardson, K. S. *Mechanism and Theory in Organic Chemistry, 3rd Edition*; HarperCollinsPublishers: New York. 1987. Chapter 12. (b) Calvert, J. G.; Pitts Jr., J. N. *Photochemistry*; John Wiley & Sons: New York. 1966.

[33] For reviews of Norrish/Yang photochemistry see: (a) Wagner, P.; Park, B. -S. In *Organic Photochemistry*; Padwa, A., Ed.; Marcel Dekker: New York. 1991; Volume 11; Chapter 4. (b) Wagner, P.J. *Acc. Chem. Res.* **1971**, *4*, 168.

[34] Norrish, R. G. W. *Trans. Faraday Soc.* **1937**, *33*, 1532.

[35] Yang, N. C.; Yang, D. -H. *J. Am. Chem. Soc.* **1958**, *80*, 2913.

[36] Weiss, R. G. In *CRC Handbook of Photochemistry and Photobiology*; Horspool, W. M., Song, P. -S., Eds.; CRC Press: Boca Raton. 1995; Chapter 39 and references cited therein.

[37] Lamola, A. A.; Hammond, G. S. *J. Phys. Chem.* **1965**, *43*, 2129.

[38] (a) Stephenson, L. M.; Cavigli, P. R.; Parlett, J. L. *J. Am. Chem. Soc.* **1971**, *93*, 1984. (b) Casey, C. P.; Boggs, R. A. *J. Am. Chem. Soc.* **1972**, *94*, 6457

[39] O'Connell, Jr., E. J. *J. Am. Chem. Soc.* **1968**, *90*, 6550.

[40] Wagner, P. J.; Kelso, P. A.; Kemppainen, A. E.; Zepp, R. G. *J. Am. Chem. Soc.* **1972**, *74*, 7500.

[41] (a) Scheffer, J. R.; Jennings, B. M.; Louwerens, J. P. *J. Am. Chem. Soc.* **1976**, *98*, 7040. (b) see also reference 15b.

[42] Bernard, M.; Yang, N. C. *Proc. Chem. Soc. London* **1958**, 302.

[43] (a) Horspool, W. M., Ed. *Synthetic Organic Photochemistry*; Plenum Press: New York. 1984. (b) Mattay, J., Griesbeck, A. G., Eds. *Photochemical Key Steps in Organic Synthesis*; John Wiley & Sons: New York, 1984.

[44] (a) Paquette, L. A.; Sugimura, T. *J. Am. Chem. Soc.* **1986**, *108*, 3841. (b) Sugimura, T.; Paquette, L. A. *J. Am. Chem. Soc.* **1987**, *109*, 3017.

[45] Chandler, W.; Goodman, L. *J. Mol. Spectrosc.* **1970**, *35*, 232.

[46] Ladd, M. F. C.; Palmer, R. A. *Structure Determination by X-ray Crystallography*; Plenum Press: New York. 1994. p. 436, 462

[47] (a) Hoffmann, R.; Swenson, J. R. *J. Phys. Chem.* **1970**, *74*, 415. (b) Wagner, P. J.; May, M.; Haug, A. *Chem. Phys. Lett.* **1972**, *13*, 545.

[48] Sauers, R. R.; Edberg, L. A. *J. Org. Chem.* **1994**, *59*, 7061.

[49] Moule, D. C.; Walsh, A. D. *Chem. Rev.* **1975**, *75*, 67.

[50] Ihmels, H.; Scheffer, J.R. *Tetrahedron* **1999**, *55*, 885 and references cited therein.

[51] (a) Bondi, A. *J. Phys. Chem.* **1964**, *68*, 441. (b) Edward, J. T. *J. Chem. Educ.* **1970**, *47*, 261.

[52] Dorigo, A. E.; Houk, K. N. *J. Am. Chem. Soc.* **1987**, *109*, 2195.

[53] (a) Kasha, M. *Radiat. Res.* **1960**, *Suppl. 2*, 243. (b) Zimmerman, H. E. *Tetrahedron* **1963**, *19*, 393.

[54] Wagner, P. J.; Kelso, P. A.; Kemppainen, A. E.; McGrath, J. M.; Schott, H. N.; Zepp, R. G. *J. Am. Chem. Soc.* **1972**, *94*, 7506.

[55] (a) Wagner, P. J.; Kemppainen, A. E. *J. Am. Chem. Soc.* **1968**, *90*, 5896. (b) Hoffmann, R.; Swaminathan, S.; Odell, B. G.; Gleiter, R. *J. Am. Chem. Soc.* **1970**, *92*, 7091.

[56] Leibovitch, M.; Olovsson, G.; Scheffer, J. R.; Trotter, J. *J. Am. Chem. Soc.* **1998**, *120*, 12755.

[57] Cheung, E.; Netherton, M. R.; Scheffer J. R.; Trotter, J. *Org. Lett.* **2000**, *2*, 77.

[58] Recent reviews on asymmetric photochemistry include: (a)Rau, H. *Chem. Rev.* **1983**, *83*, 535. (b) Inoue, Y. *Chem. Rev.* **1992**, *92*, 741. (c) Pete, J. P. *Adv. Photochem.* **1996**, *21*, 135. (d) Everitt, S. R. L.; Inoue, Y. In *Molecular and Supramolecular Photochemistry Vol. 3*; Ramamurthy, V., Schanze, K. S., Eds.; Marcel Dekker: New York, 1999; Chapter 2. (e) Griesbeck, A. G.; Meierhenrich, U. J. *Angew. Chem. Int. Ed.* **2002**, *41*, 3147.

[59] (a) Le Bel, J. -A. *Bull. Soc. Chim. Fr.* **1874**, *22*, 337. (b) van't Hoff, J. H. *Die Lagerun der Atome im Raume*; 2nd ed.; Vieweg: Braunscheig, 1894; p. 30.

[60] Kuhn, W.; Braun, E. *Naturwissenschaften* **1929**, *17*, 227.

[61] For reviews on solid-state asymmetric photochemistry see: (a) Ohashi, Y., Ed. *Reactivity in Molecular Crystals*; VCH Publishers: New York. 1993. Chapter 5. (b) Feringa, B. L.; van Delden, R. A. *Angew. Chem. Intl. Ed.* **1999**, *38*, 3418. (c) Green, B. S.; Arad-Yellin, R.; Cohen, M. D. In *Topics in Stereochemistry*; Eliel, E. I., Wilen, S. H., Allinger, N. L., Eds.l John Wiley & Sonds: NewYork. 1986. Volume 16. p. 131. (d) Green, B. S.; Lahav, M.; Rabinovich, D. *Acc. Chem. Res.* **1979**, *12*, 191. (e) Ito, Y. In *Molecular and Supramolecular Photochemistry*; Ramamurthy, V.; Schanze, K. S., Eds.; Marcel Dekker: New York. 1999. Volume 3. Chapter 1. (f) See also reference 58e.

[62] Penzien, K.; Schmidt, G. M. J. *Acc. Chem. Res.* **1969**, *8*, 608.

[63] Elgavi, A.; Green, B. S.; Schmidt, G. M. J. *J. Am. Chem. Soc.* **1973**, *95*, 2058.

[64] Evans, S. V.; Garcia-Garibay, M.; Omkaram, N.; Scheffer, J. R.; Trotter, J.; Wireko, F. *J. Am. Chem. Soc.* **1986**, *108*, 5648.

[65] Jacques, J.; Collet, A.; Wilen, S. H. *Enantiomers, Racemates and Resolutions*; John Wiley & Sons: New York. 1981. p. 1-18.

[66] For reviews of the ionic chiral auxiliary concept see: (a) Scheffer, J. R. *Can. J. Chem.* **2001**, *79*, 349. (b) Gamlin, J. N.; Jones, R.; Leibovitch, M.; Patrick, B.; Scheffer, J. R.; Trotter, J. *Acc. Chem. Res.* **1996**, *29*, 203.

[67] Pasteur, L. *C. R. Acad. Sci.* **1853**, *37*, 162.

[68] Gudmundsdottir, A. D.; Scheffer, J. R. *Tetrahedron Lett.* **1990**, *31*, 6807.

[69] Scheffer, J. R.; Wang, K. *Synthesis* **2001**, 1253.

[70] Leibovitch, M. Ph. D. Thesis, The University of British Columbia, 1997.

[71] Lewis, F. D.; Johnson, R. W.; Ruden, R. A., *J. Am. Chem. Soc.* **1972**, *94*, 4292.

[72] Buske, G. R.; Ford, W. T. *J. Org. Chem.* **1976**, *41*, 1998.

[73] Beckmann, S.; Geiger, H. *Chem. Ber.* **1961**, *94*, 48.

[74] Kwart, H.; Kaplan, L. *J. Am. Chem. Soc.* **1954**, *76*, 4072.

[75] Janz, K. Masters Thesis, The University of British Columbia, 1998.

[76] Nahm, S.; Weinreb, S. M. *Tetrahedron Lett.* **1981**, *22(39)*, 3815.

[77] Jones, T. K.; Mills, S. G.; Reamer, R. A.; Askin, D.; Desmond, R.; Volante, R. P.; Shinkai, I. *J. Am. Chem. Soc.* **1989**, *111*, 1157.

[78] Boymond, L.; Rottlander, M.; Cahiez, G.; Knochel, P. *Angew. Chem. Int. Ed.* **1998**, *37*, 1701.

[79] Shultz, D.; Boal, A. K.; Farmer, G. T. *J. Org. Chem.* **1998**, *63*, 9462.

[80] Olah, G. A.; Narang, S. C.; Gupta, B. G. B.; Malhotra, R. *J. Org. Chem.* **1979**, *44*, 1247.

[81] Ito, Y.; Yasui, S.; Yamauchi, J.; Ohba, S.; Kano, G. *J. Phys. Chem. A* **1998**, *102*, 5415.

[82] Cheung, E.; Kang, T.; Netherton, M. R.; Scheffer, J. R.; Trotter, J. *J. Am. Chem. Soc.* **2000**, *122*, 11753.

[83] Koshima, H.; Matsushige, D.; Miyauchi, M. *CrystEngComm* **2001**, *33*, 1.

[84] Lewis, T. J.; Rettig, S. J.; Scheffer, J. R.; Trotter, J. *Mol. Cryst. Liq. Cryst.* **1992**, *219*, 17.

[85] Wagner, P. J. In *Molecular Rearrangements*; de Mayo, P., Ed.; Academic Press: New York. 1980, Vol. 3, p. 381.

[86] Evidence of hydrogen abstraction in an "unreactive" benzophenone derivative in the solid state has been shown by Ito and co-workers (see ref. 81). Previous attempts within our research group to detect the biradical intermediate of alkyl-aryl ketones in the solid state has proven unsuccessful.

[87] Wagner, P. J. In *CRC Handbook of Organic Photochemistry and Photobiology*; Horspool, W. M., Song, P. -S., Eds., CRC Press: Boca Raton, 1995; Chapter 38.

[88] Burdett, J. K. *Molecular Shapes*; John Wiley & Sons: New York. 1980; p. 6.

[89] (a) Doering, W. v. E.; Roth, W. R. *Tetrahedron* **1962**, *18*, 67. (b) Hill, R. K.; Gilman, N. W. *Chem. Commun.* **1967**, 619.

[90] Ariel, S.; Ramamurthy, V.; Scheffer, J. R.; Trotter, J. *J. Am. Chem. Soc.* **1983**, *105*, 6959.

[91] Dorigo, A. E.; McCarrick, M. A.; Loncharrich, R. J.; Houk, K. N. *J. Am. Chem. Soc.* **1990**, *112*, 7508.

[92] Griesbeck, A. G.; Heckroth, H. *J. Am. Chem. Soc.* **2002**, *124*, 396.

[93] Scheffer, J. R.; Scott, C. In *The CRC Handbook of Organic Photochemistry and Photobiology*; *2nd Edition*; Horspool, W. M., Lenci, F. Eds., CRC Press: Boca Raton. 2003 (in press) and references cited therein.

[94] (a) Bijvoet, J. M.; Peerdeman, A. F.; van Bommel, A. J. *Nature* **1951**, *168*, 271. (b) Bijvoet, J. M. *Endeavour* **1995**, *14*, 71.

[95] The absolute configuration of a molecule containing only carbon, hydrogen and oxygen can be obtained by X-ray crystallography, however, the success of such methods is dependent on the intensity differences of the Friedel/Bijvoet pairs (Peerdeman, A. F.; Bijvoet, J. M. *Acta Crystallographica* **1956**, *9*, 1012). An example of such a determination concerning the mapping of the absolute steric course of a photoreaction can be found in: Garcia-Garibay, M.; Scheffer, J. R.; Trotter, J.; Wireko, F. *J. Am. Chem. Soc.* **1989**, *111*, 4985.

[96] Similar types of absolute configuration correlations using chiral auxiliaries have been previously conducted: (a) Leibovitch, M. Olovsson, G.; Scheffer, J. R.; Trotter, J. *Pure & Appl. Chem.* **1997**, *69*, 815 and references cited therein. (b) Hirotsu, K.; Okada, K.; Mizutani, H.; Koshima, H.; Matsuura, T. *Mol. Cryst. Liq. Cryst.* **1996**, *277*, 96. (c) Tanaka, K.; Mizutani, H.; Miyahara, I.; Hirotsu, K.; Toda, F. *CrystEngComm* **1999**, paper 3. (d) Tanaka, K.; Toda, F.; Mochizuki, E.; Yasui, N.; Kai, Y.; Miyahara, I.; Hirotsu, K. *Angew. Chem. Int. Ed.* **1999**, *38*, 3523. (e) Ohba, S.; Hosomi, H.; Tanaka, K.; Miyamoto, H.; Toda, F. *Bull. Chem. Soc. Jpn.* **2000**, *73*, 2075. (f) Tanaka, K.; Mochizuki, E.; Yasui, N.; Kai, Y.; Miyahara, I.; Hirotsu, K.; Toda, F. *Tetrahedron* **2000**, *56*, 6853. (g) Hosomi, H.; Ohba, S.; Tanaka, K.; Toda, F. *J. Am. Chem. Soc.* **2000**, *122*, 1818. (h) see also reference 83.

[97] (a) Lewis, F. D.; Hillard, T. J. *J. Am. Chem. Soc.* **1970**, *92*, 6672. (b) Lewis, F. D.; Hilliard, T. *J. Am. Chem. Soc.* **1972**, *94*, 3852.

[98] Wagner, P. J.; Kelso, P. A.; Zepp, R. G. *J. Am. Chem. Soc.* **1972**, *94*, 7480.

[99] Compounds with higher ω values have given varied results. (a) reactive (ω ~ 90°): (i) Popovitz-Biro, R.; Chang, H. C.; Tang, C. P.; Shochet, N. R.; Lahav, M.; Leiserowitz, L. *Pure and Appl. Chem.* **1980**, *52*, 2693. (ii) Vaida, M.; Popovitz-Biro, R.; Leiserowitz, L.; Lahav, M. In *Photochemistry in Organized and Contrained Media*; Ramamurthy, V., Ed.; VCH Publishers: New York, 1991; Chapter 6. It should be noted that these examples are all dialkyl ketones and will likely have a pyramidalized excited state carbonyl group, altering the associated angles from those found in the ground state (see ref. 48) (b)

unreactive ($\omega \sim 90°$): Lutz, G.; Pinkos, R.; Murty, B. A. R. C.; Spurr, P. R.; Fessner, W. -D.; Wörth, H. F.; Knothe, L.; Prinzbach, H. *Chem. Ber.* **1992**, *125*, 1741.

[100] Chen, S.; Cheung, E.; Filson, H.; Netherton, M. R.; Patrick, B.; Scheffer, J. R.; Scott, C.; Xia, W.; Braga, D.; Maini, L. *unpublished results.*

[101] It is interesting to note that hydrogen abstraction in the solid state for this ketone would occur from a chair-like conformation (see Section 5.5). The related spirocyclic compounds and all of the ketones discussed in this thesis undergo hydrogen abstraction from a boat-like conformation.

[102] Hyperchem™, Hypercube, Inc., 1115 NW 4th Street Gainsville, Florida 32601, USA.

[103] (a) Garcia-Garibay, M. A.; Houk, K. N.; Keating, A. E.; Cheer, C. J.; Leibovitch, M.; Scheffer, J. R.;Wu, L. -C. *Org. Lett.* **1999**, *1*, 1279. (b)Zimmerman, H. E.; Nesterov, E.E. *Acc. Chem. Res.* **2002**, *35*, 77 and references cited therein.

[104] Dunitz, J. D. *X-ray Analysis and the Structure of Organic Molecules*; Cornell University Press: Ithica, NY; 1979, 312.

[105] This has been demonstrated for a series of macrocyclic aminoketones: Cheung, E.; Netherton, M. R.; Scheffer, J. R.; Trotter, J. *J. Am. Chem. Soc.* **1999**, *121*, 2919. This study also represent another case in which the use of different auxiliaries altered the photoproduct ratio in addition to inucing enantioselectiviy.

[106] Janz, K. M.; Scheffer, J. R. *Tetrahedron Lett.* **1999**, *40*, 8725.

[107] For similar studies see: (a) Jayaraman, S.; Uppili, S.; Natarajan, A.; Joy, A.; Chong, K. C. W.; Netherton, M. R.; Zenova, A.; Scheffer, J. R.; Ramamurthy, V. *Tetrahedron Lett.* **2000**, *41*, 8231. (b) Leibovitch, M.; Olovsson, G.; Sundarababu, G.; Ramamurthy, V.; Scheffer, J. R.; Trotter, J. *J. Am. Chem. Soc.* **1996**, *118*, 1219. (c) Cheung, E.; Chong, K. C. W.; Jayaraman, S.; Ramamurthy, V.; Scheffer, J. R.; Trotter, J. *Org. Lett.* **2000**, *2*, 2801. (d) Joy, A.; Uppili, S.; Netherton, M. R.; Scheffer, J. R.; Ramamurthy, V. *J. Am. Chem. Soc.* **2000**, *122*, 728.

[108] Wittig, G.; Knauss, E. *Chem. Ber.* **1958**, *91(5)*, 895.

[109] Cristol, S. J.; Natchigall, G. W. *J. Org. Chem.* **1967**, *32*, 3727.

[110] Wilt, J. W.; Gutman, G.; Ranus, W. J., Jr.; Zigman, A. R. *J. Org. Chem.* **1967**, *32*, 893.

[111] Sauers, R. R.; Hawthorne Jr., R. M. *J. Org. Chem.* **1964**, *29*, 1685.

[112] Although all spectroscopic and analytical data are consistent with the chemical structure, the disparity between the observed and literature melting point values has not been accounted for, but could be due to the existence of a polymorphic crystal form (for a discussion on this topic see: Dunitz, J. D.; Bernstein, J. *Acc. Chem. Res.* **1995**, *28*, 193.). The literature value has been independently reported (Moriarity, R. M.; Chien, C. C.; Adams, T. B. *J. Org. Chem.* **1979**, *44*, 2206).